SURFACE-GROUNDWATER INTERACTIONS IN THE LJUBLJANSKO POLJE AQUIFER SYSTEM (SLOVENIA)

Janja Vrzel

Doctoral Dissertation
Jožef Stefan International Postgraduate School
Ljubljana, Slovenia

Supervisor: Prof. Dr. Nives Ogrinc, Jožef Stefan Institute, Ljubljana, Slovenia
Co-Supervisor: Prof. Dr. Ralf Ludwig, Ludwig-Maximilians-Universität München, Munich, Germany
Co-Supervisor: Assoc. Prof. Dr. Goran Vižintin, Faculty of Natural Sciences and Engineering, Ljubljana, Slovenia

Evaluation Board:
Prof. Dr. Radmila Milačič, Chair, Jožef Stefan Institute, Ljubljana, Slovenia
Prof. Dr. Rudolf Rajar, Member, Faculty of Civil and Geodetic Engineering, University of Ljubljana, Slovenia
Prof. Dr. Fulvio Celico, Member, Department of Chemical Sciences, Life and Environmental Sustainability, University of Parma, Italy

MEDNARODNA PODIPLOMSKA ŠOLA JOŽEFA STEFANA
JOŽEF STEFAN INTERNATIONAL POSTGRADUATE SCHOOL



Janja Vrzel

SURFACE-GROUNDWATER INTERACTIONS IN THE LJUBLJANSKO POLJE AQUIFER SYSTEM (SLOVENIA)

Doctoral Dissertation

ŠTUDIJA INTERAKCIJ MED POVRŠINSKO IN PODZEMNO VODO V VODONOSNEM SISTEMU LJUBLJANSKO POLJE (SLOVENIJA)

Doktorska disertacija

Supervisor: Prof. Dr. Nives Ogrinc

Co-Supervisor: Prof. Dr. Ralf Ludwig

Co-Supervisor: Assoc. Prof. Dr. Goran Vižintin

Ljubljana, Slovenia, May 2018

Healing sparkling water, rushing over me,
from the rain to the river to the deep blue sea,
this blessed water's always running so free,
from the glaciers on the mountain where the snow's falling down,
this blessed water feeds the thirsty ground,
. . . . . .
it's the blood of the mother as it nourishes all. (3–7,9)

(Windsong Martin, 2017)

Acknowledgments

This PhD has been truly an amazing journey and it would not have been possible to accomplish it without those who supported me in one way or the other.

First of all I would like express my sincere gratitude to my supervisor Prof. Dr. Nives Ogrinc, for her guidance and help through all stages of the thesis development, even remotely, when I have moved abroad. She has generously supported me academically and gone beyond her duties in order to allay my worries. You have inspired me and contributed to my professional and personal growth. I would like to sincerely thank to my co-supervisor Prof. Dr. Ralf Ludwig for showing me the right way towards the successful accomplishment of our ideas related to the hydrological modeling. I greatly appreciate our numerous fruitful discussions, through which new outstanding research ideas have been developed. I want to thank to my second co-supervisor Assoc. Prof. Dr. Goran Vižintin, for sharing his knowledge related to the hydrogeology in the Ljubljansko polje. Working with such successful and enthusiastic scientists was an incredible experience. Thank you all for this wonderful opportunity!

I would like to thank to the chair Prof. Dr. Radmila Milačič and members of the committee Prof. Dr. Rudolf Rajar and Prof. Dr. Fulvio Celico, for the evaluation of the thesis, all the suggestions to improve the final version of the thesis and showed interest into the thesis.

Thanks to all the colleagues at the Department of Environmental Sciences at the JSI and the Department of Geography and Remote Sensing at the LMU, for creating friendly atmosphere in our working environments. Our interesting discussions over coffee or lunch breaks have truly broadened my perspectives. Nevertheless, I would like to pass a special warm word for my office-mates (Doris Potočnik, Bor Krajnc, Viktoria Friedman, David Gampe, Verena Huber Garcia, Swen Meyer, Marinka Gams Petrišič and Ana Miklavčič Višnjevec), the *Mensa* group members at the LMU and the PhD-followers at the MPŠ program, with whom I have shared moments of anxiety, but also of great excitement. I wold also like to thank Bor for checking the Chapter 4 of the final version of the PhD.

I would like to express a gratitude to all individuals, who have credits for faster progress of the work, due to their specific expertise:

- Prof. D. Kip Solomon (University of Utah, USA) has performed the $^{3}H/^{3}He$ analysis and contributed significantly to the interpretation of the results with his rich hydrological and geochemical knowledge;
- Dr. Swen Meyer and Mr. Josef Schmid (Ludwig-Maximilians-Universität-München, Germany) have helped me when I got stuck with processing the WaSiM setup;
- Mr. Benjamin Müller (Ludwig-Maximilians-Universität-München, Germany) has been a great support when I needed help with statistics, mathematics and programming. I truly appreciate all your suggestions and many fruitful discussions;
- Dr. Patrick Keilholz (MIKE Powered by DHI, Germany) has suggested to implement ifmMIKE11 plug-in the modeling framework and shared his knowledge about its setup. Using ifmMIKE11 turned out as a great contribution to the PhD;

– Dr. rer. net. Gabriele Chiogna (Technical University of Munich, Germany) has been open for valuable hydrogeological discussions;
– Prof. John Doherty (Finders University, Australia) has given me a hint about using FePEST more effectively;
– Mag. Branka Bračič Železnik (VOKA, Slovenia), a local hydrogeological expert, has shared with me her knowledge about the Ljubljansko polje and books;
– I have met Dr. habil. Christoph Neukum (Federal Institute for Geosciences and Natural Resources, Hanover, Germany), Prof. Dr. Jan Fleckenstein (Helmholtz Center for Environmental Research (UFZ), Germany), Mag. Martin Fuchsluger (Geologische Bundesanhalt Austria, Austria) only once at different conferences, but our fruitful discussions have been an enormous help for the model improvement;
– Mr. Stojan Žigon has provided technical support and assistance for isotope analyses and taught me working with the isotope ratio mass spectrometer;
– Mrs. Veronika Degmayr has developed the WaSiM model, with the Slovenian part of the Sava River Basin as the modeling domain, for the purpose of her M. Sc. Thesis.

This work could not be accomplished without enormous amount of data. For this reason, I would like to express my gratitude to all those institutes and companies, who have shared their data:
– Slovenian Environmental Agency (ARSO),
– DHD, d.o.o.,
– Holding Slovenske Elektrarne d.o.o.,
– Institute for Water of the Republic of Slovenia (IzVRS),
– Javno Podjetje Vodovod-Kanalizacija Ljubljana (VOKA),
– Pivovarna Laško Union d.o.o.,
– Biotechnical Faculty, Infrastructural Center for Pedology and Environmental Protection, University of Ljubljana,
– The City Municipality of Ljubljana,
– The Surveying and Mapping Authority of the Republic of Slovenia.

A gratitude goes also to the MIKE Powered by Danish Hydrological Institute (DHI), who has given me an access to their powerful FEFLOW software and its plug-in ifm-MIKE11. Also, I appreciate the freely available WaSiM software, which has been developed by the Hydrology Software Consulting J. Schulla.

I would like to thank Dr. David Heath for revising the thesis.

Also, I thank to the biologists from the Institute for Biological Research "Siniša Stanković" in Belgrade, for our pleasant collaboration, the product of which is the paper, presented later in the dissertation. We had a great time together at the sampling campaign as well.

The PhD project has been financially supported by the IAEA Project under Contact No. RER8016 TC entitled "Using Environmental Isotopes for Evaluation of Stream water/Groundwater Interactions in Selected Aquifers in the Danube Basin"; and the EU 7th Research Project – GLOBAQUA (Managing the effects of multiple stressors on aquatic ecosystem under water scarcity) under Grant agreement no. 603629-ENV-2013-6.2.1. The research was partially conducted within my doctoral study financed by the European Social Fund (KROP 2012) no. C2130-12-000070. However, the application of this funding was approved due to the successful collaboration between the Jožef Stefan Institute and the Ecological engineering institute d.o.o., Maribor, Slovenia, which I appreciate very much. On this occasion, I would like to thank Mr. Željko Blažeka, director of the company Ecological engineering institute d.o.o. at that time, for his credits that my PhD could have started at all. Moreover, I would like to pass a warm word for the full IEI-team, with whom we have created nice memories on skiing and hiking. I also appreciate the approves

of the applications for even two funding programs for students: the Ad Futura (*186. Javni razpis sofinanciranja raziskovalnega sodelovanja doktroskih študentov v tujini v letu 2014* no. 11012-18/2015) from the Public Scholarships, Development, Disability and Maintenance Found of the Republic of Slovenia and the Erasmus+ (2016-1-SI01-KA103-021434) from European Union (no. 21434-MOB-00002).

Finally, I would like to express a gratitude to the people outside the working environment. Many thanks to my friends, for their patient and staying by my side despite my frequent absence. The last but not least thanks goes to my parents and sister for the unconditional love and the 24/7 support, and my nephews, for all the times you have made me laugh.

I cannot ever say this enough, but thank you all!

Abstract

All water bodies, either above or below the surface, are in constant mutual interaction. Therefore, if we are to tackle successfully environmental issues such as water scarcity and quality, both of which are global concerns, it is necessary to understand the interactions that occur between groundwater and surface water bodies and to treat them as a single system. This is also crucial in implementing properly the European Union water policy established in the EU Water Framework Directive, the purpose of which is to improve chemical and quantity status of surface and groundwater bodies.

The aim of this doctoral dissertation was to investigate the patterns of nutrients and other hydrological issues affecting groundwater and river water in order to identify stressors and the impact that they have on groundwater in an alluvial aquifer and on river water. The work goes further, since by understanding groundwater and surface water as a single system it is possible to explain the impact that these stressors have on groundwater-surface water interactions. The thesis looks at two case studies, the Sava River Basin (SRB) and a small aquifer within the SRB—the Ljubljansko polje, which is located in central Slovenia and is an important source of drinking water supply for the local population.

This research took an interdisciplinary approach to understanding groundwater-surface water interactions by combining geochemistry, hydrology, statistics, and by modeling percolation and river water and groundwater flow. It is important to stress that a combination of the various different tools used in this thesis creates a clear picture of the water cycle in the study area in space and time—not only in the past, but also in the future. First, the long-term data for the Sava River reveals a decreasing nutrient content. The ranges of isotope values ($\delta^{15}N_{NO3}$ and $\delta^{18}O_{NO3}$) suggest that nitrates in the Sava River water derive mainly from soil nitrification, sewage and/or manure—a finding supported by microbial source tracking. Second, multiple-tools were used to develop a conceptual model of the Ljubljansko polje aquifer system. The $\delta^{18}O$ and $\delta^{2}H$ values reveal the diverse impacts that the Sava River water and local precipitation have on the aquifer. According to a statistical analysis of the hydrological and meteorological chronological data, such impacts are noticeable within 24 hours at Jarški prod or up to a month later at Kleče, the time difference being due to pressure changes in the aquifer. Additionally, a short (up to 8-year) groundwater mean residence time was estimated using ^{3}H and $^{3}H/^{3}He$ methods. The thesis also involved the comprehensive numerical modeling of the steady and transient state of groundwater flow using FEFLOW, which was coupled with MIKE 11 and WaSiM software for modeling the Sava River water flow and percolation, respectively. This comprehensive modeling framework was also used to predict the groundwater and surface water behavior for the period from 2036 to 2065. This period was defined based on climate projections using the three regional climate models SMHI-RCA4, KNMI-RACMO22E and CLMcom-CCLM4-8-17 provided through the EURO-CORDEX initiative. Modeling shows that the Ljubljansko polje will retain sufficient water capacity and will not suffer due to water scarcity in the period 2036–2065.

This thesis describes a set of important tools that provide us with a deeper under-

standing of water cycling in the Ljubljansko polje and partly in the SRB. The same tools can be further applied in water protection and management strategies in the future.

Povzetek

Vodna telesa, bodisi na ali pod zemeljskim površjem, so zaradi njihove medsebojne povezanosti pod konstantnim medsebojnim vplivom. Prav zato, je razumevanje celotnega vodnega kroga kot enoten sistem, neizogibno za uspešno spopadanje z okolijskimi problemi, ki pestijo svet. Predvsem tistimi, ki se navezujejo na pomanjkanje vode ali njeno onesnaženje. Razumevanje procesov, od katerih je odvisna interakcija med površinsko in podzemno vodo, je prav tako pomembno za uspešno uveljavljanje evropske vodne politike, sprejete z Okvirno vodno direktivo, katere namen je uvajanje sanacijskih ukrepov v primeru poslabšanja količinskega stanja vodnih teles.

Eden iz med ciljev te doktorske disertacije je bil preučevanje trendov hranil v rečni in podzemni vodi v aluvialnem vodonosniku, tako kot tudi drugih v vodi skritih sporočil, z namenom, da bi identificirali stresorje in njihov vpliv na obe vodni telesi. Narejen je bil še korak naprej. Preko razumevanja površnike in podzemne vode kot enotnega sistema, je bil razložen vpliv nekaterih stresorjev na interakcijo med površinsko in podzemno vodo. Raziskave so potekale na primeru Savskega porečja in majhnega, a za lokalno prebivalstvo pomembnega, vodonosnega sistema Ljubljansko polje v centralnem delu Slovenije.

Pristop k študiji interakcije med površinsko in podzemno vodo je bil interdisciplinarni. Zajema geokemijo, hidrologijo, statistiko ter modeliranje perkolacije, pretoka reke Save in toka podzemne vode. Pomembno je izpostaviti, da rezultati različnih metod uporabljenih v tej doktorski nalogi dajejo jasno sliko o hidrologiji na preučevanem območju. Le-ta je sedaj bolj razumljiva tako v prostoru, kot v času, ne le v preteklih letih ampak tudi v prihodnjih nekaj desetletjih. V prvi raziskavi je bil v dolgem časovnem nizu podatkov ugotovljen padajoči trend hranil v reki Savi. Izotopske vrednosti ($\delta^{15}N_{NO3}$ in $\delta^{18}O_{NO3}$) nakazujejo, da so glavni viri nitratov v reki Savi nitrifikacija v tleh ter odpadne vode in/ali gnojnica. Slednji vir je bil identificirani s sledenjem mikrobov. V drugi raziskavi je bil z uporabo različnih orodij razvit konceptualni model vodonosnega sistema na Ljubljanskem polju. $\delta^{18}O$ in $\delta^{2}H$ vrednosti nakazujejo na raznolik vpliv savske vode in lokalnih padavin na vodonosnik. S statističnimi analizami hidroloških in meteoroloških kronoloških podatkov, je bilo ugotovljeno, da je ta vpliv, ki je posledica spreminjajočega se pritiska v vodonosniku, mogoče zaznati v 24-ih urah v Jarškem produ, ali pa kakšen mesec pozneje v Klečah. Ocenjen je bil tudi kratki (do osem let) zadrževalni čas podzemne vode z uporabo ^{3}H in $^{3}H/^{3}He$ metod. Disertacija zajema prav tako izčrpno numerično modeliranje stacionarnega in ne-stacionarnega toka podzemne vode. V ta namen je bil uporabljen FEFLOW, kateri je bil povezan z MIKE 11 in WaSiM-om. Slednji dva simulirata tok reke Save in perkolacijo. Pozneje je to kompleksno orodje za modeliranje bilo uporabljeno za simulacijo podzemne in površinske vode v obdobju 2036–2065. Klimatski pogoji za to obdobje so bili projicirani s tremi regionalnimi klimatskimi modeli SMHI-RCA4, DMI-HIRHAM5, KNMI-RACMO22E in CLMcom-CCLM4-8-17, kateri pa so bili izbrani preko EURO-CORDEX iniciative. Rezultati kažejo, da Ljubljansko polje v obdobju 2036–2065 ne bo trpelo zaradi pomanjkanja vode.

Doktorska disertacija opisuje uporabo pomembnih orodij, ki nam omogočajo podrob-

nejše razumevanje vodnega kroga na Ljubljanskem polju ter deloma v porečju reke Save. Ta orodja so v prihodnosti lahko prav tako v pomoč pri sprejemanju ukrepov za zaščito vode in strategij za upravljanje z vodnimi viri.

Contents

List of Figures **xvii**

List of Tables **xix**

Abbreviations **xxi**

Symbols **xxiii**

1 Introduction **1**
1.1 Work Motivation . . . 1
1.2 Methods for Identification of Processes in the GW-SW System, Recharge Areas, Fluxes, and Aquifer Responsiveness . . . 4
1.2.1 An assessment of historical patterns in long-term water quality and quantity data with a combination of meteorological data . . . 4
1.2.1.1 Spatially and temporally distributed data in hydrology . . . 5
1.2.1.2 Trend analyses in water quality data . . . 6
1.2.1.2.1 Nitrogen. . . . 6
1.2.1.2.2 Phosphorus. . . . 7
1.2.2 Isotopes in hydrology . . . 8
1.2.2.1 Stable isotopes . . . 9
1.2.2.1.1 δ^{18}O and δ^{2}H in water. . . . 9
1.2.2.1.2 Stable isotopes of nitrogen and oxygen as tracers of pollution sources. . . . 12
1.2.2.2 Radioactive isotopes . . . 13
1.3 Groundwater Flow Model . . . 13
1.3.1 Conceptual model . . . 15
1.3.2 Numerical model . . . 16
1.3.2.1 Mesh discretization . . . 17
1.3.2.2 Groundwater flow equations . . . 19
1.3.2.3 Boundary conditions . . . 20
1.3.2.4 Parameters . . . 21
1.3.2.4.1 Material property parameters. . . . 21
1.3.2.4.2 Hydrologic parameters. . . . 21
1.3.2.5 Calibration . . . 21
1.3.3 Forecasting model . . . 24
1.4 Surface Water Model . . . 24
1.4.1 Percolation/Recharge . . . 24
1.4.2 River water . . . 26

2 Aims and Hypothesis **29**

3 Publications **31**

3.1 Nutrient Variations in the Sava River Basin 31
3.2 Determination of the Sources of Nitrate and the Microbiological Sources of Pollution in the Sava River Basin 41
3.3 The Study of the Interactions Between Groundwater and Sava River Water in the Ljubljansko Polje Aquifer System (Slovenia) 55
3.4 An Integrated Simulation Approach for Studying the Hydrology of the Ljubljansko Polje Aquifer in Slovenia 71

4 Forecasting Model **109**
4.1 Introduction 109
4.2 Methods 109
4.3 Results and Discussion 110
4.4 Conclusions 113

5 Conclusions **115**

Appendix A *R*-script: The WaSiM-FEFLOW Link **119**

References **121**

Bibliography **129**

Biography **133**

List of Figures

Figure 1.1: Processes relevant to surface and groundwater interaction. The soil root zone is between the land surface and the zero flux plane, where evapotranspiration (ET) is present. Recharge crosses the water table at the top of the saturated zone. The gradient in total head (dH/dz) changes direction at the zero flux plane (whereas pressure head is zero). Modified after Lin, Wang, and Valocchi (n.d.) and Anderson, Woessner, and Hunt (2015). 2
Figure 1.2: The figures illustrate possible interactions between river water and groundwater: (A) a gaining river, (B) a losing river in which river water percolates downward and laterally to the water table, and (C) a losing river where is the river "disconnected" or "detached" from the underlying aquifer. Modified after Alley, Reilly, and Franke (1999). . . 5
Figure 1.3: The Nitrogen cycle. Modified after SAHRA (2005a). 7
Figure 1.4: The phosphorus cycle. Modified after Shreeja (n.d.). 7
Figure 1.5: Progressive rainout as clouds move across a continent causes successive rainstorms to have increasingly lower δ^{18}O and δ^{2}H values (Hoefs, 1997; Coplen, Herczeg, & Barnes, 2000; SAHRA, 2005b). 10
Figure 1.6: Effects of hydrologic processes on δ^{18}O and δ^{2}H values of water (SAHRA, 2005b). 10
Figure 1.7: A general depiction of normal ranges of δ^{18}O and δ^{15}N values for dominant sources of nitrate, adapted from Kendall and McDonnell (1998). . 12
Figure 1.8: Types of models (Anderson, Woessner, & Hunt, 2015; Essink, 2000). . . 14
Figure 1.9: Groundwater modeling workflow. The workflow assumes that the objective of a model is forecast. Modified from Anderson, Woessner, and Hunt (2015). 15
Figure 1.10: (A) A plan view of a patch of elements around the node L in a FE mesh, and (B) a 3D view of the nodal basic function $N_L(x,y)$. Modified after Wang and Anderson (1982) and Cheng (1978). 18
Figure 1.11: Equilateral triangular elements around the pumping well - node i, surrounded by six neighbouring nodes, at the distance calculated by Eq. 1.10. Adapted from Diersch (2014). 18
Figure 1.12: WaSiM structure (Schulla, 2017). 25

Figure 4.1: Climate change pressure on the water balance of Mediterranean river basins (Gampe, Nikulin, & Ludwig, 2016). 109
Figure 4.2: Modeling framework. 110
Figure 4.3: Comparison of the simulated precipitation and observed precipitation, and simulated percolation. Precipitation and percolation are given in a range that includes results of all the three RCMs. 111

Figure 4.4: The Sava River discharge—observed over the period 2002–2014 and a range of water level simulated under conditions, which were projected with three RCMs. 111
Figure 4.5: Observed, simulated and projected hydraulic heads for groups 1, 2, and 3. Locations of the groups are shown in Section 3.4, Figure 3. 112
Figure 4.6: Locations where the Sava River water leaches into the aquifer and fluxes quantification for 2010, 2011 and 2036–2065. 113
Figure 4.7: Locations where groundwater flows into the Sava River channel and fluxes quantification for 2010, 2011 and 2036–2065. 113

List of Tables

Table 1.1: Common applications of isotopes (Kendall & Doctor, 2011). 8
Table 1.2: Methods for estimating recharge and discharge in an aquifer. Modified after NRC (2004), Scanlon, Healy, and Cook (2015), Anderson, Woessner, and Hunt (2015). 22

Table 4.1: Sums of local precipitation and percolation, and mean discharge over the period 2036–2065 in the Ljubljansko polje, as well as a sum of precipitation upstream of the Ljubljansko polje, in the Alps. 114

Abbreviations

1D	... one dimensional
2D	... two dimensional
3D	... three dimensional
AS	... absorption spectroscopy
BC	... boundary conditions
DFE	... discrete feature elements
DM	... dispersion model
EU	... European Union
ET	... evapotranspiration
FD	... finite-difference
FE	... finite-element
GES	... good ecological status
GMWL	... global meteoric water line
GW-SW system	... groundwater-surface water system
IRMS	... isotope ratio mass spectrometry
LAS	... laser AS
LAI	... leaf area index
LMWL	... local meteoric water line
LSC	... liquid scintillation counting
MAE	... mean absolute value
MDF	... mass dependent fractionation
ME	... mean error
MIF	... mass independent fractionation
MRT	... mean residence time
MS	... mass spectrometer
NS	... Nash-Sutcliffe
PEST	... perimeter estimation code
RBD	... river basin districts
RMSE	... root mean squere error
SRB	... the Sava River Basin
TC	... temperature conversion
TU	... tritium unit
WFD	... water framework directive

Symbols

^{14}C	...	carbon-14 (radiocarbon)
H_2O	...	water molecule
^{3}H	...	tritium
$^{3}H/^{3}He$	...	^{3}H and helium-3 ratio
N	...	nitrogen
NH_3	...	ammonia
NH_4^+	...	ammonium
NO_3^-	...	nitrate
NO_2^-	...	nitrite
P	...	phosphorus
PO_4^{3-}	...	phosphate
δ	...	delta, relative isotopic composition, value give in parts per thousand or "per mille" (‰)
$\delta^{15}N$	...	isotopic composition of nitrogen
$\delta^{15}N_{NO_3}$	...	isotopic composition of nitrogen in NO_3^-
$\delta^{18}O$	...	isotopic composition of oxygen
$\delta^{18}O_{H_2O}$	...	isotopic composition of oxygen in water
$\delta^{18}O_{NO_3}$	...	isotopic composition of oxygen in NO_3^-
$\Delta^{17}O$	...	isotopic composition of oxygen affected by MIF
$\delta^{2}H$	...	isotopic composition of hydrogen
$\delta^{2}H_{H_2O}$	...	isotopic composition of hydrogen in water

Chapter 1

Introduction

1.1 Work Motivation

Water on the Earth is extraordinary dynamic in space and time. It constantly moves on, above and below the land surface and it changes state from liquid to vapor and ice. In fact, all water bodies, either above or below the surface, are in constant natural interaction (Figure 1.1). These processes can happen in the blink of an eye or even over millions of years (USGS, 2017b). For all these reasons, the understanding of the water cycle is extremely complicated and therefore studies devoted to different hydrologic components were and still are too often separated, although the first encouragement for understanding water as a single system appeared in the 1960s (Tóth, 1999; Bouwer & Maddock, 1997; Sophocleous, 2002). Rorabaugh (1964) provided one of the first groundwater-river interactions studies. The processes between groundwater and surface water involve also the transport of chemicals and particles. Water is a solvent that dissolves a longer list of compounds than any other solvent. For this reason, understanding of surface water and groundwater as a single system (GW-SW system) is even a necessity when hydrological problems related to water hazard due to pollutants (e.g. by nitrates, metals, pharmaceuticals or other toxic substances), degradation of aquatic environments as well as effects of climate and land cover changes need to be solved (Winter, Harvey, Franke, & Alley, 1998). Studies related to the GW-SW system, which are face extremely challenging observable or measurable processes, have grown steadily over the last two to three decades (Fleckenstein, Krause, Hannah, & Boano, 2010). Since the 1990s, the SW-GW system has been even implemented in studies from different fields: hydrology, hydrogeology, ecology, biogeochemistry and environmental management (Krause, Hannah, & Fleckenstein, 2009).

Advanced understanding of the water cycle is indirectly also vital for better understanding of natural and artificial stressors that have an impact on water quality and quantity. For instance, a contamination of surface water, either from point (e.g. water treatment plant) or diffuse sources (e.g. leaching of pesticides from farmlands), affects also groundwater through the river-groundwater interface (Lapworth, Baran, Stuart, & Ward, 2012; Meals, Dressing, & Davenport, 2010). Groundwater pumping causes water dynamic changes in an aquifer and in a river. Consequently, even a relation between river water and an aquifer can be shifted from gaining to losing river or *vice versa*. Land use change is a "shock" for the water balance, because it causes changes of infiltration, evapotranspiration, runoff characteristics and sediments yield of the land surface. A wider view of the land use change issue leads to serious economic, social and environmental consequences for communities. Further, a modification of river channels, the purpose of which is usually flood control, is another stress not only on rivers, but also on the full GW-SW system (Boano, Camporeale, & Revelli, 2010). Climate change has profound effects on the water

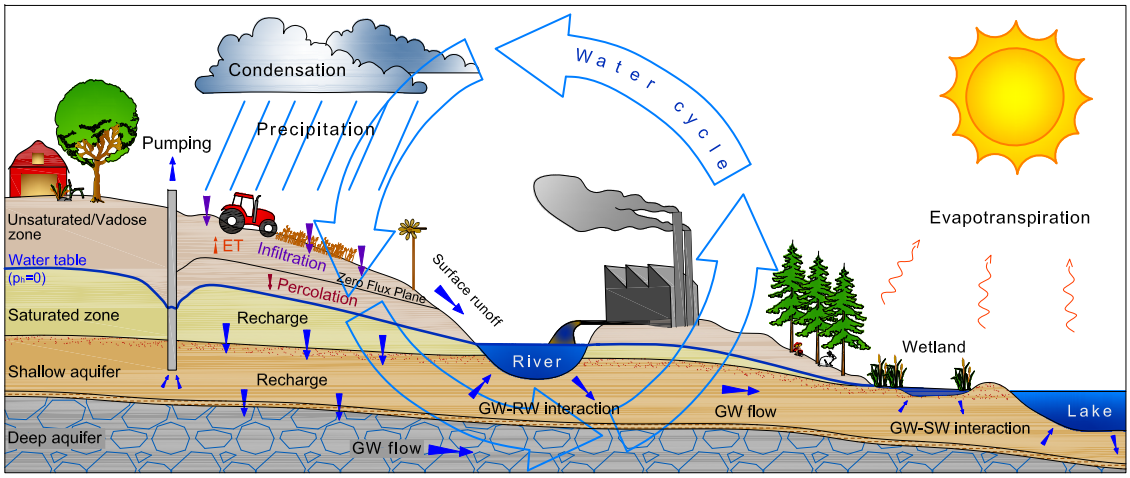


Figure 1.1: Processes relevant to surface and groundwater interaction. The soil root zone is between the land surface and the zero flux plane, where evapotranspiration (ET) is present. Recharge crosses the water table at the top of the saturated zone. The gradient in total head (dH/dz) changes direction at the zero flux plane (whereas pressure head is zero). Modified after Lin, Wang, and Valocchi (n.d.) and Anderson, Woessner, and Hunt (2015).

cycle. Its understanding is crucial also for the GW-SW system, since it has an impact on recharge, evapotranspiration, river flow and water use (Reid et al., 2009). Overall, all these stressors also have an impact on ecosystems, which are an important component of biological diversity (Poff & Zimmerman, 2009).

Interlinkages between groundwater and surface water bodies are also highly required for implementation of the European Union (EU) water policy, established in the Water Framework Directive (WFD) (published in the Official Journal – OJ L 327, see EUR-Lex (2000)) 18 years ago (EU-Commission, 2016; Krause et al., 2009). Its purpose is the introduction of remedial measures in case of deterioration of chemical and quantity status in water bodies (rivers, lakes, coastal waters and groundwater) (EU-Commission, 2016). The EU "measures" the quality of water bodies with a good ecological status (GES) index. The GES is defined as a slight variation from undisturbed conditions, from qualitative and quantitative water resource aspects. Parameters that make up ecological status include biological parameters (fish, macro-invertebrates, macrophytes and diatoms) and supporting chemical parameters (ammonia, phosphates, dissolved oxygen and 18 pollutants including some heavy metals and pesticides) (ECRR, 2014). Although more and more water bodies have the GES status, the percentage was 43% in 2009 and 10% more in 2015, the reality is still far away from the desired goals (EEA, 2016).

The motivation for this dissertation was inspired by the above-described activities in Europe and the fact that despite progress has been made in understanding the processes in the GW-SW system, knowledge remains incomplete (Fleckenstein et al., 2010). Since groundwater is the dominant source of drinking water in Europe, it is believed that there is an urgent need for better understanding of groundwater systems, in regards to identifying groundwater sources and infiltration areas, groundwater dynamics and vulnerability to contamination from industrial and agricultural activities, and to assure its sustainable development for future generations. Moreover, this research is complementary to the activities performed within the ongoing EU project GLOBAQUA (Managing the effects of multiple stressors on aquatic ecosystems under water scarcity). The main focus of

this dissertation was to understand the interaction between groundwater in an alluvial aquifer with intergranular porosity of the Ljubljansko polje aquifer, Slovenia and its main sources—local precipitation/the Sava River water. Groundwater in the Ljubljansko polje aquifer system is the main drinking water supply for Ljubljana and its surroundings. Since the Sava River water is the dominant groundwater source in this region, it is important to understand the development of its quality in the past. Therefore, the PhD also covers an investigation of annual and seasonal variations of nutrients (N and P), their temporal patterns and relationship with the Sava River discharge. In fact, due to its natural diversity the Sava River Basin (SRB) represents an excellent place for investigating both natural and anthropogenic sources of nutrients.

The SRB belongs to the second-largest basin in Europe—the Danube basin, where many activities related to the WFD have been already performed. Even though not all the Balkan countries are EU members yet, they are aware of the importance of WFD not only for humans but also for all living creatures, especially those living in water. For this reason, they also follow the European Union's environmental guidelines as much as they can. In fact, the EU has also an interest in implementing EU environmental policy in non-EU member countries, due to the water cycle complexity, which does not respect national borders. For sustainable management of water supply, agriculture, flood-drought cycles and ecosystems, as well as human health more efficient collaboration should be established among all five countries through which the Sava River channel runs. This suggestion may improve scientific understanding of water cycle processes in the SRB as a single system, for successful identification and prediction of natural (e.g. climate change, floods, etc.) and anthropogenic (e.g. industrial and agricultural activities, impacts from large cities, waste water treatment plants) impacts on sustainable development of surface and groundwater resources.

A theoretical background of available methods for identification and quantification of processes in the GW-SW system is briefly presented in the following subchapters with special attention to methods and approaches that were used in the proposed PhD thesis:

- In the Section 1.2 methods for identification of processes in the GW-SW system, determination of recharge areas, quantification of the fluxes, and aquifer responsiveness are described. The section includes analyses of historical patterns in long-term water quality and quantity data supported by meteorological data, as well as isotopes used to assess groundwater pollution and water sources and water mean residence time.
- Sections 1.3 and 1.4 describe processes of numerical modeling of groundwater and surface water flow.

Chapters 2 and 3 present the aims and objectives of the PhD dissertation, and the four relevant scientific publications, respectively. The first publication shows patterns of nutrients concentrations (N and P) over a long period in the SRB, while determination of nitrate sources is described in the second publication. In the third publication an impact of the main water sources, the Sava River and local precipitation, on groundwater over the study domain Ljubljansko polje is quantified. The last section in this chapter, which has been submitted for publication, describes a detailed overview of the hydrological modeling of the Ljubljansko polje aquifer system and its results. An example of the model application—forecasting model is presented in Chapter 4. Chapter 5 presents the conclusions of the dissertation and future work inspired by this dissertation.

1.2 Methods for Identification of Processes in the GW-SW System, Recharge Areas, Fluxes, and Aquifer Responsiveness

Methods for studying surface-groundwater interactions have to be selected carefully according to the purpose of the study. Among the common issues of such studies are the determination of water exchange locations, flow direction, quantification of fluxes or identification of temporal variation in groundwater or surface water flow. The selected method has to be also appropriate to achieve the required spatial and temporal resolution and physical and hydraulic conditions in a research domain (Rosenberry & LaBaugh, 2008; Kalbus, Reinstorf, & Schirmer, 2006). Many of the available methods are based on direct measurements of electrical, thermal, physical or (geo)chemical properties of surface water and groundwater (USGS, 2017a; Rosenberry & LaBaugh, 2008). Integrating *in situ* measurements in studies at various scales, however, remains a challenge that has not yet been completely solved. Characterising processes in the GW-SW system, with direct measurements is especially difficult due to geological, hydrological and biogeochemical heterogeneity (McLachlan, Chambers, Uhlemann, & Binley, 2017). For this reason, hydrologists are striving to develop or improve tools that are capable of handling environmental heterogeneity in space and time, such as geophysics (McLachlan et al., 2017), remote sensing (Patra, Adhikari, & Kunar, 2016), modern automated temperature sensors (Irvine, Briggs, Lautz, Ryan P. Gordon, & Cartwright, 2016), etc. These tools are capable of providing a large set of comprehensive input data for numerical models, which in many cases can only be handled by high-performance computing. Computation gets significantly longer with a larger modeling domain, rich scale or longer simulation period with high temporal resolution in transient state models. It seems that hydrological studies have slowly drifted away from lumped models, where a hydrologic system is treated as a black box, over semi-distributed to fully distributed models, where more information inside the simulated water system is available (Brunner, Therrien, Renard, Simmons, & Franss, 2017). Nevertheless, due to many possible sources of uncertainty, it is strongly recommended to use an interdisciplinary approach for studying GW-SW systems (Rosenberry & LaBaugh, 2008).

The presented PhD thesis deals with only one relatively small basin in the SRB, which is not larger than 71 km^2 and where it is still possible to successfully handle natural heterogeneity with the observed data. The Ljubljansko polje has a long history of recording hydrological and meteorological data. The next subsection describes why these data are so appreciated in most environmental studies and how we can use them. The methods are applicable for all kind of open channels, although "river" is used in the text. While most of the hydrological data were obtain only for the Ljubljansko polje aquifer, the quality of water, related to nutrients, mainly nitrogen (N) and phosphorous (P), was evaluated for the whole SRB from its source to its confluence with the Danube River.

1.2.1 An assessment of historical patterns in long-term water quality and quantity data with a combination of meteorological data

Observations of surface water levels in rivers and hydraulic heads in an aquifer give crucial information about hydrology in a study domain. Observed hydraulic heads in a piezometers' network indicate groundwater gradients that show groundwater flow direction and roughly also its velocity. Further, a comparison of observed surface water levels and adjacent hydraulic heads can be used for an identification of the direction and rate of water fluxes between water bodies on and below the land surface (Figure 1.2). If the surface

water level is higher than adjacent hydraulic heads, the direction of leaching is from a river to an aquifer and *vice versa* (Rosenberry & LaBaugh, 2008). When the hydraulic head drops below the river bed sediments, the river gets disconnected from the aquifer and river water starts to percolate into the aquifer. Another way to determine losing or gaining river characteristics is by a "seepage run" method (Harvey & Wagner, 2000). The method is based on the measurements of a surface water flow at the endpoints of a river reach. Increasing discharge over the river reach indicates gaining reach and *vice versa*. However, before any conclusions are made with this method, it has to be ensure that over the channel reach water is not lost or gained due to any other processes, for instance irrigation, released industrial water, groundwater pumping, etc. (Rosenberry & LaBaugh, 2008). Nevertheless, due to the dynamic water cycle, the rate of leaching as well as its direction varies over time scales of hours, days, months or seasons. The reverse leaching direction may be only temporary during a flood, for example. For this reason, records of hydrological parameters over longer periods (time series) are highly valued in hydrological studies. Measurements at specified time intervals are usually recorded with data loggers (Rosenberry & LaBaugh, 2008).

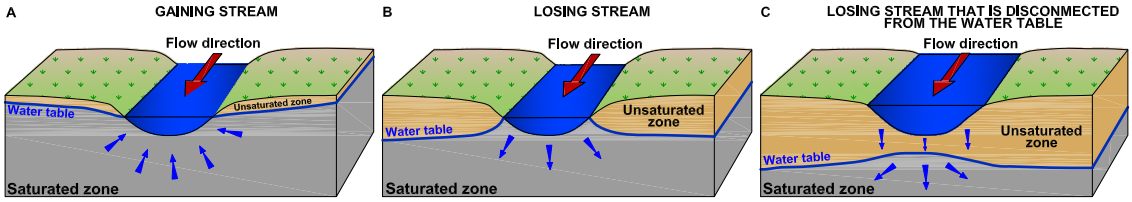


Figure 1.2: The figures illustrate possible interactions between river water and groundwater: (A) a gaining river, (B) a losing river in which river water percolates downward and laterally to the water table, and (C) a losing river where is the river "disconnected" or "detached" from the underlying aquifer. Modified after Alley, Reilly, and Franke (1999).

1.2.1.1 Spatially and temporally distributed data in hydrology

Time and space series analyses are investigations of a temporally/spatially distributed sequence of data wherein time/location is an independent variable. Most of the time series analyses can equally be applied to spatial data series and thus, the following explanation of time series does not refer only to the temporal but also to the spatial data series (Shahin, Oorschot, & Lange, 1993).

Time series have many different applications, therefore they became a major tool in hydrology. Due to fast increasing processing power in the era of digitalization and computers, time series are not used only for basic statistical analyses, but also for simulations, which are capable of generating synthetic hydrologic data. These simulations are applicable for forecasting hydrologic events, identifying trends and shifts in hydrologic data, filling in missing observations, and extending short hydrologic records (Salas, 1993; Machiwal & Jha, 2012). Increasing global interest in scientific understanding of climate change has even been enhanced using time series.

Time series consist of a systematic patterns/trends and random noises/errors, which have to be separated during data pre-processing. Time series without the noise better describe hydrology in a study domain, because the random noise makes the trend difficult to be identified in time series (Hameed, Mariño, DeVries, & Tracy, 1997; Machiwal & Jha, 2012). The random noise can be identified with a comparison of hydrological parameter with other hydrological or even meteorological parameters (Machiwal & Jha, 2012). An

example of the separation with the moving-average method is described in Section 3.3. A time series has a trend if a significant correlation between an observed parameter and time is observed. The trend is defined as an unidirectional and gradual change (falling or rising) in the mean value of a parameter (Shahin et al., 1993). The trend may be interrupted or shifted due to unusual natural events or stressors (e.g. flood, climate change, the beginning or termination of groundwater pumping), human activities, changes in measurement methods at a monitoring site, or by moving the monitoring site even a short distance away (Haan, 2002; Salas, 1993; Machiwal & Jha, 2012).

1.2.1.2 Trend analyses in water quality data

A balanced overview of how a river has been influenced by pollutants, particularly in relation to land use, can be obtained by an assessment of historical patterns of change and trend analysis using existing water quality data. Our research was focused on nutrients, mainly on the nitrogen (N) and phosphorous (P), since the lower part of the SRB is induced by agriculture and untreated waste water discharges. Nutrient enrichment or eutrophication is one of the important water quality issues limiting present and future uses of water resources. Both N and P play a key role for plant growth, since they are the main components of many molecules, including DNA (SCI, 2013; Adu-Gyamfi, 2013). In fact, human activities have already enhanced global cycles of N and P, on average 100% and 400%, respectively (Falkowski et al., 2000). Nutrient loads affect soil and water through both point and diffuse pathways, where their transportation is strongly connected to hydrology, as well as to transformation, retention, and elimination. Concentrations of nutrients and fluxes can vary significantly at different sections of a river channel in a manner related to short-term variations in hydrology and long-term changes of land use (Billen et al., 2007). Nevertheless, the ecological state of aquatic systems is often only temporary and limited to the present situation.

1.2.1.2.1 Nitrogen. N is the fourth most abundant element on the Earth, but nitrate (NO_3^-) is the only N-molecule with the ability to be dissolved in water (Stein & Klotz, 2016). The real N cycle is however a very complex system (Figure 1.3). Since N exists in many different forms, including organic and inorganic forms, it undergoes many different transformations in the ecosystem, from one to another form (Bernhard, 2010).

After over 100 years of the nitrogen cycle research, its explanation consists of five accepted nitrogen-transformation processes (Figure 1.3): (1) ammonification, including nitrogen fixation, and assimilatory and dissimilatory reduction of NO_3^-; (2) nitrification; (3) denitrification, including canonical, nitrifier-dependent and methaneoxidation-dependent denitrification; (4) anammox, as a form of coupled nitrification–denitrification; and (5) nitrite-nitrate interconversion (Stein & Klotz, 2016). The process when organisms release inorganic N back into the ecosystem as ammonia (NH_3), which later becomes available for uptake by plants and other microorganisms for growth, is known as **ammonification**. The process of converting N_2 into biologically available N is called nitrogen fixation. Mostly this process is carried out by prokaryotes (unicellular organisms). **Nitrification** is the process that converts ammonia (NH_3) to nitrite (NO_2^-) and then to NO_3^-. Nitrification occurs aerobically most of the time and is carried out by prokaryote. **Denitrification** is the process that converts NO_3^- to N_2, thus denitrification removes bioavailable N from soil and returns it to the atmosphere. **Anammox** or anaerobic ammonia oxidation is the process that oxidises NH_4^+ by using NO_2^- to gaseous N_2 under anoxic conditions (Bernhard, 2010).

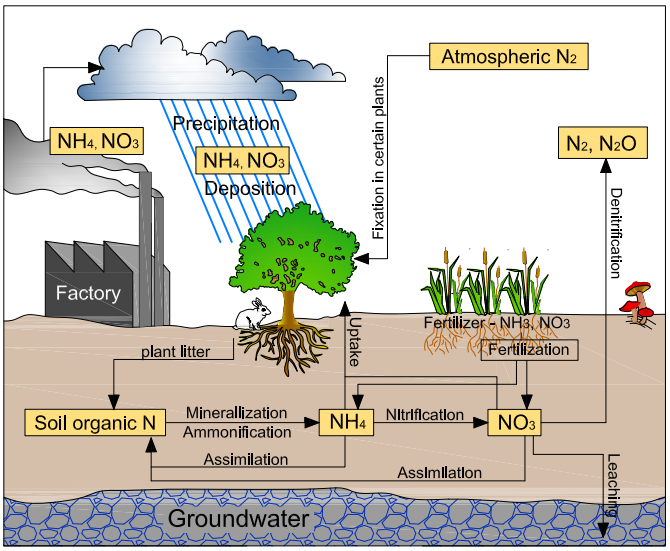


Figure 1.3: The Nitrogen cycle. Modified after SAHRA (2005a).

1.2.1.2.2 Phosphorus. P is present in the environment as inorganic and organic P, but phosphate (PO_4^{-3}) ions prevails (Figure 1.4). Rock weathering is an important source of inorganic P in soil. P may be lost from soil through leaching and water run-off. An excess PO_4^{-3} causes excessive growth of plants in surface water bodies (rivers, lakes, etc.) leading to eutrophication. Plants take up inorganic PO_4^{-3} from soil, which returns to the soil as organic P, when plants or animals, which consumed the plants, die or with manure. The mineralisation process transforms organic P back to inorganic forms of phosphorous in soil (SCI, 2013).

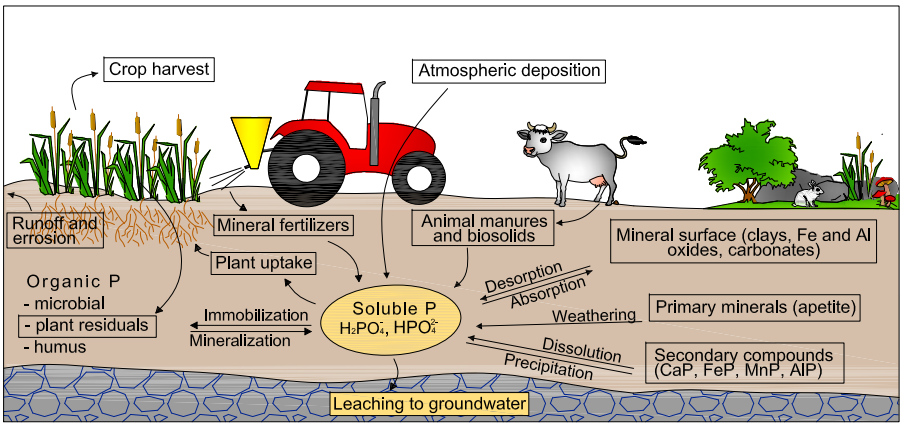


Figure 1.4: The phosphorus cycle. Modified after Shreeja (n.d.).

Detection of temporal trends is one of the most important objectives of environmental monitoring, in our case describing PO_4^{-3} and NO_3^- data. Trend analyses indicate whether concentrations of pollutants increase or decrease over time. In addition, an estimate of the trend's magnitude can help to determine whether a statistically significant trend is of practical concern. A noise in observed data adds uncertainty in detecting possible trends, which may be minimized with statistics. Additional difficulties in trend analyses of pollutants appear due to their specific characteristics: seasonality, skewness, serial correlation,

nonnormal data, "less-than" (censored) values, outliers and missing values (Hirsch, Slack, & Smith, 1982; Hirsch & Slack, 1984). Therefore, special statistical methods have been developed to deal with these different natures of data. Many different statistical approaches are currently available for detecting and estimating trends that may be present in water quality variables of interest. These approaches range from simple correlation and regression analyses, time-series analyses, and methods based on non-parametric statistics. In Section 3.1 the Weighted Regression on Time, Discharge, and Season (WRTDS) method is described, which was applied for analysing the long-term water quality data in the SRB. The method considers a concentration to be a product of three deterministic components (trend, season, and discharge) and one random component and it was proposed by Hirsch, Moyer, and Archfield (2010).

1.2.2 Isotopes in hydrology

A development of hydrogeochemistry, which uses fingerprints in water—environmental isotopes for different studies, goes back to the early 1960s. The main idea behind this method is to trace changes of neutrons number in an atom of water that is changing due to global water cycle, while the number of protons and electrons stays the same. Isotopes, both stable and radioactive of mainly light elements, are used for a wide range of applications nowadays, as presented in the Table 1.1. Nevertheless, the most widely used in hydrological studies are environmental isotopes of oxygen (δ^{16}O, δ^{17}O, δ^{18}O), hydrogen (δ^{1}H, δ^{2}H, ^{3}H) and nitrogen (δ^{14}N, δ^{15}N). Isotopes may be either part of the water molecule (H_2O) or other molecules dissolved in water (Table 1.1). All mentioned isotopes are stable isotopes of respective elements, while ^{3}H is radioactive.

Table 1.1: Common applications of isotopes (Kendall & Doctor, 2011).

Stable isotope	Substance	Applications
δ^{18}O, δ^{2}H	H_2O	Origin of water Identification of recharge areas Hydraulic connections, aquifer leakage Identification of paleowaters Interconnection with surface waters Salinization mechanisms Recycling of irrigation water Geothermal activity
δ^{15}N,δ^{18}O	NO_3, NH_4, N_2	Origin of nitrates Sources of pollution Microbial denitrification processes
Radioactive isotope	**Half-life (years)**	**Applications**
^{3}H	12.32	Identification of recent groundwater Water transport in the unsaturated zone

Stable isotopes are typically measured with a mass spectrometer (MS), or an absorption spectrometer (AS). The mass spectrometer, particularly the isotope ratio mass spectrometer (IRMS), gives characteristic series of peaks with different intensities, which give information about abundances of light stable isotopes in a sample (Morgan, 2013). The AS, particularly the laser AS (LAS), is based on absorption properties of an absorbent (analyte). Light with a frequency close to a transition frequency of the isotope under investigation is sent through a sample. The amount of absorbed light is related to the concentration of a stable isotope in the sample (Schmidt, 2007). Especially the LAS represents an important step forward towards stable isotope measurements in water. Its

biggest advantages are the conceptual simplicity and the absence of chemical sample pretreatments, which is a necessity for the traditional IRMS method. With this equipment is possible to obtain more data, which can be used in modeling approaches.

^{3}H and its daughter ^{3}He measurements are performed with liquid scintillation counting (LSC) and mass spectrometry (MS), respectively. The LSC analytic technique is based on a conversion of kinetic energy of the ^{3}H into light energy, while He analysis can be performed using a Magnetic Sector-Field mass spectrometer, with a high level of precision.

1.2.2.1 Stable isotopes

Stable isotopes in hydrological studies are conventionally expressed in per mil (‰) deviations from those of a standard using notation (Craig, 1957):

$$\delta(‰) = \left(\frac{R_{sample}}{R_{standard}} - 1\right) \cdot 10^{3} \tag{1.1}$$

R_{sample} and $R_{standard}$ are ratios (^{2}H/^{1}H, ^{18}O/^{16}O, ^{15}N/^{14}N) of a heavy isotope to a light isotope in a sample or in an international standard, respectively. The standard values are near average values of the individual isotope in nature (Engel & Macko, 1993), and are defined as δ. A positive/negative δ-value means that the isotopic ratio of the sample is higher/lower than that of the standard. For hydrogen and oxygen, the V-SMOW standard (Vienna Standard Mean Ocean Water) is used, while for nitrogen the Atmospheric Air standard is used (Craig, 1961; Kendall & Doctor, 2011).

A process that causes changes of δ-values in a substance is called fractionation, which can be mass dependent (MDF) or mass independent (MIF). MIF is mostly present in photochemical reactions in the stratosphere. It is a relatively new research tool, and therefore not so often used in hydrological studies so far (EU-Commission, 2015). MDF is partitioning of isotopes by physical or chemical processes and is proportional to differences in their masses (Sidle, 1998). According to a process that causes decomposition of binding energies in molecules, MDF may be separated into two types (Mook, 2001; Kendall & Doctor, 2011; Kendall & McDonnell, 1998): (1) kinetic fractionation happens during irreversible kinetic reactions in a system out of chemical and isotopic equilibrium. The lower the humidity and/or temperature, the greater the kinetic fractionation associated with the phase that can be expected. Lighter molecules react faster than heavier, therefore products are enriched with lighter isotopes compared to reactants; (2) equilibrium fractionation is a function of temperature. It happens during reversible thermodynamic reactions, when the redistribution of isotopes of an element along various species of compounds in a closed, well-mixed system at chemical equilibrium occurs. In this case, chemical compositions of reactants and products do not change.

1.2.2.1.1 δ^{18}O and δ^{2}H in water. Natural effects that trigger mass dependent fractionation for δ^{18}O and δ^{2}H are: latitudinal effect (lower δ-values at increasing latitude); continental effect (more negative δ-values for precipitation that occurs more inland (Figure 1.5); altitude effect (decreasing δ-values in precipitation at higher altitude); seasonal effect (in regions with temperate climate δ-values are more negative during winter); precipitation amount effect (more negative δ-values in rain during heavy storms) (Kendall & Doctor, 2011; Mook, 2001).

Craig (1961) discovered a linear relation between δ^{18}O and δ^{2}H values in precipitation, which also exist after fractionation (Figure 1.6). Based on this finding, he defined the so-called Global Meteoric Water Line (GMWL), $\delta^{2}H = 8 \cdot \delta^{18}O + 10$. Due to more available data over the years, the GMWL was upgraded into the more precise Local Meteoric

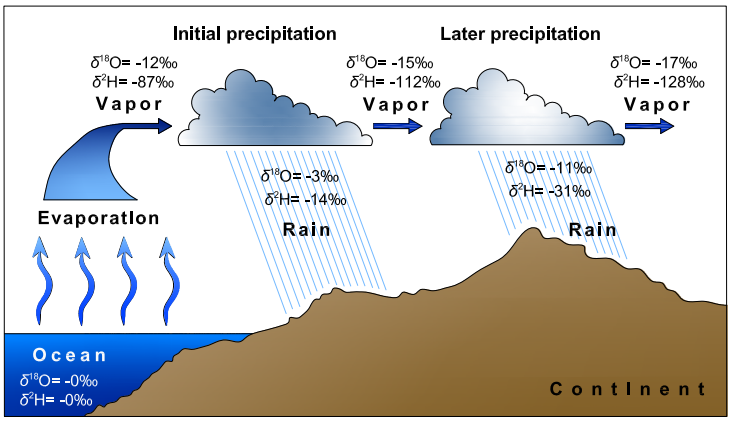


Figure 1.5: Progressive rainout as clouds move across a continent causes successive rainstorms to have increasingly lower δ^{18}O and δ^{2}H values (Hoefs, 1997; Coplen, Herczeg, & Barnes, 2000; SAHRA, 2005b).

Water Line (LMWL), $\delta^2 H = (8.07 \pm 0.02) \cdot \delta^{18}O + (9.9 \pm 0.01)$ (Kendall & McDonnell, 1998). The LMWL was implemented to specific locations around the world. The $\delta^2 H = (8.06 \pm 0.08) \cdot \delta^{18}O + (9.84 \pm 0.71)$ was developed for Ljubljana by Vreča, Bronić, Leis, and Demšar (2014).

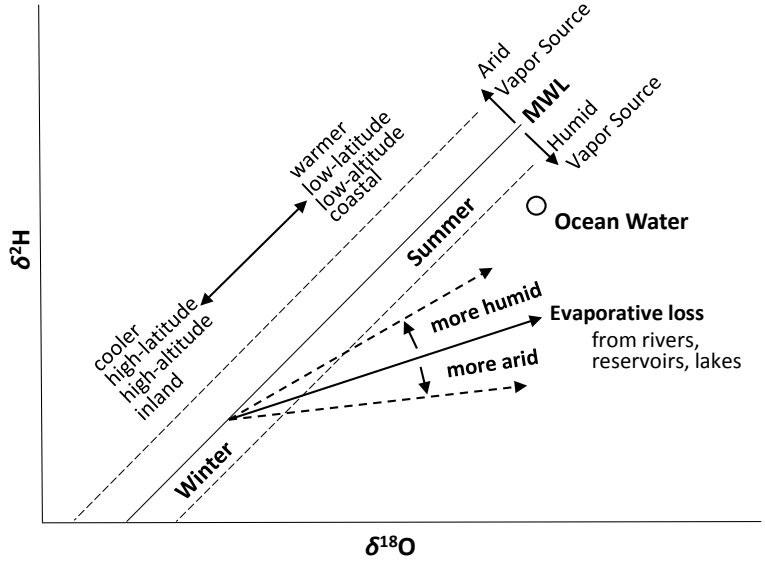


Figure 1.6: Effects of hydrologic processes on δ^{18}O and δ^{2}H values of water (SAHRA, 2005b).

The δ^{18}O and δ^{2}H correlation differ locally due to different climate and geographic influences; for this reason Dansgaard (1964) defined a difference between the GMWL and the LMWL with a deuterium excess (d-excess): $d = \delta^2 H - 8 \cdot \delta^{18}O$. The d-excess can be used as an identifier of precipitation origins or air masses, because precipitations in cooler and more humid conditions have lower d-excess value than precipitation in warmer conditions (Figure 1.6) (Kendall & Doctor, 2011). This is the reason why δ^{18}O and δ^{2}H can be used also as fingerprints of groundwater sources.

From rain water to groundwater. Percolated water through the unsaturated zone often resembles a piston flow. It means that any given water in front of the "new" water in the unsaturated zone would be pushed uniformly downwards to the aquifer. The pushed water has the same velocity and negligible dispersion and mixing. These ideal conditions enable recharge water to preserve the isotopic and chemical characteristics of precipitation. The same logic can be used for understanding transportation of tracers. The simplistic demonstration of the processes, from infiltration over percolation to recharge (Figure 1.1), with the piston flow assumes that fractionation does not occur in the unsaturated zone. There are, however, processes that have an indirect effect on the isotopic composition of water in the unsaturated zone. Nevertheless, effects of variations in rainwater chemistry, dry deposition, seasonal variations in infiltration, etc. on the groundwater chemistry can still be identified (Appelo & Postma, 2004). While δ^{18}O and δ^{2}H values of shallow groundwater reflect the mean isotopic composition of local precipitation, the δ^{18}O and δ^{2}H values of deep groundwater reflect past climatic conditions under which the recharge took place (Gat & Tzur, 1967; Kendall & Doctor, 2011; Kendall & McDonnell, 1998).

River water has a different isotopic composition to local precipitation, when rivers carry water that is derived from precipitation at a higher altitude and is therefore depleted in heavy isotopes (Figure 1.5). This is why it is possible to use stable isotopes as fingerprints of the two main groundwater sources in alluvial aquifers—river water and local precipitation. With the two-component mixing model a fraction of local precipitation versus river water in groundwater can even be calculated. The contribution of both sources can be estimated using the following equations:

$$\delta^{18}O_{GW} = f_{RW} \cdot \delta^{18}O_{RW} + f_P \cdot \delta^{18}O_P \tag{1.2}$$

$$1 = f_{RW} + f_P \tag{1.3}$$

where f_{RW} and f_P are respective river water and precipitation fractions, while $\delta^{18}\mathrm{O_{GW}}$, $\delta^{18}\mathrm{O_{RW}}$, and $\delta^{18}\mathrm{O_P}$ are the isotopic compositions of oxygen in groundwater, river water and precipitation, respectively.

Furthermore, the pulse of isotopically depleted water can be used to predict a minimum travel time, required for river water and dissolved pollutants to reach groundwater, or even for a prediction of a groundwater transit time. The later application can be done with a lumped dispersion model (Stichler, Maloszewski, & Moser, 1986; Kendall & McDonnell, 1998). Several flow models are used in the tracer studies: the piston flow model, exponential model, gamma model and the dispersion model (DM) that assumes a tracer transport which is controlled by advection and dispersion processes and was also used in our study. The g(τ) function is then defined as follows (Maloszewski & Zuber, 1982):

$$g(\tau) = \frac{1}{\tau\sqrt{4\pi(P_D)\tau/\tau_m}} exp\left[-\frac{(1-\frac{\tau}{\tau_m})^2}{4(P_D)\tau/\tau_m}\right] \tag{1.4}$$

where τ_m is the mean transit time of water, while P_D is the dimensionless dispersion parameter, which describes the variance of the distribution. In the case of bank filtration it can, in large approximation, be defined as:

$$P_D = \frac{\alpha_L}{x} \tag{1.5}$$

where α_L is dispersivity (m), and x is the mean distance between input and output locations (m).

The relationship between the input, $C_{RW}(t)$, and the output, $C_{GW}(t)$, concentrations is given by the convolution integral, which for non-decaying tracers is defined as follows:

$$C_{GW}(t) = f_{RW} \int_0^t C_{RW}(t-\tau) g(\tau) d\tau \tag{1.6}$$

where τ is the transit time of a single tracer particle between input and output and f_{RW} is a fraction of river water in a pumping well.

1.2.2.1.2 Stable isotopes of nitrogen and oxygen as tracers of pollution sources. Isotope techniques also constitute a promising tool for determining sources of nitrate (NO_3^-) in surface water and could help to identify the processes that NO_3^- has undergone in the aquatic system. This is possible because the isotopic signature in NO_3^- from fertilizer, atmospheric, soil and manure derived sources differs sufficiently to enable an unambiguous distinction to be made between them (Hebert & Wassenaar, 2001; Chang, Kendall, Silva, Battaglin, & Campbell, 2002; Mayer et al., 2002; Voss1 et al., 2006). However, the origin of NO_3^- must be linked to the entire N cycle, since values of $\delta^{15}N$ of NO_3^- can be biased due to the mixing of different NO_3^- sources or to isotope fractionation occurring during various processes (nitrification, denitrification, assimilation, remineralization) (Kendall, Elliott, & Wankel, 2008). The dual isotope approach, based on the determination of $\delta^{15}N$ and $\delta^{18}O$ values of NO_3^-, provides more conclusive information for tracing sources of NO_3^- in water (Widory et al., 2004; Seiler, 2005; Xue et al., 2009) and was also the subject of our research performed in the SRB. The dual isotope approach has three main potential benefits (Fenech, Rock, Nolan, Tobin, & Morrissey, 2012):

1. Tracking of some NO_3^- sources is more effective with $\delta^{18}O$, others with $\delta^{15}N$. However, to trace NO_3^- sources, when the spread of $\delta^{18}O$ is between -10 and +80% and of $\delta^{15}N$ between -10 and +35%, is effective only by using both isotopes;
2. Some nitrate sources that are presently indistinguishable with $\delta^{15}N$ alone (e.g. fertilizer vs soil NO_3^-, or atmospheric vs soil NO_3^-) may be identified, once $\delta^{18}O$ values are incorporated;
3. $\delta^{15}N$ compositions of NO_3^- vary systematically with $\delta^{15}N$ compositions during denitrification. Thus, in systems where dominant sources of NO_3^- are isotopically distinctive, source contributions can (in theory) be determined despite significant denitrification.

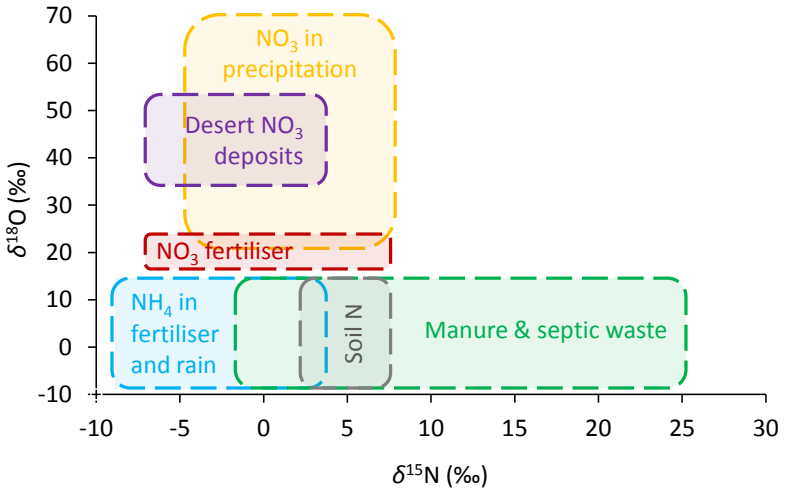


Figure 1.7: A general depiction of normal ranges of $\delta^{18}O$ and $\delta^{15}N$ values for dominant sources of nitrate, adapted from Kendall and McDonnell (1998).

A promising new technique based on MIF employs Δ^{17}O as a conservative tracer of atmospheric NO_3^- to better constrain its proportion in soils and groundwater. In most biogeochemical processes the fractionate isotopes δ^{17}O is directly related to δ^{18}O by a factor of 0.52. In contrast, the photochemical production of NO_3^- in the atmosphere has an excess ^{17}O based on what is expected from the δ^{18}O value and in the δ^{17}O signature this excess is designed as Δ^{17}O ($\Delta^{17}O = \delta^{17}O - 0.52 \cdot \delta^{18}O$).

1.2.2.2 Radioactive isotopes

The history of using ^{3}H in hydrology goes back to the 1950s and early 1960s, when a large amount of ^{3}H was released into the atmosphere due to thermonuclear bomb testing. The idea behind the method is a comparison of measured ^{3}H concentrations in water samples with ^{3}H concentrations in precipitation from the worldwide database of ^{3}H in precipitation collected by the International Atomic Energy Agency (IAEA) (EAWAG, 2018). The ^{3}H concentrations are expressed as a tritium unit (TU), where one TU represents one tritium atom per 10^{18} hydrogen atoms (Kazemi, Lehr, & Perrochet, 2006). Usability of the ^{3}H method is decreasing over time due to the loss of the high ^{3}H signal in water. The half-life of ^{3}H is 12.43 years. In hydrological studies, an electrolytic enrichment of ^{3}H is often carried out prior to analysis with liquid scintillation or proportional counters. ^{3}H in precipitation is estimated to be above 2 to 5 TU.

However, the combined measurement of ^{3}H and its decay product He (^{3}He) still provides a powerful tool for estimating groundwater residence time, recharge rate and for characterizing flow and dispersion regimes in shallow aquifers. The mean residence time (MRT), which is based on the ^{3}H/^{3}He method can be determine using the following equation (Solomon & Cook, 2000):

$$t = \lambda^{-1} ln \left(\frac{[^3He^*]}{^3H} + 1 \right) \tag{1.7}$$

where λ is the ^{3}H decay constant of 0.0556 y^{-1}, [^{3}H] is the measured ^{3}H activity and [^{3}He*] is the tritiogenic ^{3}He concentration defined as the amount of the total ^{3}He produced by the ^{3}H decay. The total amount of ^{3}He in groundwater can be expressed as:

$$^3He_{tot} = ^3He_{atm} + ^3He^* + ^3He_{nuc} + ^3He_{man} \tag{1.8}$$

where subscripts *atm*, *nuc* and *man* refer to He of the atmospheric origin and He that is produced by nuclear reactions in the subsurface, and He of the mantle origin, respectively (Solomon and Cook, 2000). Because it is difficult to separate $^3\text{He}_{\text{nuc}}$ from $^3\text{He}_{\text{man}}$, they are often lumped together and simply referred to as $^3\text{He}_{\text{terr}}$ (terrigenic ^{3}He). The determination of $^3\text{He}_{\text{terr}}$ requires additional measurements of neon and ^{4}He in the sample.

The first groundwater study related to the ^{3}H/^{3}He method was published by Takaoka and Mizutani (1987). It should be also noted that ^{3}H and ^{3}H/^{3}He methods can be successfully applied only to studies that include water in which MRT does not exceed 54 years (Kazemi et al., 2006).

1.3 Groundwater Flow Model

The content of this section is to a great extent adapted from Anderson, Woessner, and Hunt (2015).

Physical and mathematical models simplify complex nature to a level that we are capable of describing and understanding. The presented PhD thesis deals with the process-based deterministic model, while other types of models are presented in Figure 1.8. The process-based mathematical groundwater flow model describes physical processes within a model domain with governing equations, where fluxes between model domain and surroundings are defined with boundary conditions, and initial hydraulic head of a transient simulation is defined with initial conditions.

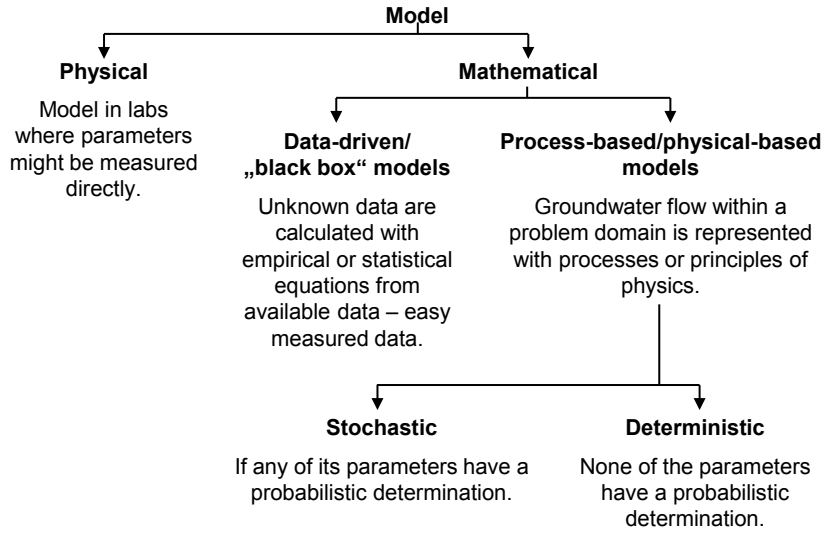


Figure 1.8: Types of models (Anderson, Woessner, & Hunt, 2015; Essink, 2000).

Groundwater flow modelers follow standard modeling steps, which are specific for different purposes. A modeling purpose defines adequacy of simplification of the modeling domain, required complexity of the conceptual model, characteristics of the mathematical model from which data have to be collected, modeling code, and physical framework design. For this reason, the purpose of modeling, like forecasting or interpretation of hydrological processes in the present or past, or looking for a solution to an engineering question, has to be clear at the very first stage of the modeling procedure. In addition, time and money constraints are important drivers of these decisions. In this section, the procedure for groundwater flow modeling, which was used in this PhD thesis, is described and presented in Figure 1.9.

A validation is excluded from the modern groundwater modeling work-flow, since modelers claim that the truth of modeling processes in the natural world is usually unknown, therefore they cannot be verified as, for instance, in laboratory experiments. Groundwater flow modelers have even noticed that people who are not experienced in modeling, do not understand the meaning of a validated model. This means that a validated model is capable of making absolute accurate forecasts, which is incorrect. A model set-up is only one of many possible combinations of model inputs that describe the observed data. Therefore, models are not unique (nonuniqueness) and have uncertainty that has to be evaluated. The uncertainty arises from a number of factors such as: quality and quantity of existing data; code selection—different codes prioritize processes for a groundwater flow simulation differently; limited definition of hydrogeological conditions; "things we do not know we do not know", etc. (Anderson et al., 2015; Hunt & Welter, 2010).

A set-up of a groundwater flow model requires a lot of effort and is time consuming. For this reason, once the model is established it should be kept "alive" and used routinely.

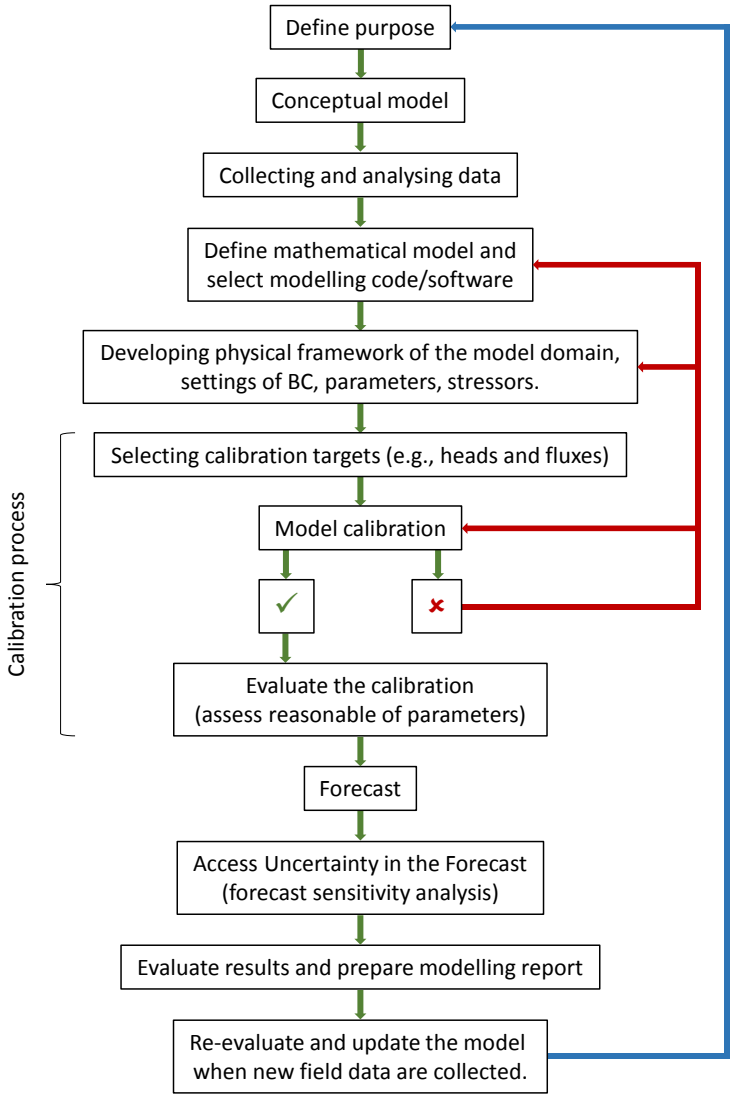


Figure 1.9: Groundwater modeling workflow. The workflow assumes that the objective of a model is forecast. Modified from Anderson, Woessner, and Hunt (2015).

Therefore, it is very handy that models can be updated later with new data. To keep a model "alive" is also one of the reasons why all the steps presented in Figure 1.9, including data sources have to be described in a modeling report.

1.3.1 Conceptual model

The purpose of model conceptualization is to summarize what is known about a hydrogeological system that we want to model. Also, all needed and available data have to be collected and analysed in this step. Unfortunately, available data are usually limited and consequently also the understanding of underground processes and a water balance. For this reason, modelers use all kinds of existing data sources: hydrology, geochemistry, climate, geophysics, geology, soils, geomorphology, vegetation, and anthropogenic sources (Kohn, 1996). Since the conceptualization and later the performance of a model depends on the modeler's understanding of the system, it is strongly recommended to visit the modeling domain before the conceptualization is completed. A field visit also helps to

make better decisions through the development of a model. In fact, the closer the conceptual model approximates the field situation, the more likely the numerical model will give reasonable results. In general, the conceptual model should give to the modeler an idea of the hydrodynamic in the system, groundwater sources and losses, stressors that have an impact on the system, and boundary conditions.

1.3.2 Numerical model

Once, the system behavior is clear for a modeler, the conceptual model can be "translated" into a numerical model. Its main driving force, which is the governing equation for a groundwater flow, includes: (1) a model simulated dependent variable—hydraulic head; (2) independent variables—spatial coordinates x, y, z and time steps, which provide a framework for the nodal and temporal networks, respectively; and (3) material property and hydrologic parameters. Material property parameters describe hydraulic characteristics of the porous media, while hydrologic parameters specify stressors to the system as sources and sinks such as recharge rates, pumping, etc. Numerical modeling relies on determination of parameters representing flow conditions for a selected model scale. For this reason, understanding of the spatial resolution is crucial (Kalbus et al., 2006). In fact, parameter values observed on a field or measured in a laboratory are usually on a different scale to that of the nodal network of the numerical model. Therefore, data preparation requires their special understanding. Data discretization over time and their initial conditions are additional requests for a transient state model.

A steady state model is usually the first step in the transient modeling procedure, since steady state model results can be applied as initials in the transient state model. The steady state model is independent from initial values, but early time transient results are strongly influenced by them. Using data observed on a field as initials in a transient model is absolutely unacceptable. It should be also mentioned that a stand-alone steady state model has also many applications, for instance: analysing average groundwater flow patterns and flow rates, estimating average annual leakage from a losing river, calculating regional water table gradients, simulating influences of long-term pumping on a hydraulic head and flow direction, providing a forecast of time-averaged stress effects (e.g. drought) on an aquifer, etc. On the other hand, the transient model can calculate hydraulic head fluctuations, recharge, or evaluate effects of transience on transport of contaminants from their sources. Since the steady state model has quite a number of applications, its simulation is much faster, easier and cheaper, it is recommended to estimate whether the transient model is needed for certain study at all. There are several methods that help to evaluate the selection of the model. One of them is a calculation of an aquifer responsiveness time (τ) with the Eq. 1.9, where L is a distance between major surface water features (m), P is a period of the forcing function (s), S is a non-dimensional storativity, K is hydraulic conductivity (m s^{-1}), b is the thickness of the saturated zone (m), and T is transmissivity (m^2 s^{-1}). When $\tau > 1$ a steady state model of time-averaged conditions is appropriate; when $0.1 < \tau < 1$ a transient model is required; and when $\tau < 0.1$ bounding or a successive steady state solution may be used. The new method for estimating responsiveness time was published recently by Carr and Simpson (2018). In Section 3.3 used of cross-correlation analysis for an estimation of the aquifer responsiveness in the Ljubljansko polje aquifer system is described.

$$\tau = \frac{1}{4P}\frac{SL^2}{Kb} = \frac{T}{4P} \tag{1.9}$$

When a transient state model is needed, its time step has to be selected carefully ac-

cording to the model application. The time step size can affect an error in the water balance and can produce unrealistic results. For instance, if time steps are too long, the numerical solution calculates unrealistic oscillating values of the pressure head (Anderson et al., 2015; Pianosi & Wagener, 2016). In general, shorter time steps are preferred to ensure that information about a stress or periodicity is included. However, from the perspective of computational time, a short time step is no longer a preference. FEFLOW handles even automatic time steps, which helps to keep an oscillation of a pressure head under control.

Depending on the modeling purpose, the groundwater flow code has to be selected. Kumar (2012) published a long list of available groundwater modeling software. However, MODFLOW by the U. S. Geological Survey (USGS) and FEFLOW by the MIKE Powered by Danish Hydrological Institute (DHI) are two of the most frequently used models in hydrology (Knödel, Lange, & Voigt, 2007). FEFLOW (finite element flow model) was also used in this PhD thesis.

The accuracy of a numerical solution is estimated with a calculated water budget. The total budget should show almost equal total inflow and outflow. If they differ by more than 1% (ideally 0.5–0.1%), the software shows an error (Konikow, 1978). A high percentage of water budget error may mean that the solution has not converged within the maximum number of iterations. The non-converged model may have errors in input data, model design, or the conceptual model does not correctly describe the modeling domain.

Numerical models may require long execution time that can be controlled with: (1) a number of nodes and layers that affect the number of calculations the software has to perform; (2) a number of iterations defined in settings as the required number of iterations for convergence; (3) the input data should approximate the final head solution very well; (4) the length of a simulated time period and number of time steps in a transient model.

1.3.2.1 Mesh discretization

A mesh discretization is very important in numerical modeling, because the governing equation (see Subsubsection 1.3.2.2) calculates heads at discrete points (nodes). There are two most commonly used numerical methods in groundwater flow modeling: the finite-difference (FD) and the finite-element (FE) methods.

A model domain is discretized into a rectangular grid with the FD method. A dependent variable is calculated within the square (2D) or rectangular prism (3D). On the other hand, the FE method, which was used also in this PhD, discretizes a model domain into a network of nodes, with triangular or rectangular shapes of elements in 2D, while 3D elements have a shape of a triangular/rectangular prism (Figure 1.10). A dependent variable (e.g. hydraulic head) within elements is defined with a trial solution, which is usually interpolated from a basic function. The basic function is often a linear function that interpolates a dependent variable within elements from surrounded nodes. Consequently, the trial solution of a hydraulic head, defined by the basic function, is not the true solution. Therefore, the governing equation includes a residual error term, which measures the degree to which the hydraulic head does not satisfy the governing equation. Nevertheless, the trial solution approaches the true solution, if residuals over the model domain are minimized.

A mash discretization around pumping wells requires more attention, because the simulated hydraulic head in the node i, which defines also a pumping well, strongly depends on the mesh discretization around this node, and indirectly also on the amount of extracted groundwater. FEFLOW simulates multi-node wells using 1D tubular discrete feature elements (DFEs). The DFE represents a feature that is smaller than the space between nodes and transmits a larger groundwater flux than the surrounding porous medium. For

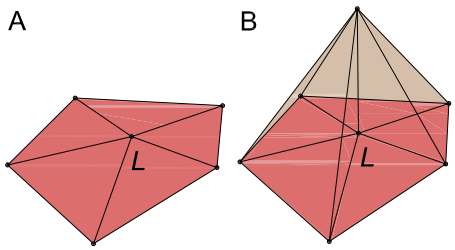


Figure 1.10: (A) A plan view of a patch of elements around the node L in a FE mesh, and (B) a 3D view of the nodal basic function $N_L(x,y)$. Modified after Wang and Anderson (1982) and Cheng (1978).

this purpose, a high conductivity is assigned to the DFE (10^6 m s^{-1}). That means, that the amount of pumped water depends on the virtual radius ($r_{virtual}$) of the pumping well (Figure 1.11), which is defined with the mesh discretization around the node i. Thus, if the mesh discretization around the node i is too coarse, the model will pump more groundwater into the node i than expected and consequently simulate lower (probably unrealistic) hydraulic head around the node i. For this reason, the distance between the node i and neighbouring nodes should meet the best physical radius of the well. Diersch (2014) introduces the following two methods for solving this issue: (1) direct estimation of nodal distances (Δ); and (2) an iterative determination of nodal distances (Δ). The iterative determination of nodal distances is applicable to the actual mesh discretization. In the proposed PhD, the direct estimation method was applied. This method gets more attention than the iterative determination method. The direct estimation method is appropriate for the ideal triangular mesh discretization, where the optimal distance between the node i and the neighbouring nodes is calculated with the Eq. 1.10, where n denotes the number of surrounding nodes (n=6 is typical for triangular horizontal meshes) (Diersch, 2014).

$$\Delta = exp\left(\frac{2\pi}{n \cdot \tan\left(\frac{\pi}{n}\right)}\right) \cdot r_{virtual} \tag{1.10}$$

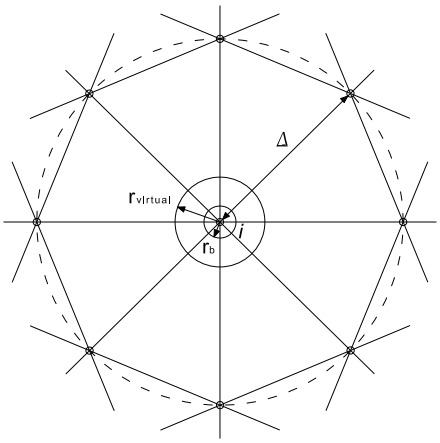


Figure 1.11: Equilateral triangular elements around the pumping well - node i, surrounded by six neighbouring nodes, at the distance calculated by Eq. 1.10. Adapted from Diersch (2014).

1.3.2.2 Groundwater flow equations

In the conceptual model, information about the groundwater flow direction may be taken from hydraulic head measurements in wells or contour maps of the water table, while a mathematical model uses the governing equation for simulation of the groundwater flow, which is derived from Darcy's law (Eq. 1.11).

$$q = -K\frac{dh}{dL} \tag{1.11}$$

where q is the specific discharge ($m^2\ s^{-1}$) and $\frac{dh}{dL}$ is the hydraulic gradient along the flow path, L (m). The law states that groundwater (a single-phase fluid) flows in the direction of decreasing gradient at a constant density in a saturated and in a continuous porous medium. The hydraulic head is an expression of potential energy of water at a point expressed as a length. Eq. 1.12 is the general differential governing the equation for a 3D transient groundwater flow for heterogeneous and anisotropic conditions (Delleur, 2007).

$$\frac{\partial}{\partial x}\left(K_x\frac{\partial h}{\partial x}\right) + \frac{\partial}{\partial y}\left(K_y\frac{\partial h}{\partial y}\right) + \frac{\partial}{\partial z}\left(K_z\frac{\partial h}{\partial z}\right) = S_s\frac{\partial h}{\partial t} - Q^* \tag{1.12}$$

where h is hydraulic head (m), K hydraulic conductivity ($m\ s^{-1}$), ∂x, ∂y, ∂z are distances (m) along which the hydraulic head ∂h has been changed (m). S_s is a specific storage (m^{-1}), which is defined as a volume of water released from a storage per unit change in the head (h) per unit volume of water (Eq. 1.13). Q^* is a volumetric inflow/outflow rate ($m^3\ s^{-1}$)(e.g. pumping or injection well) (Delleur, 2007).

$$S_s = -\frac{\Delta V}{\Delta h \Delta x \Delta y \Delta z} \tag{1.13}$$

Eq. 1.12 can slightly vary for confined and unconfined aquifers. For confined aquifer, a transmissivity ($T = K \cdot b$ in $m^2\ s^{-1}$) and a storativity ($S = S_s \cdot b$) can be implemented, where b is the aquifer thickness (m). Q^* in Eq. 1.12 becomes a flux now, expressed as a volume of water per area of an aquifer per time, R in $m\ s^{-1}$ (Delleur, 2007).

$$\frac{\partial}{\partial x}\left(T_x\frac{\partial h}{\partial x}\right) + \frac{\partial}{\partial y}\left(T_y\frac{\partial h}{\partial y}\right) + \frac{\partial}{\partial z}\left(T_z\frac{\partial h}{\partial z}\right) = S\frac{\partial h}{\partial t} - R \tag{1.14}$$

On the other hand, Eq. 1.15 is the variation of Eq. 1.12 for an unconfined aquifer (Delleur, 2007).

$$\frac{\partial}{\partial x}\left(K_x h\frac{\partial h}{\partial x}\right) + \frac{\partial}{\partial y}\left(K_y h\frac{\partial h}{\partial y}\right) + \frac{\partial}{\partial z}\left(K_z h\frac{\partial h}{\partial z}\right) = S_y\frac{\partial h}{\partial t} - R \tag{1.15}$$

where S_y is a specific yield (dimensionless) and R is a recharge rate ($m\ s^{-1}$). S_y defines storage of water in the unconfined layer. This is the ratio of the volume of water (V_w) that drains from a saturated porous matrix (V_{pm}) under the influence of gravity to the total volume of the matrix, per unit drop in the water table, see Eq. 1.16.

$$S_y = \frac{\Delta V_w}{\Delta V_{pm}} \tag{1.16}$$

Thus, the storativity of an unconfined aquifer can be defined as: $S = S_y + S_s \cdot b \cong S_y$ (Delleur, 2007).

The groundwater flow simulation in an unsaturated aquifer faces additional challenges, because parameters that control groundwater flow (soil moisture and hydraulic conductivity) depend on the pressure in an aquifer. This leads to a strong nonlinearity of the

equation (Paniconi & Putti, 2015). Such a groundwater flow is usually calculated with the Richard equation (Eq. 1.17), which is more difficult to solve than Eq. 1.12 from numerical and computational perspectives. The Richard equation is named after L. A. Richard, who published this equation in 1930 (Diersch, 2014). Eq. 1.16 is the most fundamental form of the Richard equation, where Θ is a volumetric water content (dimensionless), ψ is pressure head (m), ∂z is a vertical coordinate, ∂t is time (s) and K hydraulic conductivity (m s^{-1}) (Celia, Bouloutas, & Zarba, 1990).

$$\frac{\theta(\psi)}{\partial t} - \bigtriangledown \cdot K(\psi) \bigtriangledown \psi - \frac{\partial K(\psi)}{\partial z} = 0 \tag{1.17}$$

The advection-dispersion function is typically applied for modeling of the mass or solutes transport. This function introduces additional numerical difficulties, from time scale differences between mass transfer and transport dynamics, to the complexity of exchanges between multiple species and phases (Paniconi & Putti, 2015). However, this PhD dissertation does not include this broad-interest topic. The groundwater flow simulation, presented later in the dissertation, was performed with the Eq. 1.15—3D transient state groundwater flow model for a confined aquifer under heterogeneous and anisotropic conditions. Moreover, the governing equation must be solved under certain initial and boundary conditions described in the following section.

1.3.2.3 Boundary conditions

Boundary conditions are usually defined at important physical or hydraulic features identified from potentiometric, topographic and geologic maps in the conceptual model (Anderson et al., 2015). Mathematical models offer three types of boundary conditions for closing a model domain at these locations: Dirichlet, Neumann and Cauchy types.

- The 1^{st} type (Dirichlet-type) or the specified head boundary condition defines the known hydraulic head across the boundary (Yeh, 2000). An example: a border between the water level at surface water bodies (sea, lake, river, etc.) and groundwater table.
- The 2^{nd} type (Neumann-type) or the specified flow boundary condition is used when a derivate of the hydraulic head can be specified as an outward unit vector normal to the boundary. Normally it defines a drainage boundary, where the real flux across the boundary is calculated from Darcy's law (Yeh, 2000). An example: a connection of two aquifers.
- The 3^{rd} type (Cauchy-type) or the head-dependent boundary condition also calculates flow across the boundary from Darcy's law, but the calculation is based on differences between the water level outside the model domain and the hydraulic head simulated within the model domain. The Cauchy-type type is normally an infiltration boundary, where the flux direction is toward the lower water level (Yeh, 2000). An example: an aquifer is in direct hydraulic contact with a river, a lake or a reservoir in which the water level is known (Chiang & Kinzelbach, 2003).

In FEFLOW, a hydrogeologic judgment must be used to decide, which boundary condition in the code presents particular sources/sinks the best. The approach requires a very good understanding of hydrologic processes and the code's background.

Despite recent progress in the field of numerical models, the current modeling practice is still far away from incorporating the full complexity of surface water and groundwater interactions (Brunner et al., 2017). One of the reasons is a demanding estimation of boundary conditions in numerical models, which is even more challenging when hydraulic conditions along a boundary change over time. The latter is more realistic and often a critical step in the numerical modeling. Therefore, a suggestion for a detailed individual

simulation of these boundary conditions, which are either directly or indirectly connected to the groundwater flow model, was tested in this PhD. The groundwater flow model is mainly driven by river water and percolation of local precipitation. For this reason, the next subsubsection provides a basic theory of simulations of these boundary conditions and their state of the art.

1.3.2.4 Parameters

Mathematical models require two types of parameters: material property and hydrologic parameters.

1.3.2.4.1 Material property parameters. This group of parameters describes hydraulic characteristics of a porous medium (an aquifer). These parameters are: hydraulic conductivity (k), storativity (S), specific storage (S_s) and specific yield (S_y). They may be estimated with different aquifer tests, in the laboratory, or from literature. However, detailed information of their spatial and directional variability is rarely known and often obtained with a large uncertainty. For this reason, their initial estimations are typically refined during model calibration.

An estimation of the material property parameters is quite demanding procedure because of the heterogeneous and anisotropic geological composition of a model domain in nature. On the top of all this, the scale of the elements in the model has to be taken into account. In many cases is appropriate to assume that they are isotropic in the horizontal plane, while vertical anisotropy is common to most hydrological models. When a model domain covers structures that impart the preferential groundwater flow direction, the material property parameters in the horizontal plane should be anisotropic. The isotropic conditions in the horizontal direction were also assumed for the model described in this dissertation (see Section 3.3).

Sedimentation in a river channel forms a so-called clogging layer that affects the rate of exchanged water between a river and an aquifer. The vertical leaching is typically estimated during the calibration of a model, which is based on the equation K_z/b, where b is the thickness and K_z is the vertical conductivity of a sediment. Issues related to the vertical leaching field measurements and the estimation performed during model calibration is described in Subsection 1.4.2.

1.3.2.4.2 Hydrologic parameters. This family of parameters includes recharge, pumping/injection, and evapotranspiration. Pumping and injection rates are usually not problematic, due to the dense network over the globe and their continuous records.

Although recharge (Figure 1.1) is one of the most important parameters in groundwater modeling and despite many available methods for its measurement or estimation (Table 1.2), we still have problems with its quantification, due to its spatial and temporal variability. Recharge depends on many parameters comprising: topography, land use, soil properties, root depths, groundwater depth and climate conditions. These parameters are typically assign as an average rate over the full modeling domain, despite their diversities. Nevertheless, recharge and evapotranspiration in the model presented in this dissertation have reached spatial and temporal resolution. Their simulation was done in WaSiM. See details in Subsection 1.4.1 and Section 3.3.

1.3.2.5 Calibration

The model calibration is crucial and one of the most demanding modeling procedures. In general, the main purpose is to reach an equilibrium among all parameters implemented

Table 1.2: Methods for estimating recharge and discharge in an aquifer. Modified after NRC (2004), Scanlon, Healy, and Cook (2015), Anderson, Woessner, and Hunt (2015).

Hydrologic zone where actual measurement is made	Method
Surface water	Channel water budget Base flow discharge Seepage meters Heat tracers Isotopic tracers Solute mass balance Watershed modeling
Unsaturated zone (measurable discharge would mainly be upward exfiltration to vegetation)	Lysimeters *In situ* sensors Zero-flux plane Darcy's law Tracers (historical (^{13}C, ^{3}H, ^{2}H, ^{18}O), environmental (Cl)) Numerical modeling Thermal analysis Surface geophysics Cross-hole geophysics Gravity geophysics
Groundwater	Water table fluctuations (observation wells, geophysics) Elastic compression measurements (e.g. GIS, InSAR) Darcy's law Tracers (historical (CFCs, ^{3}H/^{3}He), environmental (Cl, ^{14}C))

in the model, which are usually barely known. Furthermore, they can be highly variable in horizontal and vertical directions and also in time. The calibration process also establishes the legitimacy of conceptual and numerical models. The history-matching method is typically used for the calibration, the idea of which is to perform the best matching of simulated and observed calibration targets, with changing calibration parameters values. The manual trial-and-error history-matching method not only improves the fit, but also important insight into the model behavior. It is also an efficient first test of the conceptual model, because it can quickly demonstrate that a specific conceptual model does not belong to the family of reasonable models. The history-matching method includes the following steps:

- Selection of calibration targets from the set of field observations. Ideally, a modeler uses as many types of available targets as can be compared to model outputs (Hunt, Doherty, & Tonkin, 2007) because one type of a target alone cannot mathematically constrain the inverse solution of the groundwater flow equation uniquely. However, none of the models is capable of matching all calibration targets equally. Thus, the importance of targets should be estimated with their ranking. The minimum recommended and most commonly used types are head and flux targets (base flow, spring flow, infiltration of losing river, groundwater inflow to a lake/river, evapotranspiration, etc.).
- Running the model with the best initial material property parameters and hydrologic parameters.
- A comparison of simulated results and observed targets. A standard procedure for evaluating model performance does not exist yet, although many scientists have highlighted its need (Ritter & Muñoz-Carpena, 2012). However, the match between

simulated and observed parameters (p) is often estimated with the following statistics:
1. The mean error (ME), which is a mean reference difference of residual errors and is considered as a weak indicator of goodness of the model fit. The ME is expressed with the following equation:

$$ME = \frac{1}{n}\sum_{t=1}^{n}(p_m - p_s)_i \tag{1.18}$$

where n is the number of targets, i is the individual location of observed values (e.g. a piezometer), and p_m and p_s are measured and simulated targets, respectively.
2. The mean absolute value (MAE), which is the mean of absolute values of residuals. The MAE ensure that both positive and negative residuals are included. Therefore, the MAE is considered as a better indicator of the model fit than the ME and is expressed as:

$$MAE = \frac{1}{n}\sum_{t=1}^{n}\mid (p_m - p_s) \mid_i \tag{1.19}$$

3. The root mean square error (RMSE), which is an average of squared residuals. This error which expresses with the following equation is less robust to the effects of outlier residuals:

$$RMSE = \Big[\frac{1}{n}\sum_{t=1}^{n}(p_m - p_s)_i^2\Big]^{0.5} \tag{1.20}$$

4. The comparison between the individual simulated and observed values can be performed with the Nash-Sutcliffe coefficient:

$$NS = 1 - \frac{\sum_{t=1}^{n}\mid (p_m - p_s) \mid_i^2}{\sum_{t=1}^{n}\mid (p_m - \overline{p}_m) \mid_i^2} \tag{1.21}$$

where p_m is the mean of observed parameter values. The NS ranges from ∞ to 1, where values close to one indicate a good fit. It should be also considered that the NS value of 0.5 may be already considered as a satisfying result, but this decision depends on the problem complexity.

– Adjustment of values of input parameters to obtain better fits of simulated values to targets. The model calibration requires multiple runs. The first step in the history-matching process involves measuring and improving the model fit with manually changed parameter values and evaluation of outputs. In the next step, the best possible match between calibration parameters and observations can be found automatically by a computer code. Nowadays, the most widely used is the parameter estimation code (PEST). PEST is a sophisticated code that uses advanced mathematical and statistical methods. FePEST (MIKE, 2016) was devloped exclusive for running FEFLOW with PEST. FePEST has a user-friendly graphical interface that enables easy integration of the FEFLOW model into PEST. FePEST is a multifunctional tool that besides the model calibration, also provides fast sensitivity and predictive analysis (MIKE, 2016). In FePEST, results that do not belong to the family of reasonable models can be reduced by quantification of reasonable ranges for the selected calibration targets.
– A selection of the model with the best possible fit of limitations in time and space. A hydrologist has to judge if the match is reasonable. Therefore, the selection of models that realistically simulate natural environment is always a subjective decision. As already mentioned, groundwater models are fundamentally non-unique. Therefore, the modeler should consider more than one possible reasonable calibrated model.

1.3.3 Forecasting model

If the best calibrated model satisfies the modeler's expectations, the model can proceed to the forecasting modeling. In this step, all the parameters in the calibrated model are kept the same, except the one whose effect on the system is forecasted. For instance: the impact of future climate projections or increase of groundwater pumping. Nevertheless, results of the forecasting model must be reported together with uncertainty analyses of the calibrated model. Even more, studies of climate change impacts on water require the use of different climate models, which leads to multiple runs. The forecasting model developed for the purpose of this PhD thesis is described in Chapter 4.

1.4 Surface Water Model

Major differences between groundwater and surface water models are the following: (1) surface water models are based on an observed river flow, while groundwater models include observed hydraulic heads and fluxes; (2) observations of surface water are typically temporally dense, but spatially sparse; while observations of groundwater are spatially dense, but temporally sparse (Anderson et al., 2015).

The development of numerical models has generally not accounted for surface-groundwater interaction because there has been limited attention given to accurately conceptualizing and parameterizing the surface-groundwater interface (Reid et al., 2009). However, lately, many scientists have expressed a need for coupling groundwater and surface water models for studying the surface-groundwater interface (Burbery & Ritson, 2010; Jolly, Rassam, Pickett, Gilfedder, & Stenson, 2010; Fleckenstein et al., 2010; Larocque & Broda, 2016; House, Thompson, Sorensen, Roberts, & Acreman, 2016). Modeling of fluxes at the surface-groundwater interface includes the modeling of percolation of local precipitation and discharge of river water. Both of them also represent the boundary conditions for a hydrological model and are described in the following subsections.

1.4.1 Percolation/Recharge

Percolation is usually calculated as a residual in a soil water balance. This method provides a physical base for estimating percolation in space, and time and can be applied to a model domain of any size. In general, in the soil water balance method, the soil root zone is defined to extend the land surface to the zero flux plane (see Figure 1.1). The infiltration at the land surface is defined as the difference between precipitation and surface runoff. Evapotranspiration in the unsaturated zone causes a loss of the infiltrated water, therefore only the residual water crosses the zero flux plane and percolates through the unsaturated zone to the water table to become recharged (Anderson et al., 2015).

WaSiM, which was used for a simulation of percolation in the model described in this dissertation, is a fully distributed, deterministic, physically based hydrological model (Schulla, 2017). Such a model provides the most sophisticated simulation of the watershed processes, which includes parameters distributed over a model domain (usually a full watershed) with a grid which has a particular spatial and temporal resolution (Anderson et al., 2015). WaSiM, whose structure is presented in Figure 1.12, contains many sub-models from which the unsaturated sub-model simulates percolation with the following procedure (Schulla, 2017):

– The model specifies a fraction with a threshold value for the precipitation intensity. That means that the fracture of precipitation that can percolate deeper into soil regions without flowing into the root zone storage depends on precipitation intensity

as follows:

$$P_{threshold} = P_{threshold,\ 1h} \cdot \triangle t^{\alpha_p} \tag{1.22}$$

where $P_{threshold}$ is a threshold of precipitation intensity (mm $(\Delta \mathrm{T})^{-1}$). If $P > P_{threshold}$ all exceeding precipitation is routed into the deep soil through macro pores; $P_{threshold,\ 1h}$ is a threshold for precipitation intensity for a time step $\triangle t =$ 1h (mm h^{-1}); $\triangle$t is a time step (h) and α_p is an empirical value (dimensionless), describing the decrease of the variance of the precipitation intensity with larger time steps.

– All precipitation below the $P_{threshold}$ flows into the root zone storage, from where it can be withdrawn by evaporation or percolated (q_v) into deeper soil regions (mm):

$$q_v = K_{korr} \cdot k_f \cdot s^{-S_i/m} \tag{1.23}$$

where K_{korr} is a scaling parameter for considering unsaturated soil and preferred flow paths (dimensionless); S_i is a local saturation deficit (mm), m is a recession parameter (mm), and k_f is a saturated hydraulic conductivity (mm h^{-1}).

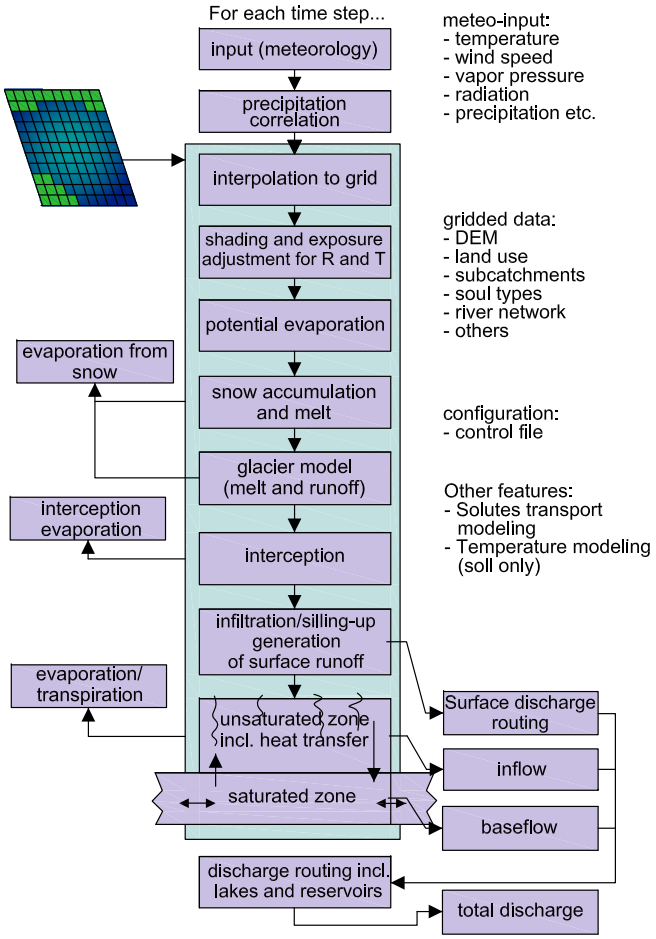


Figure 1.12: WaSiM structure (Schulla, 2017).

1.4.2 River water

At first it looks as if modeling of the river water dynamics should be easier due to easier accessibility of surface water, but this is not the case. Despite all the advanced analytical and measurement technologies, we are still facing problems related to the strong spatial and temporal variability of parameters required for modeling. First, the river channel volume is defined with its geometry. Therefore, the river channel bathymetry is important for modeling, although many numerical models still integrate it as a simplified feature. An estimation of the Manning's roughness coefficient (Manning's n) is the next critical step, since errors in computed surface water dynamics increase significantly with decreased reliability of Manning's n (Soong, Prater, Halfar, & Wobig, 2012), which is included in the following equation:

$$V = \frac{k_n}{n} R^{\frac{2}{3}} S^{\frac{1}{2}} \tag{1.24}$$

where V is velocity (m s^{-1}), S is a friction slope (m m^{-1}), R the hydraulic radius (m), k_n is a constant, $k_n = 1$ for V and R in SI units and n is Manning's n. Manning's n brings the calculated hydraulic capacity closer to realistic water flow in a natural river channels (Ding, Jia, & Wang, 2004).

The next issue is a parameterization of a river bed clogging layer, which is driven by the sedimentation and deposition of fine materials on the riverbed. This process is called colmation. The clogging layer is one of the main drivers for a simulation of river-groundwater interactions, since it defines weather conditions that enable the infiltration or ex-filtration (Doppler, Franssen, Kaiser, Kuhlmanc, & Stauffer, 2007). However, river channels are routinely simulated as static, homogeneous entities (Partington, Therrien, Simmons, & Brunner, 2017; Irvine, Brunner, Franssen, & Simmons, 2012). Brunner et al. (2017) claims this simplified conceptualization of complex river-groundwater interaction is an important source of model uncertainty. On his list of modeling uncertainty sources are also: the selection of an appropriate level of model complexity regarding processes, scale, and heterogeneity, as well as limited field observations that are used in the modeling process. Boano et al. (2010) have identified heterogeneity of the hydraulic conductivity in a river bed as a crucial issue for hyporheic zone research, while Camporeale, Perucca, Ridolfi, and Gurnell (2013) have also pointed out the importance of the riparian zone and floodplain dynamics. Rosenberry and Pitlick (2009) highlighted the importance of both, vertical and horizontal flow processes in a river bed and consequently horizontal and vertical hydraulic conductivities. However, estimating hydraulic conductivity is probably one of the most challenging endeavours in conceptualizing river channels for numerical models, due to its spatial heterogeneity, transience, and the scale dependency of any particular measurement (Brunner et al., 2017). Gianni, Richon, Perrochet, Vogel, and Brunner (2016) even showed that hydraulic conductivity can drastically change between erosion and deposition cycles, up to three orders of magnitude. Typically, hydraulic conductivities of river beds range from 10×10^{-10} to 10×10^{-2} $\mathrm{m\,s^{-1}}$ (Calver, 2001; Stewardson et al., 2016).

Doppler et al. (2007) highlighted necessity of implementing a dynamic leakage coefficient for modeling river-aquifer interactions. The leakage coefficient is the specific leakage rate or exchange per unit horizontal area of a river channel, with the specific hydraulic conductivity and thickness of a river channel. Typically the leaching coefficient and Manning's n are estimated through a model calibration (Doppler et al., 2007).

MIKE 11, developed by DHI, is one of the software tools that handle the 1D interpolation of the river water flow and the river channel bathymetry, and spatial distribution of the abovementioned parameters. The ifmMIKE11 plug-in enables exchange of infor-

mation between MIKE 11 and FEFLOW (Monninkhoff, 2014). This is a great benefit for modeling river-groundwater interactions since FEFLOW is not capable of handling river water at such a precise level. The application of these models in the proposed thesis is described in details in Section 3.4.

Chapter 2

Aims and Hypothesis

For sustainable management of water supply, agriculture, flood-drought cycles and ecosystems and human health, there is a basic need for improving the scientific understanding of the processes that makeup the water cycle in the Sava River Basin (SRB), and the ability to detect and predict natural (e.g. climate change, floods, etc.) and anthropogenic (e.g. industrial and agricultural activities, impacts from large cities) impacts on the sustainable development of groundwater resources. The outcome of the thesis will help improve the conceptual model of the Sava River watershed and the Ljubljansko polje aquifer system and guide future efforts in the management and protection of groundwater and surface water resources. The European Water Framework Directive (WFD) and the Water management plan for 2015–2021 require the introduction of remedial measures to restore or prevent the deterioration of groundwater chemical and quantity status. Obtaining information on the water mean residence time, its dynamics and groundwater recharge are indispensable for assessing the impact of such measures, i.e. in which time period and to what extent an improvement in groundwater status can be expected.

Within the proposed thesis the following hypotheses were tested:

- The implementation of the Urban Waste Water Treatment Directive (UWWTD) 2000/60/EC and Nitrate Directive (ND) 91/676/EEC implemented by EU member states, and the development of waste water infrastructure in the non-EU member countries has led to a measurable decrease the nutrient content (NO_3^- and PO_4^{3-}) of groundwater.
- The mean residence time of groundwater in the aquifer is less than 10 years.
- Locally presented layers with low hydraulic conductivity, which cover the aquifer and form perched aquifers have a measurable influence on the hydrodynamics of the aquifer in the south-western part of the Ljubljansko polje.

My research work covers the following two complementary research areas: (1) short and long-term evaluation of nutrient levels in the SRB and source identification using stable isotopes; and (2) the study of surface-groundwater interactions in the Ljubljansko polje aquifer using hydrological, geochemical and a modeling approach. The tasks involved can be summarized as follows:

1. The first comprehensive evaluation of the long-term water quality data, in terms of major nutrient concentrations (N and P) in the SRB at selective locations in Slovenia, Croatia and Serbia during 2006–2012, 2003–2012 and 1989–2012, respectively. The annual seasonal variations and influence of river discharge on nutrient concentrations were investigated, while temporal trends were assessed using trend analysis. In addition stable isotope composition of nitrogen and oxygen in nitrates were used to identify sources of nitrates in the SRB during high and low flow conditions (2014 and 2015).

2. A hydrological and geochemical characterization of groundwater system in the Ljubljansko polje aquifer was performed. Since the use of isotopes is a useful tool for studying hydrodynamics, monthly isotopic measurements (March to November) of groundwater, Sava River water and of precipitation were obtained in order to: (1) determine the proportion of infiltrated river water into groundwater using $\delta^{18}O$ and $\delta^{2}H$ measurements, (2) to estimate the mean residence time of groundwater using ^{3}H and $^{3}H/^{3}He$ mdating, and (3) determining the levels of ^{3}H and NO_3^- to check the vulnerability of groundwater to pollution. The work represents the first time that the $^{3}H/^{3}He$ was used to date groundwater in Slovenia.
3. The main challenge of the proposed PhD thesis was the modeling. Although a few hydrological models have been developed for the Ljubljansko polje aquifer (e.g. Janža, Meglič, and Šram (2011)), the main advantage of the hydrological model reported herein is the accuracy of the upper boundary conditions that define the two main groundwater sources: local precipitation and river water. This approach was to my knowledge reported for the first time not only for the Ljubljansko polje aquifer, but also elsewhere. Another advantage includes the use of environmental tracers as tracers of hydrological processes or as calibration targets. Using natural tracers, such as isotopes, in hydrological modeling is a priority, because they provide information about groundwater flow and the time scales of groundwater and the movement of contaminants, and on the transformation of reactive contaminants (Wachniew, 2015).

The proposed work, which can be later implemented into other fields (e.g. ecology), is also important from a social and economic perspective, a fact that is proven by the interest of different companies in this research including the following: (1) Javno podjetje Vodovod-Kanalizacija Ljubljana, which is responsible for drinking water management in Ljubljana and its surroundings, (2) Pivovarna Laško Union d.o.o. brewery uses water for their beverage products, and (3) Holding Slovenske elektrarne d.o.o., which is responsible for the hydroelectric power plants on the River Sava in Slovenia.

Chapter 3

Publications

3.1 Nutrient Variations in the Sava River Basin

In this part, the paper "Nutrient variations in the Sava River Basin" by Janja Vrzel and Nives Ogrinc is presented. The paper was published in the Journal of Soils and Sediments, in 2015 and describes the initial research I undertook during my PhD.

The paper presents the first comprehensive evaluation and trend analysis of long-term nitrogen and phosphorous concentrations in the Sava River basin in Slovenia, Croatia and Serbia. During this research two issues were exposed: (1) merging data obtained from different countries into one data base and (2) the lack of data from Bosnia and Herzegovina. However, I hope that the work presented in this paper will encourage people to manage the Sava River water in collaboration with all the countries in the catchment, which will require the implementation of harmonized measurement methods and procedures. Behmel, Damour, Ludwig, and Rodriguez (2016) points out how crucial is a reliable assessment of water quality (through water quality monitoring programs, WQMPs) for decision-makers to understand, interpret and use this information in support of management activities aimed at protecting the resource. They even introduce an intelligent decision support system (IDSS) as a future approach for planning a monitoring program at a specific site with unique characteristics (regulatory requirements, water quality standards, geographical and geological differences, land-use variations, and other site specifications).

My main observation was the decrease in the levels of NO_3^- and PO_4^{3-} in the Croatian and Serbian parts of the Sava River channel, where anthropogenic pressure on the Sava River is high, due to dense human populations and intensive agricultural activities. My next observation shows how important discharge is on the distribution of NO_3^- and PO_4^{3-}. The minimal and maximal concentrations on the annual mean NO_3^- data series were recorded over the summer and winter months, respectively. The increase in NO_3^- levels is because of the higher flow conditions that leach NO_3^- from the soil and from the riverbanks into the river. At the same time, the annual mean PO_4^{3-} levels reach a maximum as inorganic phosphorous is released from the sediments. A reduction in nutrients, observed at the majority of sampling locations (8 to 58%), indicates a significant improvement in the water quality of the Sava River Basin. However, there remains a need to apply appropriate remedial technologies in order to reduce nutrient loads into the Sava River Basin. My research illustrates the utility of long-term water quality monitoring data for providing a basis for empirical analysis and is useful for management-related studies.

In this paper, I contributed to the development of the research question, collected all the chronological data (NO_3^- and PO_4^{3-} concentration, river discharge) at each of the eight sampling locations: Otoče (SI), Šentjakob (SI), Jesenice na Dolenjskem (SI), Zagreb (HR), Črnac (HR), Slavonski Brod (HR), Županja (HR), Sremska Mirovica (RS) and Šabac

(RS). I also collated all the information for example on the land use and performed data processing and statistical analyses. I also wrote the paper and prepared the manuscript for publication.

J Soils Sediments
DOI 10.1007/s11368-015-1190-7

IASWS 2014: THE INTERACTIONS BETWEEN SEDIMENTS AND WATER

Nutrient variations in the Sava River Basin

Janja Vrzel[1,2] · **Nives Ogrinc**[2,3]

Received: 1 September 2014 / Accepted: 21 June 2015
© The Author(s) 2015. This article is published with open access at Springerlink.com

Abstract
Purpose The first comprehensive evaluation and trend analysis of long-term nitrogen (N) and phosphorus (P) data was performed for the Sava River Basin (SRB) at locations in Slovenia, Croatia, and Serbia.
Materials and methods Data on long-term water quality at eight selected locations were evaluated statistically based on the period of reporting, availability of flow data, and the experience from our previous investigations. Trends in NO_3^- and PO_4^{3-} concentrations at locations were identified using simple linear regressions on log-transformed data.
Results and discussion Analysis indicated spatial and seasonal variability between locations. The highest long-term annual mean NO_3^- and PO_4^{3-} concentrations were observed in Croatia and Serbia at locations that are susceptible to anthropogenic nutrient loading arising from high human population densities and intensive agricultural land use. Temporal variations indicate that river flow plays an important role in the distribution of NO_3^- and PO_4^{3-} concentrations. Low flow during the summer months promotes reductive conditions leading to a minimum in annual mean NO_3^- concentrations and a maximum in annual mean PO_4^{3-} concentrations resulting from the release of inorganic P from sediments. The highest annual mean NO_3^- concentrations were observed in winter/autumn under higher flow conditions that leach NO_3^- from soil and banks into the river. The results of trend analysis show a reduction of nutrients at the majority of locations ranging from 8 to 58 %.
Conclusions Although trends in NO_3^- and PO_4^{3-} concentrations indicate a decrease at the majority of selected locations, it is still necessary to apply appropriate removal technologies in order to reduce the nutrient loads into the Sava River Basin and thereby improve water quality.

Keywords Computational methods · Nutrients · Sava River Basin · Statistics

1 Introduction

Nutrient enrichment or eutrophication is one of the important water quality issues limiting present and future uses of water resources. Although nutrients—mainly nitrogen (N) and phosphorus (P)—are necessary for the growth and survival of animals, plants, and other organisms, human activities have enhanced their global cycles by, on average, 100 and 400 %, respectively (Falkowski et al. 2000). Nutrient loads operate through both point and diffuse pathways linking land to water and are dependent on hydrology and in-stream processes such as transformation, retention, and elimination. Their concentrations and flux can vary significantly at different parts of the river in a manner related to short-term variations in hydrology and long-term changes of land use (Billen et al. 2007). Knowledge of mechanisms influencing the distribution of nutrients and assessment of the ecological state of aquatic systems is often only temporary and limited to the present situation. Assessment of historical patterns of change and trend analysis using existing water quality data are required in order

Responsible editor: Fred Ellery

✉ Nives Ogrinc
nives.ogrinc@ijs.si

[1] Ecological Engineering Institute, Ltd, Maribor, Slovenia
[2] Jožef Stefan International Postgraduate School, Ljubljana, Slovenia
[3] Department of Environmental Sciences, Jožef Stefan Institute, Jamova 39, 1000 Ljubljana, Slovenia

Published online: 03 July 2015

to gain a balanced overview of how a river has been influenced, particularly in relation to land use.

The Sava River Basin (SRB) is an excellent area on which to investigate both natural and anthropogenic inputs influencing nutrient dynamics in a riverine ecosystem. Our studies have shown that upper reaches are largely regulated by natural processes, middle reaches by agricultural activity and biological processes related to eutrophication, while lower reaches are influenced mainly by stressors related to high pollution from industrial processing, along with untreated municipal waste water discharges (Markovics et al. 2010). Agricultural and industrial sources contribute significantly to the increase in Na^+, K^+, Cl^-, SO_4^{2-}, and NO_3^- concentrations in stream waters. Nitrate inputs are controlled by land use, and the high isotope composition of nitrate at some sites is attributed to sewage and/or animal waste (Ogrinc et al. 2008a, 2015). It was also found that the low discharges, higher temperature, and nutrient enrichment observed in autumn promoted the eutrophication of a river in agricultural areas (Ogrinc et al. 2008a; Markovics et al. 2010). However, the rate of change has not been assessed, and it is important to know this information so that remedial efforts can be targeted and be effective.

We present the first comprehensive evaluation of the long-term water quality data in terms of major nutrient concentrations (N and P) in the SRB at selected locations in Slovenia, Croatia, and Serbia. Annual seasonal variations and the influence of river discharge on nutrient concentrations have been investigated, and temporal trends assessed using trend analysis.

2 Materials and methods

2.1 Site selection

The Sava River is located in southeast Europe and is a tributary of the Danube River, joining at Belgrade (Fig. 1). It is 990-km long, with a catchment area of 97,713 km^2. It flows through four countries: Slovenia, Croatia, Bosnia and Herzegovina, and Serbia. It drains a significant portion of the Dinaric Alps region, via the tributaries of Krka, Kupa, Una, Vrbas, Bosna, and Drina.

The SRB is divided into three climatic areas Alpine, Pannonian, and Continental. Mean annual precipitation and temperature differ over the length of the river. In the upper reaches (alpine headwaters), mean annual precipitation is in the range of 2000–3000 mm yr^{-1} with a mean annual temperature of approximately 6 °C. At the confluence of the Sava with the Danube, annual precipitation is <660 mm yr^{-1}, and mean annual temperatures are higher at about 13 °C. In general, the discharge of the Sava is greatest in the winter and lowest in the summer. However, seasonal and annual discharges vary by location. The long-term average discharges are 84, 255, and 1722 $m^3\ s^{-1}$ in Ljubljana, Zagreb, and Belgrade, respectively. These values correspond to similar area-normalized discharge values of 17.4, 20.5, and 18.0 $l\ km^{-2}\ s^{-1}$. The mean residence time of stream water is similar at all sampling points, with a mean value of 1.32 years, generally characterized as being relatively short, indicating that the catchments have relatively low groundwater storage capacity (Ogrinc et al. 2008b).

Land use of the SRB is diverse and complex, reflecting the differences in relief, climate, and stream flow. The greatest population density occurs near the large cities, while agriculture is the dominant activity in the Croatian and Serbian part of the watershed. The upper part of the SRB (in Slovenia) is covered mainly by forests (>50 %) with subalpine vegetation occupying ~35 %. In Croatia, forests cover 25 % and agriculture >40 % of the basin area. The Bosnian part of the SRB has valleys and hills with about 30 % agriculture and 20 % forest. The majority of the watershed area in Serbia is used for agriculture. Other anthropogenic impacts in the watershed comprise thermo- and hydroelectric plants, oil and gas refinery stations with pipelines, metallurgical, chemical and textile industries, and mining.

Data on water quality were evaluated at eight selected monitoring stations listed in Table 1 and displayed in Fig. 1. These stations were selected on the basis of availability of flow and water quality data and our previous research experience. Three locations were selected in Slovenia (Otoče, Šentjakob, and Jesenice na Dolenjskem) and four in Croatia (Zagreb, Črnac, Slavonski Brod, and Županja). Two locations in Serbia—Sremska Mitrovica and Šabac (location 8)—were treated together, since the data complement each other. Otoče (location 1) is a predominantly forested area and was treated as a background site as it had the lowest observed nutrient concentrations (Table 1). $\delta^{15}N_{NO3}$ is <6‰ indicating the presence of natural soil-derived nitrogen (Ogrinc et al. 2008a). Šentjakob (location 2) and Zagreb (location 4) are influenced by large cities Ljubljana and Zagreb. Jesenice na Dolenjskem (location 3) is located amid nuclear and hydroelectric plants, while Črnac (location 5), Slavonski Brod (location 6), Županja (location 7), Sremska Mitrovica, and Šabac (location 8) are locations highly impacted by agricultural activities (Table 1). In addition, the highest $\delta^{15}N_{NO3}$ values (+24.4‰) were observed at Šabac during our study in autumn 2006 when flow was low indicating the influence of animal waste and/or poorly treated sewage (Ogrinc et al. 2008a).

Daily averaged flow rates ($m^3\ s^{-1}$) and water quality data (usually monthly) were provided by the Environmental Agency of the Republic of Slovenia (ARSO; URL: http://www.arso.gov.si/), Hrvatske vode (URL: http://www.voda.hr) and Republic Hydrometeorological Service of Serbia (http://www.hidmet.gov.rs). The analysis covers periods from 2006 to 2012, 2003 to 2012, and 1989 to 2012 in

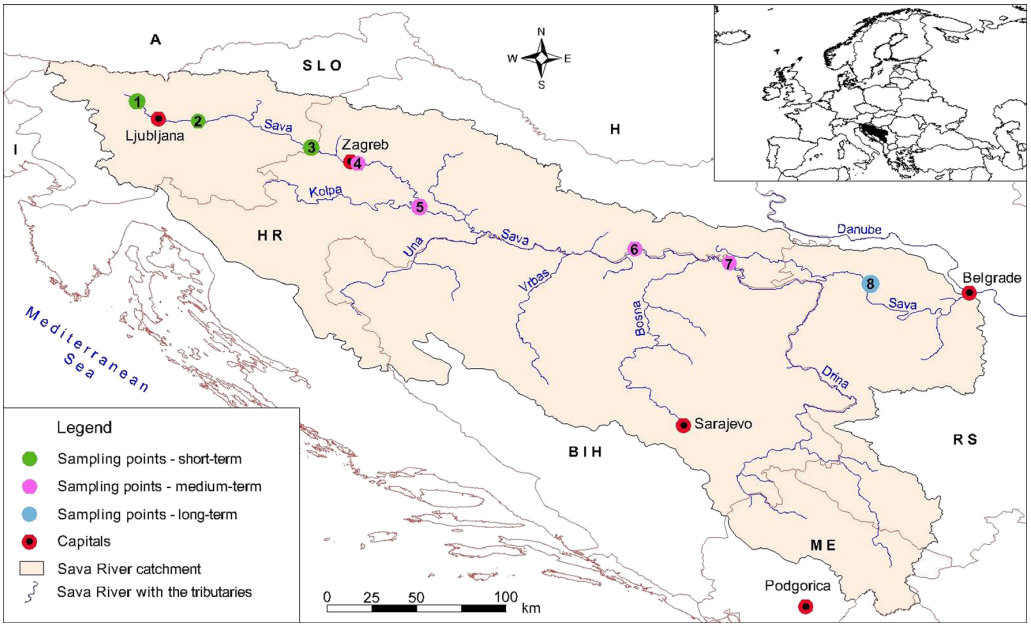


Fig. 1 Map of the selected monitoring locations in the Sava River Basin. These are the following: *1* Otoče, *2* Šentjakob, *3* Jesenice na Dolenjskem, *4* Zagreb, *5* Črnac, *6* Slavonski Brod, *7* Županja, and *8* Sremska Mitrovica and Šabac

Slovenia, Croatia, and Serbia, respectively. Standardized protocols have been used for water sampling and laboratory analysis to obtain comparable monitoring results.

2.2 Statistical analysis

Statistical evaluation of the data was performed using Statistica version 7.0 (Statsoft, Tulsa, USA). Normally distributed data were analyzed by ANOVA to test for the temporal and spatial differences in flow and water quality parameters.

The model proposed by Hirsch et al. (2010) was used to estimate concentrations for the entire recorded period. The model considers concentration to be a product of three deterministic components (trend, season, and discharge) and one random component described by the following equation:

$$\ln(c) = \beta_0 + \beta_1 t + \beta_2 \ln(Q) + \beta_3 \sin(2\pi t) + \beta_4 \cos(2\pi t) + \varepsilon \quad (1)$$

where c is the concentration (mg l^{-1}), Q is discharge (m^3 s^{-1}), t is the time (years), ε is the unexplained variations, and β_{0-4} are fitted coefficients.

Trend analysis at selected locations was performed using linear regressions. This involved first regressing log-transformed concentration data with log-transformed flow

Table 1 Selected monitoring locations with short, medium, and long-term data collection with their distances from the source, height above sea level, and cumulative land use

Location number	Sampling location	Country	Latitude N	Longitude E	Distance from the source (km)	Height above sea level (m)	Forest (%)	Agriculture (%)	Urban and industry (%)	Other (%)
1	Otoče	Slovenia	46° 18′	14° 14′	40	415	0.9	0.1	0.01	0.004
2	Šentjakob	Slovenia	46° 06′	14° 47′	115	245	3.8	1.4	0.2	0.038
3	Jesenice na Dolenjskem	Slovenia	45° 51′	15° 41′	213	140	6.0	2.8	0.3	0.056
4	Zagreb	Croatia	45° 41′	16° 14′	268	100	7.9	4.7	0.4	0.069
5	Črnac	Croatia	45° 25′	16° 28′	376	95	9.8	7.9	0.7	0.110
6	Slavonski Brod	Croatia	45° 09′	18° 00′	564	82	28.5	22.0	1.2	0.405
7	Županja	Croatia	45° 04′	18° 41′	685	81	36.3	28.0	1.6	0.485
8	Sremska Mitrovica	Serbia	44° 58′	19° 35′	804	74	52.3	36.6	2.0	0.653
	Šabac	Serbia	44° 44′	19° 44′	837	73	52.6	37.8	2.1	0.671

data, taking the residual scores from this regression and then regressing them with time (Jones and Armstrong 2001). This procedure minimizes the influence of the correlation between concentration and flow. Trends were considered significant if $p<0.05$. The Shapiro-Wilcox W test was used to test whether the regression residuals were normally distributed.

3 Results and discussion

3.1 Temporal and spatial variations

The temporal and spatial variations were related to the obtained data and divided into three stages:

- Long-term evaluation of the data (from 1989 to 2012) at location 8;
- Medium-term evaluation of the data (from 2003 to 2012) at locations 4 to 8; and
- Short-term evaluation of the data (from 2006 to 2012) from all locations.

Annual flows varied considerably at each location. At location 8, where a long-term record of flow exists, the lowest mean annual flow was observed in 1990, but for all those stations where a short-term record exists, the lowest mean annual flow was observed in 2011. The highest mean annual flow was observed in 2010 at all locations. Concentrations of the two nutrients N and P were correlated significantly with flow at all locations except at location 8. Negative slopes, signifying a dilution effect, were observed at locations 1, 2, 3, 4, and 6. At locations 5 and 7, a positive correlation between NO_3^- concentrations and flow was recorded indicating a continuous input of NO_3^- into the riverine system. Variations in rainfall and temperature were found to contribute greatly to the monthly variation in NO_3^- concentration.

The data from location 8 covered the period from 1989 to 2012, where the greatest changes in NO_3^- concentrations were observed after 1989. These changes could be related to several factors associated with the political and economic situations in Serbia. Due to the former, a large percentage of productive farms were abandoned, while industrial activity decreased. Furthermore, statutory regulation of the price of artificial fertilizers declined such that they became more expensive, resulting in a decline in their application. In addition to these socioeconomic factors, two major EU directives controlling nutrient losses to waters were implemented: the Nitrates Directive and the Urban Waste Water Treatment Directive.

Spatial variations in nutrient concentrations were treated statistically for two periods: locations from 4 to 8 were compared for the period from 2003 to 2012, and all locations were compared for the period 2006 to 2012. Significant differences in nutrient concentrations (ANOVA, $p<0.05$) were observed between locations 4 to 8 over the last 10 years. Values for locations 4 and 5 differed significantly from those at locations 6, 7, and 8; higher values were observed at locations 4 and 5 with mean values of 1.53±0.36 and 1.25±0.34 mg N l^{-1}. PO_4^{3-} concentrations differed at all locations, such as the highest mean concentration of 0.094±0.077 mg P l^{-1} was observed at location 5. Statistically significant spatial differences were also observed when short-term data were compared. Values of mean annual NO_3^- and PO_4^{3-} concentrations differed significantly between all locations for both nutrients (ANOVA, $p<0.05$), except for NO_3^- concentrations, which are similar at locations 3 and 4 and at locations 6 and 7. As expected, the lowest values were at location 1 with average values of 0.70±0.12 mg N l^{-1} and 0.01±0.01 mg P l^{-1}. The average NO_3^-concentrations at other locations ranged from 1.00±0.46 to 1.64±0.41 mg N l^{-1} with the lowest concentration observed at location 8 and the highest observed at location 2. Location 2 is close to Ljubljana city where exchange between surface water and groundwater is high. Agriculture is the main source of nitrate pollution in this area, but the discharges from urban areas with no or unregulated sewage systems could also contribute to the lower groundwater quality. The average nitrate concentrations in the Ljubljansko polje groundwater are not of immediate serious concern, but the groundwater quality can only be kept at the same level or improved if appropriate remedial measures are taken immediately (Jamnik and Urbanc 2000). The average PO_4^{3-} concentrations ranged from 0.03±0.03 to 0.063±0.037 mg P l^{-1}, with the lowest observed at location 3 and the highest observed at location 5, which is influenced by intensive agricultural activities.

In addition to changes from year to year, there were clear seasonal fluctuations in nutrient concentrations. Seasonal changes were statistically evaluated for each location separately. Seasonal changes in nutrient concentrations are illustrated using data for locations 5 and 8 as examples (Fig. 2). Statistically significant seasonal variations in NO_3^- concentrations (ANOVA, $p<0.05$) were observed for all locations, except location 2. Values were consistently higher in winter/autumn months than in spring/summer. The timing of this maximum reflects factors such as leaching of nitrate (which accumulates in the soil in summer and autumn), the high rates of soil water movement in the winter months, and the absence of nitrogen uptake by plants due to low temperatures in the winter period. In contrast, diminished soil water movement and increased plant uptake of nitrogen during low flow conditions causes NO_3^- concentrations to decrease to a minimum in July and August. Denitrification is not present since hypoxic/anoxic conditions are usually not present in the system. Concentrations of dissolved oxygen (DO) ranged from 6.07 to 18.9 mg l^{-1}. The study performed in late summer 2006 indicates that reductive conditions were present at locations 5, 6, and 7 at low flows and high temperatures (Ogrinc et al. 2008a). The concentration of oxygen was also low

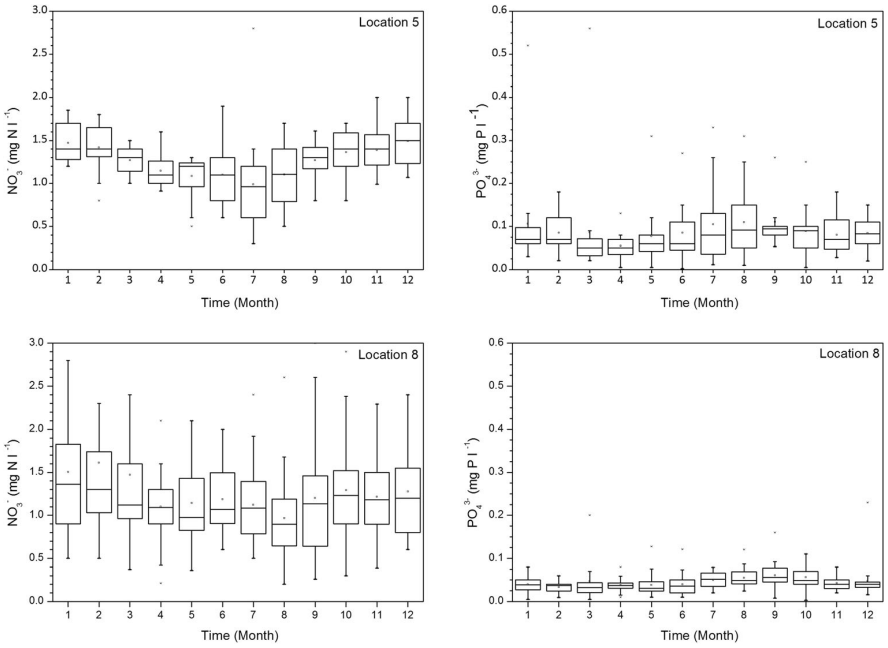


Fig. 2 Boxplots of NO_3^- and PO_4^{3-} concentrations grouped by month at locations 5 and 8 during the observation period

(5.5 mg l^{-1}), which was below the minimum state standard DO concentration of 6 mg l^{-1}. These conditions occurred as a consequence of nutrient enrichment and were confirmed by the presence of the diatom algae *Stephanodiscus hantzschii*. These algae are usually present in eutrophic environments, and their dynamics are also influenced by temperature and silica content (Jung et al. 2009). The reductive conditions were further indicated by the presence of framboidal pyrite on suspended particulate material (Ogrinc and Ščančar 2013).

No statistically significant temporal differences were observed in PO_4^{3-} concentrations at locations 1, 2, 3, 4, and 5. On the other hand, the differences at locations 6 and 8 were statistically significant, with the highest values observed in summer. The higher concentrations could be related to the lower flow conditions observed during the summer and the presence of reductive conditions that could release inorganic P from sediments into the water column (Billen et al. 2007). At both of these locations, there were higher concentrations of P in sediments (860±25 mg kg^{-1} and 930±30 mg kg^{-1}, respectively) compared to other locations (Milačič et al. 2009).

3.2 Trend analysis in water quality

The results of the trend analysis for nitrate and phosphate are presented in Table 2. The results of the trend analysis performed on NO_3^- concentrations show that there was a significant trend of decreasing levels, except for location 5 where NO_3^- concentrations exhibited no significant trend over the reporting period (p=0.77942). The reduction in NO_3^- concentrations ranged from 6 to 58 %, with the highest being observed at location 2 from 2006 to 2011 and the lowest at location 7 from 2003 to 2011. The trend in PO_4^{3-} concentrations exhibits different behavior. No significant trend was observed at location 1, which is located in a predominantly forested area, suggesting that most of the PO_4^{3-} is of natural origin. Furthermore, no significant trend was observed at locations 2 and 8. Trends at locations 3 to 6 show significant declines in PO_4^{3-} concentrations of 18–34 %. Trend data from rivers in other European countries have shown that about 30 % of the monitoring stations show a decreasing trend and 10 % an increasing trend in nutrient concentrations (both N and P) during the period 1991–2005 (Kronvang et al. 2008; Bouraoui and Grizzetti 2011).

Although there was no significant trend in PO_4^{3-} concentrations at location 8 (p=0.32283), the switch from a negative slope in the regression line for location 6 to a positive slope for location 8 suggests that inputs of PO_4^{3-} had been increasing downstream. This is possible given that location 8 has been more susceptible to nutrient inputs, mainly from wastewater effluent discharges. This assumption was further supported by our previous investigation conducted in 2006 (Ogrinc et al. 2008a). At this location and in the Sava River near Belgrade, elevated $\delta^{15}N_{NO3}$ values of up to +25.5‰ fall within the range of animal waste and sewage (Aravena et al. 1993; Fogg et al. 1998; McClelland and Valiela 1998; Wankel et al. 2006), and were only found in autumn 2006. During the high discharge in spring 2006, $\delta^{15}N_{NO3}$ values of ~7‰ did not show such a predominance of sewage-derived N. Previous studies have indicated that point sources could be relatively important at low flows when the contribution from diffuse catchment sources is lower (Bowes et al. 2005; Arnscheidt et al. 2007).

Table 2 Statistical results for linear regression (trend analysis) together with the minimum, maximum, and mean NO_3^- and PO_4^{3-} concentrations

No. of location	NO_3^- concentrations					
	Slope	Mean (mg N l^{-1})	Min (mg N l^{-1})	Max (mg N l^{-1})	R^2	p
1	−3.630E-5±1.399E-5	0.704±0.116	0.535	1.00	0.1752	0.0153
2	−7.945E-5±1.141E-5	1.640±0.412	0.967	2.69	0.5829	<0.001
3	−4.519E-5±8.289E-6	1.453±0.308	0.587	2.69	0.1390	<0.001
4	−3.691E-5±6.033E-6	1.512±0.359	0.60	3.30	0.1503	<0.001
5	−2.294E-6±8.181E-6	1.250±0.332	0.30	2.80	−0.004	0.7794
6	−3.855E-5±9.140E-6	1.075±0.323	0.30	2.60	0.0898	<0.001
7	−2.858E-5±6.906E-5	1.137±0.342	0.10	2.30	0.0593	<0.001
8	−4.668E-6±5.239E-6	1.171±0.590	0.05	5.20	0.2575	<0.001
	PO_4^{3-} concentrations					
	Slope	Mean (mg P l^{-1})	Min (mg P l^{-1})	Max (mg P l^{-1})	R^2	p
1	−5.854E-5±4.015E-5	0.009±0.006	0.0033	0.033	0.0431	0.15778
2	−5.879E-5±5.490E-5	0.038±0.028	0.0059	0.112	0.00471	0.29281
3	−1.457E-4±1.798E-5	0.034±0.031	0.0049	0.175	0.26534	<0.001
4	−1.231E-4±1.473E-5	0.071±0.053	0.005	0.35	0.25022	<0.001
5	−1.213E-4±1.158E-5	0.090±0.075	0.002	0.56	0.34428	<0.001
6	−7.116E-5±1.125E-5	0.066±0.034	0.01	0.20	0.18584	<0.001
7	–	–	–	–	–	–
8	8.530E-6±8.605E-6	0.050±0.033	0.003	0.25	−9.402E-5	0.32283

Trend analysis were performed for the period 1989–2012 at location 8, 2003–2012 at locations 4–7 and 2006–2012 at locations 1–3

It is known that point sources are the main source of nutrients in the SRB, constituting 54 % of the total N and P loads (ISRBC 2013). For N pollution, the input from agriculture (manure, fertilizers) is an important source with a contribution of 36.1 % of the total emission. For P, input from urban settlements is the most important source with a contribution of 63.5 % of the total emission. Nutrient input via atmospheric deposition as a pathway is <1 % of the total emission for both N and P (ISRBC 2013). In the SRB, there are either no or poorly performing urban wastewater treatment plants (UWWTP). The best wastewater collecting systems are in Slovenia, while in Serbia, 68 % of urban areas have no infrastructure for providing wastewater treatment services (ISRBC 2013). In addition, as of 2007, processes for nutrient removal at UWWTPs were implemented only in Slovenia (ISRBC 2013).

Many industrial facilities are also sources of nutrient pollution. Over the past two decades, the political and economic situation has caused changes in industrial activity in the SRB countries. This process has influenced the generated pollution load and the discharges of industrial wastewater, of which the chemical sector and intensive livestock production are the most important contributors. In 2007, it was identified that 40 % of industrial waste is discharged directly into surface water ecosystems, from which 71 % of industrial wastewater is discharged without treatment (ISRBC 2013).

Since the SRB belongs to the Danube watershed, the criteria established for sensitive areas have to be respected. The implementation of the Urban Wastewater Treatment Directives (UWWTD; Directive 91/271/EC) in the EU Member States and the development of wastewater infrastructure in non-EU countries are the most important measures to reduce nutrient pollution in SRB by 2015 and beyond. The transition period in Slovenia for implementation of UWWTD ends in 2017, and the results of the Croatian accession negotiation process with deadlines until 2023 were taken into consideration. At present, extensive improvements in urban wastewater treatment are being implemented throughout the basin, and the overall application of nutrient removal technologies is expanding. Based on the pollution reduction scenarios, the final effect of N and P reduction in 2015 relative to the year 2007 was estimated to be 55.1 and 61.2 %, respectively (ISRBC 2013). However, it must be pointed out that even if the nutrient management is successful, the results of other studies have indicated that at least 4 years will be required to detect any change (Stow et al. 2001; Kronvang et al. 2005; Bouraoui and Grizzetti 2011).

4 Conclusions

Comparison of results of nutrient concentrations at selected locations suggests that there is significant temporal and spatial

variability within the system. Spatial variability in the medium-term data showed that significantly higher annual mean concentrations of NO_3^- and PO_4^{3-} occurred in Croatia and Serbia at locations influenced by intensive agricultural activity. The temporal variability in nutrient concentrations is controlled by riverine flow, with the highest NO_3^- concentrations usually being observed during winter/autumn when leaching from soil was most intensive. The lowest NO_3^- concentrations, observed during summer, are mainly related to the reduction of NO_3^- due to phytoplankton uptake. On the other hand, the highest PO_4^{3-} concentrations are related to low flow conditions during the summer and the presence of reducing conditions that release inorganic P from sediments into the water column.

The results of trend analysis indicated that, at most locations, nutrient concentrations decreased by up to 58 %. However, sources have either varied (point vs. diffuse) or are uncertain. Nevertheless, the data suggest point sources, especially UWWTPs, are an important source of nutrients at most locations. Hence, all countries within the SRB should consider nutrient removal technologies during the upgrading of existing, or the construction of new, UWWTPs. This research illustrates the utility of long-term water quality monitoring data to provide the basis for empirical analysis and is thus useful for management-related studies.

Acknowledgments This study was supported financially by the EU 7th Research Project—GLOBAQUA (Managing the effects of multiple stressors on aquatic ecosystem under water scarcity). The research was partially conducted within a PhD study of Janja Vrzel financed by the European Social Fund. We thank the staff of Hrvatske vode and the Republic Hydrometeorological Service of Serbia who helped us obtain the discharge and water quality data. Special thanks are given to Roger H. Pain for linguistic corrections and two anonymous reviewers for their constructive comments that improved the quality of the paper.

Open Access This article is distributed under the terms of the Creative Commons Attribution 4.0 International License (http://creativecommons.org/licenses/by/4.0/), which permits unrestricted use, distribution, and reproduction in any medium, provided you give appropriate credit to the original author(s) and the source, provide a link to the Creative Commons license, and indicate if changes were made.

References

Aravena R, Evans ML, Cherry JA (1993) Stable isotopes of oxygen and nitrogen in source identification of nitrate from septic systems. Ground Water 31:180–186

Arnscheidt J, Jordan P, Li S, McCormick S, McFaul R, McGrogan HJ, Neal M, Sims JT (2007) Defining the sources of low-flow phosphorus transfers in complex catchments. Sci Total Environ 382:1–13

Billen G, Garnier J, Némery J, Sebilo M, Sferratore A, Barles S, Benoit P, Benoît M (2007) A long-term view of nutrient transfers through the Seine river continuum. Sci Total Environ 375:80–97

Bouraoui F, Grizzetti B (2011) Long term change of nutrient concentrations of rivers discharging in European seas. Sci Tot Environ 409: 4899–4916

Bowes MJ, Hilton J, Irons GP, Hornby DD (2005) The relative contribution of sewage and diffuse phosphorus sources in the River Avon catchment, southern England: implications for nutrient management. Sci Total Environ 344:67–81

Falkowski P, Scholes RJ, Boyle E, Canadell J, Canfield J, Elser J, Gruber J, Hibbard K, Högberg P, Linder S, Mackenzie FT, Moore B III, Pedersen T, Rosenthal Y, Seitzinger S, Smetacek V, Steffen W (2000) The global carbon cycle: a test of our knowledge of earth as a system. Science 290:291–296. doi:10.2307/3078125

Fogg GE, Rolston DE, Decker DL, Louie DT, Grismer ME (1998) Spatial variation in nitrogen isotope values beneath nitrate contamination sources. Ground Water 36:418–426

Hirsch RM, Douglas L, Moyer L, Archfield A (2010) Weighted regression on time, discharge, and season (WRTDS) with an application to Chesapeake bay river inputs. J Am Wat Res Assoc 46:857–880

ISRBC (2013) Sava River Basin management plan. Background paper no. 3: Significant pressures identified in the Sava River Basin, International Sava River Basin Commission, Zagreb, Croatia, 80 pp

Jamnik B, Urbanc J (2000) Origin and quality of groundwater from Ljubljansko polje. RMZ 47:167–178

Jones G, Armstrong N (2001) Long-term trends in total nitrogen and total phosphorus concentrations in Manitoba streams. Water Quality Management Section, Water Branch, Manitoba Conservation. Manitoba Conservation Report No. 2001-07, Winnipeg, Manitoba, Canada, 154 pp

Jung SW, Kwon OY, Lee JH, Han MS (2009) Effects of water temperature and silicate on the winter blooming diatom Stephanodiscus hantzschii (Bacillariophyceae) growing in eutrophic conditions in the Lower Han River, South Korea. J Freshwat Ecol 24:219–226

Kronvang B, Jeppesena E, Conley DJ, Søndergaarda M, Larsen SE, Ovesen NB, Carstensen J (2005) Nutrient pressures and ecological responses to nutrient loading reductions in Danish streams, lakes and coastal waters. J Hydrol 304:274–288

Kronvang B, Andersen HE, Børgesen C, Dalgaard T, Larsen SE, Bøgestrand J, Blicher-Mathiasen G (2008) Effects of policy measure implemented in Denmark on nitrogen pollution of the aquatic environments. Environ Sci Pol 11:144–152

Markovics R, Kanduč T, Szramek K, Golobočanin D, Milačič R, Ogrinc N (2010) Chemical dynamics of the Sava riverine system. J Environ Monit 12:2165–2176

McClelland JW, Valiela I (1998) Linking nitrogen in estuarine producers to land-derived sources. Limnol Oceanogr 43:577–585

Milačič R, Ščančar J, Murko S, Kocman D, Horvat M (2009) A complex investigation of the extent of pollution in sediments of the Sava River. Part 1: selected elements. Environ Monit Assess 163:263–275. doi:10.1007/s10661-009-0832-x

Ogrinc N, Ščančar J (2013) Suspended particulate matter and water quality of the Sava River Basin. River Syst 20:197–211

Ogrinc N, Markovics R, Kanduč T, Walter LM, Hamilton SK (2008a) Sources and transport of carbon and nitrogen in the River Sava watershed, a major tributary of the River Danube. Appl Geochem 23:3685–3698

Ogrinc N, Kanduč T, Stichler W, Vreča P (2008b) Spatial and seasonal variations in $\delta^{18}O$ and δD values in the River Sava in Slovenia. J Hydrol 359:303–312

Ogrinc N, Kanduč T, Kocman D (2015) Integrated approach to the evaluation of chemical dynamics and anthropogenic pollution sources in the Sava River Basin. In: Milačič R, Ščančar J, Paunović M (eds) The handbook of environmental chemistry vol. 31: the Sava River. Springer, Heidelberg, New York, Dordrecht, London, UK, pp 75–94

Stow CA, Borsuk ME, Stanley DW (2001) Long-term changes in watershed nutrient inputs and riverine exports in the Neuse River, North Carolina. Wat Res 35:1489–1499

Wankel SD, Kendall C, Francis CA, Paytan A (2006) Nitrogen sources and cycling in the San Francisco Bay Estuary: a nitrate dual isotope approach. Limnol Oceanogr 51:1654–1664

3.2 Determination of the Sources of Nitrate and the Microbiological Sources of Pollution in the Sava River Basin

In this sub-chapter I present the paper "Determination of the sources of nitrate and the microbiological sources of pollution in the Sava River Basin" by Janja Vrzel, Branka Vuković-Gačić, Stoimir Kolarević, Zoran Gačić, Margareta Kračun-Kolarević, Jovana Kostić, Mustafa Aborgiba, Andreas Farnleitner, Georg Reischer, Rita Linke, Momir Paunović and Nives Ogrinc. The paper was published in the journal Science of the Total Environment in 2016.

The observed decrease in nutrient concentrations in the Sava River Basin (SRB), should not make us satisfied with the current situation. The European Environmental Agency estimates that concentrations of nitrate in many European streams remain above natural levels (European-Environmental-Agency, 2018). Therefore, it is believed that even more effort should be put into the river "recovery" procedures. The presented paper deals with the determination of nutrient sources. I made an assessment of the levels of NO_3^- using a combination of N and O stable isotope and the level of microbial pollution in the Sava River under different hydrological conditions i.e., high and low river flow in 2014 and 2015, respectively. The study was intended to fill the information gaps related to riverine nutrient cycling and to evaluate whether the isotopic composition of riverine nitrate provides information about sources or processes, or a combination of both. The paper also includes the work of my colleagues from Belgrade, who applied biogeochemical and molecular methodologies to identify hotspots of pollution, and the use of microbial source tracking to identify the main sources of pollution.

The major finding is the significant spatial variability that exists in the levels of nutrients. In the areas where the Sava River is under stress due to intensive agricultural activity. I observed higher annual mean concentrations of NO_3^- and PO_4^{3-}. The temporal correlation between the river flow and the nutrient concentrations (already reported in the previous paper) supports my observation of significant temporal and spatial nutrient patterns in the Sava River, which correlate strongly with diverse land use and climatic conditions. In the upstream sampling location at Otoče, where forests predominate, the natural source of nitrogen is soil (Ogrinc, Markovics, nd Lynn M. Walter, & Hamilton, 2008). In addition, the climate conditions in the SRB are very heterogeneous comprising three main climatic interactions: Alpine, Pannonian, and Continental. This diversity means that the SRB represents an excellent location for environmental studies.

For the purpose of this paper I participated in a nine day sampling campaign, which was organized together with my Serbian colleagues in September 2014 within the project GLOBAQUA. Samples for water quality and biological analysis were collected at eight locations along the Sava River from its source in Zelenci in Slovenia to its confluence with the Danube River in Belgrade, Serbia. I also wrote and prepared the manuscript for publication.

Science of the Total Environment 573 (2016) 1460–1471

Contents lists available at ScienceDirect

Science of the Total Environment

journal homepage: www.elsevier.com/locate/scitotenv

Determination of the sources of nitrate and the microbiological sources of pollution in the Sava River Basin

Janja Vrzel [a,b], Branka Vuković-Gačić [c], Stoimir Kolarević [c], Zoran Gačić [d], Margareta Kračun-Kolarević [e], Jovana Kostić [d], Mustafa Aborgiba [c], Andreas Farnleitner [f], Georg Reischer [f], Rita Linke [f], Momir Paunović [e], Nives Ogrinc [b,g,*]

[a] Department of Geography, University of Munich, Luisenstraße 37, 80333 Munich, Germany
[b] Jožef Stefan International Postgraduate School, Jamova ulica 39, 1000 Ljubljana, Slovenia
[c] University of Belgrade, Faculty of Biology, Chair of Microbiology, Center for Genotoxicology and Ecogenotoxicology, Studentski trg 16, 11000 Belgrade, Serbia
[d] University of Belgrade, Institute for Multidisciplinary Research, Kneza Višeslava 1, 11030 Belgrade, Serbia
[e] University of Belgrade, Institute for Biological Research "Siniša Stanković", Bulevar despota Stefana 142, 11060 Belgrade, Serbia
[f] Vienna University of Technology, Institute for Chemical Engineering, Research Group Environmental Microbiology and Molecular Ecology, The Interuniversity Cooperation Centre Water & Health, Gumpendorfer Straße 1a, 1060 Vienna, Austria
[g] Department of Environmental Sciences, Jožef Stefan Institute, Jamova ulica 39, 1000 Ljubljana, Slovenia

HIGHLIGHTS

- There are spatial and temporal differences in nutrient concentrations in the Sava River Basin.
- The combination of soil nitrification and admixture of nitrate from wastewater and manure are the main sources of nitrate in autumn.
- Microbiological analyses showed the existence of hot spots of fecal pollution.
- Microbial source tracking analyses confirmed that the pollution is human associated.

GRAPHICAL ABSTRACT



ARTICLE INFO

Article history:
Received 14 June 2016
Received in revised form 29 July 2016
Accepted 29 July 2016
Available online 10 August 2016

Keywords:
Nutrients

ABSTRACT

Coupled measurements of nitrate (NO_3^-), nitrogen (N), and oxygen (O) isotopic composition ($\delta^{15}N_{NO3}$ and $\delta^{18}O_{NO3}$) were used to investigate the sources and processes of N cycling, while the microbial source tracking (MST) method was used to identify microbiological pollution in the surface water of the Sava River Basin (SRB) in autumn in 2014 and 2015 during high and low water discharge. Atmospheric nitrate deposition or nitrate-containing fertilizers were found not to be significant sources of riverine nitrate in the SRB. The ranges of isotope values suggest that NO_3^- in the SRB derives from soil nitrification, sewage, and/or manure, which were further supported by MST analysis. Microbiological indicators show the existence of hotspots of fecal pollution

* Corresponding author at: Jožef Stefan International Postgraduate School, Jamova ulica 39, 1000 Ljubljana, Slovenia.
E-mail addresses: j.vrzel@iggf.geo.uni-muenchen.de (J. Vrzel), brankavg@bio.bg.ac.rs (B. Vuković-Gačić), stoimirk@bio.bg.ac.rs (S. Kolarević), zorga@imsi.rs (Z. Gačić), margareta.kracun@ibiss.bg.ac.rs (M. Kračun-Kolarević), kosticjovana@hotmail.com (J. Kostić), mustafab@bio.bg.ac.rs (M. Aborgiba), andreas.farnleitner@wavenet.at (A. Farnleitner), georg.reischer@tuwien.ac.at (G. Reischer), rita.linke@tuwien.ac.at (R. Linke), mpaunovi@ibiss.bg.ac.rs (M. Paunović), nives.ogrinc@ijs.si (N. Ogrinc).

http://dx.doi.org/10.1016/j.scitotenv.2016.07.213
0048-9697/© 2016 The Authors. Published by Elsevier B.V. This is an open access article under the CC BY-NC-ND license (http://creativecommons.org/licenses/by-nc-nd/4.0/).

Stable isotopes
Microbial source tracking
Fecal indicators
Sava River Basin

in the SRB, which are human associated. Long-term observations indicate persistent fecal contamination at selected locations caused by continuous discharge of untreated wastewaters into the SRB.

© 2016 The Authors. Published by Elsevier B.V. This is an open access article under the CC BY-NC-ND license (http://creativecommons.org/licenses/by-nc-nd/4.0/).

1. Introduction

During the last two decades, much effort has been invested into understanding the nutrient cycles, heightened by problems associated with global, regional and local environmental problems (Heatwaite, 2010). These problems result in part from increased fluxes of nutrients such as nitrogen (N) and phosphorous (P) compounds into water bodies that can lead to eutrophication, causing ecological changes including loss of plant and animal species. In addition, these fluxes can influence the quality of water for human consumption and other purposes. In many river catchments the main source of N pollution is run-off from agricultural land, although discharges from wastewater treatment works can also be significant. According to the European Environmental Agency current concentrations of nitrate are still above what might be considered to be 'background' or natural levels, except in the northern European countries (EEA, 2015). Thus control of these nutrient discharges is needed to reduce pollution levels in water bodies.

For solving problems related to loading of nutrients such as N, tools are needed for identifying sources of N, often a challenging task. Isotope techniques constitute a promising tool for determining sources of nitrate (NO_3^-) in surface water and could help to identify the processes that NO_3^- has undergone in the aquatic system. This is possible because the isotopic signature in NO_3^- from fertilizer, atmospheric, soil and manure-derived sources differs sufficiently to enable an unambiguous distinction to be made between them (Hebert and Wassenaar, 2001; Chang et al., 2002; Mayer et al., 2002; Voss et al., 2006). However, the origin of NO_3^- must be linked to the entire N cycle, since values of $\delta^{15}N$ of NO_3^- can be biased due to the mixing of different NO_3^- sources or to isotope fractionation occurring during various processes (nitrification, denitrification, assimilation, remineralization) (Kendall et al., 2008). The dual isotope approach, based on the determination of $\delta^{15}N$ and $\delta^{18}O$ values of NO_3^-, provides more conclusive information for tracing sources of NO_3^- in water (Widory et al., 2004; Seiler, 2005; Xue et al., 2009). However, in the case of discriminating between sewage and manure the $\delta^{15}N$ and $\delta^{18}O$ values of NO_3^- overlap and this approach could not be used to differentiate between these two sources. The contamination of water bodies by sewage or manure is generally determined using the detection of Fecal Indicator Bacteria (Kirschner et al., 2014). Specific differentiation between sources of fecal contamination is of particular importance, because the risk to humans is usually considered higher from human fecal contamination (sewage) than from animal fecal contamination. New approaches based on PCR quantification and biomarker analysis could be used to track microbiological sources of contamination. The human-associated fecal marker BacHum (Kildare et al., 2007) and a recently modified version of the HF183II (Green et al., 2014) could be used to track human associated fecal pollution, while the ruminant-associated BacR qPCR assay (Reischer et al., 2006) and the pig-associated Pig2Bac qPCR assay (Mieszkin et al., 2009) are the methods for detecting animal fecal pollution sources. The contamination of water by fecal pollution leads to exposure to pathogens via drinking water production, recreation or irrigation. However, monitoring the microbiological quality of surface waters is quite neglected despite its importance for human health (Kittinger et al., 2013).

In the case of the Sava River Basin (SRB), many of the settlements situated on the river banks discharge large quantities of untreated or improperly treated wastewaters directly into surface waters (Kapetanović et al., 2015; Aborgiba et al., 2016). On the other hand, in the middle and lower course, the Sava River flows through regions of intense agriculture: the Slavonija in Croatia, the Bosanska Posavina and the Semberija in Bosnia and Herzegovina and the Srem in Serbia, together cover an area >100,000 km^2 (Paunović et al., 2012). The results of long-term trend analysis show a reduction of NO_3^- at the majority of locations in the SRB, ranging from 8 to 58%, the highest being observed at Litija in Slovenia from 2006 to 2011 and the lowest at Županja in Croatia from 2003 to 2011 (Vrzel and Ogrinc, 2015). In addition, a switch from a negative to a positive trend in phosphate (PO_4^{3-}) concentration was observed at Sremska Mitrovica indicating that this location has been more susceptible to nutrient inputs, mainly from wastewater effluent discharges. This assumption was further supported by the investigation performed in autumn 2006. At this location and in the Sava River near Belgrade, elevated $\delta^{15}N_{NO3}$ values of up to +25.5‰ were determined (Ogrinc et al., 2008). The high $\delta^{15}N_{NO3}$ values obtained fall within the range of animal waste and sewage (Aravena et al., 1993; Fogg et al., 1998; McClelland and Valiela, 1998; Wankel et al., 2006), and were only found in autumn 2006 during extremely low water discharge. Due to the use of water for irrigation, evaluation of the microbiological quality of the Sava River becomes essential for further river management. One of the pathways of exposure to contaminated water that must not be neglected is flooding. The study of Casteel et al. (2006) indicated that flooding can result in extensive fecal contamination of nearby agricultural soil with pathogens.

The aim of the present study was to assess the sources of NO_3^- using a combination of the N and O stable isotope approach and the level of microbial pollution in the SRB under different hydrological conditions – in 2014 during high water levels and in 2015 during low water levels. This study was performed to fill the gaps in the information related to riverine nutrient cycling and to evaluate whether the isotopic composition of riverine nitrate provides source or process information, or a combination of both. Related work performed in 2005 and 2006 published by Ogrinc et al. (2008) quantifies the sources of riverine N throughout the SRB using only stable isotope composition of N in NO_3^-, while to our knowledge no research including biomarker analysis to track microbiological sources of contamination has been performed in the whole SRB. Thus, this interdisciplinary study taking into account biogeochemical and molecular approaches has been applied for the first time in the SRB and was used to identify the hotspots of pollution, while microbial source tracking was used to identify the major sources of pollution.

2. Materials and methods

2.1. Study site

The main characteristics of the Sava watershed are summarized according to the report of the International Sava River Basin Commission (ISRBC, 2011). The River Sava is 990 km long, including the 45 km Sava Dolinka headwater rising at Zelenci, Slovenia. It is the greatest tributary of the Danube in terms of volume of water, and the second-largest after Tisza in terms of its catchment area of 97,713 km^2. The Sava flows through four countries in the Balkan Peninsula: Slovenia, Croatia, along the northern border of Bosnia and Hercegovina, and through Serbia. Climatic conditions and physical features, such as morphology, geology, pedology and vegetation, of the SRB are highly heterogeneous. The Sava flows through a variety of landscape types, including alpine, karstic, deep river valleys and shallow Pannonian flats. The average bottom slope of 15.8% qualifies the Sava as a typical lowland or middle course river starting in the central flow in Slovenia.

The SRB is divided into three climatic areas: Alpine, Pannonian and Continental. In the Alpine areas, in Slovenia, the mean annual precipitation is the highest (2000–3000 mm/y) and the mean annual temperature the lowest (6 °C). On the other hand, in the Continental area, in

Serbia, annual precipitation decreases to around 660 mm/y and the mean annual temperature increases to about 13 °C. The average discharge of the Sava increases downstream from 84 m^3/s at Ljubljana to 255 m^3/s at Zagreb, to 1722 m^3/s at Belgrade. Further, the increase gradient of solar radiation was observed in the SRB from 3713 MJ m^{-2} determined in the Alpine region, through 4013 MJ m^{-2} in Continental region to 4135 MJ m^{-2} in Pannonian region (http://solarelectricityhandbook.com/solar-irradiance.html).

The large retention areas of the Sava are one of the most effective flood control systems in Europe. Its management is seen as an international model for sustainable flood management. The backwater effect of the Iron Gate Dam (Djerdap I) during low flow of Sava is observed almost up to the town of Šabac at 105 km from Belgrade.

The geology of the River Sava basin is diverse. The most important geological characteristic influencing the regime of water and sediment of the SRB is the presence of the karst regions in the southern part of the river basin. The rest of the river basin, between the External Dinarides and the border of the Sava catchment belongs to the Inner Dinarides zone and Pannonian basin. In this zone the following lithological units are present: sandstone, marls, claystones, intrusive and extrusive igneous rocks (diabase, spilite, dacite, andesite etc.), metamorphic rocks (serpentinite, phylite, argiloshist etc.). The main aquifers are formed in alluvial deposits representing the large reserves of groundwater (Ogrinc et al., 2010). According to Harmonized World Soil database, the soils with the largest extent are the Cambisols (weakly to moderately developed soils) that cover 46.4% of the basin. Other important soil groups are the Luvisols, Leptosols, Podzoluvisols (leached soils) and Fluvisols. Geology and soils play an important role in sediment formation in the SRB. Previous research indicates that soil was the dominant source of particulate organic matter (Ogrinc et al., 2008). A rather sharp transition from a gravel-bed river (at the Upper Sava) to a sand-bed river (at the Middle Sava) is present in the SRB. Grain size distribution shows the presence of silt or clay and except at the Šabac (location 11) a uniform composition of sand particles was observed. However no clear correlation between the part of fine fraction and location was obtained, although in the lower, flat part of the river the percentage of fine particles in sediments can reach up to 90% of the total sediment content (Globevnik et al., 2010).

Land use of the SRB reflects the differences in relief, climate and stream flow. The greatest population density is located near large cities. Three capitals are located near the Sava: Ljubljana, Zagreb and Belgrade. Agriculture is the dominant activity in the Croatian (40%) and Serbian (~100%) parts of the watershed, while the upper part, in Slovenia, is mainly covered by forest (>50%). The Bosnian part of the watershed is dominated by valleys and hills, with about 30% agricultural area and 30% forest. For these four countries, the basin catchment area comprises 60–70% of their land and is the source of >80% of total available water. Due to important hydropower generation, industrial and agricultural activities, and a high population density, especially near large cities (Ljubljana, Zagreb, Belgrade), strong anthropogenic influences on water quality are expected.

2.2. Sampling

2.2.1. Sample collection

Two sampling campaign at the SRB, performed within the scope of the GLOBAQUA project (Navarro-Ortega et al., 2015), are presented in this paper and cover the period of the high and the low water discharge in September 2014 and 2015, respectively, at 12 locations from its source in Slovenia to the confluence with the Danube in Serbia (Fig. 1). At some sampling stretches two sampling locations were selected (marked as 'a') in order to obtain a representative water body for further investigation. Thus, altogether 17 locations were selected in 2014, while samples from 15 locations were obtained in 2015. For microbiological characterization additional samples were collected from 4 wastewater outlets detected in 2015 at the following locations: Radovljica – location 2 (RWW), Zagreb – location 6 (ZWW), Sremska Mitrovica - location 10a (SMWW) and Šabac – location 11 (ŠWW).

Discharge and water quality data for long-term periods 2006–2012, 2003–2012 and 1989–2012 were provided by the Environmental Agency of the Republic Slovenia (ARSO; URL: http://www.arso.gov.si/), Hrvatske vode (URL: http://www.voda.hr) and the Republic Hydrometeorological Services of Serbia (http://www.hidmet.gov.rs).

Hydrologic balance depends primarily on climatic conditions and physical features of the catchments and its spatial distribution is heterogeneous. In general, Sava has the largest discharge in spring and the lowest in late summer. However, seasonal and annual maxima and minima of discharge vary according to the locations (ISRBC, 2011).

2.2.2. Field measurements

Temperature (T), pH, electrical conductivity (ElCo) and dissolved oxygen (DO) were measured in the field. T and DO were measured directly in the stream, using a VTV OXI model 91 m. ElCo was measured using a Corning 316 m with a two point calibration at 0 μS and 1413 μS. The precisions of DO saturation and ElCo measurements were within ±5%. Because pH is sensitive to degassing and warming, water samples were collected in a large volume, air-tight container and pH was measured at least twice to verify electrode stability, using a Corning 315 high sensitivity pH meter coupled with an Orion Ross electrode. The pH meter was calibrated on the NBS scale using two buffers (pH 4.10 and 6.97) with a reproducibility of ±0.02 pH units.

Sample aliquots collected for chemical analysis were passed through 0.45 μm membrane filters into bottles and kept refrigerated until analysed. Samples for anions, total alkalinity and stable isotope analysis of nitrate ($\delta^{15}N_{NO3}$, $\delta^{18}O_{NO3}$) were collected in HDPE bottles. Samples for determining the stable isotope composition of oxygen ($\delta^{18}O$) were stored in HDPE bottles without filtering. Samples for carbon isotope analyses of dissolved inorganic carbon ($\delta^{13}C_{DIC}$) were capped in glass serum vials filled with no headspace. Particulate material for stable C and N isotopic analyses was collected on precombusted Whatman glass fiber filters (GF/F) by filtering 1–2.5 L of water using a pump connected to a Teflon filter holder. Filters were wrapped in aluminum foil.

The samples for microbiological analysis were collected within 10 days of survey at approximate the same time of the day. In all cases, water samples were collected in sterile, 1 L glass bottles from about 30 cm below the water surface. Samples were kept in dark, cool boxes prior to analysis and analysed within 3 h of arrival in the laboratory.

2.3. Chemical and stable isotope analysis

2.3.1. Chemical analysis

Total alkalinity (TA) was determined within 24 h of sample collection by the Gran titration method, with a precision of ±1%. Concentrations of nitrate (NO_3^-), nitrite (NO_2^-), ammonium (NH_4^+) and phosphate (PO_4^{3-}) were analysed using standard colorimetric methods (Grasshoff et al., 1983) with a precision of measurement ±3%. Concentrations of dissolved organic carbon (DOC) were measured with a Shimadzu TOC-5000 instrument with an analytical precision of ±2%.

2.3.2. Stable isotope analysis

The isotopic composition of oxygen ($\delta^{18}O$) was determined by standard water–CO_2 equilibration technique (Epstein and Mayeda, 1953) on a Multiflow continuous flow isotope ratio mass spectrometer (Isoprime GV Instruments).

Isotope analyses of nitrogen and oxygen of NO_3^- were carried out by Hydroisotop GmbH, Schweitenkirchen, Germany using the denitrifier method (Sigman et al., 2001; Casciotti et al., 2002), which is based on the isotopic analysis of nitrous oxide (N_2O) produced by denitrifying *Pseudomonas* strains. The measurements were performed on a Gas

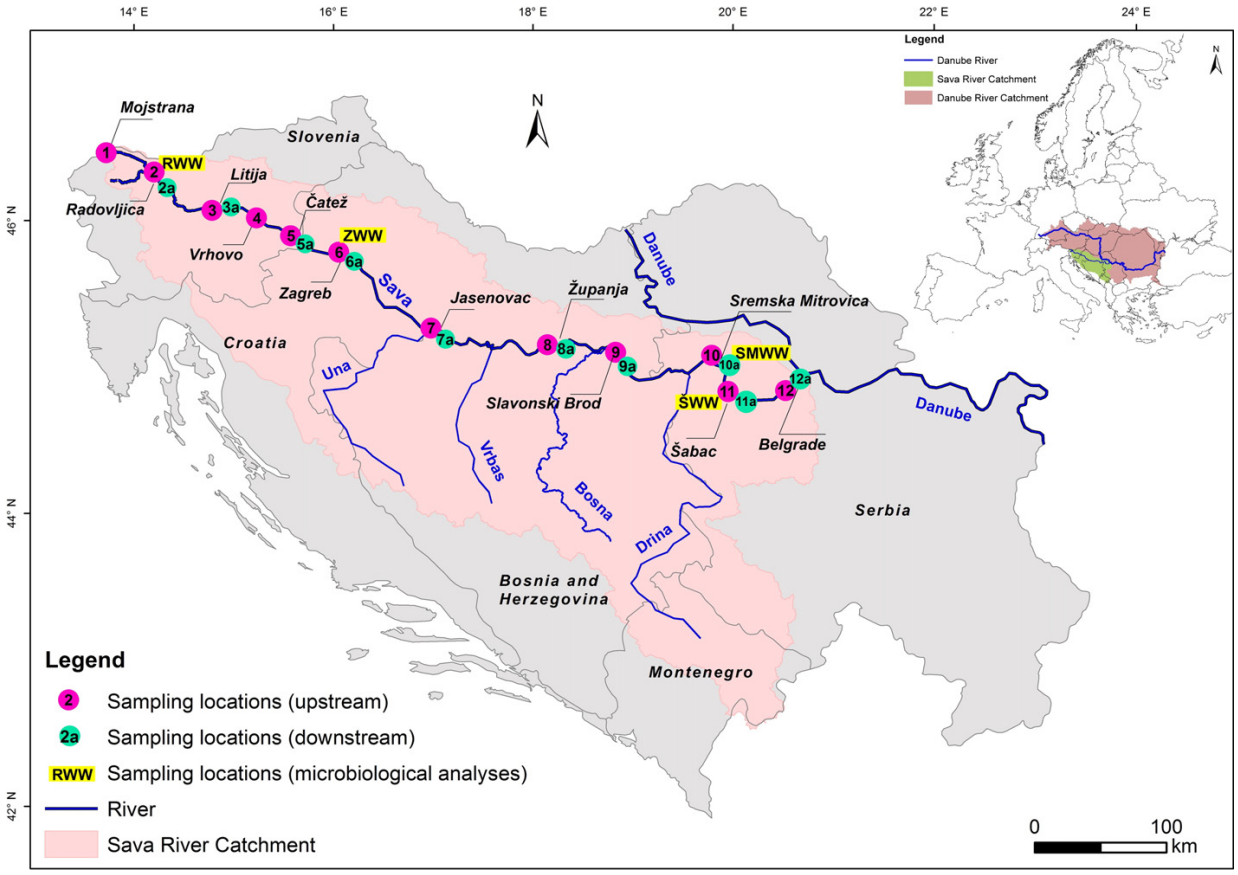


Fig. 1. Map of selected monitoring locations in the Sava River Basin in September 2014 and 2015.

Bench (Thermo Finnigan Gas Bench II) coupled to an isotope ratio mass spectrometer Delta Plus XP.

$\delta^{13}C_{DIC}$ values were determined after extraction as CO_2 in glass septum tubes (VACUTAINER Septum Tubes, Labco Limited, UK) by Europa Scientific 20–20 mass spectrometer with an ANCA-TG preparation module for trace gas samples using the procedure described by Ogrinc et al. (2008). The samples collected on Whatman GF/F filters for carbon and nitrogen isotopic analysis ($\delta^{15}N_{TPN}$ and $\delta^{13}C_{POC}$) were first dried at 40 °C. $\delta^{13}C_{POC}$ values were determined after treatment with 1 M HCl to remove carbonate minerals, while $\delta^{15}N_{TPN}$ values were determined on the bulk samples without acidification. $\delta^{13}C_{POC}$ and $\delta^{15}N_{TPN}$ values were measured with a Europa Scientific 20–20 mass spectrometer with an ANCA-SL preparation module.

All stable isotope results are reported using conventional delta (δ)-notation in per mil (‰) relative to a suitable standard: for oxygen VSMOW standard was used, while for carbon and nitrogen VPDB and AIR standards were used, respectively. The results were calibrated against the following international reference materials: IAEA-CH-7 (polyethylene; $\delta^{13}C = -32.15 \pm 0.05$‰) and IAEA-CH-6 (sucrose; $\delta^{13}C = -10.45 \pm 0.03$‰) for carbon; IAEA-N-1 (ammonium sulfate; $\delta^{15}N = 0.4 \pm 0.2$‰) and IAEA-N-2 (ammonium sulfate; $\delta^{15}N = 20.3 \pm 0.2$‰) for nitrogen; IAEA-NO-3 (potasium nitrate; $\delta^{15}N = 4.7 \pm 0.2$‰ and $\delta^{18}O = 25.6 \pm 0.4$‰) for nitrogen and oxygen; SLAP2 (Standard Light Antarctic Precipitation; $\delta^{18}O = -55.50 \pm 0.02$‰) and GISP (Greenland Ice Sheet Precipitation; $\delta^{18}O = -24.76 \pm 0.09$‰) for oxygen. Reproducibility of the measurements was ±0.1‰ for $\delta^{18}O$, ±0.2‰ for $\delta^{13}C_{DIC}$ and ±0.3‰ for $\delta^{15}N$ and $\delta^{18}O$ in NO_3^-. The mean standard deviations for replicate POM samples were higher: 0.4‰ and 0.5‰ for $\delta^{13}C_{POC}$ and $\delta^{15}N_{TPN}$, respectively, perhaps reflecting more subsampling error in these particulate samples.

2.4. Microbiological analysis

2.4.1. Detection of total coliforms, Escherichia coli and enterococci

Defined Substrate Technology (DST) was used to detect total coliforms (TC), *E. coli* (EC) and enterococci (FE). This enables isolation and identification of certain groups of bacteria by enzymatic hydrolysis of specific substrates (Buckalew et al., 2006). Quantification was performed with Colilert Quanti-Tray 2000 system, which provides a Most Probable Number (MPN) result, based on color/fluorescence change in 97 wells. For coliform bacteria two dilutions were analysed (1:10 and 1:1000) while for enterococci only one dilution was analysed (1:10). Powdered reagents Colilert-18 and *E*-enterolert were used for cultivation of coliforms and enterococci respectively. A diluted water sample was mixed with powdered reagents and poured into Quanty-Tray, a sterile plastic disposable 97-well tray. For coliforms, trays were incubated at 37 °C for at least 18 h. Enterococci were incubated for at least 24 h at 44 °C.

After incubation, an appearance of yellow color in wells was indicative of the presence of total coliforms. Fluorescence in wells, under UV illumination (365 nm) was used as an indication of the presence of *E. coli*, in Colilert, and enterococci in Enterolert-E. The number of positive wells was scored and converted to MPN using tables provided by the manufacturer. Assessment of the water quality was based on the total

coliforms, *E. coli* and enterococci classification scheme suggested by Kirschner et al. (2009) and was expressed as MPN/100 mL.

2.4.2. Detection of presumptive Clostridium perfringens by the membrane filtration method

Before the filtration, water samples were pasteurized for 15 min at 60 °C. *C. perfringens* (CP) were enumerated by membrane filtration and incubation on Tryptose Sulphite Cycloserine (TSC) media according to ISO 14189:2013 and the number of cells expressed as CFU/100 mL of sample.

2.4.3. Microbial fecal source tracking

2.4.3.1. Sample preparation and DNA extraction. Water samples for MST were collected, only during the 2015 survey from all 15 studied locations. Triplicate subsamples, between 150 and 200 mL, were filtered through 0.2 μm polycarbonate filters. Filtration volume was. Filters were immediately frozen at −20 °C. Clean filters were frozen and stored alongside the sample filters as filtration controls. DNA was extracted from two series of filters by a phenol-chloroform extraction combined with bead-beating (Reischer et al., 2008). DNA was dissolved in 100 μL Tris buffer. Extraction controls were routinely run alongside each extraction batch. Prior to the qPCR assays, DNA concentration in the extracts was measured by the PicoGreen assay according to the manufacturer's instructions (QuantiFluor® dsDNA Sytem, Promega, Madison, WI, USA) on a Anthos Multimode Fluorometer Zenyth 3100 (UK-Biochrom Ltd.).

2.4.3.2. qPCR quality assurance and inhibition control. Sample DNA was diluted 1:4 and 1:16 and the AllBac assay (Layton et al., 2006) applied to ensure the presence of amplifiable bacterial DNA and the absence of inhibition. An internal amplification control was also included in the AllBac assay.

2.4.3.3. Microbial fecal source tracking assays. The human-associated fecal marker BacHum (Kildare et al., 2007) and a recently modified version of the HF183II (Green et al., 2014) were enumerated by quantitative PCR (qPCR), to indicate human associated fecal pollution. The ruminant-associated BacR qPCR assay (Reischer et al., 2006) and the pig-associated Pig2Bac qPCR assay (Mieszkin et al., 2009) were included as methods for detecting animal fecal pollution sources. All these qPCR assays were adapted to run on the Rotor-Gene Q thermocycler with the Rotor-Gene Multiplex PCR mastermix (Qiagen Inc.). Quantification was achieved by running plasmid standard dilution series of known concentration. No template controls (containing no DNA) were applied in all instrument runs.

For the AllBac qPCR reaction the mixture was composed of 2.5 μL of the 1:4 or 1:16 sample DNA dilution, 600 nmol/L primer AllBac296f, 600 nmol/L primer AllBac412r, 25 nmol/L TaqMan MGB AllBac375Bhqr, 0.4 μg/μL of bovine serum albumin (Roche, Vienna, Austria), 7.5 μL of Rotor-Gene Multiplex PCR Kit (total volume of 15 μL). An internal amplification control was included in the AllBac qPCR reaction mixture comprised 500 nmol/L primer IPC-ntb2-F, 500 nmol/L primer IPC-ntb2-R, 200 nmol/L probe IPC-ntb2-P and IAC template (1000 copies/2.5 μL).

For the BacHum qPCR reaction, the mixture was composed of the following: 2.5 μL of the 1:4 sample DNA dilution, 400 nmol/L primer BacHum-160f, 400 nmol/L primer BacHum-241r, 80 nmol/L TaqMan probe BacHum-193p, 0.4 μg/μL of bovine serum albumin (Roche, Vienna, Austria), 7.5 μL of Rotor-Gene Multiplex PCR Kit (total volume of 15 μL).

For the HF183II qPCR reaction, the mixture was composed of the following: 2.5 μL of the 1:4 DNA dilution, 1 μmol/L primer HF183, 1 μmol/L primer BacR287, 80 nmol/L TaqMan probe BacP234MGB, 0.4 μg/μL of bovine serum albumin (Roche, Vienna, Austria) and 7.5 μL of Rotor-Gene Multiplex PCR Kit (total volume of 15 μL).

For the BacR qPCR reaction, the mixture was composed of the following: 2.5 μL of 1:4 sample DNA dilution, 100 nmol/L primer BacR_f, 500 nmol/L BacR_r, 100 nmol/L TaqMan MGB probe BacR_p, 0.4 μg/μL of bovine serum albumin (Roche, Vienna, Austria) and 7.5 μL of Rotor-Gene Multiplex PCR Kit (total volume of 15 μL).

For the Pig-2-Bac qPCR reaction, the mixture was composed of the following: 2.5 μL of 1:4 sample DNA dilution, 300 nmol/L primer Pig-2-Bac41F, 300 nmol/L Pig-2-Bac163R, 200 nmol/L TaqMan MGB probe Pig-2-Bac113MGB, 0.4 μg/μL of bovine serum albumin (Roche, Vienna, Austria) and 7.5 μL of Rotor-Gene Multiplex PCR Kit (total volume of 15 μL).

The PCR program was as follows: 95 °C for 5 min, 45 cycles of 95 °C for 30 s (AllBac) and for 15 s (all other assays), 60 °C for 45 s (AllBac) and 60 s (all other assays).

All reactions were performed in duplicate. A total of seven 10-fold serial dilutions of plasmid standard (1–10^6 gene copies) were run in duplicate as well as a no-template control. The results of quantitative

Table 1
Physico-chemical, nutrient and stable isotope parameters in late summer 2014.

Sampling site				Physico-chemical parameters					Nutrients					Isotopes					
Code	Date	Latitude (N)	Longitude (E)	T °C	pH	O_2 %	ElCo μS/cm	TA meq/kg	NO_3^- mg L^{-1}	NO_2^-	NH_4^+	PO_4^{3-}	DOC mg L^{-1} C	$\delta^{18}O$ ‰	$\delta^{15}N_{NO3}$	$\delta^{18}O_{NO3}$	$\delta^{15}N_{TPN}$	$\delta^{13}C_{DIC}$	$\delta^{13}C_{POC}$
2	01/09/2014	46.34	14.17	10.84	7.70	93.3	277	1.747	2.11	0.07	0.09	3.2	3.2	−10.0	0.1	11.1	1.0	−7.9	−26.7
2a	01/09/2014	46.29	14.26	11.52	8.44	91.2	286	1.900	2.33	0.05	0.15	0.10	2.5	−10.2	1.1	10.6	2.9	−9.1	−26.5
3	02/09/2014	46.06	14.81	12.24	7.55	96.8	279	n.a.	3.73	n.a.	n.a.	n.a.	1.6	−9.6	3.7	9.4	1.1	−8.4	−26.5
3a	02/09/2014	46.07	14.85	13.53	7.81	82.6	290	2.177	3.27	0.06	0.1	1.6	2.4	−9.3	4.7	9.8	1.1	−11.1	−26.1
5	03/09/2014	45.90	15.63	14.07	7.85	130	340	1.825	3.77	0.17	0.1	10.6	2.9	−9.3	3.4	9.0	2.2	−11.6	−27.3
5a	03/09/2014	45.87	15.65	13.33	7.73	117	381	2.194	1.69	0.04	0.35	0.48	2.7	−9.1	3.7	8.9	2.9	−12.3	−26.6
6	04/09/2014	45.78	16.00	13.98	7.52	96.8	361	2.150	1.77	0.04	0.76	<0.06	3.6	−9.1	4.5	9.4	4.0	−12.4	−26.8
6a	04/09/2014	45.76	16.05	14.12	7.96	97.4	363	2.358	2.53	0.06	0.09	1.6	2.5	−9.1	4.9	11.9	3.5	−12.0	−27.2
7	05/09/2014	45.26	16.89	15.06	8.14	68.3	283	2.415	3.58	0.04	0.05	6.8	4.8	−8.8	5.0	10.8	6.4	−13.1	−26.9
7a	05/09/2014	45.25	16.95	14.32	7.99	78.2	246	2.274	3.22	0.05	<0.02	0.16	2.5	−9.0	4.3	11.1	0.3	−12.9	−27.2
8	06/09/2014	45.15	18.01	15.25	7.66	81.6	320	2.038	1.82	0.07	<0.02	0.16	3.6	−9.0	3.1	8.1	3.5	−11.8	−26.1
8a	06/09/2014	45.13	18.09	15.84	7.65	76.2	352	2.338	0.73	0.24	0.19	<0.06	2.9	−8.8	4.2	8.6	3.6	−12.9	−26.4
9	07/09/2014	45.08	18.69	15.73	7.55	74.0	350	1.982	3.22	0.04	0.2	1.4	3.0	−8.8	3.2	8.5	4.5	−12.3	−25.7
9a	07/09/2014	45.02	18.74	16.12	7.95	75.2	367	1.880	2.55	0.05	0.2	2.3	3.9	−8.9	4.2	10.0	4.1	−11.7	−25.8
10	08/09/2014	45.97	19.60	16.49	7.61	79.8	327	1.912	3.52	0.05	0.07	1.3	3.0	−8.9	4.7	9.9	3.8	−12.6	−26.2
10a	08/09/2014	44.91	19.75	16.66	8.71	80.0	320	2.501	3.60	0.05	0.06	1.5	4.8	−8.9	4.5	10.1	4.8	−12.6	−25.7
12	09/09/2014	44.77	20.81	17.26	7.57	77.5	340	2.343	2.26	0.06	0.13	0.8	3.0	−8.9	4.4	8.8	5.6	−11.3	−26.8
12a	09/09/2014	44.81	20.44	17.16	8.03	76.2	334	2.762	3.86	0.05	0.06	0.9	2.6	−8.9	4.6	9.9	3.8	−12.2	−26.4

n.a. – not analysed.

Table 2
Physico-chemical, nutrient and stable isotope parameters in late summer 2015.

Sampling site				Physico-chemical parameters					Nutrients					Isotopes					
Code	Date	Latitude (N)	Longitude (E)	T °C	pH	O_2 %	ElCo µS/cm	TA meq/kg	NO_3^- mg L^{-1}	NO_2^-	NH_4^+	PO_4^{3-}	DOC mg L^{-1} C	$\delta^{18}O$ ‰	$\delta^{15}N_{NO3}$	$\delta^{18}O_{NO3}$	$\delta^{15}N_{TPN}$	$\delta^{13}C_{DIC}$	$\delta^{13}C_{POC}$
1	01/09/2015	46.49	13.74	9.9	7.10	80.7	210	2.921	1.44	<0.02	<0.05	n.a.	1.41	−10.82	−2.7	8.9	4.1	−8.2	−26.9
2	01/09/2015	46.34	14.17	14.5	8.20	103	230	2.908	2.92	0.034	0.158	n.a.	1.66	−10.02	1.6	8.9	0.0	−7.8	−27.2
3	02/09/2015	46.06	14.81	17.6	8.80	101	260	3.790	6.48	n.a.	n.a.	0.108	1.93	−9.29	3.4	9.6	9.3	−10.2	−28.7
3a	02/09/2015	46.07	14.85	17.7	7.62	94.6	100	3.882	6.69	0.128	<0.05	0.154	1.93	−9.30	4.0	8.8	4.3	−10.2	−29.2
4	02/09/2015	46.04	15.24	20.2	7.82	96.6	280	3.843	6.53	0.034	0.086	0.024	2.12	−9.21	4.5	10.1	n.a.	−10.2	−28.3
5	03/09/2015	45.90	15.63	23.1	7.75	106	320	3.924	4.57	0.032	<0.05	n.a.	2.14	−9.35	5.0	7.1	4.0	−10.0	−29.4
6	04/09/2015	45.78	16.00	22.6	7.72	107	285	4.077	4.23	0.03	<0.05	n.a.	2.32	−9.22	6.1	7.5	5.5	−10.2	−29.4
7	05/09/2015	45.26	16.89	23.8	7.41	69.0	270	4.080	5.39	0.106	<0.05	0.151	2.84	−9.25	4.2	10.9	5.9	−10.8	−28.6
8	05/09/2015	45.15	18.01	24.8	7.83	100	336	3.969	4.32	0.032	<0.05	0.094	2.78	−9.31	6.6	10.1	6.8	−10.3	−27.3
9	06/09/2015	45.08	18.69	24.1	8.32	82.2	427	3.716	4.56	0.034	0.053	0.127	3.08	−9.26	6.7	9.5	6.0	−10.5	−25.6
10	07/09/2015	44.97	19.60	23.1	8.22	84.9	325	3.405	2.52	0.036	<0.05	n.a.	2.53	−9.53	5.7	11.0	5.7	−10.1	−28.1
10a	07/09/2015	44.91	19.75	22.6	8.48	89.2	293	3.229	2.11	0.022	<0.05	n.a.	2.29	−9.69	5.6	8.0	7.5	−10.4	−29.5
11	08/09/2015	44.75	19.72	22.4	8.08	94.2	336	3.389	2.21	0.02	<0.05	0.372	2.58	−9.59	6.1	8.1	7.7	−10.5	−29.2
11a	08/09/2015	44.74	19.82	22.5	8.94	115	313	3.525	2.05	0.022	<0.05	0.088	2.43	−9.65	4.8	9.7	1.0	−10.5	−29.1
12	09/09/2015	44.77	20.81	23.7	8.44	85.9	324	3.635	2.42	<0.02	0.088	0.087	2.40	−9.65	4.7	7.4	4.5	−10.0	−27.5

n.a. – not analysed.

microbial source tracking were expressed as marker equivalents (ME), taking account of the filtration volume and the DNA sample dilution to yield the result (Reischer et al., 2006, 2008).

2.5. Computational methods/statistics

Considering that the data were in line for usage of parametric tests, differences of the variables between the sampling sites were investigated by one-way ANOVA followed by Duncan's multiple range test. A 95% confidence interval was used for the confidence level. Based on the physical and chemical parameters studied, Euclidian distances were calculated and used to construct an Unweighted Pair-Group Method with Arithmetic mean (UPGMA) phenogram to reveal overall similarity between the sites studied in 2014 and 2015. Logarithmic transformations (log + 1) of microbiological data were performed by calculating log10 after addition of 1 to a given value. All statistical analyses were performed using Statistica 6.0 Software (StatSoft, Inc.).

3. Results and discussion

3.1. Distribution of nutrients in the Sava River Basin

3.1.1. Long-term nutrient trends

Long-term nutrient trends are presented in Vrzel and Ogrinc (2015). Here only a brief summary is reported for the same locations, but using the new location numbers from Fig. 1. Concentrations of both nutrients (NO_3^- and PO_4^{3-}) were correlated significantly with flow at all locations, except at location 10. A dilution effect was detected at locations 2, 3, 4, and 8 while, at location, 9, a continuous input of NO_3^- into the riverine system was indicated. Variations in rainfall and temperature were found to contribute greatly to the monthly variation in NO_3^- concentration.

Temporal variability in nutrient concentrations was controlled by riverine flow and indicated that the highest NO_3^- concentrations were usually observed during winter/autumn when leaching of soil from slopes and banks was more intensive. The lowest NO_3^- concentrations observed during the summer were related to the limiting leaching

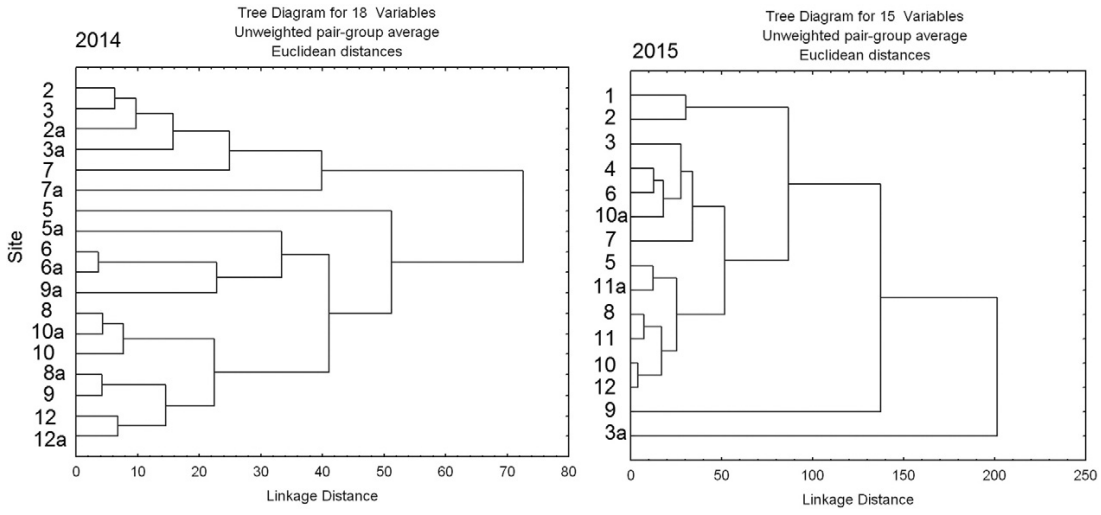


Fig. 2. UPGMA (Unweighted Pair-Group Method with Arithmetic mean) tree derived from Euclidian distances for the sites studied in 2014 and 2015 and based on physical and chemical parameters.

from the catchment and reduction of NO_3^- caused by phytoplankton uptake. Occurrence of denitrification was unlikely, since hypoxic/anoxic conditions are usually not present in the river. On the other hand, during the summer the highest PO_4^{3-} concentrations were related to low flow conditions and to the presence of reductive conditions releasing inorganic P from sediments into the water column.

The results of trend analysis show a reduction of nutrients at the majority of selected locations, ranging from 6 to 58% (Vrzel and Ogrinc, 2015). The trend in PO_4^{3-} concentrations exhibits different behavior. No significant trend was observed at locations 3 and 10 while, at locations 4 to 9, trends show significant decline in PO_4^{3-} concentrations with reductions in PO_4^{3-} concentrations of 18–34%. Although there was no significant trend in PO_4^{3-} concentration at location 10, the switch from a negative slope in the regression line for location 9 to a positive slope for location 10 suggests that inputs of PO_4^{3-} had been increasing downstream. This is possible, given that location 10 has been more susceptible to nutrient inputs, mainly from wastewater effluent discharges (Ogrinc et al., 2008; Ogrinc et al., 2015).

3.1.2. Nutrients in late summer in 2014 and 2015

The data regarding environmental parameters in late summer 2014 and 2015 are presented in Tables 1 and 2. The water temperature (T) usually increased with distance from the source (location 1) (Ogrinc et al., 2008). Statistically significant differences in the temperature of water, T, between locations was observed ($p < 0.0001$) with the lowest value of T always observed at location 1 and the highest usually found in the lower reaches of the Sava (18.4 °C at location 12 in 2014 and 24.8 °C at location 8 in 2015). A statistically significant difference in water temperature was also observed between 2014 and 2015 ($p < 0.0001$) with the highest value observed in 2015.

Specific conductivity (ElCo) ranged from 210 to 427 μS cm^{-1}, with the lowest and highest values observed in 2015 at locations 1 and 9, respectively. Significant differences in ElCo were observed between sampling locations ($p = 0.003$) in 2015. No statistically significant temporal differences in ElCo were observed in 2015 compared to 2014 ($p = 0.066$).

pH ranged from 7.10 to 8.94, with the lowest and highest values obtained in 2015 at locations 1 and 11, respectively. No significant spatial ($p = 0.652$ in 2014 and $p = 0.507$ in 2015) and yearly ($p = 0.1627$) differences were observed in pH values.

Concentrations of NO_3^- ranged from the limits of detection (LOD) determined at location 1 to 6.69 mg L^{-1} at location 3 (Tables 1 and 2). Significant differences between NO_3^- concentrations were observed between 2014 and 2015 ($p = 0.0213$), with higher values observed in 2015, but no significant differences between sampling locations were observed in 2014 and 2015.

The measured NH_4^+ concentrations were between <0.05 and 0.76 mg L^{-1}, with the highest values observed in 2015. Concentrations of NO_2^- were very low, ranging from 0.02 to 0.24 mg L^{-1}. NO_2^- is the intermediate inorganic species of the interconversion of NO_3^- and NH_4^+. In an aquatic ecosystem, NO_2^- is rapidly converted to NO_3^- under oxidizing conditions. NO_3^- is, therefore, usually far more abundant in the aquatic environment. This explains the relatively high concentrations of NO_3^- compared to those of NO_2^- during the whole study period (Tables 1 and 2). The concentrations of PO_4^{3-} ranged from 0.02 to 10.6 mg L^{-1} and were, on average, higher in 2014. Spatial and year differences were not significant in the cases of NH_4^+, NO_2^-, and PO_4^{3-}.

DOC concentrations ranged from 1.41 to 4.83 mg C L^{-1} and were statistically higher in 2014 than in 2015. Spatial distribution indicated that observed values were statistically higher in the lower part of the Sava River in 2014 and 2015.

Values of $\delta^{15}N_{NO3}$ for riverine samples ranged from −2.7 to 6.7‰ (Tables 1 and 2) and displayed significant differences between those in 2014 and 2015 (higher values in 2015; $p = 0.0492$) and also between headwater/mouth locations (higher values at the mouth; $p = 0.054$). $\delta^{18}O_{NO3}$ values were quite uniform, with an average value of 9.4 ± 1.2‰. No significant differences were observed in relation to year of sampling or sample location.

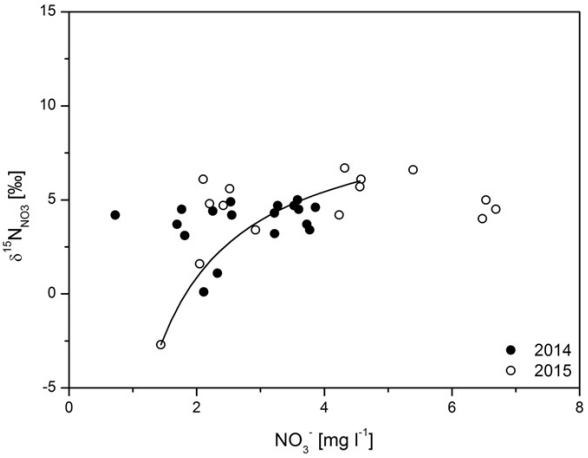


Fig. 3. The relation between $\delta^{15}N_{NO3}$ values and NO_3^- concentrations in the Sava River Basin. The following isotope-mixing curve was used to describe the observed data: $\delta^{15}N = \frac{\delta^{15}N_1 \times f \times N_1 + \delta^{15}N_2 \times (1-f) \times N_2}{N}$ where N, N_1 and N_2 are concentrations of NO_3^- in the sample, two end-members and $\delta^{15}N$, $\delta^{15}N_1$ and $\delta^{15}N_2$ are corresponding $\delta^{15}N$ values. The first end-member, with an NO_3^- concentration of 1.44 mg L^{-1} and $\delta^{15}N_{NO3}$ of −2.7‰, was chosen for the sample observed in a pristine area, while the second end-member was selected from location 9 where the highest $\delta^{15}N_{NO3}$ value of 6.7‰ was observed with NO_3^- concentration of 4.56 mg L^{-1}.

Values of $\delta^{13}C_{DIC}$ ranged from −13.1 to −7.8‰ and of TA from 1.747 to 4.080 meq/kg. Statistically significant spatial differences were observed in both parameters in 2014 ($p < 0.001$) and 2015 ($p < 0.001$). Locations 1 and 2, with higher values of $\delta^{13}C_{DIC}$ and lower TA, differed significantly from other locations. The higher values of $\delta^{13}C_{DIC}$ indicate that dissolution of carbonates prevails while, at the downstream locations, degradation of organic matter appeared to be more important. The difference from measurements at other locations in the SRB was not significant in 2015 and relatively similar $\delta^{13}C_{DIC}$ values were observed in the whole lower part of the River Sava (average $\delta^{13}C_{DIC}$ − 10.3 ± 0.7‰). A similar finding was observed in the study performed in 2005 and 2006 (Ogrinc et al., 2008).

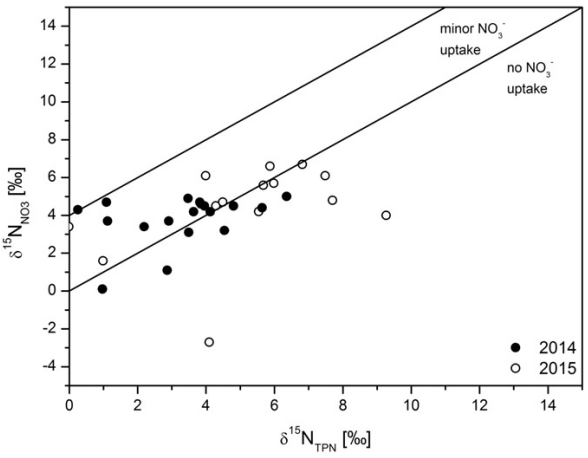


Fig. 4. Values of $\delta^{15}N_{NO3}$ versus $\delta^{15}N_{PN}$ for the Sava River Basin. The diagonal lines indicate the expected $\delta^{15}N$ values if there was no isotopic fractionation during uptake (lower line), and the expected $\delta^{15}N$ values if the fractionation was 4‰ (upper line), a typical fraction for uptake of NO_3^- (Finlay and Kendall, 2007). The further the data plot below the lower line, the less likelihood of NO_3^- uptake occurring.

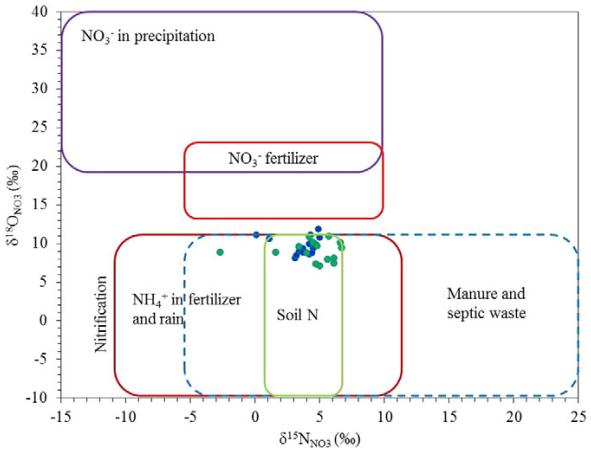


Fig. 5. $\delta^{15}N$ and $\delta^{18}O$ values of riverine nitrate in the Sava River Basin (adopted by Kendall et al., 2008). Ranges of isotope compositions for four major nitrate sources are indicated by boxes: (a) atmospheric nitrate deposition, (b) nitrate-containing fertilizers, (c) nitrate derived from nitrification e.g. in soils, and (d) nitrate in manure and/or sewage.

Values of $\delta^{13}C_{POC}$ ranged from −29.5 to −25.6‰ and of $\delta^{15}N_{PN}$ from 0.0 to 9.3‰. No significant differences were observed in $\delta^{15}N_{PN}$ values in relation to sampling location, while significant differences in $\delta^{13}C_{POC}$ values were observed in 2015, where location 9 differed significantly from locations 5, 6, and 7.

The differences between 2014 and 2015 sampling periods in TA, $\delta^{13}C_{DIC}$, $\delta^{13}C_{POC}$ and $\delta^{15}N_{TPN}$ values ($p = 0.038$, $p < 0.001$, $p < 0.001$ and $p = 0.012$, respectively) were statistically significant, with lower $\delta^{13}C_{DIC}$ and higher TA, $\delta^{13}C_{POC}$ and $\delta^{15}N_{TPN}$ values obtained in 2014.

The UPGMA phenogram derived from the matrix of Euclidian distances for the sites studied in 2014 and 2015 is shown in Fig. 2. With some exceptions, in both years the grouping of the sites belonging to upper, middle and lower stretches of the river is observed, supporting our previous observation in 2005 and 2006 (Markovics et al., 2010) where only chemical composition of the Sava River and its tributaries were investigated. In 2014 the major driving forces for distances among the sites were water temperature, concentrations of NO_3^- and DOC, $\delta^{13}C_{DIC}$ and $\delta^{15}N_{NO3}$ values, while in 2015 the concentrations of NO_3^- and $\delta^{15}N_{NO3}$ had the highest impact. In 2015 the locations 3a and 9 differed most distinctly from the other sites.

3.1.2.1. Determination of nitrate sources. A clear trend of increasing $\delta^{15}N_{NO3}$ values with increasing NO_3^- concentrations is evident from Fig. 3, suggesting that riverine nitrate in River Sava contained contributions from at least two different sources: one source generating low concentrations and $\delta^{15}N_{NO3}$ values below 2‰, and another with higher concentrations and a $\delta^{15}N_{NO3}$ value above 6‰. An isotope mixing line with two different riverine end-members was therefore constructed. The first end-member, with an NO_3^- concentration of 1.44 mg L^{-1} and $\delta^{15}N_{NO3}$ of −2.7‰, was chosen from the sample observed in a pristine area at the source of the River Sava (location 1; Fig. 1), while an NO_3^- concentration of 4.56 mg L^{-1} and a $\delta^{15}N_{NO3}$ of 6.7‰ were selected as the second source, with the highest $\delta^{15}N_{NO3}$ value observed at location 9 (Table 2). The results indicate that most of the data fall on the mixing line in 2014, while higher deviations from the mixing line were observed in 2015.

The low NO_3^- concentrations and low $\delta^{15}N_{NO3}$ values observed at locations 1 and 2 in 2014 and 2015 were indicators of NO_3^- leaching from pristine soils, the river in the upper watershed draining mainly a forested catchment (Harrington et al., 1998; Voss et al., 2006). $\delta^{15}N_{NO3}$ values range from −3 to 5‰ for NO_3^- leaching from non-fertilized soils (Fogg et al., 1998; Mayer et al., 2002) while, on the other hand, NO_3^- originating from animal manure and sewage generally shows a $\delta^{15}N_{NO3}$ value >7‰ (Aravena et al., 1993; Fogg et al., 1998; McClelland and Valiela, 1998; Wankel et al., 2006). The highest $\delta^{15}N_{NO3}$ value of 6.7‰ was observed at location 9 in 2015, but higher values could not be detected, as was the case in autumn in 2006, when the river discharge was even lower than in 2015 (Ogrinc et al., 2008).

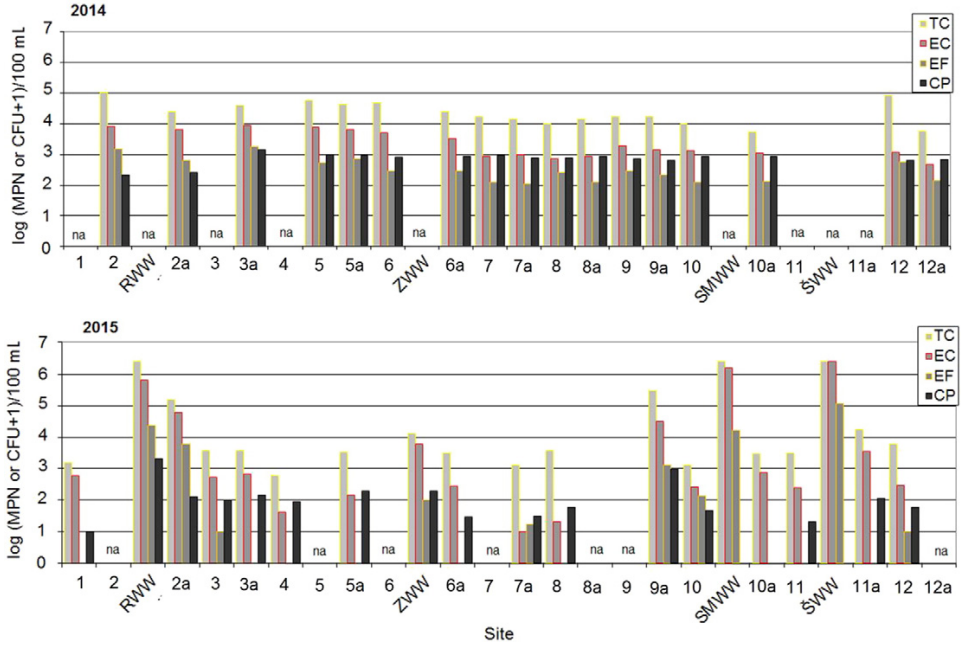


Fig. 6. Numbers of indicator bacteria (log (MPN or CFU + 1) / 100 mL) measured in water samples of the Sava River and in wastewater samples (WW) collected during the survey; TC - total coliforms, EC – *E. coli*, EF – enterococci, CP – *C. perfringens*; n.a. – not assessed.

The increase in $\delta^{15}N_{NO3}$ above the values expected from simple mixing indicates the consumption of NO_3^- by photosynthetic uptake or denitrification processes. Denitrification was not an important process, since neither hypoxic nor anoxic conditions were present in the River Sava. Thus, the stable isotope data and the decrease in NO_3^- concentrations observed at these locations (Tables 1 and 2) indicate higher assimilation rates of NO_3^-. Plotting values of $\delta^{15}N_{NO3}$ against those of $\delta^{15}N_{TPN}$ provides a useful means for determining whether NO_3^- uptake could be significant for various sites, since the $\delta^{15}N$ of algae should always be equal or lower than that of the N source (Finlay and Kendall, 2007). In Fig. 4 are two diagonal lines that indicate the $\delta^{15}N$ values expected if there was no isotopic fractionation during uptake (lower line) and, likewise, the expected values of $\delta^{15}N$ if the fractionation was 4‰ (upper line), a typical fraction for uptake of NO_3^- (Finlay and Kendall, 2007). As shown in Fig. 4, no locations show differences in $\Delta\delta^{15}N$ as high as 4‰. Most of the data plot near the lower diagonal line defined by $\delta^{15}N_{TPN} = \delta^{15}N_{NO3}$, consistent with minor uptake of local nitrate, while the data below the lower diagonal line indicate the insignificant uptake of NO_3^-.

In addition, and based on values of $\delta^{13}C_{POC}$ (Tables 1 and 2), the presence of phytoplankton was detected. The $\delta^{13}C$ value of phytoplankton was estimated from the $\delta^{13}C_{DIC}$ and a C isotope discrimination of 21‰ on photosynthetic C assimilation (Mook and Tan, 1991; Hellings et al., 1999; Hoffman and Bronk, 2006). The mean values of $\delta^{13}C$ for phytoplankton in the lower part of River Sava from location 3 could be estimated to be -33.6 ± 0.6‰ in 2014 and -31.3 ± 0.2‰ in 2015. Our previous investigation indicated that, at 59% of the locations, the main source of POC is derived from soil OC (Ogrinc et al., 2008). Thus, it was assumed that two main sources dominated the POC in River Sava in the autumns of 2014 and 2015: soil and phytoplankton. The proportion of these two sources was estimated using isotope mass balance, taking into account two end-members: the average $\delta^{13}C$ value of −26‰ for soil OC and the calculated mean $\delta^{13}C$ values for phytoplankton. The calculations indicate that >90% of POC is of soil origin at all locations in 2014, while in 2015 phytoplankton was found to be the main source of POC, accounting for >60% at locations 3, 5, 6, 10 and 11.

The data plotted below the mixing line indicate the additional source of NO_3^- in the River Sava, which was more pronounced in 2015 at locations 3, 5, 7 and could be related to nitrification. Since nitrification leaves an imprint on $\delta^{18}O_{NO3}$ values, these values were used to identify the origin of NO_3^- derived from nitrification processes in manure, sewage, or soils (Fig. 5). Based on the assumption that $\delta^{18}O_{NO3}$ of microbially-produced NO_3^- is determined by the two oxygens derived from H_2O and one from atmospheric O_2 (Hollocher, 1984; Anderson and Levine, 1986; Böhlke et al., 1997; Durka et al., 1994; Kendall, 1998; Wassenaar, 1995; Mayer et al., 2001), the expected range of $\delta^{18}O$ values of NO_3^- produced by nitrification can be calculated from the known $\delta^{18}O$ values for atmospheric oxygen and ambient water by the equation (Mayer et al., 2001): $\delta^{18}O_{NO3} = 2/3\ \delta^{18}O$ (in water) $+ 1/3\ \delta^{18}O\text{-}O_2$. The atmospheric oxygen is known to have a $\delta^{18}O$ value of 23.5‰ (Kroopnick and Craig, 1972), while the ambient water is expected to display an isotope value similar to that in the river water, as shown in Tables 1 and 2. The calculated $\delta^{18}O_{NO3}$ values for nitrate from nitrification were around 2‰ and differed significantly from those of our measured data with an average value of 9.4 ± 1.2‰ (Tables 1 and 2). However, $\delta^{18}O$ values of microbially-produced NO_3^- have been observed to be up to 5‰ higher than the calculated values (Aravena et al., 1993; Kendall, 1998; Mayer et al., 2001) and thus more closely related to our data. Further, it is possible to conclude that atmospheric deposition, with high $\delta^{18}O_{NO3}$ values between 25 and 70‰ (e.g. Durka et al., 1994; Kendall, 1998), does not contribute significantly to river NO_3^-, nor do the nitrates originating from fertilizers, with $\delta^{18}O_{NO3}$ values of ~+22‰ (Fig. 5). This is in line with studies carried out on USA and German rivers (Mayer et al., 2002; Johannsen et al., 2008). The absence of a trend of increasing $\delta^{18}O_{NO3}$ values with increasing agricultural land-use could be due to two reasons, the uptake of fertilizer-nitrate by crops and microbes and the subsequent re-mineralization and nitrification, producing nitrate with $\delta^{18}O_{NO3}$ values below +15‰ (Mayer et al., 2001) and thus changing the original oxygen isotope ratio of the fertilizer-nitrate. NO_3^- derived from nitrification of ammonium or urea-based fertilizers is also characterized by $\delta^{18}O_{NO3}$ values of less than +15‰, since nitrogen from ammonium or urea-containing fertilizers must be nitrified before it can contribute to riverine nitrate.

3.2. Microbiology

3.2.1. Comparative data for the whole Sava River

To compile long-term data for the whole Sava River, the same strategy proposed by Kirschner et al. (2009) for the Danube River was used. The data from two whole river surveys (2014 and 2015) and long-term data from the TransNational Monitoring Network (TNMN) of the International Commission for the Protection of the Danube River (ICPDR) were integrated. The data from TNMN are available at the http://www.icpdr.org/main/activities-projects/tnmn-transnational-

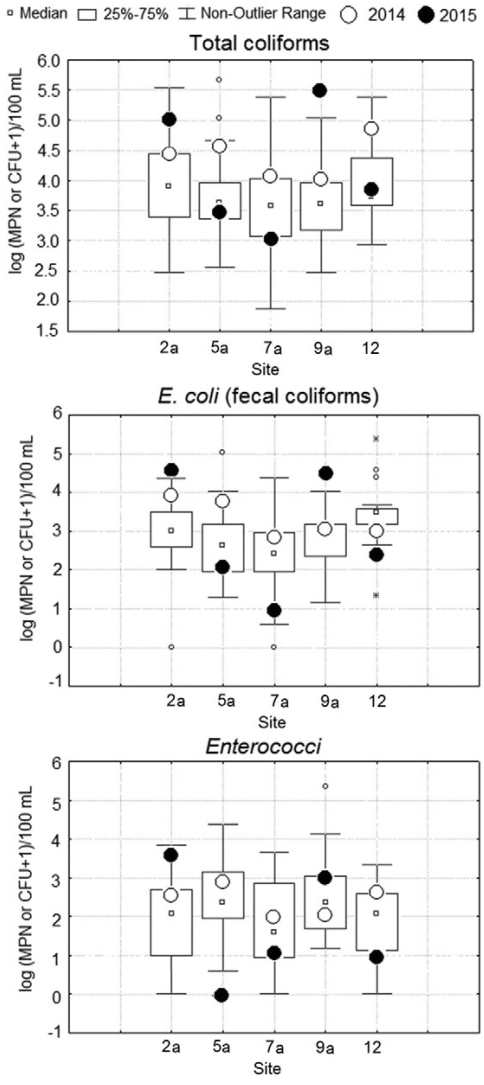


Fig. 7. Long term monitoring data on the numbers of the indicator bacteria (log (MPN-CFU + 1) / 100 mL) at 5 sites used in routine monitoring (Box-Whiskers); white circles – samples collected in 2014, black circles – samples collected in 2015.

monitoring-network. The dataset comprised five years of monthly monitoring (the only period available in the database was 2000–2004) from four TNMN locations: Jesenice (SI), Jasenice (HR), Jasenovac (HR) and Županja (HR). For Belgrade, pooled data obtained during five years of monthly monitoring (2010–2014) and provided by the Belgrade City Institute of Public Health were used. Selected locations overlap or are within 5 km of the locations studied in the whole river sampling campaigns: Jesenice (SI) - Litija, Jasenice (HR) - Čatež, Jasenovac - Jasenovac, Županja – Županja and Belgrade – Belgrade.

The long-term monitoring data are summarized in Fig. 6. For all three groups of bacteria, the majority of values showed grouping within the class II (moderate pollution) and class III (critical pollution). It is alarming that, at the locations 3a, 9a and 12, over 50% of the samples were critically polluted, indicating continuous presence of fecal pollution at these locations and is consistent with our previous results (Kapetanović et al., 2015). The lowest medians were observed at location 7a.

3.2.2. Sampling survey in 2014 and 2015

Primarily, the focus was on microbiological indicators of fecal pollution (*E. coli*, fecal enterococci), which are used as surrogates for the possible presence of intestinal pathogens (Kirschner et al., 2014). The numbers of total coliforms were assessed, as this group is still included in the national regulations of Serbia in assessing the ecological status of surface waters. We have also quantified *C. perfringens* as a potential indicator for point source emissions from wastewater (Sorensen et al., 1989). The results of the two whole river surveys are summarized in Fig. 6.

During the survey 2014, the numbers of total coliforms ranged from 3.73 (location 10a) to 5.03 (location 2) log (MPN + 1) / 100 mL. As indicated in Fig. 7, samples were scattered within the classes II and III (moderate to critical pollution). The numbers of *E. coli* ranged from 2.84 (location 8a) to 3.94 log (MPN + 1) / 100 mL (location 3a). The numbers of enterococci ranged from 2.03 (location 8a) to 3.26 (location 3a) log (MPN + 1) / 100 mL. The numbers of *C. perfringens* ranged from 2.03 (location 5a) to 3.13 (location 3a) log (CFU + 1) / 100 mL.

In 2015, the river samples were scattered within the classes I and II (slight to moderate pollution). The numbers of total coliforms ranged from 2.79 (location 4) to 5.49 (location 9a) log (MPN + 1) / 100 mL. The numbers of *E. coli* ranged from 1.0 (location 7a) to 4.51 log (MPN + 1) / 100 mL (location 9a). At 9 out of 15 locations the numbers of enterococci were below the limit of detection (<1 log (MPN + 1) / 100 mL), the highest numbers being recorded at location 9a (3.12 log (MPN + 1) / 100 mL). The numbers of CP ranged from 0 (location 10a) to 3.98 (location 9a) times log (CFU + 1) / 100 mL. By all monitored indicators, samples collected from the WW discharge points at locations 2, 10 and 11 were excessively contaminated. The effects were evident downstream at the location 11a, but especially at the location 2a.

For comparison, data obtained within the surveys were included into Fig. 8. At locations 5a and 7a a shift towards the upper quartile of the range was observed for samples collected in 2014 while a shift towards the lower quartile of the range was observed for samples collected in 2015. On the other hand, at locations 2a and 9a, the ones heavily impacted by wastewaters, we have noted the opposite situation. High water velocity, in combination with high water level, in 2014 resulted in homogeneity of water quality along the river. This is also valid for other parameters, since no statistically significant differences between sampling locations were found in pH, concentration of O_2, ElCo, concentrations of NO_2^-, NH_4^+, PO_4^{3-} or DOC and $\delta^{18}O_{NO3}$ values. Therefore, in 2014, the hotspots of pollution were hard to identify. In contrast, in 2015 we found WW outlets at 4 locations, but the effect was only evident at location 2a. It was interesting that a critical level of pollution was found at location 9a, although the direct point of discharge was not defined. This observation could be further supported by the high NO_3^- and DOC concentrations and the highest $\delta^{15}N_{NO3}$ value of 6.7‰ and the $\delta^{13}C_{POC}$ value of −25.6‰. According to the statistical evaluation this location differed most from the other sites in 2015 (Fig. 2). Besides the point discharges of WW, diffuse pollution, originating from households of the nearby located villages, was considered as a possible pathway of contamination. Also in the middle and lower sections of the river, the use of animal manure as a fertilizer in agriculture is commonly employed without strict legislative regulations, which should not be neglected.

Since the standard indicators, *E. coli* and enterococci, cannot provide any reliable information regarding the origin of fecal pollution (Kirschner et al., 2014), we have employed the MST technique to identify the major source of pollution. Quantitative PCR (qPCR)-based assays for the analysis of general-, human-, wastewater-, or animal-associated genetic *Bacteroidetes* fecal markers have gained increasing popularity in the field of fecal pollution analysis and microbial source tracking (MST) during recent years (Mayer et al., 2016). The human-associated fecal markers BacHum and HF183II were detected at 12 and 13 locations, respectively. The ruminant-associated BacR and the pig-associated Pig-2-Bac markers were not detected in any of the samples. As indicated in Table 3, high correlation was observed between the standard indicators (coliforms and enterococci) and human associated fecal markers. This is consistent with previous studies that support the fact that fecal pollution based on qPCR quantification can be performed with at least equal precision compared with traditional ISO-based cultivation techniques (Stapleton et al., 2009; Mayer et al., 2016). The lowest correlation was observed with numbers of *C. perfringens*. Among the indicators studied, *C. perfringens* numbers show the lowest degree of variation along the river, as reported earlier (Byamukama et al., 2005).

4. Conclusions

The combined use of the isotope compositions of N and O in NO_3^- provides evidence that NO_3^- is affected primarily by two different

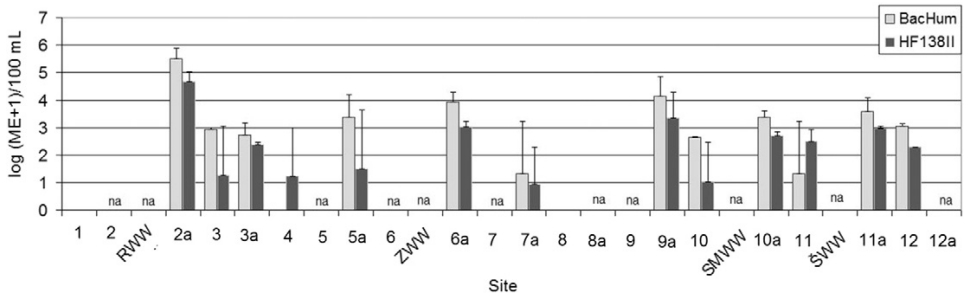


Fig. 8. Concentration of the human-associated fecal markers BacHum and HF183II expressed as log (ME + 1) / 100 mL, values are means ± SD obtained from two filter series; n.a. – not assessed.

Table 3
Correlation between the standard indicators (TC, EC, EF and CP) and the human-associated fecal markers BacHum and HF183II monitored. Marked correlations are significant for $p < 0.003$ (p value adjusted for multiple comparisons).

Spearman	EC		EF		CP		BacHum		HF138II	
	r	*p*	*r*	*p*	*r*	*p*	*r*	*p*	*r*	*p*
TC	0.63	0.012	0.28	0.318	0.64	0.010	0.65	0.009	0.60	0.018
EC			0.26	0.349	0.29	0.301	0.70	0.004	0.70	0.004
EF					0.30	0.278	0.36	0.187	0.19	0.508
CP							0.40	0.135	0.32	0.252
BacHum									0.89	**0.000**

sources: one source originating from pristine soils, and another originating from wastewater and manure, although processes such as phytoplankton assimilation and nitrification have also been observed, especially in autumn 2015. According to the analyses of the $\delta^{15}N_{NO3}$ and $\delta^{15}N_{TPN}$ values the minor and/or zero uptake of local nitrate was detected in most locations. Particulate organic carbon (POC) is mainly of soil origin in 2014 while, in 2015, phytoplankton was found to be the main source of POC at locations 3, 5, 6, 10 and 11. According to the $\delta^{18}O_{NO3}$ values it is possible to conclude that atmospheric deposition does not contribute significantly to river NO_3^- nor do the nitrates originating from commercial fertilizers. We therefore suggest that the comparatively low isotopic enrichment factors for nitrogen and oxygen arise from a combination of soil nitrification and an admixture of NO_3^- from wastewater and manure. This assumption could be further confirmed by microbiological analyses. These analyses comprised analysis of the standard indicators of fecal pollution and microbial source tracking (MST) analyses based on the human-associated BacHum and HF183II, the ruminant-associated BacR and the pig-associated Pig2Bac genetic Bacteroidetes fecal markers. The results reveal the existence of hotspots of fecal pollution of human associated origin in the SRB. Long-term data at selected locations indicated persistent fecal contamination, showing that the locations are impacted by continuous discharge of untreated wastewaters. This study describes the present nutrient and microbiological pollution status in the SRB, and indicates the urgent need for effective wastewater treatment plants in water management.

Acknowledgements

This study was conducted within the EU Seventh Framework Programme – GLOBAQUA (managing the effects of multiple stressors on aquatic ecosystem under water scarcity) under Grant agreement no. 603629-ENV-2013-6.2.1. It also represents a part of the activities within the projects funded by the Ministry of Education, Science and Technological Development of the Republic of Serbia projects no. 173045 and 173025 and the bilateral project Serbia and Austria: Implementation of Microbial Source Tracking (MST) method for assessment of faecal pollution in the Sava River and its relation (potential relationship) to the presence of genotoxic agents. The research was conducted partially within the PhD study of Janja Vrzel financed by the European Social Fund no. C2130-12-000070. We acknowledge the staff of Hrvatske vode and the Republic Hydrometeorological Service of Serbia, who helped us to obtain the discharge and water quality data, and the International Commission for the Protection of the Danube River (ICPDR) for data obtained from the Transnational Monitoring Network. The authors thank Prof. R. Pain for linguistic corrections.

References

Aborgiba, M., Kostić, J., Kolarević, S., Kračun-Kolarević, M., Elbahi, S., Knežević-Vukčević, J., Lenhardt, M., Paunovć, M., Gačić, Z., Vuković-Gačić, B., 2016. Flooding modifies the genotoxic effects of pollution on a worm, a mussel and two fish species from the Sava River. Sci. Total Environ. 540, 358–367.

Anderson, I.C., Levine, J.S., 1986. Relative rates of nitric oxide and nitrous oxide production by nitrifiers, denitrifiers, and nitrate respirers. Appl. Environ. Microbiol. 51, 938–945.

Aravena, R., Evans, M.L., Cherry, J.A., 1993. Stable isotopes of oxygen and nitrogen in source identification of nitrate from septic systems. Ground Water 31, 180–186.

Böhlke, J.K., Ericksen, G.E., Revesz, K., 1997. Stable isotope evidence for an atmospheric origin of desert nitrate deposits in northern Chile and southern California, USA. Chem. Geol. 136, 135–152.

Buckalew, D.W., Hartman, L.J., Grimsley, G.A., Martin, A.E., Register, K.M., 2006. A long-term study comparing membrane filtration with Colilert defined substrates in detecting fecal coliforms and *Escherichia coli* in natural waters. J. Environ. Manag. 80, 191–197.

Byamukama, D., Mach, R.L., Kansiime, F., Manafi, M., Farnleitner, A.H., 2005. Discrimination efficacy of fecal pollution detection in different aquatic habitats of a high-altitude tropical country, using presumptive coliforms, *Escherichia coli*, and *Clostridium perfringens* spores. Appl. Environ. Microbiol. 71, 65–71.

Casciotti, K.L., Sigman, D.M., Hastings, M., Böhlke, J.K., Hilkert, A., 2002. Measurement of the oxygen isotopic composition of nitrate in seawater and freshwater using the denitrifier method. Anal. Chem. 74, 4905–4912.

Casteel, M.J., Sobsey, M.D., Mueller, J.P., 2006. Fecal contamination of agricultural soils before and after hurricane-associated flooding in North Carolina. J. Environ. Sci. Health A 41, 173–184.

Chang, C.C.Y., Kendall, C., Silva, S.R., Battaglin, W.A., Campbell, D.H., 2002. Nitrate stable isotopes: tools for determining nitrate sources among different land use in the Mississippi River Basin. Can. J. Fish. Aquat. Sci. 59, 1874–1885.

Durka, W., Schulze, E.D., Gebauer, G., Voerkeliust, S., 1994. Effects of forest decline on uptake and leaching of deposited nitrate determination from ^{15}N and ^{18}O measurements. Nature 372, 765–767.

Epstein, S., Mayeda, T., 1953. Variations of ^{18}O content of waters from natural sources. Geochim. Cosmochim. Acta 4, 213–224.

European Environment Agency (EEA), 2015. Indicator Assessment, Prod-ID: IND-8-en, CSI 020, WAT 003. Nutrients in Freshwater.

Finlay, J.C., Kendall, C., 2007. Stable isotope tracing of temporal and spatial variability in organic matter sources to freshwater ecosystems, chapter 10. In: Michener, R.H., Lajtha, K. (Eds.), Stable Isotopes in Ecology and Environmental Science, second ed. Blackwell Publishing, Oxford, pp. 283–333.

Fogg, G.E., Rolston, D.E., Decker, D.L., Louie, D.T., Grismer, M.E., 1998. Spatial variation in nitrogen isotope values beneath nitrate contamination sources. Ground Water 36, 418–426.

Globevnik, L., Mikoš, M., Padežnik, M., Petan, S., Petkovšek, A., Vidmar, A., Milačič, R., Ščančar, J., Heath, E., Ogrinc, N., Brilly, M., 2010. SARIB: chapter 13. In: Brilly, M. (Ed.), Hydrological Processes of the Danube River Basin: Perspectives From the Danubian Countries. Springer, Dordrecht, Heidelberg, pp. 389–428 http://dx.doi.org/10.1007/978-90-481-3423-6.

Grasshoff, K., Ehrhardt, K., Ehrhardt, M., 1983. Methods of Seawater Analysis. Verlag Chemie, New York.

Green, H.C., Haugland, R.A., Varma, M., Millen, H.T., Borchardt, M.A., Field, K.G., Walters, W.A., Knight, R., Kelty, C.A., Shanks, O.C., 2014. Improved HF183 quantitative real-time PCR assay for characterization of human fecal pollution in ambient surface water samples. Appl. Environ. Microbiol. 80, 3086–3094.

Harrington, R.R., Kennedy, B.P., Chamberlain, C.P., Blum, J.D., Folt, C.L., 1998. ^{15}N enrichment in agricultural catchments: field patterns and applications to tracking Atlantic salmon (*Salmo salar*). Chem. Geol. 147, 281–294.

Heatwaite, A.L., 2010. Multiple stressors on water availability at global to catchment scales: understanding human impact on nutrient cycles to protect water quality and water availability in the long term. Freshw. Biol. 55, 241–257.

Hebert, C.G., Wassenaar, L.I., 2001. Stable nitrogen isotopes in waterfowl feathers reflect agricultural land use in western Canada. Environ. Sci. Technol. 35, 3482–3487.

Hellings, L., Dehairs, F., Tacks, M., Keppens, E., Baeyens, W., 1999. Origin and fate of organic carbon in the freshwater part of the Scheldt estuary as traced by stable carbon isotope composition. Biogeochemisty 47, 167–186.

Hoffman, J.C., Bronk, D.A., 2006. Interannual variation in stable carbon and nitrogen isotope biogeochemistry of the Mattaponi River, Virginia. Limnol. Oceanogr. 51, 2319–2332.

Hollocher, T.C., 1984. Source of the oxygen atoms of nitrate in the oxidation of nitrite by *Nitrobacter agilis* and evidence against a P–O–N anhydride mechanism in oxidative phosphorylation. Arch. Biochem. Biophys. 233, 721–727.

ISRBC, 2011. International Sava River Basin Commission. Sava River Basin Management Plan. Draft Version 6.2. 241 pages http://www.savacommission.org/srbmp/.

Johannsen, A., Dähnke, K., Emeis, K., 2008. Isotopic composition of nitrate in five German rivers discharging into the North Sea. Org. Geochem. 39, 1678–1689.

Kapetanović, D., Smrzlić, I.V., Valić, D., Teskeredžić, E., Kolarević, S., Sunjog, K., Tomović, J., Kračun-Kolarević, M., Knežević-Vukčević, J., Paunović, M., Gačić, Z., Vuković-Gačić, B., 2015. Microbial characterisation of the Sava River. In: Milačič, R., Ščančar, J., Paunović, M. (Eds.), The Sava River. Springer Berlin Heidelberg, Berlin, pp. 201–228.

Kendall, C., 1998. Tracing sources and cycling of nitrate in catchments. In: Kendall, C., McDonnell, J.J. (Eds.), Isotope Tracers in Catchment Hydrology. Elsevier, Amsterdam, pp. 519–576.

Kendall, C., Elliott, E.M., Wankel, S.D., 2008. Tracing anthropogenic inputs of nitrogen to ecosystems. In: Michener, R., Lajtha, K. (Eds.), Stable Isotopes in Ecology and Environmental Science, second ed. Blackwell Publishing Ltd, Oxford, pp. 375–449.

Kildare, B.J., Leutenegger, C.M., McSwain, B.S., Bambic, D.G., Rajal, V.B., Wuertz, S., 2007. 16S rRNA-based assays for quantitative detection of universal, human-, cow-, and dog-specific fecal *Bacteroidales*: a Bayesian approach. Water Res. 41, 3701–3715.

Kirschner, A.K., Kavka, G., Reischer, G.H., Sommer, R., Blaschke, A.P., Stevenson, M., Vierheilig, J., Mach, R.L., Farnleitner, A.H., 2014. Microbiological water quality of the Danube River: status quo and future perspectives. In: Liska, I. (Ed.), The Danube River Basin. Springer Berlin Heidelberg, Berlin, pp. 439–468.

Kirschner, A.K.T., Kavka, G., Velimirov, B., Mach, R.L., Sommer, R., Farnleitner, A.H., 2009. Microbiological water quality along the Danube River: integrating data from two

whole-river surveys and a transnational monitoring network. Water Res. 43, 3673–3684.
Kittinger, C., Marth, E., Reinthaler, F.F., Zarfel, G., Pichler-Semmelrock, F., Mascher, W., Mascher, F., 2013. Water quality assessment of a central European river—does the directive 2000/60/EC cover all the needs for a comprehensive classification? Sci. Total Environ. 447, 424–429.
Kroopnick, P., Craig, H., 1972. Atmospheric oxygen: isotopic composition and solubility fractionation. Science 175, 54–55.
Layton, A., McKay, L., Williams, D., Garrett, V., Gentry, R., Sayler, G., 2006. Development of bacteroides 16S rRNA gene TaqMan-based real-time PCR assays for estimation of total, human, and bovine fecal pollution in water. Appl. Environ. Microbiol. 72, 4214–4224.
Markovics, R., Kanduč, T., Szramek, K., Globočanin, D., Milačič, R., Ogrinc, N., 2010. Chemical dynamics of the Sava riverine system. J. Environ. Monit. 12, 2165–2176.
Mayer, R.E., Bofill-Mas, S., Egle, L., Reischer, G.H., Schade, M., Fernandez-Cassi, X., 2016. Occurrence of human-associated bacteroidetes genetic source tracking markers in raw and treated wastewater of municipal and domestic origin and comparison to standard and alternative indicators of faecal pollution. Water Res. 90, 265–276.
Mayer, B., Bollwerk, S.M., Mansfeldt, T., Hütter, B., Veizer, J., 2001. The oxygen isotope composition of nitrate generated by nitrification in acid forest floors. Geochim. Cosmochim. Acta 65, 2743–2756.
Mayer, B., Boyer, E.W., Goodale, C., Jaworski, N.A., Breemen, N.V., Howarth, R.W., Seitzinger, S., Billen, G., Lajtha, K., Nadelhoffer, K., Van Dam, D., Hetling, L.J., Nosal, M., Paustian, K., 2002. Sources of nitrate in rivers draining sixteen watersheds in the northeastern U.S.: isotopic constraints. Biogeochemisty 57, 171–197.
McClelland, J.W., Valiela, I., 1998. Linking nitrogen in estuarine producers to land derived sources. Limnol. Oceanogr. 43, 577–585.
Mieszkin, S., Furet, J.P., Corthier, G., Gourmelon, M., 2009. Estimation of pig fecal contamination in a river catchment by real-time PCR using two pig-specific *Bacteroidales* 16S rRNA genetic markers. Appl. Environ. Microbiol. 75, 3045–3054.
Mook, W.G., Tan, F.C., 1991. Stable carbon isotopes in rivers and estuaries. In: Degens, E.T., Kampe, S., Richey, J.E. (Eds.), Biochemistry of Major World Rivers. J. Wiley and Son, Ltd, Chicester, pp. 245–264.
Navarro-Ortega, A., Acuña, V., Bellin, A., Burek, P., Cassiani, G., Choukr-Allah, R., Dolédec, S., Elosegi, A., Ferrari, F., Ginebreda, A., Grathwohl, P., Jones, C., Rault, K., Kasper Kok, P., Koundouri, P., Ludwig, R.P., Merz, R., Milacic, R., Muñoz, I., Nikulin, G., Paniconi, C., Paunović, M., Petrovic, M., Sabater, L., Sabater, S., Skoulikidis, N.T., Slob, A., Teutsch, G., Voulvoulis, N., Barceló, D., 2015. Managing the effects of multiple stressors on aquatic ecosystems under water scarcity. The GLOBAQUA project. Sci. Total Environ. 503–504, 3–9.
Ogrinc, N., Kanduč, T., Globočanin, D., Kocman, D., Miljević, N.R., 2010. A Hydrogeochemical and Isotope Investigation of the River Sava Watershed. Nova Science Publishers Inc., New York.
Ogrinc, N., Kanduč, T., Kocman, D., 2015. Integrated approach to the evaluation of chemical dynamics and anthropogenic pollution sources in the Sava River Basin. In: Milačič, R., Ščančar, J., Paunović, M. (Eds.), The Sava River Vol. 31. Springer Berlin Heidelberg, pp. 75–94.
Ogrinc, N., Markovics, R., Kanduč, T., Walter, L.M., Hamilton, S.K., 2008. Sources and transport of carbon and nitrogen in the river Sava watershed, a major tributary of the river Danube. Appl. Geochem. 23, 3685–3698.
Paunović, M., Tomović, J., Kovačević, S., Zorić, K., Žganec, K., Simić, V., Atanacković, A., Marković, V., Kračun, M., Hudina, S., Lajtner, J., Gottstein, S., Lucić, A., 2012. Macroinvertebrates of the natural substrate of the Sava River – preliminary results. Water Resour. Manag. 2, 33–39.
Reischer, G.H., Haider, J.M., Sommer, R., Stadler, H., Keiblinger, K.M., Hornek, R., Zerobin, W., Mach, R.L., Farnleitner, A.H., 2008. Quantitative microbial faecal source tracking with sampling guided by hydrological catchment dynamics. Environ. Microbiol. 10, 2598–2608.
Reischer, G.H., Kasper, D.C., Steinborn, R., Mach, R.L., Farnleitner, A.H., 2006. Quantitative PCR method for sensitive detection of ruminant fecal pollution in freshwater and evaluation of this method in alpine karstic regions. Appl. Environ. Microbiol. 72, 5610–5614.
Seiler, R.L., 2005. Combined use of ^{15}N and ^{18}O of nitrate and ^{11}B to evaluate nitrate contamination in groundwater. Appl. Geochem. 20, 1626–1636.
Sigman, D.M., Casciotti, K.L., Andreani, M., Barford, C., Galanter, M., Böhlke, J.K., 2001. A bacterial method for the nitrogen isotopic analysis of nitrate in seawater and freshwater. Anal. Chem. 73, 4145–4153.
Sorensen, D.L., Eberl, S.G., Dicksa, R.A., 1989. *Clostridium perfringens* as a point source indicator in non-point polluted streams. Water Res. 23, 191–197.
Stapleton, C.M., Kay, D., Wyer, M.D., Davies, C., Watkins, J., Kay, C., McDonald, A.T., Porter, J., Gawler, A., 2009. Evaluating the operational utility of a bacteroidales quantitative PCR-based MST approach in determining the source of faecal indicator organisms at a UK bathing water. Water Res. 43 (19), 4888–4899.
Voss, M., Deutsch, B., Elmgren, R., Humborg, C., Kuuppo, P., Pastuszak, M., Rolff, C., Schulte, U., 2006. Source identification of nitrate by means of isotopic tracers in the Baltic Sea catchments. Biogeosciences 3, 663–676.
Vrzel, J., Ogrinc, N., 2015. Nutrient variations in the Sava River Basin. J. Soils Sediments 15, 2380–2386.
Wankel, S.D., Kendall, C., Francis, C.A., Paytan, A., 2006. Nitrogen sources and cycling in the San Francisco Bay Estuary: a nitrate dual isotope approach. Limnol. Oceanogr. 51, 1654–1664.
Wassenaar, L.I., 1995. Evaluation of the origin and fate of nitrate in the Abbotsford aquifer using the isotopes of ^{15}N and ^{18}O in NO_3^-. Appl. Geochem. 10, 391–405.
Widory, D., Kloppmann, W., Chery, L., Bonnin, J., Rochdi, H., Guinamant, J.L., 2004. Nitrate in groundwater, an isotope multi-tracer approach. J. Contam. Hydrol. 72, 165–188.
Xue, D., Botte, J., De Baets, B., Accoe, F., Nestler, A., Taylor, P., Van Cleemput, O., Berglund, M., Boeckx, P., 2009. Present limitations and future prospects of stable isotope methods for nitrate source identification in surface- and groundwater. Water Res. 43, 1159–1170.

3.3 The Study of the Interactions Between Groundwater and Sava River Water in the Ljubljansko Polje Aquifer System (Slovenia)

The third paper is "The study of the interactions between groundwater and Sava River water in the Ljubljansko polje aquifer system (Slovenia)" by Janja Vrzel, D. Kip Solomon, Željko Blažeka and Nives Ogrinc. The paper was published in the Journal of Hydrology in 2018.

In this paper I present the various impacts of the two main groundwater sources in the Ljubljansko polje aquifer system – Sava River water and local precipitation. The groundwater mean residence time over the study domain was also estimated. The study is the main driver for the development of a conceptual model of the aquifer in the Ljubljansko polje, which was later transformed into a numerical model and developed using advanced modeling tools.

The main aims included: (1) determining the fractions of the Sava River water in groundwater samples using $\delta^{18}O$ and $\delta^{2}H$ values in relation to precipitation levels (2010 and 2011) using a two-component mixing model. This is the first detailed study of the Ljubljansko polje aquifer system in terms of understanding the system in space and under different conditions (2010 and 2011 were wet and dry years, respectively); (2) estimating the mean residence time for which I used the ^{3}H and $^{3}H/^{3}He$ methods. The combination of these two methods is particularly valuable, since, until this study, the $^{3}H/^{3}He$ method had not been used in Slovenia and because the ^{3}H method has become less reliable (see Section 1.2); (3) estimating the vulnerability of groundwater to pollution and the relationship between ^{3}H and NO_3^- concentrations.

The main findings were that local precipitation ($> 86\%$) is the main source of water in the wells Kleče 11, Hrastje 3, and Hrastje 8, while similar fractions of the both sources river water and precipitation made up the groundwater pumped from the wells Kleče 8, Kleče 12 and Jarški prod 3. In addition, Sava River water dominates the groundwater pumped from the well Jarški prod 1. The fraction of both sources is influenced by the distance of the well from the Sava River and the depth of the screens in the well. In terms of groundwater resource management, the groundwater MRT is an important parameter. The ^{3}H analyses indicated the presence of mostly modern water with a short mean residence time (MRT). However, noble gas analyses revealed that up to 10% of the groundwater at Kleče 8 and Kleče 12 is much older. The exact age of water should be precisely determined by other methods, such as ^{14}C. Alternatively, groundwater with a long MRT is not present in the Jarški prod area. The highest concentrations of NO_3^- were observed at Hrastje, where local precipitation is the dominant groundwater source. Thus, groundwater at the Hrastje pumping station is more vulnerable to pollution from agricultural sources, whereas the wells in Jarški prod are more vulnerable to pollution from the Sava River.

The Ljubljansko polje aquifer is a complex system that represents an excellent case study for understanding groundwater-surface water interactions. Here the Sava River can change its role from losing to gaining stream within a few kilometers making it an ideal model domain for studying these two different relationships on a small scale. Other benefits of this study domain include the following: the system is very dynamic, has easily controlled boundary conditions, is composed of diverse bedrock that has a major influence on groundwater dynamics (but the role of which is too often not well presented), has a diverse geometry and can be extended from the surface to 100 m below the surface. The area is also occupied by different anthropogenic activities, which offers the possibility to study the vulnerability of groundwater to different pollution sources. Because of the strategic location of Ljubljansko polje–south from the Alps and close to the Adriatic see, the iso-

topic composition of the Sava River and local precipitation can be easily distinguished, which is not the case in many studies.

In this paper, I contributed to the development of the research question, performed measurements of isotope ratio mass spectrometric measurements of δ^2H at the Jožef Stefan Institute, and analysed and interpreted the data. I also interpreted (both temporally and spatially) the isotopic composition of groundwater, river water and local precipitation data and evaluated them together with the hydrological and meteorological data. The study represents a valuable opportunity to gain a deeper knowledge of the hydrology, geochemistry and geology of groundwater systems.

Journal of Hydrology 556 (2018) 384–396

Contents lists available at ScienceDirect

Journal of Hydrology

journal homepage: www.elsevier.com/locate/jhydrol

Research papers

The study of the interactions between groundwater and Sava River water in the Ljubljansko polje aquifer system (Slovenia)

Janja Vrzel [a,b], D. Kip Solomon [c], Željko Blažeka [d], Nives Ogrinc [b,e,*]

[a] Department of Geography, Ludwig-Maximilians-Universität München, Luisentraße 37, 80333 Munich, Germany
[b] Jožef Stefan International Postgraduate School, Jamova cesta 39, 1000 Ljubljana, Slovenia
[c] Department of Geology and Geophysics, The University of Utah, 115 S 1460 E RM 205, Salt Lake City, USA
[d] Ecological Engineering Institute d.o.o., Ljubljanska ulica 9, 2000 Maribor, Slovenia
[e] Department of Environmental Sciences, Jožef Stefan Institute, Jamova cesta 39, 1000 Ljubljana, Slovenia

ARTICLE INFO

Article history:
Received 2 November 2017
Accepted 11 November 2017
Available online 14 November 2017
This manuscript was handled by C. Corradini, Editor-in-Chief, with the assistance of Bartolomé Andreo-Navarro, Associate Editor

Keywords:
Environmental isotopes
$^3H/^3He$
Groundwater
Precipitation
Sava

ABSTRACT

River basin aquifers are common sites for drinking water wells as bank filtration can be a cost effective pretreatment technology. A groundwater vulnerability to pollution depends on a groundwater mean residence time and on a relative contribution of river water versus local precipitation to groundwater. Environmental isotopes of oxygen and hydrogen ($\delta^{18}O$ and δ^2H), tritium (^3H) and concentrations of nitrate (NO_3^-) were used to investigate hydrological pathways, mean residence time and interactions between surface water and groundwater in the Ljubljansko polje aquifer system in Slovenia. $\delta^{18}O$ and δ^2H values indicate a spatial variability of the influence of individual groundwater sources inside the aquifer – local precipitation and the Sava River water. Fractions of river water in groundwater depend on the depth of perforated screens in the pumping wells and their distance from the Sava River. It was estimated that groundwater at wells Kleče 11, Hrastje 3, and Hrastje 8 is mostly composed of recently infiltrated local precipitation, while the Sava River is the dominant source of groundwater at the well Jarški prod 1. Groundwater at wells Kleče 8, Kleče 12, and Jarški prod 3 contains on average between 41% and 48% of the Sava River water. The ^3H and $^3H/^3He$ methods indicate short mean residence time of groundwater present at Jarški prod (2–7 years) and Hrastje (7–8 years). A small fraction (<10%) of old groundwater is present at Kleče. Furthermore, infiltration of local precipitation influenced the levels of NO_3^- at Hrastje. These data extend our understanding of groundwater flow in the Ljubljansko polje aquifer system, interactions between the Sava River water/local precipitation and groundwater, and the utility of isotope tracers in evaluating the spatial distribution of groundwater vulnerability to pollution.

© 2017 The Authors. Published by Elsevier B.V. This is an open access article under the CC BY-NC-ND license (http://creativecommons.org/licenses/by-nc-nd/4.0/).

1. Introduction

The European Water Framework Directive (WFD) requires the introduction of remedial measures in case of deterioration of groundwater chemical and quantity status. Information about a water mean residence time (MRT) and dynamics of a groundwater recharge are an indispensable basis for assessing the effects of remedial measures, i.e. in which time period and to what extent an improvement in groundwater status can be expected.

Generally, groundwater within a river basin aquifer is a mixture of two main sources (a) precipitation, which infiltrates through a soil layer into an aquifer, and (b) river water. In some cases the third important groundwater source might also be very old groundwater that is accumulated in deeper layers of an aquifer. Understanding of relative contributions of these sources to groundwater are important for prediction of potential impacts of pollutants on water supplies, a development of management practices to preserve water quality, and a diversity of remediation plans for sites that are already polluted. Environmental isotopes (e.g. $\delta^{18}O$, δ^2H, ^3H) have been widely applied in groundwater studies for better understanding of groundwater origin, infiltration areas, groundwater dynamics, its MRT and vulnerability to pollution (Aggarwal et al., 2006; Gat, 1996; Lachniet and Patterson, 2002). Tracers of groundwater MRT are particularly useful because complex patterns of flow are integrated and the vulnerability of groundwater resources to both pollution and climate change depend on the groundwater MRT in aquifer systems (Kendall and Doctor, 2004). Also, there are regional and temporal variations of

* Corresponding author at: Department of Environmental Sciences, Jožef Stefan Institute, Jamova cesta 39, 1000 Ljubljana, Slovenia.
E-mail address: nives.ogrinc@ijs.si (N. Ogrinc).

https://doi.org/10.1016/j.jhydrol.2017.11.022
0022-1694/© 2017 The Authors. Published by Elsevier B.V.
This is an open access article under the CC BY-NC-ND license (http://creativecommons.org/licenses/by-nc-nd/4.0/).

isotopic fractionation because of latitudinal, continental, altitude and seasonal effects (Cappa et al., 2003; Kendall and Doctor, 2004; Urresti-Estala et al., 2015) that can help to define flow patterns.

Over the past three decades, interpretation of the $\delta^{18}O$, $\delta^{2}H$ and ^{3}H isotopic signatures of water have provided insight into identifying groundwater recharge areas or flow paths under different flow conditions and estimating groundwater MRT in catchments (Cook and Herczeg, 1998; Kendall and McDonnell, 1998). When initial concentrations of ^{3}H in the atmosphere is not known or when the mid-1960s ^{3}H peak cannot be clearly defined, the $^{3}H/^{3}He$ method for estimation of the MRT can be used (Schlosser et al., 1988; Poreda et al., 1988; Solomon et al., 1992; Solomon et al., 1993; Ekwurzel et al., 1994; Solomon and Cook, 2000; Kipfer et al., 2002).

The specific aims of the present study are: (1) to determine fractions of the Sava River water in groundwater samples using isotopes $\delta^{18}O$ and $\delta^{2}H$ in relation to low and high precipitation levels in 2010 and 2011; (2) to estimate groundwater MRTs using ^{3}H and $^{3}H/^{3}He$ methods; (3) to check the groundwater vulnerability to pollution using ^{3}H and NO_3^- concentrations. These new hydrological data would serve as a base for an improvement of the hydrogeological conceptual models of the Ljubljansko polje aquifer system and especially $^{3}H/^{3}He$ data, which are to our knowledge obtained for the first time in this area. They might be even used as calibration targets for groundwater flow and transport models.

2. Material and methods

2.1. Site description

The Ljubljansko polje aquifer system is one of the most important groundwater sources for the Slovenian capital Ljubljana and its surroundings. Groundwater is exploited from four pumping stations: Šentvid, Kleče, Hrastje, and Jarški prod. Natural conditions are characterized by fast groundwater flow, strong interconnection between surface and groundwater, and elevated vulnerability to pollution (Bračič Železnik and Jamnik, 2005).

The Ljubljansko polje is located at the eastern part of the Ljubljanska kotlina (Fig. 1). This tectonic depression formulated in the early Pleistocene along the main neotectonic fault system, running in the east-west direction (Premru, 2005). Occasional seismic activities indicate that the basin formation is still in progress. Its elevations vary from 324 m in Stanežiče to the 270 m in Zalog, which are located in the eastern and western sides of the Ljubljansko polje, respectively. Geographical boundaries of the basin are defined by surrounded hills with elevations up to 669 m at the Šmarna gora, which are composed of Permian and Carboniferous slate claystone and sandstone. These layers form a bedrock with variable depths over the Ljubljansko polje (Žlebnik, 1971; Premru, 1983). Remainders of Paleozoic rocks were also detected at the western and south-western areas at depths ranging from 0 to 30 m. They represent so-called perched aquifers (Šram, 2011) and have an influence on chemical properties of groundwater and transport of pollutants (Šram et al., 2012). A graphical presentation of the perched aquifer is shown in Fig. 2.

The Sava River accumulated Pleistocene and Holocene silty sandy gravels and sandy gravel with lenses of conglomerate in the Ljubljansko polje basin (Fig. 2). These fluvial sediments represent the main aquifer in the area with an increased thickness towards the centre of the Ljubljansko polje where it exceeds even 100 m (Bračič Železnik et al., 2005). The thickness of the aquifer is 80 m at Kleče, 65 m at Jarški prod and 58 m at Hrastje (Bračič Železnik, 2002). The aquifer is protected from polluted subsurface water by layers of clay or clay with gravel only at isolated areas in the central part of the Ljubljansko polje and at its western, southwestern and southern marginals (Bračič Železnik et al., 2005).

In general, the direction of the groundwater flow is toward the southeast (Fig. 1). In relation to the Ljubljansko polje aquifer system, the Sava River might be considered as a losing river from Medno to Šentjakob, and as a gaining river downstream of Šentjakob (Fig. 1). However, the interaction highly depends on the water level and the river bed geology. The Sava River water do not interact with groundwater, where it flows directly over the bedrock. The Ljubljanica River is a gaining river starting at Fužine and continues to gain as it traverses the Ljubljansko polje (Petauer and Hiti, 2013). Another important source of groundwater is local precipitation, since the area exhibits a large quantity of precipitation due to its geographic position and subalpine climate. The mean annual rainfall of 1400 mm and the mean air temperature between 8 °C and 10 °C were observed (ARSO; URL: http://meteo.arso.gov.si/met/en/archive), however in the 60 years long time period the maximum and minimum precipitation amount of 1798 mm and 998 mm were observed in the years 2010 and 2011, respectively (ARSO; URL: http://meteo.arso.gov.si/met/en/archive). In addition, underground groundwater recharge from the neighbouring groundwater bodies should be mentioned, but it occurs only at edges segments of the Ljubljansko polje aquifer system, where the bedrock is deep. Therefore, the Ljubljansko polje aquifer system is also recharged by groundwater from the Ljubljansko Barje aquifer (Ljubljana moors) in the south as well as from the Kamniško–Bistriško polje and the Kranjsko–Sorško polje in the north (Jamnik et al., 2000). High groundwater table may also change this interaction from recharging to discharging. Although the underground recharge is still not well known its fraction in the aquifer was estimated to be negligible in relation to other groundwater sources (Cerar and Urbanc, 2013). The hydrodynamic in the Ljubljansko polje aquifer is also influenced by groundwater pumping for water supply and industrial needs (Andjelov et al., 2005). Oscillations of the piezometric groundwater table shown in Fig. 3 occurred because of variations in pumping rates, especially at the well Kleče 11. The Ljubljansko polje aquifer system has intergranular porosity and an unconfined groundwater table, which is located on average around 20–25 m below the surface. The main permeable formation is composed of gravels and sands with lenses of conglomerates and muddy gravels, and has variable properties: transmissivity ranges from 43.2 to 4752 $m^2\,d^{-1}$, storage capacity from 0.01 to 0.1 and effective porosity from 5 to 15% (Bračič Železnik et al., 2005; Vižintin et al., 2009).

2.2. Sampling and analysis

Samples were collected monthly over one hydrological cycle from March 2010 to December 2011 from: (1) the aquifer under ambient (non-pumping) conditions at seven wells at three different water supplies: Kleče, Hrastje and Jarški prod, (2) the Sava River at Šentjakob, and (3) precipitation at Geological Survey in Ljubljana (Bežigrad). The sampling locations with some descriptive parameters are summarized in Table 1 and graphically presented in Fig. 1. Perforated screens in the pumping wells range between 205 m and 278 m a.s.l. (Fig. 2).

Dissolved oxygen and water temperature were measured using a YSI model 58 meter and a YSI 5239 DO probe with high-sensitivity membranes. Electrical conductivity was measured using a Corning 316 meter with a two-point calibration of 0 and 1413 $\mu S\,cm^{-1}$. Dissolved oxygen and electrical conductivity measurements had precision of ±5%. A Corning 315 high-sensitivity pH meter with an Orion Ross combination pH electrode, calibrated with low ionic strength buffers of 4.1 and 6.97 (corrected for temperature), was used to measure pH in the field as close to the water temperature

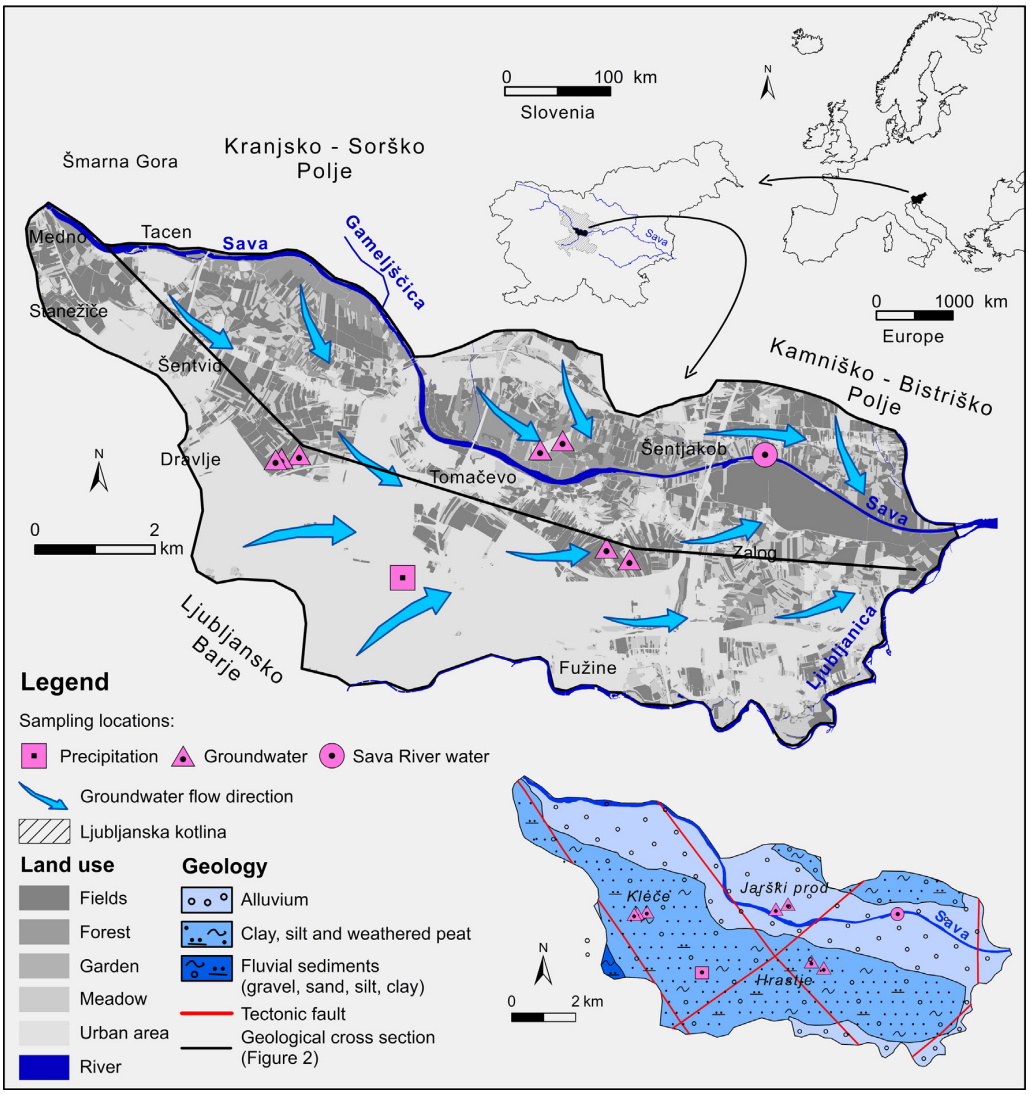


Fig. 1. Land use map (from http://rkg.gov.si/GERK/) of the Ljubljansko polje with the groundwater flow direction (after Andjelov et al., 2005) and the geological map (from http://www.arso.gov.si/).

as possible. The reproducibility of field pH determinations was ±0.02 pH units.

Stable isotope measurements of oxygen (O) and hydrogen (H) were performed in 260 samples. Results for O and H are reported using conventional delta (δ) notation $\delta^{18}O$ and $\delta^{2}H$, respectively, in permil (‰) relative to VSMOW. The isotopic composition of oxygen ($\delta^{18}O$) was measured after equilibration with reference CO_2 (Epstein and Mayeda, 1953) on a Multiflow continuous flow isotope ratio mass spectrometer (Isoprime GV Instruments), while reduction on Cr at 800 °C was used to determine the isotopic composition of hydrogen ($\delta^{2}H$) in water (Gehre et al., 1996) on a Varian MAT 250 mass spectrometer. The accuracy of the measurements were ±0.1‰ for $\delta^{18}O$ and ±1‰ for $\delta^{2}H$.

The ^{3}H measurements were performed at HYDROSYS LABOR Analytical Laboratory Ltd., Budapest, Hungary according to standard procedure FS-78-15-AKU (1995). Volumes of the water samples were reduced from 250 ml to 14–15 ml by electrolytic enrichment, factor of tritium enrichment is about 15–16. The tritium activities of enriched water samples were counted by super low level Liquid Scintillation Counter (LSC). The tritium (^{3}H) concentration in water is expressed in terms of the tritium unit (TU) with accuracy of ±0.4 TU.

Concentrations of NO_3^- were determined in 109 samples (previously filtered through 0.45 μm nylon filter) on a Dionex ICS-2500 IC (accuracy ±2%).

Seven samples taken at Kleče, Hrastje and Jarški prod wells in June 2010 were used for groundwater dating by the $^{3}H/^{3}He$ method. Helium isotope analyses were performed using a Mass Analyzers Products – Model 215-50 Magnetic Sector-Field mass spectrometer (±1%) and Ne, Ar, Kr, and Xe were measured using a Standard Research SRS – Model RGA 300 quadrupole mass spectrometer (±2%) at the University of Utah, USA. In these samples also ^{3}H measurements were performed by the ^{3}He in-growth method (Clarke et al., 1976) with an accuracy of ±3%. The uncertainty in $^{3}H/^{3}He$ dating depends on measurement errors and upon the suitability of models used to determine the component of total ^{3}He

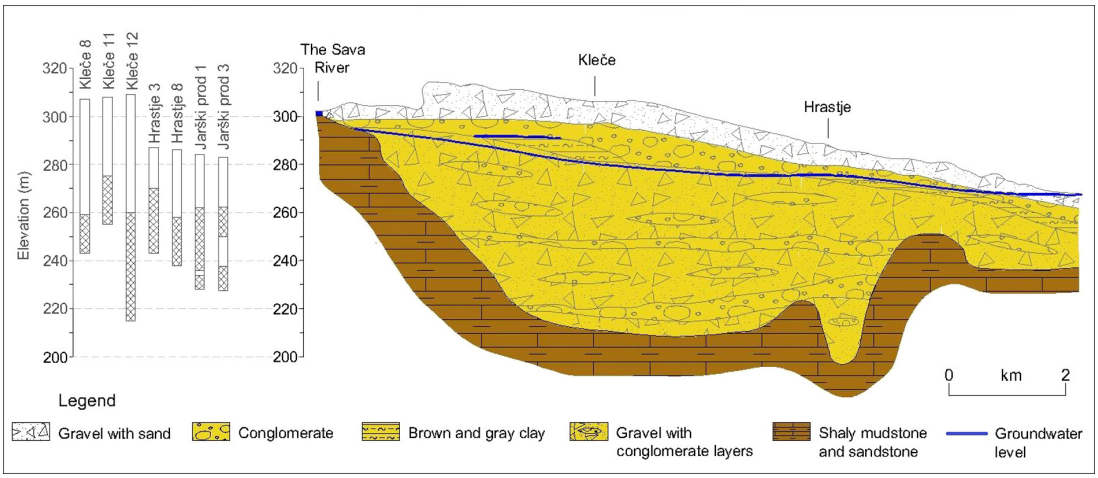


Fig. 2. Geological cross section of the Ljubljansko polje aquifer system (after Bračič Železnik et al., 2005) and depth of perforated screens in wells.

that comes from tritium decay ($^3He_{trit}$). The $^3He_{trit}$ component is estimated by subtracting the atmospheric and terrigenic (both crustal and mantle) components from total ^3He (Solomon and Cook, 2000). The atmospheric component of ^3He was determined from Ne, Ar, Kr, and Xe measurements using the Closed Equilibrium (CE) model (Aeschbach-Hertig et al., 2000). The terrigenic component ($^3He_{terr}$) depends on the $^3He/^4He$ ratio of mantle rocks, mantle fluids, and lithospheric (crustal) He production, and can vary over several orders of magnitude. The $^3He_{trit}$ component for samples with large concentrations of total He (more than an order of magnitude above atmospheric solubility) or mantle-derived fluids with high $^3He/^4He$ ratios are sensitive to the assumed terrigenic $^3He/^4He$ ratio, making dating problematic (Solomon and Cook, 2000). We assumed a $^3He/^4He$ ratio of 2×10^{-8} for terrigenic He (Mamyrin and Tolstikhin, 1984) but let this value vary up to 1×10^{-7} when calculating the uncertainty of $^3H/^3He$ ages. The measured $^3He/^4He$ ratio is presented as R/R_a where R is the $^3He/^4He$ ratio measured in the sample and R_a is the $^3He/^4He$ ratio in the air (1.384×10^{-6}).

The Sava River discharge and precipitation in Ljubljana collected at daily intervals were obtained from Environmental Agency of the Republic of Slovenia (ARSO; www.arso.si).

2.3. Calculation methods

Data analysis – Normally distributed data were analysed by the one-way ANOVA for testing differences in measured parameters according to a season and a location. In the statistical test probability (p) values of less than .05 were used to indicate a significance level. If the significance was noted in a response factor, the calculation was followed by post-hoc testing using the Tukey's Honestly Significant Difference (HSD) test. All statistical analyses were performed using STATISTICA software package v.7 (StatSoft Inc., Tulsa, OK, USA).

Groundwater dating by the $^3H/^3He$ method – The mean residence time (MRT), which is based on the $^3H/^3He$ method, was computed using the following equation (Solomon and Cook, 2000)

$$t = \lambda^{-1} ln\left(\frac{[^3He^*]}{[^3H]} + 1\right) \quad (1)$$

where λ is the ^3H decay constant of 0.0556 y^{-1}, $[^3H]$ is the measured ^3H activity and $[^3He^*]$ is the tritiogenic ^3He concentration defined as the amount of the total ^3He produced by the ^3H decay. The total amount of ^3He in groundwater can be expressed as:

$$^3He_{tot} = {}^3He_{atm} + {}^3He^* + {}^3He_{nuc} + {}^3He_{man} \quad (2)$$

where subscripts *atm*, *nuc* and *man* refer to He of the atmospheric origin and He that is produced by nuclear reactions in the subsurface, and He of the mantle origin, respectively (Solomon and Cook, 2000). Because it is difficult to separate $^3He_{nuc}$ from $^3He_{man}$, they are often lumped together and simply referred to as $^3He_{terr}$ (terrigenic ^3He). When a mixture of water with longer and shorter MRT is present, the MRT, estimated with the $^3H/^3He$ method, is biased towards the shorter MRT (Małoszewski and Zuber, 1982).

Isotope mass balance – A fraction of local precipitation versus the Sava River water in groundwater was calculated by the two-component mixing model. The contribution of both sources could be estimated using the following equation:

$$\delta^{18}O_{GW} = f_{RW} \times \delta^{18}O_{RW} + f_P \times \delta^{18}O_P \quad (3)$$

$$1 = f_{RW} + f_P \quad (4)$$

where f_{RW} and f_P are respective river water and precipitation fractions, while $\delta^{18}O_{GW}$, $\delta^{18}O_{RW}$, and $\delta^{18}O_P$ are the isotopic compositions of oxygen in groundwater, river water and precipitation, respectively.

Lumped dispersion model – Transit time distribution was performed by the lumped Dispersion Model (Stichler et al., 1986), which assumes a tracer transport controlled by advection and dispersion processes. The $g(\tau)$ function is then defined as follows (Małoszewski and Zuber, 1982):

$$g(\tau) = \frac{1}{\tau\sqrt{4\pi(P_D)\tau/\tau_m}} exp\left[-\frac{(1-\frac{\tau}{\tau_m})^2}{4(P_D)\tau/\tau_m}\right] \quad (5)$$

where τ_m is the mean transit time of water, while P_D is the dimensionless dispersion parameter, which describes the variance of the distribution. In the case of bank filtration it can, in large approximation, be defined as:

$$P_D = \frac{\alpha_L}{x} \quad (6)$$

where α_L is the dispersivity (m), and x is the mean flow-distance between the input and output locations (m). P_D of 0.2 was used in our calculation.

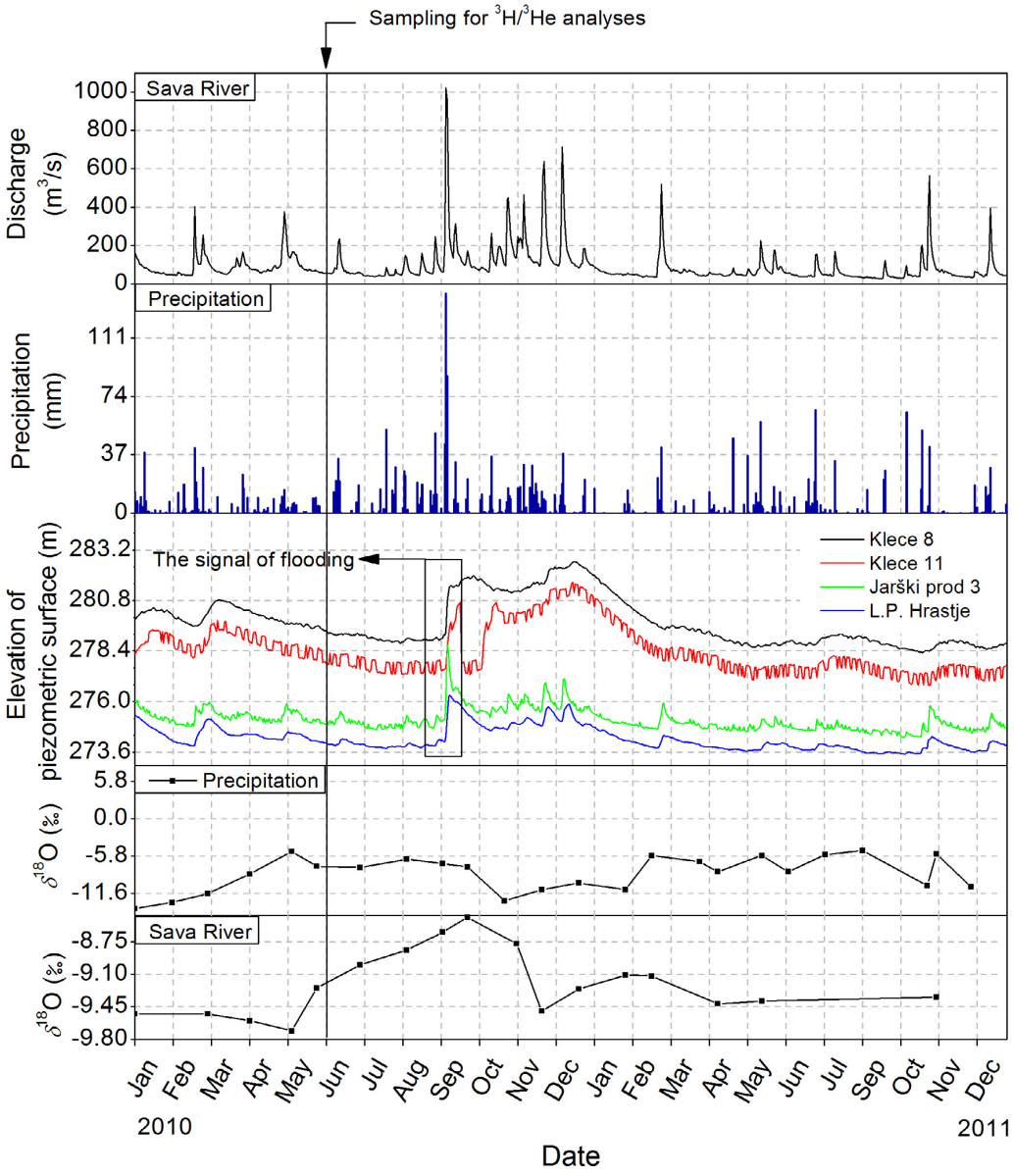


Fig. 3. Discharge of the Sava River (ARSO), amount of daily precipitation (measured at 7 am) in Ljubljana (ARSO), elevation of piezometric surface (VO-KA), $\delta^{18}O$ values in precipitation and the Sava River for the period 2010–2011.

Table 1
Sampling locations with some descriptive parameters (latitude, longitude, elevation, mean pumping rate over the time period 2010–2011 (SOURCE: VO-KA)) of sampling locations together with the type of sampling water and depth of perforated screens.

Sampling location	Latitude (°)	Longitude (°C)	Elevation (m)	Mean pumping rate over the period 2010–2011 (l s^{-1})	Type of sampled water	Elevation of perforated screens (m)
Kleče 8	46.086	14.495	308.7	54.22	groundwater	278–241
Kleče 11	46.085	14.491	308.2	48.47	groundwater	275–255
Kleče 12	46.085	14.490	308.7	48.54	groundwater	260–205
Hrastje 3	46.072	14.562	287.4	40.43	groundwater	270–243
Hrastje 8	46.070	14.567	286.3	1.41	groundwater	270–237
Jarški prod 1	46.087	14.547	282.5	52.53	groundwater	235–230 263–238
Jarški prod 3	46.088	14.552	282.8	54.53	groundwater	238–228 262–250
Sava River	46.085	14.599	266.1	/	surface water	/
Bežigrad	46.871	14.515	300.0	/	precipitation	/

Table 2
Minimum, maximum, average, standard deviations (SD) and number of samples for $\delta^{18}O$, $\delta^{2}H$ and ^{3}H values, *d-excess* and NO_3^- concentrations at sampling locations for the period 2010–2011. The mean values for precipitation were weighted by amount of precipitation.

Name of the sample	$\delta^{18}O$ (‰)					$\delta^{2}H$ (‰)					^{3}H (TU)					*d*-excess (‰)	NO_3^- (mg l^{-1})				
	Mean	Min	Max	SD	No. of samples	Mean	Min	Max	SD	No. of samples	Mean	Min	Max	SD	No. of samples	Mean	Mean	Min	Max	SD	No. of samples
Kleče 8	−8.86	−9.18	−8.42	0.16	16	−59.4	−63.6	−56.1	2.4	14	5.4	4.0	6.3	0.8	13	11.5	10.6	1.40	13.7	3.25	13
Kleče 11	−8.65	−8.88	−8.48	0.10	16	−58.1	−61.1	−55.5	1.8	16	5.8	4.5	6.8	0.6	13	11.1	25.4	20.9	50.1	7.17	12
Kleče 12	−8.83	−9.06	−8.60	0.13	15	−60.3	−63.8	−56.6	2.3	14	5.6	4.9	6.4	0.4	13	10.3	18.3	12.8	35.7	6.69	14
Hrastje 3	−8.66	−9.04	−8.50	0.12	16	−58.5	−62.8	−55.0	2.2	15	5.4	3.6	6.1	0.6	13	10.9	24.1	5.74	50.3	9.13	13
Hrastje 8	−8.66	−8.71	−8.60	0.05	4	−58.7	−60.1	−56.5	1.9	3	6.0	5.9	6.2	0.2	3	10.6	34.3	26.2	42.4	11.5	2
Jarški prod 1	−9.11	−9.38	−8.90	0.14	15	−60.4	−62.6	−57.1	1.4	14	5.6	4.4	7.0	0.7	11	12.5	7.10	5.30	22.6	4.47	13
Jarški prod 3	−8.87	−9.27	−8.62	0.17	16	−59.7	−63.0	−57.4	1.7	14	6.0	4.6	6.8	0.6	13	11.2	9.49	7.24	14.1	1.66	13
Sava River	−9.19	−9.71	−8.49	0.36	15	−62.0	−66.4	−57.6	2.9	12	6.4	4.5	8.7	1.3	12	11.5	4.55	3.45	6.82	1.29	8
Bežigrad	−8.67●	−13.91	−4.92	2.73	10	–	–	–	–	–	–	–	–	–		–	–	–	–	–	–
Precip.–$LJ_{07\text{-}10}$*	−8.57●	−14.52	−4.65	2.90	44	−59.1●	−115.1	−27.9	23.6	44	9.9	1.0	18.0	4.9	44	8.3	–	–	–	–	–

* Data from Vreča et al. (2014).
● Mean weighted values (our results and Vreča et al. (2014)).

Table 3
Results of $^{3}H/^{3}He$ analyses at the groundwater sampling locations in June 2010.

Sample ID	^{3}H (TU)	+/−	Total Ne (ccSTP g^{-1})	Total Ar (ccSTP g^{-1})	Total Kr (ccSTP g^{-1})	Total Xe (ccSTP g^{-1})	Total N_2 (ccSTP/g) values are approximate	He^4 (ccSTP g^{-1})	R/R_a	Age (yr) (CE model)	+/− (yr)	Rech. Temp (°C)	Ae	F	Terrigenic ^{4}He (ccSTP g^{-1})	Chi^2	Rech Elev (m)
Kleče 8	5.82	0.20	2.25E−07	4.13E−04	9.11E−08	1.34E−08	9.05E−03	3.49E−07	0.153	NA	–	9.6	0.028	0.81	3.0E−07	1.1	307
Kleče 11	6.08	0.24	2.48E−07	4.13E−04	9.48E−08	1.36E−08	8.74E−03	6.93E−08	0.822	0	4.2	8.6	0.005	0.30	9.9E−09	0.01	308
Kleče 12	5.80	0.22	2.39E−07	3.92E−04	8.26E−08	1.21E−08	8.46E−03	1.87E−07	0.298	NA	–	12.9	0.011	0.59	1.3E−07	2.2	309
Hrastje 3	5.76	0.23	2.15E−07	4.10E−04	1.00E−07	1.42E−08	8.23E−03	7.18E−08	0.700	2.8	6.2	7.1	0.035	0.91	2.2E−08	0.8	287
Hrastje 8	6.68	0.26	2.10E−07	3.90E−04	9.33E−08	1.28E−08	7.62E−03	6.58E−08	0.843	8.4	3.3	11.2	0.31	0.91	1.7E−08	0.7	287
Jarški prod 1	6.20	0.24	2.17E−07	4.29E−04	1.09E−07	1.52E−08	9.75E−03	4.93E−08	1.006	2.1	3.1	6.0	0.46	0.93	3.6E−10	2.5	284
Jarški prod 3	6.37	0.21	2.19E−07	4.19E−04	9.97E−08	1.43E−08	8.40E−03	5.36E−08	1.027	6.7	2.8	6.6	0.021	0.50	3.0E−09	0.46	283

NA: Not applicable because sample contains significant amounts of terrigenic ^{4}He; the groundwater is probably a mixture of modern and pre-modern water.

The relationship between input, $C_{RW}(t)$, and output, $C_{GW}(t)$, concentrations, in our case $\delta^{18}O$ values, is given by the convolution integral, which for non-decaying tracers is defined as follows:

$$C_{GW}(t) = f_{RW} \int_0^t C_{RW}(t-\tau) g(\tau) d\tau \quad (7)$$

where τ is the transit time of a single tracer particle between input and output and f_{RW} is the fraction of river water in the pumping well.

3. Results

The entire data set of basic physical and isotopic parameters obtained over the two years period (2010–2011) are presented in the electronic supplement (Table S1). The main focus of the paper is related to $\delta^{18}O$, $\delta^{2}H$, ^{3}H and NO_3^-, thus the means, ranges and standard deviations in groundwater, the Sava River water and the weighted means, ranges and standard deviations in precipitation are shown in Table 2, while concentrations of the noble gases determined in June 2010 are presented in Table 3. Unusual high ^{3}H activities up to 12.5 TU in the Sava River water and groundwater were observed in November 2010 (Table S1). It is assumed that they are related to a systematic analytical error and thus excluded from the further analysis. The decision was accepted according to the following reasons: (1) as reported by Vreča et al. (2014) there was no high ^{3}H activity in precipitation observed at that time; (2) the event is not correlated with any other hydrological or isotopic parameters; and (3) the rapid increase in ^{3}H activity in the Sava River water and in groundwater was observed at the same time period, which would require unrealistic nearly zero transit time from the river to the wells.

3.1. Precipitation

As already mentioned, minimum and maximum annual precipitation over the 60 years period before 2011 were observed exactly over the sampling period (2010–2011) (ARSO; URL: http://meteo.arso.gov.si/met/en/archive). The total annual rainfall amount of 1798 mm and 998 mm were observed in 2010 and 2011, respectively. The maximum monthly precipitation of 140 mm and the maximum discharge of the Sava River at Šentjakob of 1022 $m^3 s^{-1}$ were observed in September 2010. At the same time, the signal of flooding was recorded and its influence on the piezometric groundwater table in the aquifer was observed (Fig. 3).

In precipitation only $\delta^{18}O$ values were determined. Values ranged from −13.9‰ to −4.9‰ with a weighted mean of −8.7 ± 2.7‰. Significant differences in $\delta^{18}O$ values in precipitation in different seasons were observed ($p = .01$). The marked seasonal variation is typical for the Northern Hemisphere (Vreča et al., 2008). Fig. 3 shows that the mean $\delta^{18}O$ values in precipitation over periods from October 2010 to March 2011 and from April to September in 2010 and 2011 were different: −10.6‰ and −7.0‰, respectively. Thus, winter precipitation was more ^{18}O-enriched mainly due to the lower temperature.

The previous investigation indicated that the Local Meteoric Water Line in Ljubljana, so-called Ljubljana Meteoric Water Line (LMWL): $\delta^2H = (8.06 \pm 0.08)\ \delta^{18}O + (9.84 \pm 0.71)$ is close to the Global Meteoric Water Line and shows the predominant influence of Atlantic air masses in Ljubljana, although the influence of Mediterranean air masses could not be excluded. This contribution was estimated to be in the range 15–26% (Vreča et al., 2008). In addition, a recent study of precipitation at the Reactor Centre in Ljubljana over the period 2007–2010 was performed by Vreča et al. (2014) and the obtained data in 2010 are comparable to our $\delta^{18}O$ values. In their study the Local Meteoric Water Line was calculated and the slope and the intercept was found to be similar to the LMWL calculated from the long-term data (from 1981 to 2006). Thus, the weighted mean $\delta^{18}O$ and $\delta^{2}H$ values together with ^{3}H activities obtained in the study provided by Vreča et al. (2014) are included in Table 2. In addition $\delta^{2}H$ values were calculated from the LMWL for each month in 2011 (Vreča et al., 2014) and included in Table S1. The measured ^{3}H activities in precipitation are comparable to those from the past studies in Slovenia and neighbouring countries. The mean annual ^{3}H activity is 9.1 TU for the period 1998–2010 in Ljubljana, while the mean values for Zagreb (Croatia) precipitation are 8.6 TU and 9.0 TU for periods 1998–2010 and 2007–2010, respectively (Vreča et al., 2014). Horvatinčič et al. (2011) presented precipitation data observed in Zagreb over the year 2010 that ranged from 4 to 14 TU with the highest values observed in summer.

3.2. The Sava River

Water temperature of the Sava River varied from 4.9 °C in March 2011 to 16.1 °C in July 2010 (Table S1), electrical conductivity (EC) from 236 to 392 μS cm^{-1} and pH from 7.57 to 8.46, while NO_3^- concentrations ranged from 3.47 mg l^{-1} to 6.82 mg l^{-1} with the mean value of 4.55 ± 1.29 mg l^{-1} (Tables 2 and S1). Temporal differences were not significant in the cases of all three parameters: EC ($p = .091$), pH ($p = .097$), NO_3^- ($p = .142$).

The discharge and $\delta^{18}O$ values for the Sava River over the sampling period 2010–2011 are presented in Fig. 3. Over this period similar trend in $\delta^{18}O$ values in the Sava River water and precipitation was observed (Fig. 3). Previous investigation indicated that the Sava River responds quickly to precipitation, which is further reflected in the isotopic composition of the Sava River water (Ogrinc et al., 2008). $\delta^{18}O$ values of the Sava River water ranged from −9.7‰ to −8.5‰ and $\delta^{2}H$ values ranged from −66.4‰ to −57.6‰ with the mean $\delta^{18}O$ value of −9.2 ± 0.4‰ and the mean $\delta^{2}H$ value of −62.0 ± 2.9‰ (Table 2). Marked seasonal variability was reflected in the isotopic composition of the Sava River water ($p = .04$) with intra-seasonal variations. Under average flow conditions, the Sava River water tends to be isotopically depleted in ^{18}O relative to local precipitation. The depletion in heavy isotopes in the Sava River water likely reflects the dominance of precipitation infiltrating at higher altitude areas (the Alps) rather than locally at the Ljubljansko polje (Ogrinc et al., 2008).

The ^{3}H activity of the Sava River water ranged from 4.5 to 8.7 TU with the highest value observed in August 2010 (Fig. 4). The mean ^{3}H activity was 6.4 ± 1.3 TU. Significant temporal differences were observed in ^{3}H activity ($p \leq 0$).

3.3. Groundwater

Groundwater temperature ranged from 10.2 to 13.6 °C, the highest temperature was measured at Hrastje 8 and the lowest at Jarški prod 1 (Table S1). Statistical analyses showed significant differences in temperatures between locations ($p = .034$). Temperature observed at Jarški prod 1 differed significantly from temperature at Hrastje 3 and Hrastje 8. On the other hand, no significant temporal differences in groundwater temperatures were observed ($p = .103$). pH ranged from 6.98 to 8.44, with the mean value of 7.75 ± 0.33 (Table S1). The lowest pH was observed at Kleče 8 in August 2010 and the highest at Hrastje 3 and Kleče 8 in April 2011. Spatial and temporal differences in pH were not statistically significant ($p = .070$, $p = .098$). In the case of electrical conductivity (EC) and NO_3^- concentrations significant differences between locations were observed for both parameters ($p = .0001$), while temporal differences were not significant ($p = .098$, $p = .477$). This indicates different geological and anthropogenic influences on

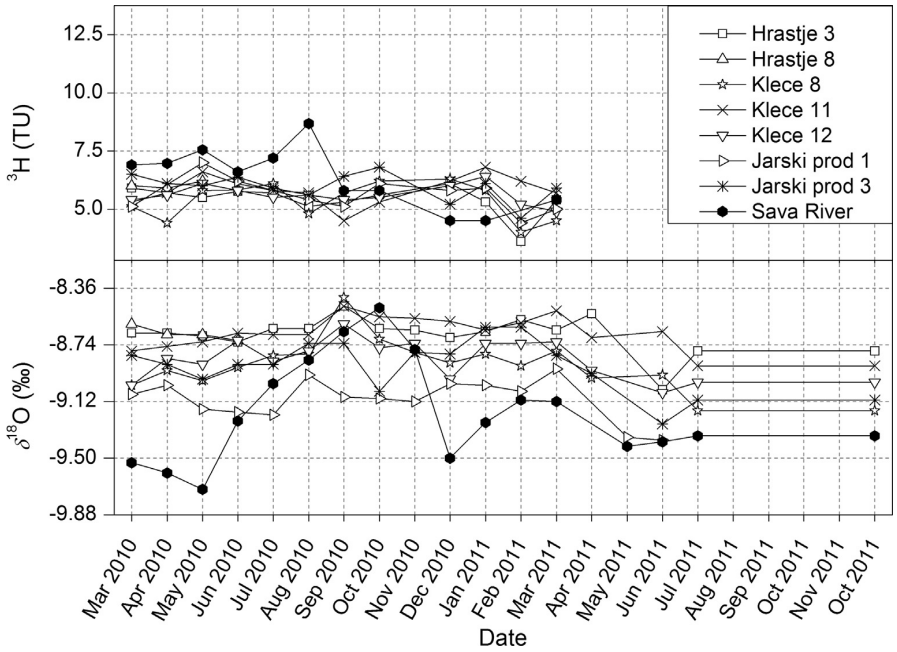


Fig. 4. Variations of ^{3}H and δ^{18}O values in groundwater and the Sava River for the period 2010–2011.

groundwater at different sampling locations due to changes of the aquifer properties and the land use at a local scale. EC ranged from 203 to 640 μS cm^{-1} with the lowest values observed at Kleče 12 in June 2010 and the highest at Hrastje 8 in April 2010 (Table S1). EC in Jarški prod differed significantly from the other locations. In addition, the difference in EC was also observed between Kleče and Hrastje and was found to be higher at Hrastje then at Kleče. The NO_3^- concentrations in groundwater ranged from 1.40 to 50.3 mg l^{-1} at Kleče 8 and Hrastje 3, respectively (Table S1), with the mean values ranging from 7.10 ± 4.47 to 34.3 ± 11.5 mg l^{-1} (Table 2). The lowest and the highest mean NO_3^- concentrations were observed at Jarški prod 1 and Hrastje 8, respectively.

The δ^{18}O values of groundwater ranged from −9.4‰ at Jarški prod 1 to −8.4‰ at Kleče 8 with the mean δ^{18}O value of −8.8 ± 0.2‰. The δ^2H values ranged from −63.8‰ at Kleče 12 to −55.0‰ at Hrastje 3 with the mean δ^2H value of −59.1 ± 2.2‰ (Tables 1 and 2). The ^{3}H activities of groundwater ranged from 3.6 to 7.0 TU at Hrastje 3 and Jarški prod 1, respectively, with the mean values ranging from 5.4 ± 0.8 TU to 6.0 ± 0.6 TU (Table 2) and can be classified as "modern waters". No significant differences according to the location and the season were observed for any of the three environmental isotopes: δ^{18}O (p = .207, p = .062), δ^2H (p = .247, p = .534), ^{3}H (p = .200, p = .130).

Noble gases were also determined in groundwater (Table 3). Values of R/R$_a$ range from 0.153 at Kleče 8 to 1.027 at Jarški prod 3. Measured ^{4}He values range from 3.49 × 10^{-7} ccSTP g^{-1} to 4.93 × 10^{-8} ccSTP g^{-1} and are highly correlated with the helium isotope ratio (as given by R/R$_a$). Calculated concentrations of terrigenic ^{4}He (^{4}He produced in the subsurface from the decay of U and Th) are significant in some samples, with a maximum occurring at Kleče 8 of 3 × 10^{-7} ccSTP g^{-1}. All samples have Ne concentrations near equilibrium with the atmosphere with values ranging from only 2.10 × 10^{-7} to 2.48 × 10^{-7} ccSTP g^{-1}. Mean residence time (MRT), calculated with the Eq. (1), ranged from 2.1 to 8.4 years with uncertainties ranging from 2.8 to 6.2 years (Table 3). Uncertainties in the estimated MRTs were evaluated using the Monte Carlo method in which the input parameters, used to calculate the MRT, were varied by plus/minus one standard deviation from the mean (measured) value (Table 3). However, it was not possible to estimate a ^{3}H/^{3}He age/MRT for the wells at Kleče due to significant levels of the terrigenic ^{4}He and the uncertainty in the ^{3}He/^{4}He ratio of this He.

4. Discussion

4.1. Stable isotope composition

The mean δ^{18}O and δ^2H values of groundwater samples plot between the LMWL (Vreča et al., 2008) and the Sava River regression line (Ogrinc et al., 2008) showing that groundwater is directly influenced by both sources: the infiltration of local precipitation and the recharge from the Sava River water (Fig. 5). Despite the fact that water supplies effect groundwater MRT, groundwater flow dynamics, fastest recharge of the Sava River water over days without precipitation and consequently also isotopic composition of groundwater, the environmental isotope fingerprints still detect infiltrated local precipitation. Thus, it is assumed that production wells should not have significant influence on our data interpretation.

The groundwater samples scatter around the regression line characterised by the equation: $\delta^2H = 3.47 \times \delta^{18}O - 28.61$ with $R^2 = 0.87$. The mean d-excess ($d = \delta^2H - 8 \times \delta^{18}O$) of 11.4‰ for the Ljubljansko polje aquifer system is similar to d-excess of 11.3‰ found in the Sava River water at Šentjakob (Table 2). Thus, the Sava River water reflected the contribution of precipitation of the mixed Atlantic-Mediterranean origin (Ogrinc et al., 2008).

Based on the mean average δ^{18}O and δ^2H values two groups of wells can be clearly defined (Fig. 5):

- Group 1: Jarški prod 1, Jarški prod 3, Kleče 8 and Kleče 12 where the Sava River water represents a significant or dominant contribution to groundwater.

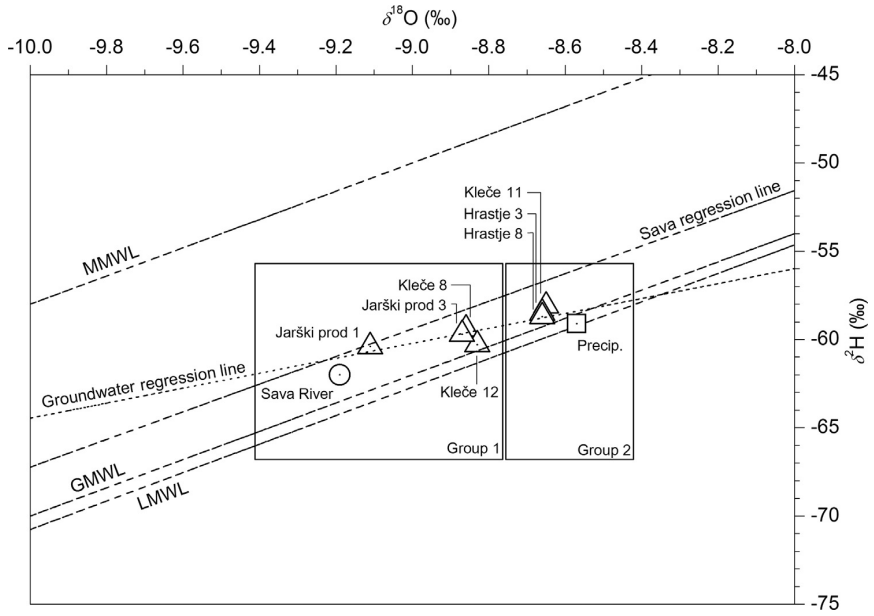


Fig. 5. Relationships between mean $\delta^{18}O$ and $\delta^{2}H$ of groundwater and the Sava River water with the regression line, the Global Meteoric Water Line (GMWL), the Mediterranean Meteoric Water Line (MMWL), the Ljubljana Meteoric Water Line (LMWL) (Vreča et al., 2006) and the Sava River regression line (Ogrinc et al., 2008).

- Group 2: Hrastje 3, Hrastje 8 and Kleče 11 with higher $\delta^{18}O$ and $\delta^{2}H$ values than the Group 1 indicating greater influence of local precipitation.

The $\delta^{18}O$ and $\delta^{2}H$ values show that isotopic composition of groundwater samples taken from individual wells is either more similar to that of local precipitation, or to the isotopic composition of the Sava River water (Urbanc and Jamnik, 1998). The enrichment with both heavy isotopes ^{18}O and ^{2}H along the regression line indicates mixing of water from a river with infiltrated local precipitation in an aquifer. Higher $\delta^{18}O$ and $\delta^{2}H$ values observed in groundwater in the Group 2 could not be explained by evaporation of the Sava River water, since the Sava River is a torrential river where the evaporation effect can be neglected (Ogrinc et al., 2008). It is also known that the Ljubljansko polje aquifer system is partly recharged with groundwater from the Ljubljansko Barje aquifer (Jamnik et al., 2000), which could have an influence on the isotopic composition of groundwater at Kleče. However, in the study provided by Cerar and Urbanc (2013) it was shown that the contribution of groundwater from the Ljubljansko Barje aquifer at Kleče is of minor importance. This estimation was performed based on molar Ca/Mg ratios ranging between 2.5 and 3.0 and HCO_3^- data. Ljubljansko polje has higher Ca/Mg ratios and lower HCO_3^- concentrations comparing to Ljubljansko Barje aquifer.

The two groups of groundwater determined in Fig. 5 could be further justified by geological properties of the aquifer and spatial distribution of the wells. There are two main areas where the Sava River recharges the aquifer: (1) from Tacen to the Gameljščica tributary and (2) from Tomačevo to Šentjakob (Fig. 1). The water inflow from the upstream river section reaches Kleče, while the water inflow from the downstream river section reaches Jarški prod. The Sava River water needs more time to reach Hrastje, more likely due to the complicated bedrock geometry in this area, therefore the signal of the Sava River water is smaller there. The wells in Jarški prod, especially the well Jarški prod 1, are located close to the Sava River bed on the permeable Sava River floodplain, which is mainly composed of gravel mixed with sand and silt. Thus, it is expected that groundwater in Jarški prod has higher fraction of the Sava River water (Fig. 6). The Kleče and Hrastje pumping stations are located on the higher terrace, where the aquifer is deeper under the surface and where conglomerate and clay appear (Fig. 1). The area around Kleče pumping station may also be locally covered with thick lenses of poorly permeable sediments, since perched aquifers are present near the Kleče station (Šram, 2011). For this reason leaching of the subsurface water is stymied. The geological composition of the aquifer at Kleče might be one of the reasons why the groundwater mixture at the well Kleče 11 differs from the groundwater mixtures at the wells Kleče 8 and Kleče 12, although they are located close to each other (Fig. 1). In fact, perforated screens in the wells at Kleče are located at different depths (Fig. 2). It can be seen that the wells Kleče 8 and Kleče 12 pump groundwater from deeper layers of the aquifer than the well Kleče 11. Thus, different isotopic composition between shallow and deep groundwater might be also an effect of smaller hydraulic conductivity in vertical direction than in horizontal direction.

Statistically significant differences between $\delta^{18}O$ values in the Sava River water and local precipitation ($p = .0315$) were observed. Thus, a simple isotope mass-balance calculation was performed to estimate fractions of each recharge water types in the aquifer. First, a time-constant mixing calculation was performed using Eqs. (3) and (4). In this calculation for $\delta^{18}O_{RW}$ a mean $\delta^{18}O$ value of −9.2‰ for the Sava River was applied (Table 2), while for $\delta^{18}O_P$ the mean annual weighted value of −8.6‰ reported by Vreča et al. (2014) was used. The results of this calculation are presented in Fig. 6. It was found that local precipitation dominates in the groundwater samples taken from the wells Kleče 11, Hrastje 3, and Hrastje 8, where their fractions are even higher than 85%. Groundwater pumped from the well Kleče 12 has also higher fraction of precipitation (59%), while both sources equally contribute to groundwater at the wells Kleče 8 and Jarški prod 3. The main source of groundwater pumped from the well Jarški prod 1 is the Sava River.

It should be mentioned that an influence of both end-members are changing during time, therefore a possibility of using a

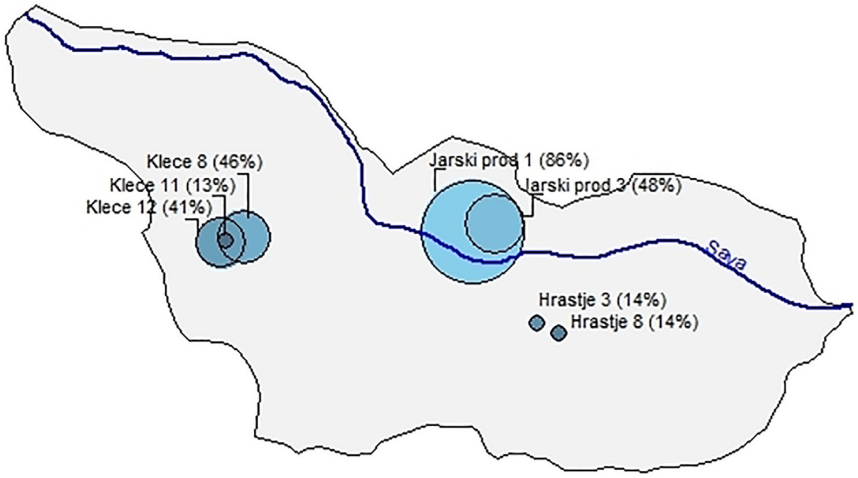


Fig. 6. The calculation of the fractions of the Sava river water versus local precipitation in groundwater over the period 2010–2011 calculated using the time-constant mixing model.

time-dependent mixing ratios was also investigated. The transport of ^{18}O from the Sava River towards a production well (e.g. Jarški prod 1) was performed with the Transit analysis (Eqs. (5)–(7)). A one-dimensional solution to the advection dispersion equation with the observed $\delta^{18}O$ in the Sava River during the sampling period from March 2010 to October 2011 as input was used. Fig. 7 shows the simulated value of $\delta^{18}O$ at the well with the assumption that the virtual well pumps groundwater, which has only one source – the Sava River water (f_{RW} = 1 in Eq. (7)). If the groundwater MRT between the Sava River and the well is only 10 days, then (as shown in the dark brown curve in Fig. 7) the $\delta^{18}O$ value in the well Jarški prod 1 should have dropped down to −8.5‰ shortly after the $\delta^{18}O$ value of the Sava River did in September 2010. As it can be seen in Fig. 7, the longer the MRT is, the greater is a delay of the $\delta^{18}O$ peak in the Sava River, which is also getting more attenuated in time. For example, if the MRT is 500 days (1.36 years) the $\delta^{18}O$ in the well would only change to a value about −9.2‰ and this change would occur in 500 days after it occurs in the Sava River. The $\delta^{18}O$ values at the well Jarški prod 1 do not show this change. The time-constant mixing model shows that groundwater from the well Jarški prod 1 has the highest fraction of the Sava River water, thus if this change is not observed in the well Jarški prod 1, it is not likely to occur in any of the other wells. If the MRT between the Sava River and the well Jarški prod 1 is about 200 days or longer, the expected change would only be about 0.4‰ or less. The data showed that the $\delta^{18}O$ variation in the well Jarški prod 1 were only slightly larger than the measurement uncertainty of 0.1‰ and much smaller than the variation observed in the Sava River (about 1.0‰). Thus, the only plausible explanation why in the well Jarški prod 1, where the Sava River water is the dominant groundwater source, the observed $\delta^{18}O$ variations of the Sava River water could not be seen is the MRT longer than one year. In this case, the dispersion would smooth out variations observed during a year, which indicate that the MRT is longer than the period of the oscillation. Therefore, a time-constant analysis using mean values is appropriate for this study.

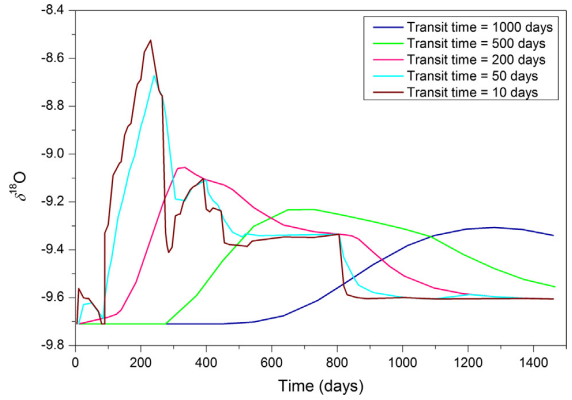


Fig. 7. The changes of the simulated $\delta^{18}O$ values at the well Jarški prod 1 vs. mean residence time (MRT). As an example, the model assumes that the well is pumping 100% of the Sava River water.

4.2. ^{3}H and $^{3}H/^{3}He$ values and mean residence time

According to Vreča et al. (2014) the highest mean weighted ^{3}H activity of 9.9 ± 4.9 TU was observed in precipitation. The mean ^{3}H activity in the Sava River water was estimated to be 6.4 ± 1.3 TU. The mean ^{3}H activities in groundwater were 5.6 ± 0.5 TU and 5.8 ± 0.6 TU in the Groups 1 and 2, respectively (Table 2). The lowest ^{3}H activity of 3.6 TU was observed at Hrastje 3 in February 2011. Based on the decay of ^{3}H and measurements of ^{3}H activities in groundwater, it was estimated, that the mean residence times (MRTs) 2–5 years best fit the data of groundwater samples indicating that mostly modern water is present in the Ljubljansko polje aquifer system (Table 3). A similarity in ^{3}H activities between groundwater and the Sava River water indicates that the Sava River water reaches the wells in less than 10 years (Al-Charideh and Hasan, 2013).

More accurate information about the groundwater MRT could be obtained by the $^{3}H/^{3}He$ method, which results are given in Table 3 and are summarized as follows:

- *Kleče 8 and 12*: Significant amounts of terrigenic ^{4}He and low R/R_a suggest a mixture of mostly very young water probably from the Sava River with some very old water. This old water must come from deeper parts of the aquifer with a long (but unknown) MRT, since it has accumulated such a large amount of terrigenic ^{4}He. However, the ^{3}H data suggest that

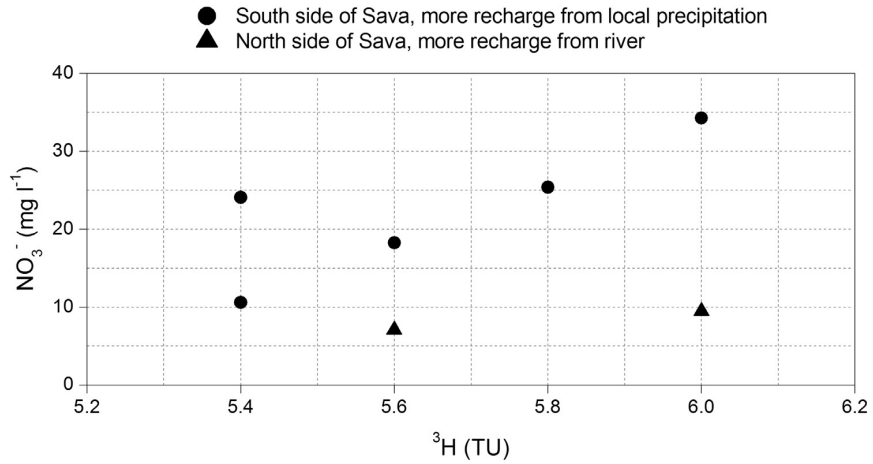


Fig. 8. Relationships between the average ^{3}H activity and NO_3^- concentrations in the wells divided by the northern and southern parts of the Sava River.

groundwater contain no more than 10% of this old water, otherwise the ^{3}H value would be much lower than the measured ones. The presence of very old water in Kleče could be a consequence of tectonic factors, probably of still active Ljubljanski fault. At these locations the ^{3}H/^{3}He method could not be used to determine the age or MRT of the groundwater, since the presence of very old water can influence this estimation.

- *Kleče 11*: Low R/R_a suggests a mixture of mostly very young water with some very old water, but with a lesser amount than in wells Kleče 8 and Kleče 12. In this well, the calculated tritiogenic ^{3}He was slightly negative, but our uncertainty analysis showed that the MRT could be of 4 years.
- *Hrastje 3 and 8*: Modest amounts of terrigenic ^{4}He and low R/R_a suggest a water mixture of young and a small amount of old water with a long MRT. The MRTs are between 3 and 8 years with differences possibly related to the difference in the screened intervals.
- *Jarški prod 1* and *3:* Samples do not have component of old water. This is young groundwater with the variable MRTs of 2 and 7 years.

4.3. Nitrate concentrations

In terms of the groundwater resources management with respect to the high NO_3^- levels, the mean residence time (MRT) of groundwater is an important parameter. Higher values of ^{3}H and NO_3^- concentrations should demonstrate shorter MRTs and thus higher vulnerability of the aquifer system to pollution (Al-Charideh and Hasan, 2013). Positive correlations were observed between ^{3}H and NO_3^- concentrations for the wells located on the south side of the Sava River, which receive more water from local precipitation, as well as for the wells located on the north side of the Sava River that receive more water from the Sava River (Fig. 8). The correlation (R^2) between ^{3}H and NO_3^- in the wells on the south side of the Sava River is 0.54.

However, the slopes of both correlations are different, probably due to greater dilution by the Sava River water and/or different concentrations of NO_3^- near the wells in Jarški prod. Graphical position of the wells in Figs. 1 and 6show that greater fractions of the Sava River water are present in groundwater pumped from the wells located closer to the Sava River and thus the Sava River water dilutes the NO_3^- signal in groundwater. The highest NO_3^- concentrations were observed in the Group 2 (Hrastje 3, Hrastje 8, Kleče 11), where local precipitation was the main source of groundwater. This indicates that precipitation leaches NO_3^- from soil in these agriculturally active areas (Kladnik et al., 2005). The atmospheric deposition of NO_3^- at these locations (as estimated using stable isotopes in N and O; (Tamše, per.com.) contributes only about 10% of the total NO_3^-. Thus, Hrastje is the most endangered pumping station in the Ljubljansko polje in terms of pollution from agricultural sources. In addition, the positive correlation between ^{3}H and NO_3^- might be also a consequence of the damaged pipeline, since these processes modify the water quality (NO_3^- concentrations) and have an influence on ^{3}H activities. The damaged and old pipeline is a well known problem. It was estimated that up to 37% of pumped groundwater was lost in 2003 in the Ljubljansko polje (Andjelov et al., 2005). Further investigation, based on the stable isotope composition of nitrate, should give us better understanding of the NO_3^- sources in the selected study area.

5. Conclusions

An isotopic investigation of precipitation, river water and groundwater shows spatial variability of groundwater composition in the Ljubljansko polje aquifer system in the central part of Slovenia over the period 2010–2011. The Sava River and local precipitation are the main sources of groundwater in this alluvial aquifer. A binary mixing model indicates that groundwater pumped from the wells Kleče 11, Hrastje 3, and Hrastje 8 is mostly composed of local precipitation (>86%), while similar fractions of both sources were calculated for groundwater pumped from the wells Kleče 8, Kleče 12 and Jarški prod 3. The Sava River water especially dominates in groundwater pumped from the well Jarški prod 1. Fraction of both sources is influenced by the distance of the well from the Sava River and the depth of the screens in the well.

^{3}H analyses indicated a presence of mostly modern water with a short mean residence time (MRT) in the Ljubljansko polje aquifer system. However, noble gas analyses show that up to 10% of groundwater in Kleče 8 and Kleče 12 is very old, the exact age of which should be precisely determined by another method, such as ^{14}C. On the other hand, groundwater with a long MRT is not present at the Jarški prod area. In the future, these data will be used in groundwater flow simulations and for delineation of groundwater protection areas and capture zones.

In terms of groundwater resource management the groundwater MRT is an important parameter. The highest concentrations of NO_3^- were observed at Hrastje, where local precipitation is the main source of groundwater. Thus, groundwater at Hrastje

pumping station is more vulnerable to potential pollution from agricultural sources, whereas the wells in Jarški prod are more vulnerable to a potential pollution from the Sava River.

Selection of this study area is crucial in hydrology, especially for investigation of so complex hydrological processes such as surface-groundwater interactions. The important issues can be highlighted as follows: the Sava River might change its role from losing to gaining stream within a few kilometres making it an ideal place for modelling of two different relationships on a small scale; the system is very dynamic since groundwater table responds to increased river discharge or amount of precipitation within a day or a month; its boundary conditions can be controlled very well; the bedrock, which has a large influence on groundwater dynamic but it is often just a sideline, has a diverse geometry here and can be extended from the surface to even 100 m below the surface; and the area is occupied by different anthropogenic activities, which offer the possibility to study the vulnerability of groundwater to pollution sources. As it was also illustrated, because of its strategic location – south from the Alps and close to the Adriatic see, isotopic composition of the Sava River and local precipitation can be easily distinguished, which is not the case in many studies. The paper further shows how dynamic, varied and sensitive the aquifer system in Ljubljansko polje is, making it an excellent case study not only to investigate surface-groundwater interactions, but also influences of climate change in the future.

Acknowledgement

The project was financially supported by the IAEA Project under Contact No. RER8016 TC entitled "Using Environmental Isotopes for Evaluation of Stream water/Groundwater Interactions in Selected Aquifers in the Danube Basin" and by the EU 7th Research Project – GLOBAQUA (Managing the effects of multiple stressors on aquatic ecosystem under water scarcity) under Grant agreement no. 603629-ENV-2013-6.2.1. The research was partially conducted within a PhD study of Janja Vrzel financed by the European Social Fund (KROP 2012) no. C2130-12-000070. The authors would like to thank all those who helped us, especially Mrs. Branka Bračič Železnik (VO-KA) and Mr. Janko Urbanc (GeoZS). The technical support and assistance for isotope analyses provided by Mr. Stojan Žigon is greatly appreciated.

Appendix A. Supplementary data

Supplementary data associated with this article can be found, in the online version, at https://doi.org/10.1016/j.jhydrol.2017.11.022.

References

Aeschbach-Hertig, W., Peeters, F., Beyerle, U., Kipfer, R., 2000. Palaeotemperature reconstruction from noble gases in ground water taking into account equilibration with entrapped air. Nature 405, 1040–1044.
Aggarwal, P.K., Gat, J., Froehlich, K.F.O., 2006. Isotopes in the Water Cycle: Past, Present and Future of a Developing Science. Springer, Dordrecht.
Al-Charideh, A., Hasan, A., 2013. Use of isotopic tracers to characterize the interaction of water components and nitrate contamination in the arid Rasafeh area (Syberia). Environ. Earth Sci. 70, 71–82.
Andjelov, M., Bat, M., Frantar, P., Mikulič, Z., Savić, V., Uhan, J., 2005. Pregled elementov vodne balance. In: Rejec Brencelj, I., Smrekar, A., Kladnik, D. (Eds.), Podtalnica Ljubljanskega polja (in Slovene). Založba ZRC, Ljubljana, pp. 27–38.
Bračič Železnik, B., 2002. Kje so meje rabe prostora in izkoriščanja podtalnice vodonosnika Ljubljanskega polja in barja. In: Brilly, M., Jamnik, B., Bračič Železnik, B. (Eds.), Zaščita vodnih virov in vizija oskrbe s pitno vodo v Ljubljani: zbornik. Faculty of Civil Engineering and Geodetic Engineering, Chair of Hydrology and Hydraulic Engineering and Javno podjetje Vodovod-Kanalizacija Ljubljana, Ljubljana, pp. 117–127.
Bračič Železnik, B., Jamnik, B., 2005. Javna oskrba s pitno vodo. In: Rejec Brencelj, I., Smrekar, A., Kladnik, D. (Eds.), Podtalnica Ljubljanskega polja (in Slovene). Založba ZRC, Ljubljana, pp. 101–120.
Bračič Železnik, B., Pintar, M., Urbanc, J., 2005. Naravne razmere vodonosnika. In: Rejec Brencelj, I., Smrekar, A., Kladnik, D. (Eds.), Podtalnica Ljubljanskega polja (in Slovene). Založba ZRC, Ljubljana, pp. 17–26.
Cappa, C.D., Hendricks, M.B., DePaolo, D.J., Cohen, R.C., 2003. Isotopic fractionation of water during evaporation. J. Geophys. Res. 108 (D16), 1–10.
Cerar, S., Urbanc, J., 2013. Carbonate chemistry and isotope characteristics of groundwater of Ljubljansko polje and Ljubljansko Barje aquifers in Slovenia. Sci. World J. 2013, 1–11.
Clarke, W.B., Jenkins, W.J., Top, Z., 1976. Determination of tritium by mass spectrometric measurement of ^{3}He. Int. J. Appl. Radiat. Isot. 27 (9), 515–522.
Cook, P., Herczeg, A., 1998. Groundwater chemical methods for recharge studies. CSIRO Publishing, Collingwood.
Ekwurzel, B., Schlosser, P., Smethie, W.M., Plummer, L.N., Busenberg, E., Michel, R.L., Weppering, R., Stute, M., 1994. Dating of shallow groundwater: comparison of the transient tracers ^{3}H/^{3}He, chlorofluorocarbons, and ^{85}Kr. Water Resour. Res. 30, 1693–1708.
Epstein, S., Mayeda, T.K., 1953. Variations of ^{18}O of waters from natural sources. Geochim. Cosmochim. Acta 4, 213–224.
Gat, J.R., 1996. Oxygen and hydrogen isotopes in the hydrologic cycle. Ann. Rev. Earth Planet Sci. 24, 255–262.
Gehre, M., Hoefling, R., Kowski, P., Strauch, G., 1996. Sample preparation device for quantitative hydrogen isotope analysis using chromium metal. Anal. Chem. 68, 4414–4417.
Horvatinčič, N., Barešić, J., Krajcar Bronić, I., Karman, K., Forizs, I., 2011. Study of the bank filtered groundwater system of the Sava River at Zagreb (Croatia) using isotope analysis. Cent. Eur. Geol. 54, 121–127.
Jamnik, B., Kristensen, M., Anderson, U., Sorensen, H.R., Refsgaard, A., Gustavsson, L., 2000. Water resources management model for Ljubljansko polje and Ljubljansko Barje, Final Report Project No. 98-50228, DHI Water & Environment, Denmark, in association with Geological Survey of Slovenia, Hydro– Engineering and Hydro-Consulting, Slovenia.
Kendall, C., Doctor, D.H., 2004. Stable Isotopes Applications in Hydrologic Studies. In: Drever, J.I. (Ed.), Surface and groundwater weathering, and soils: treatise on geochemistry, 5. Elsevier, New York, pp. 319–364.
Kendall, C., McDonnell, J.J., 1998. Isotope Tracers in Catchment Hydrology. Elsevier, Amsterdam.
Kipfer, R., Aeschbach-Hertig, W., Peeters, F., Stute, M., 2002. Noble gases in lakes and ground waters. In: Porcelli, D. (Ed.), Noble gases in geochemistry and cosmochemistry, reviews in mineralogy and geochemistry. Mineral. Soc. of Am, Washington, pp. 615–700.
Kladnik, D., Rejec Brancelj, I., Smrekar, A., 2005. Kmetijsko obremenjevanje. In: Rejec Brencelj, I., Smrekar, A., Kladnik, D. (Eds.), Podtalnica Ljubljanskega polja (in Slovene). Založba ZRC, Ljubljana, pp. 134–163.
Lachniet, M.S., Patterson, W.P., 2002. Stable isotope values of Costa Rican surface waters. J. Hydrol. 260, 135–150.
Małoszewski, P., Zuber, A., 1982. Determining the turnover time of groundwater systems with the aid of environmental tracers: 1. Models and their applicability. J. Hydrol. 57 (3–4), 207–231.
Mamyrin, B.A., Tolstikhin, I.N., 1984. Helium Isotopes in Nature (Vol. 3). Elsevier.
Ogrinc, N., Kanduč, T., Stichler, W., Vreča, P., 2008. Spatial and seasonal variations in δ^{18}O and δD values in the Sava River in Slovenia. J. Hydrol. 359, 303–312.
Petauer, D., Hiti, T., 2013. Vpliv črpanja iz vodnjakov vodarne Hrastje na podzemno vodo vodonosnika Ljubljanskega polja (in Slovene). GEORAZ, d.o.o., Ljubljana.
Poreda, R.J., Cerling, T.E., Salomon, D.K., 1988. Tritium and helium isotopes as hydrologic tracers in a shallow unconfined aquifer. J. Hydrol. 103 (1–2), 1–9.
Premru, U., 2005. Tektonika in tektogeneza Slovenije = Tectonics and tectogenesis of Slovenia (in Slovene). Geological Survey of Slovenia, Ljubljana.
Premru, U., 1983. Osnovna geološka karta SFRJ. Tolmač lista Ljubljana: L 33–66. Beograd: Zvezni geološki zavod, pp. 111.
Schlosser, P., Stute, M., Dorr, H., Sonntag, C., Munnich, K.O., 1988. Tritium/^{3}He dating of shallow groundwater, Earth Planet. Sci. Lett. 89, 353–362.
Solomon, D.K., Cook, P.G., 2000. ^{3}H and ^{3}He. In: Cook, P.G., Herczeg, A.L. (Eds.), Environmental tracers in subsurface hydrology. Kluwer Academic Publishers, Boston, pp. 397–424.
Solomon, D.K., Poreda, R.J., Schiff, S.L., Cherry, J.A., 1992. Tritium and helium 3 as groundwater age tracers in the Borden aquifer. Wat. Resour. Res. 28, 741–755.
Solomon, D.K., Schiff, S.L., Poreda, R.J., Clarke, W.B., 1993. A validation of the ^{3}H/^{3}He method for determing groundwater recharge. Water Resour. Res. 29, 2951–2962.
Šram, D., 2011. Hidrogeologija visečih vodonosnikov na Ljubljanskem polju = Hydrogeology of Ljubljansko polje perched aquifers (in Slovene). University of Ljubljana Faculty of Natural Sciences and Engineering, Department of Geology, Ljubljana.
Šram, D., Brenčič, M., Lapajne, M., Janža, M., 2012. Prostorski model visečih vodonosnikob na Ljubljanskem polju = Perched aquifers spatial model: a case study for Ljubljansko polje (central Slovenia) (in Slovene). Geologija 55, 107–116.
Stichler, W., Małoszewski, P., Moser, H., 1986. Modelling of river water infiltration using oxygen-18 data. J. Hydrol. 83, 355–365. https://doi.org/10.1016/0022-1694(86) 90161-7.
Urbanc, J., Jamnik, B., 1998. Isotope investigation of groundwater from Ljubljansko polje (Slovenia). Geoloija 41, 355–364.
Urresti-Estala, B., Vadillo-Pérez, I., Jiménez-Gavilán, P., Soler, A., Sánchez-García, D., Carrasco-Cantos, F., 2015. Application of stable isotopes (δ^{34}S-SO$_4$, δ^{18}O-SO$_4$,

$\delta^{15}N\text{-}NO_3$, $\delta^{18}O\text{-}NO_3$) to determine natural background and contaminant sources in the Guadalhorce River Basin (souther Spain). Sci. Total Environ. 506–507, 46–57.

Vižintin, G., Souvent, P., Veselič, M., Cencur Curk, B., 2009. Determination of urban groundwater pollution in alluvial aquifer using linked process models considering urban water cycle. J. Hydrol. 377, 261–273.

Vreča, P., Krajcar Bronić, I., Horvatinčić, N., Barešić, J., 2006. Isotopic characteristics of precipitation in Slovenia and Croatia: comparison of continental and maritime stations. J. Hydrol. 330, 457–469.

Vreča, P., Krajcar Bronić, I., Leis, A., Brenčič, M., 2008. Isotopic composition of precipitation in Ljubljana (Slovenia). Geologija 51, 169–180.

Vreča, P., Krajcar Bronić, I., Leis, A., Demšar, M., 2014. Isotopic composition of precipitation at the station Ljubljana (Reaktor), Slovenia – period 2007–2010. Geologija 57 (2), 217–230.

Žlebnik, L., 1971. Pleistocen Kranjskega, Sorškega in Ljubljanskega polja (in Slovene). Geologija 17, 477–491.

3.4 An Integrated Simulation Approach for Studying the Hydrology of the Ljubljansko Polje Aquifer in Slovenia

This sub-chapter represents the main research I performed in the scope of the proposed PhD thesis, which is presented in the paper "An Integrated simulation approach for studying the hydrology of the Ljubljansko polje aquifer in Slovenia" by Janja Vrzel, Ralf Ludwig, Goran Vižintin and Nives Ogrinc. The paper is currently under review in Environmental Modelling & Software.

The paper presents details of the full modeling procedure: data processing, set-up of all four models—WaSiM, MIKE 11 and steady and transient state FEFLOW models, their settings, coupling, calibration, validation and interpretation. The main contribution of this study is the information obtained about groundwater behavior that is hidden behind the data from different sources and can be combined in a hydrological model.

The aim of the study was to create a visual understanding of the hydrology of the Ljubljansko polje, described on the basis of isotopic analyses (Section 3.3). Conceptualization of the study area revealed that the two main groundwater sources impact differently on groundwater at different locations in the aquifer. These impacts vary not only in space, but also in time. Among the chronological data of the hydraulic heads it was possible to observe five oscillation patterns on the basis of which the piezometers were divided into five groups. Cross-correlation analyses showed also the different responsiveness of these five groups to the two main groundwater sources—the Sava River and local precipitation. Later, with the simulated mean residence time I was able to explain the five oscillations patterns with different recharge areas.

A cross-correlation analysis showed that groundwater responsiveness on the surface water, particularly on the Sava River water can be especially fast, within 24 hours in Jarški prod or less than a month in Kleče. For this reason I developed a transient state model. In order to provide a reliable simulation of groundwater flow in an aquifer where interactions between groundwater and surface water are very important (as it was shown in the conceptual model) multiple models were combined. The groundwater flow was simulated with FEFLOW, which was coupled with the ifmMIKE11 plug-in for the simulation of the Sava River dynamic and leaching of river water into the aquifer and vice versa in MIKE 11. Percolation was simulated in WaSiM, thus a link between FEFLOW and WaSiM was also established.

The transient groundwater flow model is based on the data obtained during 2010–2011, since the isotopic analyses of water on which the conceptual model is based were performed during this period. It should be noted that the year 2010 was extremely wet and the year 2011 extremely dry. Therefore daily simulations show fluxes and the behavior of groundwater, surface water and groundwater-surface water interactions under extreme conditions.

Resolving hydrological issues related to sensitive hydrological systems is time consuming and challenging. However, the results provide extraordinary valuable and unique information about the studied aquifer. It even gives a possibility to quantify the important components of the water balance from surface water to the groundwater in space and time. Thus, such an approach gives an excellent basis particularly for studies related to influences of climate or land use changes on hydrology.

In this work, I developed the research question, collect and processed all the data, performed field work, developed all of the three models (WaSiM, MIKE 11 and FEFLOW), developed a link between WaSiM and FEFLOW, and analyzed and interpreted the results. The created database includes:

– meteorological data: precipitation, temperature, wind speed, global radiation, and

humidity;
- hydrological data: groundwater table, water level in the Sava and Ljubljanica Rivers, pumping rates from pumping wells in the Ljubljansko polje, roughness coefficient (Manning's n coefficient) in the Sava River; location of all the pumping wells and piezometers;
- geological data: drilling reports, bedrock geometry, and other reports of geological studies in the Ljubljansko polje; the soil map and data needed for its parametirization, soil moisture;
- digital elevation model data, LiDAR, the Sava River channel cross-sections; land use map and data needed for its parametirization;

Data analysis included statistical analyses of the collected chronological data, and their preparation for modeling, which includes their transformation into specific forms requested for each of the models. Most of this work was done in *R*-software. I also unified all the drilling reports and sediment names. The wells were drilled by different companies, over more than three decades, therefore different names for the same sediment were used. I also showed that the chronological data are appropriate for simulating the conceptual model, the development of which was based on isotopes. Finally, I selected the best calibrated model from the family of all calibrated models, and performed the interpretation of the results.

An integrated simulation approach for studying the hydrology of the Ljubljansko polje aquifer in Slovenia

Authors: Janja Vrzel[1,2*], Ralf Ludwig[1], Goran Vižintin[3], Nives Ogrinc[2,4]

[1]Department of Geography, Ludwig-Maximilians-Universität-München, Luisenstraße 37, 80333 Munich, Germany
[2]Jožef Stefan International Postgraduate School, Jamova cesta 39, 1000 Ljubljana, Slovenia
[3]Department of Geotechnology, Mining and Environment, University of Ljubljana, Aškerčeva cesta 12, 1000 Ljubljana, Slovenia
[4]Department of Environmental Sciences, Jožef Stefan Institute, Jamova cesta 39, 1000 Ljubljana, Slovenia

*Corresponding author: Tel.: +49 (0) 89/ 2180 - 6648; e-mail: j.vrzel@iggf.geo.uni-muenchen.de

Environmental Modelling & Software
May 2018

Abstract

Surface water and groundwater are strongly connected. In fact, quality and quantity changes in one water body can impact water quality and quantity in the other. Therefore, understanding these interactions is important when studying the water balance in a complex aquatic system. In this paper, an integrated and comprehensive approach to studying hydrological system behavior including surface-groundwater interactions is presented. The study is based on knowledge obtained from a multivariate statistics on data collected over a long term period (precipitation levels, river discharge, hydraulic head, and groundwater pumping rate), and their comparison with the isotopic composition of groundwater, river water and precipitation. The hydrology in the study domain was also simulated using a comprehensive modeling framework. Since boundary conditions are very important for simulating groundwater flow in a sensitive aquifer, MIKE 11 and WaSiM were used to model river dynamics and percolation of local precipitation, respectively. The results were used as boundary conditions for a transient state groundwater flow model performed in FEFLOW 6.8 and 7.0. The study used the Ljubljansko polje aquifer (Slovenia) as a case study, which represents a hydrological system highly sensitive to surface-groundwater interactions. The study revealed that a combination of the MIKE11-FEFLOW-WaSiM tools offers a good solution for performing parallel simulations of groundwater and surface water dynamics.

Keywords: surface-groundwater interaction, multivariate statistical methods, hydrological modeling, aquifer responsiveness

Software availability:

- FEFLOW 6.8 and 7.0 and ifmMIKE11 from the MIKE Powered by Danish Hydraulic Institute (DHI), Agern Allé 5, Hørsholm 2970, Denmark, +45 45169333, mike@dhigroup.com, URL: https://www.mikepoweredbydhi.com/;
- WaSiM from the Hydrology Software Consulting J. Schulla, Regensdorferstrasse 162, CH 8049 Zurich, Switzerland, j.schulla@wasim.ch, URL: http://www.wasim.ch/en/;
- R, URL: https://www.r-project.org/;
- ArcMap: URL: http://desktop.arcgis.com;

Data availability:

- Javno podjetje Vodovod-Kanalizacija d.o.o., Vodovodna ulica 90, 1000 Ljubljana, Slovenia, +386 1 580 81 00, E: voka@vo-ka.si, URL: http://www.vo-ka.si: Geological and hydrogeological data.
- Mestna občina Ljubljana (Municipality of Ljubljana), Mestni trg 1, 1000 Ljubljana, Slovenia +386 1 306 10 00, E: glavna.pisarna@ljubljana.si, URL: https://www.ljubljana.si/: River bed cross-sections.
- Pivovarna Laško Union d.o.o., Pivovarniška ulica 2, 1000 Ljubljana, Slovenia, +386 1 471 72 17, E: info.plu@heineken.com, URL: www.pivovarnalaskounion.si: hydrogeological data.
- Savske elektrarne Ljubljana d.o.o., Gorenjska cesta 46, 1215 Medvode, Slovenia, +386 1 474 9 221, E: info@sel.si, URL: http://www.sel.si/, LiDAR data.

- Slovenian Environmental Agency, Vojkova cesta 1b, 1000 Ljubljana, Slovenia, +386 1 4784 000, E: gp.arso@gov.si, URL: http://www.arso.gov.si – hydrological and meteorological data.
- University of Ljubljana, Biotechnical Faculty - Infrastructural Centre for Pedology and Environmental Protection (ICPVO), Jamnikarjeva ulica 101, 1000 Ljubljana, +386 1 3203 000, E: info@bf.uni-lj.si, URL: http://www.bf.uni-lj.si: Soil texture map.
- [dataset] European Environmental Agency, 2016. CORINE Land Cover database of the year 2006. https://www.eea.europa.eu/data-and-maps/data/clc-2006-raster-4#tab-european-data.

1. Introduction

All water bodies, either above or below the land surface, are in constant mutual interaction. Therefore, if we are to tackle successfully environmental issues such as water scarcity and quality, both of which are global concerns, it is necessary to understand the interactions that occur between groundwater and surface water bodies and to treat them as a single system. It is also important to understand these processes in space and time. This because the relation between river water and groundwater can change from either gaining or losing stream or *vice versa*, over the short-term due to groundwater extraction, increased river discharge, and precipitation, or over the long-term due to land use changes, stream regulations and climate change. These stressors also impact ecosystems, which are important component of the biological diversity, and on the water balance, which is directly related to changes in percolation, evapotranspiration, runoff characteristics and sediment yield from the land surface. When combined, all these effects can have serious economic, social and environmental consequences for communities (Reid et al., 2009).

The European Union has attempts to add knowledge of the dynamic processes that connect surface water and groundwater (Fleckenstein et al., 2010). The European Water Framework Directive and the related River Basin Management Plans for the current period 2015–2021 and beyond, require, if needed, remedial measures to ensure a good chemical and quantity status for groundwater and generally prohibits any deterioration. To achieve these aims, the EU encourages significant research activities aimed at improve the understanding of the complex water cycle, including the following: groundwater interactions at sensitive interfaces, identifying percolation areas and other sources of groundwater recharge, and the vulnerability of ground water to different contaminants.

The aim of this paper is to present a novel approach to simulating groundwater behavior at the reach-scale using multi-tools, in a system where surface-groundwater interactions are significant. Characterizing and measuring the processes that occur at the interface of surface water and groundwater is an extremely challenging task. Usually, surface water and groundwater are studied individually. In this study, we deal exclusively with the connections between river level, percolation from local precipitation and groundwater in an alluvial aquifer with an intergranular porosity. The Ljubljansko polje, located within the Sava River Basin (SRB), is a suitable case study for testing such an approach, since it is highly sensitive to changes in its two main groundwater sources: the Sava River water and local precipitation (Urbanc and Jamnik, 1998; Vrzel et al., 2018). Understanding the hydrology of the Ljubljansko polje aquifer system is also important for local inhabitants, since it represents the main source of drinking water. Much of the basin is covered by the city of Ljubljana, and is crossed by a major highway that connects central Europe with the Mediterranean.

Multivariate statistical methods were used to compare geochemical data that forms the basis of the conceptual model (Vrzel et al., 2018), with the long-term data (precipitation levels, river discharge, hydraulic head, groundwater pumping rate) to develop the hydrological model. An understanding of the observed field data was also a great help in the making the right decisions concerning the calibration of the groundwater flow model. Although several hydrological models have been developed for this area (Janža et al., 2011), the advanced hydrological model used herein accurately determines the upper boundary conditions of the two main groundwater sources. In addition, the complexity of the surface-subsurface interactions demand the coupling of various model-types to represent all critical processes. The plug-in ifmMIKE11 and WaSiM software simulate river water-groundwater interactions and percolation, respectively and provide boundary conditions for simulating groundwater flow in FEFLOW. An additional evaluation of the models was performed by comparing groundwater mean residence time, defined using the

$^3H/^3He$ method and simulated by the steady state groundwater flow model. The traveling time of particles in water in the transient-state groundwater flow model was also compared with aquifer responsiveness estimated using statistical analyses.

2. The Ljubljansko polje

The Ljubljansko polje is a 71 km^2 basin located between latitudes 46.12 °N, 46.08 °N and longitudes 14.43 °E and 14.64 °E in central Slovenia (Figure 1). Its elevation ranges from 259.5 to 327.5 m, and is separated from its neighboring geographic units—the Kamniško-Mengeško polje and the Ljubljansko Barje, by hills up to 450 m in height. The Sava River is the main river that flows in the basin together with its three main tributaries: the Ljubljanica, the Kamniška Bistrica and the Gamlejščica Rivers.

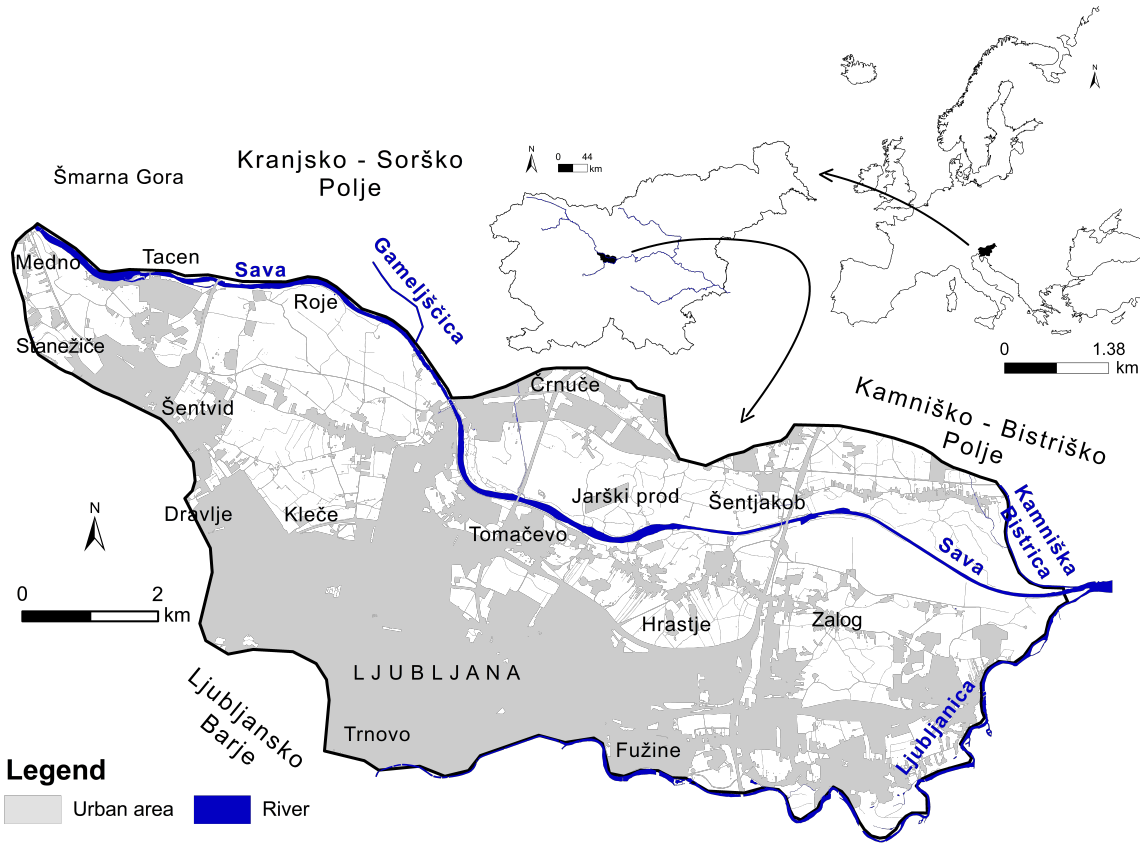


Figure 1: Map of the case study area—the Ljubljansko polje.

The basin is filled with alluvial sediments—Pleistocene and Holocene gravel, which may also contain silt and sand, interspersed with conglomerate lenses. Layers of clay or clay with gravel-stone are located only at local spots, mainly in the western part of the basin (Šram et al., 2012). The sediments have an intergranular porosity, while the bedrock with its diverse geometry is composed of impermeable Permian and Carboniferous slate clay-stone and sandstone, which extends from the surface (Šentjakob, Črnuče, Tacen and surrounding hills) to a depth of 100 m in the central part of the basin.

Local precipitation, leaching water from the Sava River, and the lateral underground inflows from neighboring groundwater bodies are the main sources of groundwater in the Ljubljansko polje aquifer system (Cerar and Urbanc, 2013; Auersperger et al., 2005; Vrzel et al., 2018). Since the Ljubljansko polje is a small depression surrounded with

impermeable bedrock outcrops, the lateral boundary conditions can be well controlled in a hydrological model. Exceptions are the narrow boundary sections where bedrock sinks deeper under the surface and thus underground inflows from the neighboring groundwater bodies are enabled. However, these underground inflows are still not well studied (Cerar and Urbanc, 2013).

An important loss of groundwater is through water extraction. Besides the Pivovarna Laško Union d.o.o. brewery which extracts groundwater there are four pumping stations in the Ljubljansko polje: Kleče, Jarški prod, Hrastje and Šentvid (Figure 3). The largest pumping station is located at Kleče, which produced approximately 60% of the daily drinking water needs (Bračič Železnik and Jamnik, 2005). Groundwater extraction influences the groundwater flow in the Ljubljansko polje aquifer system, which has the general direction is to the southeast (Auersperger et al., 2005).

3. Conceptualization of the modeling approach

3.1 Modeling tools

Combining multiple tools to represent a complex system is challenging because its behavior cannot simply be expressed as the sum of its components or subsystems. Complex interactions and feedback between processes can dominate the evolution of the system. The ability to represent effectively information that must pass between subsystem models in order to establish feedback and interaction processes poses many software challenges (NASEM, 2016). Figure 2 shows the different tools used in this study to simulate groundwater flow and its two main sources: percolation and river water leaching.

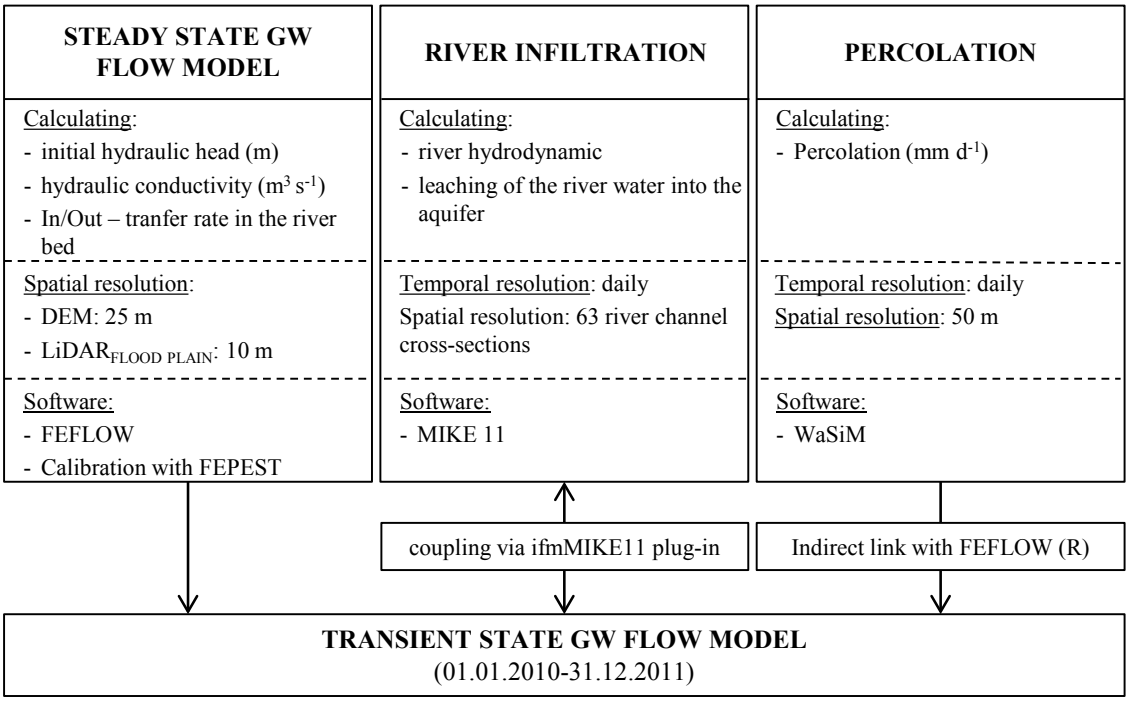


Figure 2: A hydrological modeling framework.

Percolation was simulated using the physically-based fully distributed hydrological model—Water Flow and Balance Simulation Model (WaSiM). Depending on the general availability of data and the hydrological problem to be solved, several algorithms designed for simulating specific processes on various temporal and spatial scales are available in

WaSiM. In addition, WaSiM uses the ASCII format, which allows easy and optimal data exchange with many other software packages (Schulla, 2015).

The effects of riverbed morphology on river water level and groundwater exchange are known (Diem et al., 2014; Cardenas, 2009, Cardenas et al., 2004; Woessner, 2000). Therefore, an important prerequisite for modeling groundwater flow in a real surface-groundwater system is an accurate description of the river water level (Diem et al., 2014). MIKE 11 from the MIKE Powered by the Danish Hydraulic Institute (DHI) is an implicit finite difference model, developed by Abbott and Ionescu (1967). MIKE 11 is capable of creating a detailed model of rivers, since the water level (in h points) is calculated at each cross section and at model interpolated interior points located evenly and specified by the user-entered maximum distance. The flow is then calculated at points midway between neighboring h-points and at structures (Fleenor et al., 2003). MIKE 11 is capable of dealing with kinematic, diffusive and dynamic Saint Venant equations and thus able to solve one-dimensional unsteady flow problems, simulate mass transport, sedimentation and erosion processes (Monninkhoff, 2011). For this reason, MIKE 11 was used to simulate unsteady flow in the Sava River.

FEFLOW also belongs to the MIKE Powered by the DHI software family, and is an advanced finite element subsurface flow and transport modeling system. One advantage of creating a three-dimensional complex hydrological model in FEFLOW is the software's compatibility with different file formats. The combination of FEFLOW and a GIS package (e.g., ArcMap) creates a powerful tool for performing hydrological analyses (Trefry and Muffels, 2007; Diersch, 2014).

FEFLOW can also be coupled to MIKE 11 *via* the FEFLOW Inter Face Manager (ifmMIKE11), developed by the DHI. The ifmMIKE11 enables the user to define not only the surface water (reference) level at a single boundary node, but also the water exchange area represented by the node and the nodal transfer rate. Another advantage is its ability to successfully deal with the situation where the hydraulic head drops below the bottom of the river (Monninkhoff and Hartnack, 2009; Monninkhoff, 2011).

3.2 A link between FEFLOW and WaSiM

FEFLOW is unable to directly handle raster files i.e., WaSiM outputs. Therefore, an indirectly communication link between WaSiM results and FEFLOW was established with the open source R-software (URL: http://www.R-project.org). The simulated daily percolation data are reported as ASCII files, which were then converted into a *.dat file where the second and third columns contain the coordinates of the central points of each raster cell, while the subsequent columns contain the amount of percolation for each time step. An extra file containing the mean percolation values for the study period was then created for the steady state groundwater flow model.

Daily percolation data from the *.dat file could then be assigned to the in/outflow on the top/bottom parameter in FEFLOW through four different options. In the present case, the "assign material data to time stages" option was used. Unfortunately, connecting so many time steps is time consuming.

3.3 Input Data

Hydraulic head. Daily and monthly hydraulic head values from 52 and 25 piezometers, respectively were provided by VOKA. The observed hydraulic head was from 260.47 to 299.08 m a.s.l. Only those piezometers with daily data and minimal gaps of available data were used in the simulation (Figure S1). Locations of the piezometers are shown in Figure 3.

Groundwater pumping. Daily rates of groundwater abstractions from the 32 wells were obtained from VOKA for all four pumping stations and from Pivovarna Laško Union d.o.o. Kleče is the most important, since it pumped five times more groundwater (53.0 l s^{-1}) than the other pumping stations during the study period (Figure 3).

River Discharge. Discharges observed in the Sava and the Ljubljanica Rivers were used to simulate spatially-explicit percolation (WaSiM model), while only the Sava River discharge was used in the transient state groundwater flow model (MIKE 11 and FEFLOW models). The Ljubljanica River was not included in the groundwater flow model, due to its negligible effect on the aquifer (Auersperger et al., 2005). Further, the Ljubljanica River discharge represented only 20–30% of the Sava River discharge in 2010 and 2011, when the observed recorded discharge in the Sava River was 1021.66 m^3 s^{-1}. The Sava River water level is a required input data for the steady state groundwater model and was obtained from ARSO (URL: http://vode.arso.gov.si).

Underground recharge/discharge. The amount of subsurface groundwater recharge/ discharge were estimated during the calibration process of the steady state groundwater flow model in FEFLOW (Table 4).

Mean residence time (MRT). An estimation of MRT was made using the $^3H/^3He$ method for water samples collected on the 01.06.2010 at Kleče 8, Kleče 11, Kleče 12, Hrastje 3, Hrastje 8, Jarški prod 1 and Jarški prod 3 (Vrzel et al., 2018, Table 3). The MRT could not be estimated for Kleče, due to the presence of old water, thus only Hrastje and Jarški prod data were used to calibrate the model.

Meteorological data. Daily data of temperature (°C), precipitation (mm), global radiation (Wh m^{-2}), humidity (1/1) and wind speed (m^3 s^{-1}) were obtained from ARSO for the period 2003–2015 (URL: http://meteo.arso.gov.si). The inverse distance weighting interpolation (IDW) method was used for the horizontal interpolation of the meteorological data (Schulla, 2015)

2010 was one of the wettest years in Ljubljana (1798 mm y^{-1}) and a large flood event affected the Ljubljansko polje at that time of sampling. Only in 1965 was a higher yearly precipitation (1848 mm) recorded (Cegnar, 2011). In contrast, 2011 recorded the lowest amount of precipitation (Cegnar, 2012).

Soil map. A precise soil texture map was provided by the University of Ljubljana, Biotechnical Faculty—Infrastructural Centre for Pedology and Environmental Protection (ICPVO). The model parameterization of soil texture classes (Table 1) was adapted from various relevant literature for Central Europe (UNSW, 2007; Wessolek et al., 2009; Renger et al., 2008).

Table 1: Soil texture classes for the Ljubljansko polje (ICPVO).

Code	Soil texture type	Description	%
1	Artificial area	Data cannot be defined	39.60
2	Coarse	Sand/Loamy/Sand/Sandy Loam	30.05
3	Coarse–Medium	Sand/Loamy Sand/Sandy Loam/Sandy Clay Loam/Clay Loam/Loam/Silt Loam	27.51
4	Medium	Sandy Clay Loam/Clay Loam/Loam/Silt Loam	2.77
5	Medium – Fine-Fine	Sandy Clay Loam/Clay Loam/Loam/Silt Loam/ Silt/Silty Clay Loam/Silty Clay/Sandy Clay/Clay	0.06
6	Very fine	Silt/Silty Clay Loam/Silty Clay/Sandy Clay/Clay	0.01

Land use map. Land use data for the Slovenian part of the Sava River basin was taken from the CORINE Land Cover database (CLC2006). The original data had a spatial

resolution of 25 m, which were downscaled to a resolution of 50 m for the Ljubljansko polje. Table 2 gives the land use classes for the Ljubljansko polje.

Table 2: Land use classes for the Ljubljansko polje (CLC2006).

Code	Land use type	Description
1	Agriculture	15.72
2	Arable land	22.70
3	Meadow	0.31
4	Mixed forest	4.74
5	Urban	30.44
6	Trans wood land	0.92
7	Industrial area	19.30
8	Pastures	2.92
9	Water	2.97

Digital Elevation Model (DEM). The DEM at a spatial resolution of 5 m was obtained from the Surveying and Mapping Authority of the Republic Slovenia. The DEM was downscaled to a resolution of 50 m for the WaSiM model. LiDAR data for the floodplain of the Sava River in the Ljubljansko polje were obtained from Savske elektrarne Ljubljana d.o.o.

The River channel cross-sections. The Sava River channel cross-sections were measured in 2007, 2010 and 2013. Sixty-three cross-sections were used in the MIKE 11 model (Figure 3). The data were obtained from the Municipality of Ljubljana.

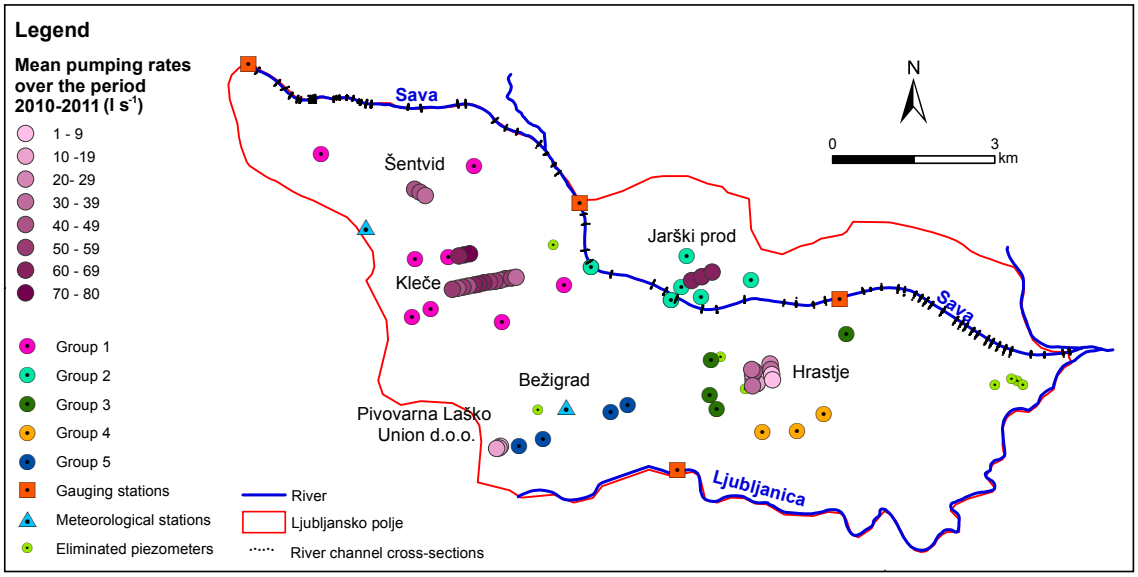


Figure 3: Locations of pumping stations and wells along with mean pumping rates in ls^{-1} for 2010–2011. Also shown are the locations of the formulated groups with representative piezometers, three meteorological stations, three gauging stations on the Sava River and one on the Ljubljanica River. The Sava River cross-sections used in MIKE 11 are also indicated.

A counter map of the bedrock in Ljubljansko polje was obtained from the VOKA, which had been prepared by local hydrologists. However, the map was updated and extended with information obtained from the latest drilling reports (from VOKA and Pivovarna Laško Union d.o.o. 115 in total).

3.4 Analysis of hydrochronological data

3.4.1 Testing the usability of the data needed for a definition of the groundwater sources

Before applying multivariate statistical analysis, the database was reduced in size using linear correlation. The 47 piezometers, where the hydraulic heads were measured between 2005–2015 are shown in Figure 3. The hydraulic head measurements were divided into five groups. Each group included piezometers with high correlation coefficients $R^2 \geq 0.95$, , due to similar patterns of hydraulic heads. Only one piezometer from each group, with minimal data gaps in their sets, were considered representative and used for data analyses. Due to the high correlation (> 0.99) between the Sava River discharges observed at the three gauging stations, only the discharges measured in Šentjakob were analyzed. The reason for the high correlations is the short distance ($\sim$ 6.5 km) between the gauging stations. Since the Ljubljanica River discharge, does not correlate with that observed at the other gauging stations, these data were also analyzed. Precipitation, which was recorded at the meteorological station in Ljubljana (Bežigrad, Figure 3), did not correlate with the discharges of the Sava and Ljubljanica Rivers due to the remoteness of their springs where different climate conditions prevail.

Any uncertainty in the hydro-chronological data, which appears due to a combination of measurement error, systematic error, natural variation and inherent randomness were eliminated using different data analysis (Pignotti et al., 2017). In addition, piezometer data showing significantly different patterns of hydraulic heads were also excluded from the database (Figure S2).

The hydraulic head pattern in group 2 (Figure S3), which is located adjacent to the Sava River bed, stands out from the other groups and has the strongest correlation with the water level in the Sava River. Alternatively, the hydraulic head in group 3 correlates most strongly with local precipitation. Both observations are likely related to the leaching of the river water and local precipitation into the aquifer, respectively, a fact supported Vrzel et al. (2018) using stable isotope measurements.

The groundwater budget components summarized by Andjelov et al. (2005) are given in Table S4.

3.4.2 Estimation of the system responsiveness

Groundwater responsiveness to the Sava River discharge (river events) or local precipitation (precipitation events) was estimated using the moving window method. The method was used to cross-correlate the hydraulic heads and local precipitation levels/river discharge. In this method a defined time "window" (30 days) is moved over the daily data-set obtained for 2003–2015, where the distance moved is equal to the width of the "window". All data located within the "window" are statistically summarized (GITTA, 2013).

Despite the small cross-correlation coefficients (0.12 and 0.25) in Figure 4, results show a discrepancy in the time delay of groundwater responsiveness to local precipitation events and the Sava River discharge dynamics in the Ljubljansko polje. In general, the groundwater responsiveness responds more rapidly to the river events than to the precipitation events, due to the higher horizontal than vertical hydraulic conductivity. Group 2 responds to both of the main groundwater sources within 24 hours (Figure 4), while mboxgroup 1 responds a month later. The distance between piezometers and the Sava River channel is the main factor in determining groundwater responsiveness, although the Sava River is not the dominant groundwater source at a certain point. Further, response time is not equal to the groundwater MRT, but is related exclusively to pressure changes.

Understanding the system's responsiveness is also important for determining the time step in a transient groundwater flow model. Since in certain areas it was estimated that surface water pressure can impact the Ljubljansko polje aquifer within 24 hours, a daily time step for the transient state groundwater flow model was determined.

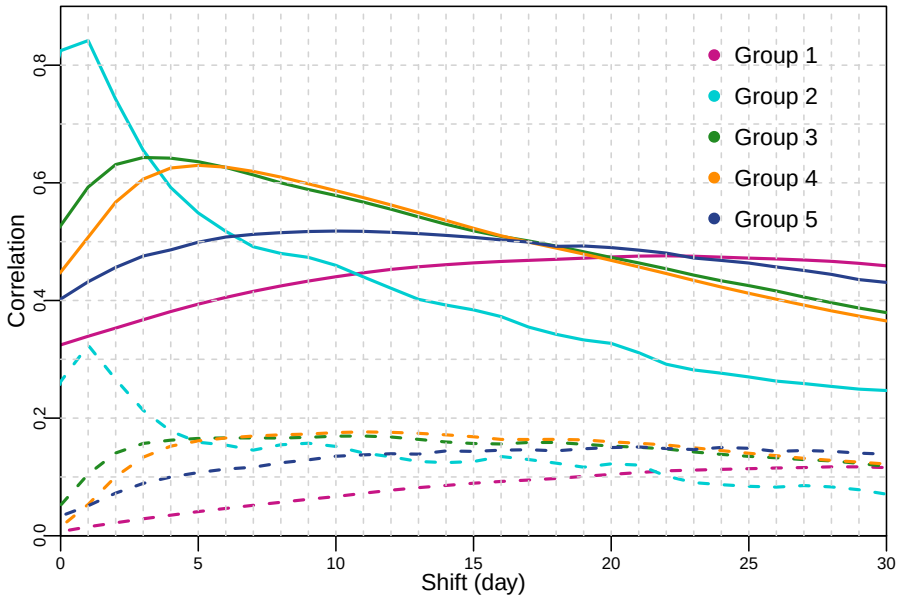


Figure 4: Cross-correlogram between the hydraulic heads and local precipitation levels (dash line)/Sava River discharge (full line) in different time lag data of the hydraulic head. Locations of the groups is shown in Figure 3.

4. Numerical model

4.1 WaSiM model—simulation of percolation

The WaSiM requires spatial data in a raster format with unique spatial resolution and time-dependent data with temporal resolution (Schulla, 2015). The grid data includes topology, land use soil features, and aspect and slope with a spatial resolution of 50 m. Climate conditions are defined by the station-based daily time sets of temperature (°C), precipitation (mm), global radiation (Wh m^{-2}), humidity (1/1) and wind speed (m s^{-1}) recorded in 2005–2015. All these drivers play an important role in the water balance modeling. For this reason, spending time collecting these data and later filtering good quality and useful data is a good investment for setting up a high quality hydrological model in WaSiM (Rieger et al., 2010; Schulla, 2015).

Unlike the raster data, meteorological data do not require special processing or parameterization. The WaSiM connects soil texture and land use maps with the look up tables in the Control File, where their properties are defined. Soil hydraulic properties for each horizon in each soil texture class (Table 1) are described by following parameters: saturated hydraulic conductivity, saturated hydraulic conductivity recession with depth, saturated water content, residual water content, van Genuchten Parameter Alpha, van Genuchten Parameter n, Mualem Parameter in van-Genuchtens, number of numerical layers and numerical layer thickness (Schulla, 2015). In this case, soil parameterization is based on four soil horizons. Land use classes (Table 2) for 12 Julian days over a year are parameterized by the following parameters: albedo, leaf surface resistance, leaf area index,

roughness length, vegetation covered fraction, root depth, altitude correction, interception surface resistance and soil surface resistance (Schulla, 2015).

Simulation of the surface water percolation for the Ljubljansko polje also requires information about the lateral inflow of the surface water in the study area from the upstream area of the Sava River catchment. For this reason, the hydrological model of the Slovenian part of the Sava River catchment, with a daily temporal and spatial resolution of 1 km, while only the Ljubljansko polje was later down-scaled to a spatial resolution of 50 m. These two models were coupled with a routing model, which is one of the modules in the WaSiM set-up file. The framework of the WaSiM model is shown in Figure 5.

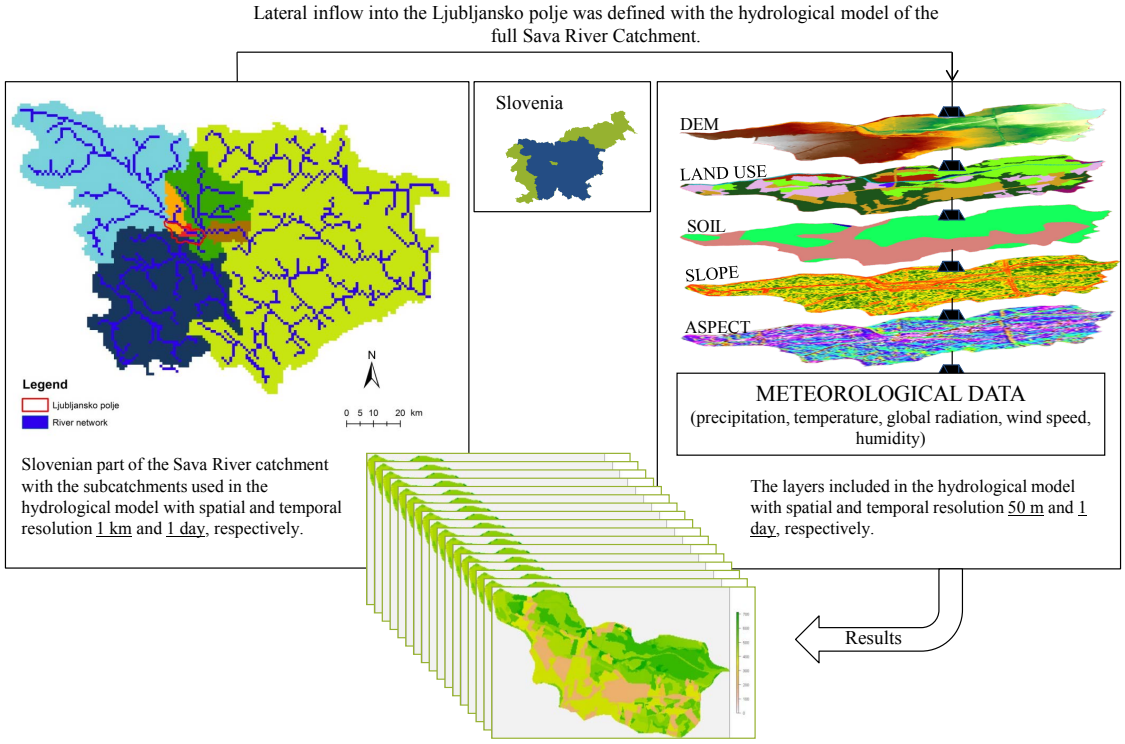


Figure 5: A framework of the modeling procedure with WaSiM.

Precipitation events. Precipitation events that cause hydraulic head oscillations were used for the calibration of the WaSiM model. These events were extracted from the full database in four steps by: (1) calculating the two day moving average for the hydraulic head, precipitation, river discharge and groundwater abstraction; (2) extracting days when hydraulic heads, precipitation and the river discharge were higher than the previous day; (3) extracting days with increased hydraulic heads and precipitation and decreased river discharge ($\uparrow$ *hydraulic head* $|\uparrow$ *precipitation* $|\downarrow$ *the river discharge*); (4) plotting the extracted days vs. hydraulic heads/precipitation/the river recharge/groundwater abstraction.

4.2 MIKE 11 model

Leaching of the Sava River water into the aquifer, the river water level and its discharge were simulated using the MIKE 11 model. The only thing, which cannot be tested without coupling with FEFLOW, is the simulation period. For this purpose, the MIKE 11 model was run before coupling. It is also recommended to test the numerical stability of the

stand-alone MIKE 11 model, since a numerically unstable model cannot be used with FEFLOW.

A detailed river water flow simulation using MIKE 11 requires four input files, namely, Network, Cross-section, Boundary and Hydrodynamic (HD) Parameters. The river network and reference cross-sections must be defined in the Network file. The Sava River channel in the study domain is 17.83 km long. Sixty-three Sava River channel's cross-sections and their Manning's n coefficients are defined in the Cross-Section file. By comparing the natural situation and figures described in the Jarret (1985) and with the help of local studies (Steinman et al., 2008), the Manning's n coefficients was estimated to be between 0.027 and 0.030 in the steady domain. The Manning's n coefficient was later corrected for each cross-section over the calibration process of the transient state groundwater flow model, after which the Manning's coefficient is from 0.032 to 0.037.

Upstream and downstream of the model domain, Inflow and Q-h Boundary types were defined, respectively. Daily discharges observed in Medno between 2010–2011 were used as input data for the Inflow Boundary type, while the Auto calculation of Q-h Table tool was used for the Q-h Boundary type. The calculation is based on the Manning formula, with a river slope of 0.02 and Manning's n parameter of 0.0285. In the HD Parameters file, the following parameters were defined: initial water level in the Sava River (observed at two gauging stations), Groundwater Leakage and Bed Resistance. The Manning formula was chosen as the resistance formula, which uses 0.0324 as a global resistance number. The local groundwater leakage coefficient was defined for each cross-section for the calibration of the groundwater flow model ($0–10^{-6}$).

4.3 FEFLOW model

4.3.1. Development of the physical framework

Differences in the spatial and temporal discretization and in the model complexity are reflected in the response of a simulated system (Borah and Bera, 2003; Daniel et al., 2011; Wellen et al., 2011). For this reason the level of discretization, based on subjective judgment, must be defined carefully since it should reflect the scale of interest of the intended application (Pignotti et al., 2017).

The outlines of the model domain (Ljubljansko polje: 15 x 8.3 km) must first be defined as a "super-element". Within this frame, a 2D unstructured triangle mesh was generated with 110,249 elements per sub-layer. The mesh was refined around the central river line, the pumping wells and the domain border. The elements' volume ranged from 0.98 to 31241.7 m^3, the maximal interior angle of the triangles was no smaller than 60° and the Delaunay criterion violations is zero for all elements.

The 3D groundwater flow model can be divided into five model layers according to the geological composition (Table S1) (Vrzel et al., 2015). However, the set-up of the groundwater flow model is defined as being only a one-layer aquifer, due to non-existing hydraulic conductivity and isotopic composition data for each of the five suggested model layers. Nevertheless, to guarantee numerical stability the vertical resolution of the model was refined by subdividing the layer into eight sub-layers. For the same reason the layers were moved slightly lower from the river bed in the areas where the bedrock outcrops appear. After making mesh corrections, these local areas are located at an elevation of 275 m (Figure 8, red colored areas). In this way the continuity criterion was fulfilled (Kaiser et al., 2011). The model depth varies from 4.2 to 124 m (Figure 6).

The simulated hydraulic head in a single node i that defines also the pumping wells depends on the so-called virtual radius, which itself depends upon the mesh discretization around the node i. Therefore, the mesh has to be generated around the singular nodes

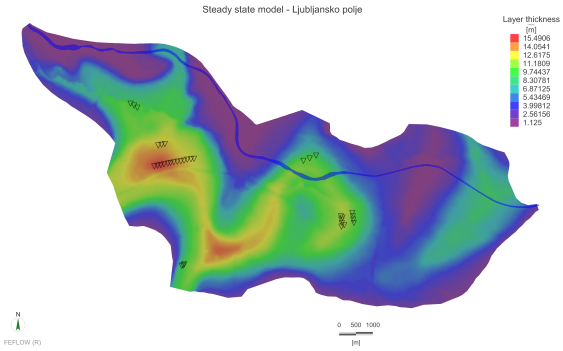


Figure 6: The aquifer thickness.

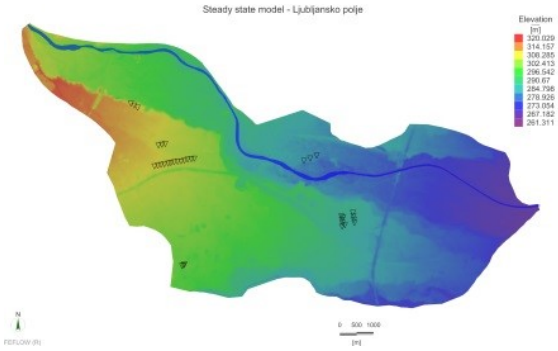


Figure 7: Topography.

i in such a way that the virtual radius meets at best the physical radius of the well. A direct estimation of the nodal distance method was used to calculate the relevant distance between the pumping wells and their adjacent nodes (Diersch, 2014).

An interpolation of the model topography is based on a 25 m-resolution DEM (Figure 7), while the interpolation of the Sava River floodplain or so-called low terrace topography is based on even more precise LiDAR data at a resolution of 10 m. Because the LiDAR technique fails when the land surface is covered with water, the Sava's bed geometry was generated using the 63 Sava river channel cross-sections data-sets, from 2007 and 2010. The distances between the cross-sections are approximately 20 m to 900 m along the flow path. Interpolation of the river bathymetry with the river channel cross-sections is important in the reach-scale model because an inappropriate elevation of a node in a riverbed can produce unwanted or uncontrolled stream water-groundwater exchanges. The lithological composition of the aquifer, its thickness, extension into the vertical direction downwards to the bedrock was based on drilling reports and a bedrock counter map. Outcrops of the bedrock and the Ljubljanica River were used as the main criteria for defining the lateral boundary of the model domain.

The kriging method was used for the interpolation of the DEM and bedrock, while the Sava River channel was interpolated using the 1D linear interpolation method. The kriging method is still the most accurate geostatistical interpolation method in FEFLOW, since it takes into account both the distance and the degree of variation between known data points when estimating values in unknown areas (Gis Resources, 2015). This is important since the surface is interpolated from a grid and interpolation is based on a mesh of varying density. Every 10 neighboring points were used in the interpolation. Unfortunately, the 1D linear interpolation method cannot be used with geometric data in FEFLOW, therefore the Sava River bed geometry was interpolated from the Fluid Transfer BC from the channel cross-sections. The interpolated data were then copied and used for the elevation of the river channel.

4.3.2. Set-up of the steady state & transient state groundwater flow models

It is assumed that the Ljubljansko polje aquifer system is in an approximate equilibrium in the steady state groundwater flow model. This means that inflows into the steady state groundwater flow model are equal to the outflows resulting in no overall net change in the aquifer storage. On the other hand, a transient groundwater flow model represents a dynamic system with changes in inflows, outflows, and aquifer storage (Ackerman et al., 2010). Thus, the steady state groundwater flow represents the basic conditions in the Ljubljansko polje aquifer during 2010–2011. Its initial material properties (except in/outflow at the top/bottom) were estimated from consultants' reports. The initials were

later changed over the calibration process using a manual and an automatic trial-and-error method. For the steady state groundwater flow model the calibration procedure, initial conditions of material parameters and boundary conditions for the transient state groundwater flow model were simulated. The transient state model was calibrated separately. According to the authors' knowledge, the hydraulic conductivity of the alluvial sediments in the modeling domain was not measured, for this reason its estimation was even more challenging.

Daily observed hydraulic heads, pumping ratios and the Sava River water level were imported into the FEFLOW through a time-series editor. Hydraulic heads are linked with the observation points in FEFLOW, pumping ratios with the Multilayer Well BC, and the Sava River water level with the Fluid-Transfer BC. The latter is coupled also with the ifmMIKE11 plug-in. Percolation was assigned to time steps through the Material property—In/Outflow on the top/bottom. The Hydraulic Head BC was defined for all nine slices in the areas where the bedrock is deep, and along the outer model domain boundary (Figure 8). Here, interactions between the aquifer and neighboring water bodies are present.

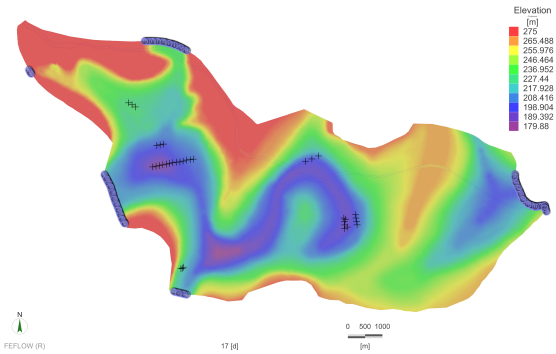


Figure 8: Hydraulic head BC and elevation of bedrock. Black triangles show locations of the Multilayer Well BC.

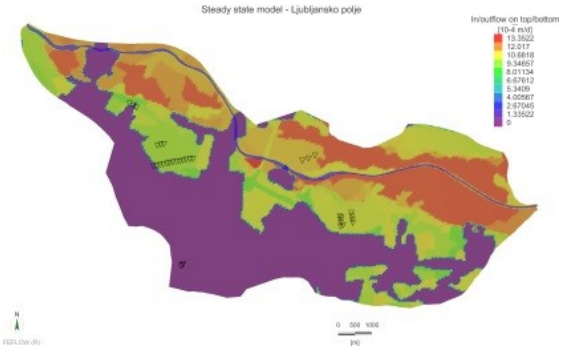


Figure 9: In/outflow on top/bottom BCs—the mean percolation for the period 2010–2011 or the steady state groundwater flow model.

Groundwater flows in the steady and transient state models are simulated using the standard (saturated) groundwater flow equation—Darcy's law (Darcy, 1856), which is also capable of handling unconfined/phreatic conditions in an aquifer (Diersch, 2014). Therefore, the upper slice was defined as phreatic (fixed slice topping of an unconfined layer) and the bottom slice as fixed, while the sub-slices depend on the top and bottom slices of the model. In the case, when groundwater rises above the surface, the aquifer is treated as a confined. As head limits for unconfined conditions, the unconstrained head at the top of the model domain and the constrained boundary at the bottom of the model domain were selected. A residual water depth for the unconfined layers was estimated at 0.1 m.

In FePEST (a graphical interface, a link between the FEFLOW and Parameter Estimation code—PEST), a "pilot points" method was used for automatic trial-and-error history matching of the hydraulic heads and the MRT, and the kriging method for spatial interpolation of values from pilot points to the model domain (Doherty, 2003). Pilot points were located manually and have a higher density where a higher heterogeneous hydraulic conductivity was expected.

5. Results and discussion

5.1 WaSiM model

Among the different hydrologic stresses including groundwater pumping, evapotranspiration and groundwater recharge in the Ljubljansko polje, the latter is the most challenging task. Percolation of local precipitation was modeled using WaSiM.

The trial-and-error method was used to calibrate the model, which implies a manual parameter assessment through a number of calibration runs in order to determine realistic lower and upper limits of the adjustable parameters (Refsgaard and Storm, 1996). The parameters used for the calibration are given in Table 3.

Table 3: Parameters used for the calibration (C) and/or validation (V) of the WaSiM model with time periods.

Use	Module	Parameter	Period	Description
C	ET	Real ET	01.01.2010–31.12.2014	Calculated real ET was compared with the referential ET in Bežigrad* (46° 3′ 5″ N, 14° 30′ 45″ E, altitude 299 m), which were calculated by ARSO (Source: http://meteo.arso.gov.si)
V			01.01.2008–31.12.2009	
C	Unsaturated zone	Soil moisture within the root zone (%)	01.01.2012-31.08.2012	Calculated soil moisture was compared with the observed soil moisture data in Kleče (46° 5′ 11″ N, 14° 29′ 56″ E, altitude 308 m) during the period Jan 201–Aug 2012 (Pintar et al., 2012).
C	Unsaturated zone	Hydraulic head below surface (m)	01.01.2010–31.12.2014	Trends of calculated percolation were compared with trends of the observed hydraulic head.
V			01.01.2009–31.12.2009	

*Referential evapotranspiration is an amount of water, which has evaporated from the referential plant and soil. As the referential surface is considered growing grass, which completely covers the soil, is 0.12 m high, with a resistance of 70 sm^{-1} and an albedo of 0.23. For the calculation, the Penman-Monteith method was used incorporating four meteorological inputs: temperature, relative air humidity, wind speed and global radiation (Source: http://meteo.arso.gov.si/met/sl/agromet/period/etp/)

Table S2 shows linear correlations between the observed and simulated real evapotranspiration and hydraulic head. The calculated soil moisture with WaSiM and soil moisture observed by Pintar et al. (2012) in the lysimeter in Kleče show a good correlation (R^2 = 0.87) (Figure 10). Further, a high Nash-Sutcliffe model Efficiency (NSE = 0.87) between the real evapotranspiration calculated using WaSiM and the referential evapotranspiration calculated by ARSO give adequate modeled values for the actual evapotranspiration in the Ljubljansko polje.

A lower correlation between the observed and calculated hydraulic heads were expected. This is because of the known "hidden" precipitation event signals that result from diverse groundwater responsiveness over the steady domain and the presence of a second groundwater source, the Sava River (Vrzel et al., 2018). Built-up areas and locally presented layers with low hydraulic conductivity obstruct percolation in the aquifer. Also, the impact of groundwater abstraction on the hydraulic head was not taken into account in the WaSiM model. Nevertheless, R^2 = 0.90 for the well P-102 in the year 2013 (Table S2).

Due to a lack of available data, model validation was performed only for the year 2009 at an hourly time step and a grid size of 50 m. The warming up period for the model was three years. The calibrated parameter set yielded a good agreement between the observed and the simulated real evapotranspiration and the hydraulic head for the validation period. The R^2 values for the real evapotranspiration and the well P-102 were estimated to be 0.47

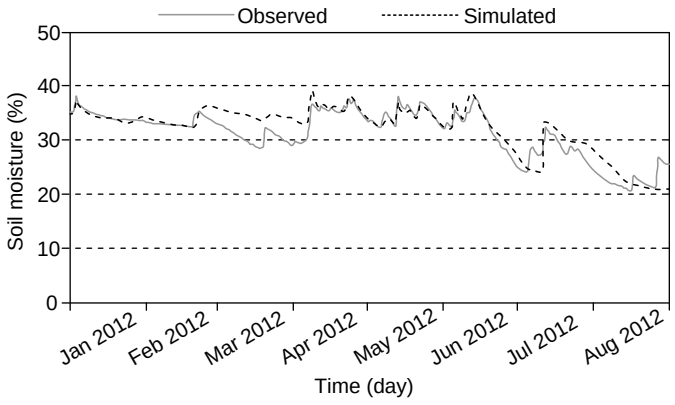


Figure 10: Comparison of the calculated and observed soil moisture (Pintar et al., 2012).

and 0.87 (Table S3), respectively. The influence of the Sava River water on the hydraulic head in the well P-013 and the longer transient time of the groundwater at Kleče (Vrzel et al., 2018) explains the lower correlation ($R^2 = 0.53$) between the hydraulic heads in the well.

5.2 FEFLOW-WaSiM-ifmMIKE 11

The material properties in the set-up of the steady and transient state groundwater flow models (except percolation; an example of the percolation raster is in Figure 9) were estimated during the calibration procedure. These parameters were: hydraulic conductivity for $K_x = K_y$ and K_z, In and Out transfer rates, specific yield and specific storage. The base of the aquifer (the bedrock) and most of the outer boundaries along the bedrock outcrops were designed as non-flow boundaries.

Anderson et al. (2015) quotes that using the term validation and even performing validation results is not necessary in the 21st century. Many modelers agree and defend the statement that a hydrogeological model cannot be validated, but it can be invalidated at a certain confidence level (Oreskes et al., 1994; Anderson et al., 2015). Doherty (2011) also quotes that a properly constructed model can only promise that the right answer for predictions is in a range of uncertainty limits. Nevertheless, model validation is still used and was performed in this study according to the following five steps:

STEP 1: The steady state groundwater flow model was calibrated using manual and automatic trial-and-error history matching of the hydraulic heads in FEFLOW and FePEST, respectively.

STEP 2: A simulation of the groundwater MRT was activated in FEFLOW. The initial MRT for the full aquifer is 4.99 years, which was calculated in FEFLOW based on the $^3H/^3He$ results (Vrzel et al., 2018). This step turned out as extremely useful, because it is a good indicator of the model's instability, either due to an inappropriate mesh discretization or parameter estimation. If the results after this step were unsatisfying, steps one and two were repeated.

The simulated MRT (Figure 11) reveals recharge areas of the aquifer (purple areas on Figure 11), which should get the most attention for sustainable groundwater management. The MRT, estimated using the $^3H/^3He$ data, is 8.4 years (Vrzel et al., 2018, Table 3), while simulations show an even longer MRT at certain spots. Nevertheless, the old water (red spots on Figure 11) in the northern part of the basin and around the Rožnik hill may not be representative due to the influence of the model domain border. Figure 11 explains that the five oscillation patterns of the hydraulic heads (Figure S3) and the diverse aquifer

responsiveness over the steady domain (Figure 4) are related to the different recharge areas and groundwater flow directions.

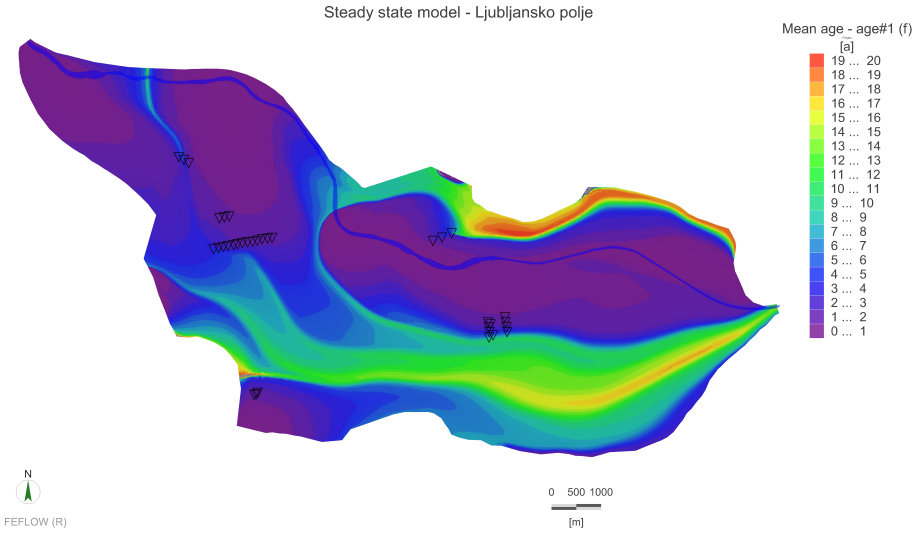


Figure 11: Simulated mean residence time. The black triangles show the position of the pumping wells.

STEP 3: The steady state model was validated using mean data obtained between 2013–2014.

STEP 4: The steady state groundwater flow model was upgraded to a transient state groundwater model and calibrated using the daily data record (April 2010), which was made in combination with manual and automatic trial-and-error history matching of the hydraulic heads. The model was coupled to the MIKE 11 *via* the ifmMIKE11 plug-in and daily input data for percolation, simulated with WaSiM, were applied.

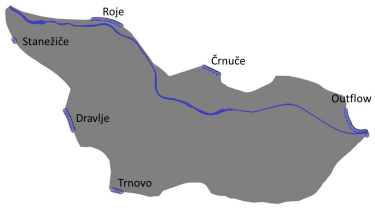
STEP 5: Validation of the transient state model was performed during 01.01.2010–31.12.2011. Unfortunately, the initial results did not satisfy expectations, therefore several corrections to the model parameterization were made.

The steady state groundwater flow model. This model was calibrated using the mean hydraulic head elevations, the mean water levels of the Sava River, the mean percolation and the mean quantity of pumped water from 2010–2011 and validated with data from 2013–2014. The results (Table S5) show that simulated and estimated (Table S4) water balances are in the same range. A discrepancy between the observed and simulated underground recharge is not critical, since fluxes through these boundary conditions have very rough estimations in the limited number of published studies and in the model. Simulated groundwater leaching into the Sava River is smaller than estimated, while an estimation of the underground outflow does not exist. Simulated percolation is also smaller than was previously estimated (Table S4 and S5).

Estimating the Fluid-flux BC is very demanding and uncertain due to limited knowledge. To provide a minimal uncertainty of the model under the boundary conditions, the model's reactions to various fluid-fluxes, from extremely high to extremely low values, were tested many times (even more than 100 times). Setting up a high outflow around the Kamniška Bistrica and Ljubljanica Rivers was the only way to stabilize the model due to the many assumptions in the parametrization and the design of the eastern part of the steady domain, which was limited by the amount of available data (hydraulic head, bedrock). Nevertheless, the model was stable when the fluxes presented in Table 4 were used.

Table 4: Fluid-flux BC set up parameters.

Location	Hydraulic head BC
Trnovo	P_102 + 0.48 m
Dravlje**	P_038 + (−2.00–2.20 m)
Roje	P_097 + (2.00–2.20 m)
Črnuče*	P_008 + (0.04–0.64 m)
Stanežiče	P_098 + 0.66 m
Otflow	P_017 + (−3.69–0.51 m)



*The Fluid-Flux BC in Črnuče was removed from the transient state groundwater flow model, due to the better stability of the model

**The Fluid-Transfer in Dravlje cause the strange behavior of the hydraulic head around the boundary of the model domain at this place. The reason for the strange behavior might be that the groundwater flux through this border is not crucial for the groundwater flow simulation or that the border set-up was not precise enough

Simulated K_x and K_y in the steady state model vary between 9.21×10^{-7} and 0.12 $m\,s^{-1}$, and K_z between 8.65×10^{-6} and 0.1 $m\,s^{-1}$. The findings agree with the literature data and describes the poorly permeable layers in the area where the lower hydraulic conductivity was simulated (Šram et al., 2012). In and Out Transfer Rates in the Sava River bed vary between 5.0×10^{-3} and 2.9 d^{-1}.

To ensure that the steady state model performs adequately, the travel time of particles in groundwater between their sources and the wells, for which the Sava River water fractions in groundwater mixtures were estimated (Vrzel et al., 2018), was compared with these fractions and with the estimated system responsiveness (Figure 4). In Figure S4 shorter pathlines of particles between the Sava River and Hrastje than those between the Sava River and Kleče can be seen. This is the reason for the quick responsiveness of the system to the Sava River water in Hrastje than in Kleče, although the fraction of the Sava River water is higher in Kleče than in Hrastje. Very short paths of particles in Jarški prod explain why the Sava River water dominates in this area and why it has the shortest MRT (Vrzel et al., 2018, Table 3).

The steady state model gives a clear direction of groundwater flow recharge areas and boundary conditions. However, for understanding the system in time and under different conditions, a transient state groundwater flow model was developed.

Transient state groundwater flow model. The calibration of this model was challenging due to the eight unknown parameters that had to be mathematically estimated. Much of the effort and time was invested into parameterization, which still has a potential for improvement. Hydraulic conductivity ranged from 6.57×10^{-3} to 3.89×10^{-2} $m\,s^{-1}$ and from 3.24×10^{-3} to 4.57×10^{-3} $m\,s^{-1}$ for $K_x = K_y$ and K_z, respectively. The In and Out transfer rates were up to 30.44 d^{-1}. All of these four parameters have values higher than that calculated from the calibration of the steady state model. The simulated specific yield (Drain-/fillable porosity) and specific storage (compressibility effect) was from 1.09×10^{-2} to 1.25×10^{-2} and 9.9×10^{-5} m^{-1}, respectively. Minimal effort was invested into calculating the specific storage due to its negligible influence on the results. The MIKE 11 model was calibrated *via* the ifmMIKE11 plug-in module in FEFLOW with the trial-and-error history matching of the Sava River discharge and hydraulic heads. The Manning's n coefficient and the leakage coefficient for each of the Sava River's channel cross sections were estimated during this step. The groundwater leakage was estimated to be up to 8.00×10^{-5}, while the Manning's n coefficient was between 3.24×10^{-2} and 3.70×10^{-2}.

A water balance for the transient state model (Table S6) was estimated for the 02.11.2010

(high water level in the Sava River) and for the 01.07.2010 (low water level in the Sava River). In general, water exchange rates are higher in the transient state model than in the steady state model (Table S5), as well as in the water balance calculated from the literature (Table S4). The simulated leaching of the Sava River water in the aquifer was higher, when the Sava River water level was lower, than for wet conditions (02.11.2010). The explanation for this observation may be a higher pressure in the aquifer on the 02.11.2010, due to a recent flood prior to the 02.11.2010 in the Ljubljansko polje (Figure 12).

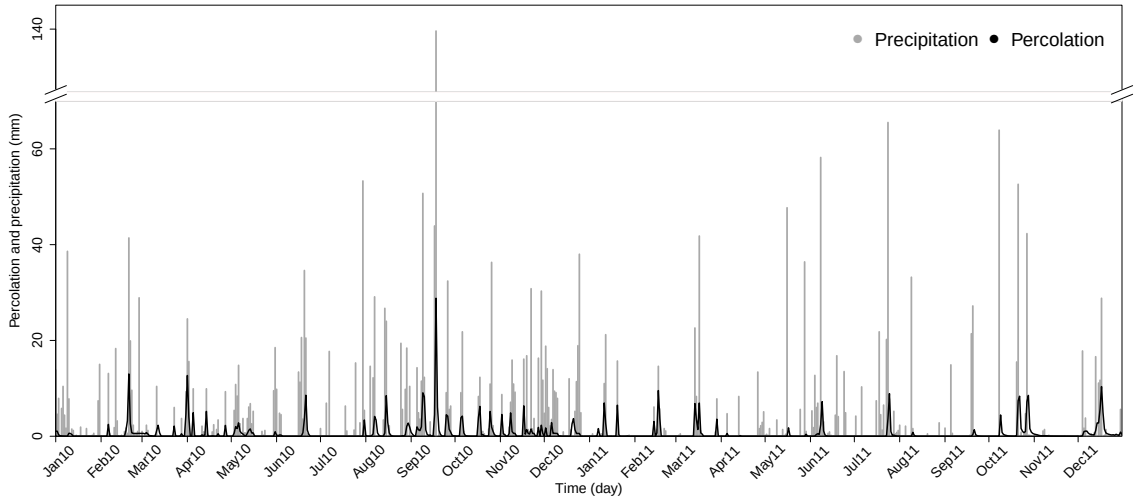


Figure 12: Daily precipitation observed in Bežigrad (mm) and percolation simulated in WaSiM (mm) for the full model domain—the Ljubljansko polje.

A comparison between the observed and simulated hydraulic heads after validation of the transient state model is shown in Figure 13. Their time series also match their maximal values. Only subtle shifts that are not critical were observed. Deviations between the observed and simulated hydraulic head might be due to the use of only one model layer, since multiple model layers regulate pressure in the aquifer more realistically. A precise parameterization of the geological layers, either using geostatistics or fieldwork, is one way of improving the model. Realistic oscillations of the hydraulic head in the piezometers located near the Sava River (P-017) and a good agreement between the observed and simulated discharges and water levels in the Sava River (Figure S5) confirm that the groundwater flow boundary conditions are well defined.

The simulated Sava River discharge was only slightly lower than the observed one, while their oscillation patterns match closely (Figure S5). The lower level of recharge downstream along the Sava River is another indicator of the leaching of the Sava River water into the aquifer. Simulated outflow and inflow can be as high as 20 $m^3\ s^{-1}$ or 0.26 $m^3\ s^{-1}$, respectively. The outflow and inflow react on the Sava River discharge in the opposite direction. When the Sava River discharge increases the outflow also increases, but the inflow decreases. Exact locations of the river water-groundwater interactions are presented in Figure 14 and Table S6.

In the literature, it is reported that groundwater drains into the Sava River only downstream of Šentjakob, however model simulations indicate that this process already occurs upstream from Šentjakob (Figure 14).

Groundwater flow under different conditions—a high (02.11.2010) and low (01.07.2010) discharge in the Sava River, is shown in Figure S6. It has to be considered that the data from 02.11.2010 is not representative of normal wet conditions. The system was

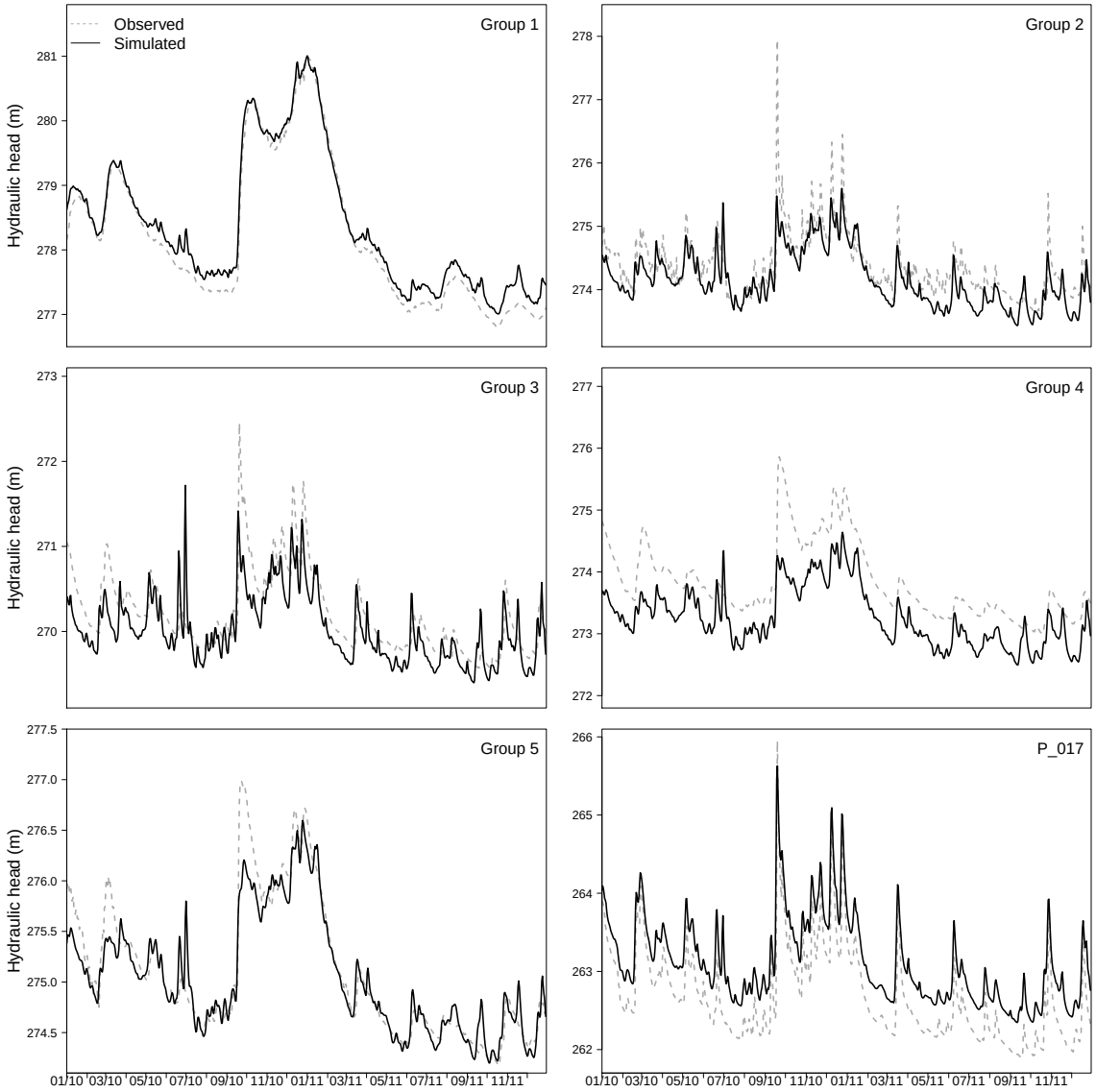


Figure 13: Observed and simulated hydraulic heads for the groups presented in Figure S3. Hydraulic heads were simulated in FEFLOW for the period 01.01.2010–31.12.2011.

still under the recovery phase after a recent flooding event on that day. However, a connection between the traveling time of particles in groundwater between their sources and piezometers and the estimated system responsiveness can be observed (Figure 4).

The travel time of the particles differs from the MRT estimated using the $^{3}H/^{3}He$ method and the simulated MRT (Figure 11). The reason is the different mathematical background of both tools. The calculation of particle travel time does not take into account the mixing of water from different sources, unlike in the simulation of the MRT. The logics behind the particle travel time calculation is similar to the piston flow by assuming that a parcel of water moves as a discrete volume along a flow path (Anderson et al., 2015). The results also show how Trnovo represents an important underground inflow of groundwater from the Ljubljansko barje into the system.

There are deviations between the groundwater flow paths in the steady and transient state models. For instance, Roje is the main recharge area for Hrastje in the transient state model and Tomačevo in the steady model. Figure 11 shows the mixing of groundwater

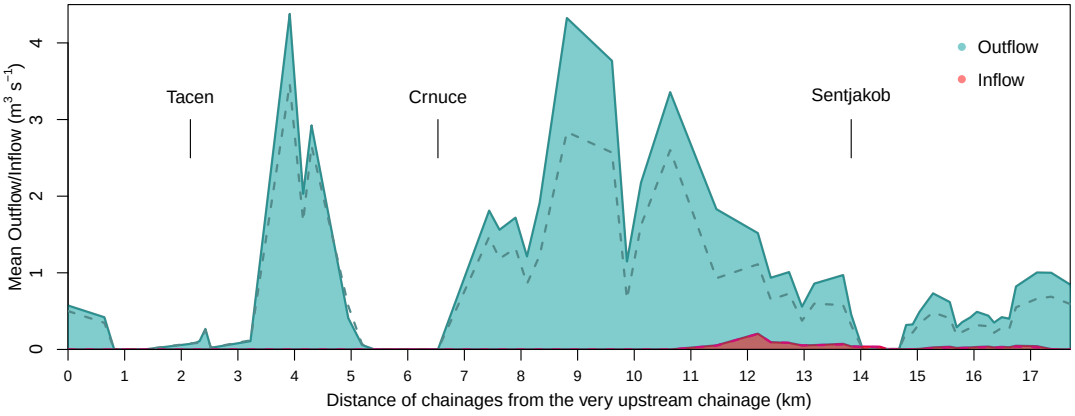


Figure 14: The Sava River water—groundwater interactions areas, and mean seepage of river water into the aquifer (inflow) and *vice versa* (outflow) over 2010 (full line) and 2011 (dash line).

around Hrastje from different recharge areas. The determination of the recharge area for groundwater in Hrastje might be ambiguous. However, given the long MRT (Vrzel et al., 2018, Table 3) and the small estimated Sava River water fraction in Hrastje (Vrzel et al., 2018, Figure 6), it is feasible that the main recharge area for groundwater in Hrastje is in the north-western part of the Ljubljansko polje.

According to Table 5, the observed and simulated values are most similar when the system contains more water. The highest discrepancy between the observed and simulated hydraulic heads is in the area around Group 4 (Figure 13). One reason for this might be a lack of information about the depth of the bedrock. The dynamic bedrock elevation in this area was predicted based on limited information. A second reason might be an underestimation of the underground recharge in Trnovo.

Table 5: Statistics of the calibrated models after steps one, two and five. Statistics for the calibrated transient state model (after the step five) are presented for two days (02.11.2010 and 01.07.2010), when the Sava River recharge was high and low, respectively.

	STEP 1 (steady state GW flow model)	**STEP 2** (steady state GW flow model + MRT)	**STEP 5** 02.11.2010	**STEP 5** 01.07.2010
$\overline{E}$	0.125	0.260	0.445	0.943
RMS	0.169	0.343	0.563	1.062
σ	0.173	0.351	0.575	1.085

*$\overline{E}$—Absolute error, RMS—the root mean square, σ—standard deviation

6. Conclusions

An integrated approach using geochemical and multivariate statistical methods were used to study surface-groundwater interactions in the Ljubljansko polje aquifer system. This involved collecting and processing a large amount of chronological data and defining the isotopic composition of groundwater. The main success of the work was the unraveling of information about groundwater behavior "hidden" in the data obtained from different sources and combining this into a hydrological model.

651 The first part of this paper presents the conceptualization of the study domain us-
652 ing chronological data, while the second part describes the hydrological modeling. The
653 chronological data of the hydraulic heads observed in many piezometers show five oscil-
654 lation patterns that led to dividing them into five groups, due to their similarity. The
655 cross-correlation analyses showed a varying responsiveness of these five groups to the two
656 main groundwater sources—the Sava River and local precipitation. Further, the sim-
657 ulated mean residence time can explain these patterns for the different recharge areas,
658 which should receive special attention regarding groundwater protection.
659 Cross-correlation analyses reveals how crucial it was to understand the system in time,
660 since the response to an increase in the high-water level of the Sava River or in local
661 precipitation could be very fast, even within 24 hour. For this reason, a transient state
662 model was developed. In order to provide a reliable simulation of the complex interac-
663 tions between groundwater and surface water that dominate the system's evolution (as
664 shown in the conceptual model) multiple models were combined. The groundwater flow
665 was simulated using FEFLOW, which was coupled with the ifmMIKE11 plug-in for the
666 simulation of the Sava River discharge, and the leaching of river water into and out of the
667 aquifer as simulated by MIKE 11. Percolation was simulated in WaSiM, for this reason a
668 link was established between FEFLOW and WaSiM.
669 Solving hydrological issues related to sensitive hydrological systems can be time con-
670 suming and complex. However, the results provide valuable and unique information about
671 the studied system. It is even possible to quantify important components in the water
672 balance of the basin under different conditions. This study also provided a complete pic-
673 ture of the full water cycle in the Ljubljansko polje, while the existing groundwater flow
674 model has great potential for many other applications such as the following: (1) Testing
675 the impact of changing land use on the water cycle. Particularly interesting would be to
676 observe the impact on groundwater-surface water interactions. Huber-Garcia et al. (2018)
677 already projected land use in the Sava River Basin up to 2050. (2) Running the forecasting
678 model with daily time steps over the full 30-year period and testing the impacts of climate
679 data at different spatial resolutions, i.e., 12 km and 1 km is possible. Climate data with
680 spatial resolution of 12 km and 1 km were already downscaled by Gampe et al. (2016).
681 (3) The model could also be converted into a tracing model for simulating water tracers
682 (e.g., isotopes) and pollutants (e.g., nutrients, pharmaceuticals, heavy metals). The study
683 results can also aid in the decision making process regarding sustainable groundwater
684 management in the Ljubljansko polje aquifer system, which is the main drinking water
685 source for the growing population of Ljubljana.

Acknowledgements

The Project was financially supported by the EU 7th Research Project—GLOBAQUA (Managing the effects of multiple stressors on aquatic ecosystem under water scarcity) under Grant agreement no. 603629-ENV-2013-6.2.1. The research was partially conducted within the doctoral study of Janja Vrzel financed by the European Social Fund (KROP 2012) no. C2130-12-000070. The authors would like to thank all those institutes and companies who shared their data including the following: ARSO, DHD, d.o.o., Holding Slovenske Elektrarne d.o.o., Institute for Water of the Republic of Slovenia (IzVRS), Javno Podjetje Vodovod-Kanalizacija Ljubljana (VOKA), Pivovarna Laško Union d.o.o., University of Ljubljana, Biotechnical Faculty—Infrastructural Centre for Pedology and Environmental Protection, The City Municipality of Ljubljana, The Surveying and Mapping Authority of the Republic of Slovenia. The authors would also like to thank MIKE Powered by DHI for the use of their software FEFLOW and its plug-in ifmMIKE11. The WaSiM model for the Slovenian part of the SRB was developed by Veronika Degmayr for the purpose of her M. Sc. Thesis entitled *Hydrologische Modellierung mit WaSiM zur Ermittlung von 759 Süßwasserökosystemdienstleistungen im Einzugsgebiet der oberen Sava, Slowenien.*

Authorship: J. V. together with R. L. and N. O. were responsible for research design, developing the conceptual and numerical model and for writing the manuscript. J. V. collected all the required data, statistically analyzed them, constructed the conceptual and numerical model and did the interpretation of the results. G. V. supported the research with specific local hydrological knowledge.

Reference

Abbott, M.B., Ionescu, F., 1967. On the numerical computation of nearly-horizontal flows. J. Hydraul. R. 5, 97–117.

Ackerman, D.J., Rousseau, J.P., Rattray, G.W., Fischer, J.C., 2010. Steady-State and Transient Models of Groundwater Flow and Advective Transport, Eastern Snake River Plain Aquifer, Idaho National Laboratory and Vicinity, Idaho. U.S. Geological Survey, Reston, Virginia.

Anderson, M.P., Woessner, W.W., Hunt, R.J., 2015. Applied Groundwater Modelling, Simulation of Flow and Advective Transport, second ed. Elsevier Inc., London.

Andjelov, M., Mikulič, Z., Uhan, J., Dolinar, M., 2013. Vodna bilanca z modelom GROWA-SI za količinsko ocenjevanje vodnih virov Slovenije (in Slovene), 24. Mišičev vodarski dan, 127–133.

Andjelov, M., Bat, B., Frantar, B., Mikulič, Z., Savić, V., Uhan, J. 2005. Pregled elementov vodne bilance (in Slovene), in: Rejec Brancelj, I., Smrekar, A., Kladnik, D. (Eds.), Podtalnica Ljubljanskega polja. Založba ZRC, Ljubljana, pp. 27–38.

Auersperger, P., Čenčur Curk, B., Jamnik, B., Janža, M., Kus, J., Prestor, J., Urbanc, J., 2005. Dinamika podzemne vode, in: Rejec Brancelj, I., Smrekar, A., Kladnik, D. (Eds.), Podtalnica Ljubljanskega polja. Založba ZRC, Ljubljana, pp. 39–61.

Borah, D.K., Bera, M., 2003. Watershed-scale hydrologic and nonpoint-source pollution models: Review of mathematical bases. Trans. ASAE 46, 1553–1566.

Bračič Železnik, B., Jamnik, B., 2005. Javna oskrba s pitno vodo (in Slovene), in: Rejec Brancelj, I., Smrekar, A., Kladnik, D. (Eds.), Podtalnica Ljubljanskega polja. Založba ZRC, Ljubljana, pp. 101–120.

Cardenas, M.B., 2009. Stream–aquifer interactions and hyporheic exchange in gaining and losing sinuous streams. Water Resour. Res. 45, 1–13.

Cardenas, M.B., Wilson, J.L., Zlotnik, V.A., 2004. Impact of heterogeneity, bed forms, and stream curvature on subchannel hyporheic exchange. Water Resour. Res. 40, 1–13.

Cegnar, T., 2012. Climate in Slovenia in 2011 (Slovene: Podnebne razmere v Sloveniji leta 2011), Ujma 26, 20–32.

Cegnar, T. (Ed.), 2011. Agencija Republike Slovenije za okolje v letu 2010 (in Slovene). Slovenian Environmental Agency, Ljubljana.

Cerar, S., Urbanc, J., 2013. Carbonate chemistry and isotope characteristics of groundwater of Ljubljansko polje and Ljubljansko barje aquifers in Slovenia, The Sci. World J. 2013, 1–11.

Daniel, E.B., Camp, J.V., LeBoeuf, E.J., Penrod, J.R., Dobbins, J.P., Abkowitz, M.D., 2011. Watershed modeling and its applications: A state-of-the-art review. Open Hydrol. J. 5, 26–50.

Darcy, H., 1856. Les fontaines publiques de la ville de Dijon (in French). Dalmont, Paris.

Diem, S., Renards, P., Schirmer, M., 2014. Assessing the effect of different river water level interpolation schemes on modelled groundwater residence times. J. Hydrol. 510, 393–402.

Diersch, H.J., 2014. FEFLOW, Finite Element Modeling of Flow, Mass and Heat Transport in Porous and Fractured Media. Springer, Verlag Berlin Heidelberg.

Doherty, J., 2011. Modeling: Picture perfect or abstract art? Groundw. 49, 455.

Doherty, J., 2003. Ground water model calibration using pilot points and regularization. Groundw. 41, 170–177.

Fleckenstein, J.H., Krause, S., Hannah, D.M., Boano, F., 2010. Groundwater-surface water interactions: New methods and models to improve understanding of processes and dynamics. Adv. in Water Resour. 33, 1291–1295.

760 Fleenor, W.E., Ache, M., Jensen, R., 2003. Evaluation of Numerical Models... HEC-
761 RAS and DHI-MIKE 11. Draft version submitted to J Hyd Eng, http://www.water.ca.
762 gov/floodsafe/fessro/docs/north_HECRAS_Mike11.pdf (accessed 27 December 2017).
763 Gampe, D., Nikulin, G., Ludwig, R., 2016. Using an ensemble of regional climate
764 models to assess climate change impacts on water scarcity in European river basins. Sci.
765 Total. Environ., 573, 1503–1518.
766 Gis Resources, 2015. Interpolation methods. http://www.gisresources.com (accessed
767 06 July 2017).
768 GITTA – Geographic Information Technology Training Alliance. 2013. Moving Win-
769 dows. http://www.gitta.info/ContiSpatVar/en/html/SpatDependen_learningObject2.xhtml
770 (accessed 27 December 2017).
771 Huber-García, V., Meyer, S., Kok, K., Verweij, P., Ludwig, R., 2018. Deriving spatially
772 explicit water uses from land use change modelling results in four river basins across
773 Europe. Sci. Total. Environ. 628–629, 1079–1097.
774 Janža, M., Meglič, P., Šram, D., 2011. Numerical hydrological modelling, Final report.
775 Geological Survey of Slovenia, Ljubljana.
776 Jarret, R.D., 1985. Determination of roughness coefficients for streams in Colorado,
777 Water-Resources Investigations Report 85-4004. U. S. Geological Survey, Lekewood, Col-
778 orado.
779 Kaiser, B.O., Cacace, M., Scheck-Wenderoth, M., Lewerenz, B., 2011. Characteriza-
780 tion of main heat transport processes in the Northern German Basin: Constraints from
781 3-D numerical models. Geochem. Geophys. Geosyst. 12, 1–17.
782 Monninkhoff, B., 2011. ifmMIKE11 2.0, Coupling the groundwater model FEFLOW®
783 and the surface water model MIKE11®, User Manual. DHI-WASY GmbH, Berlin.
784 Monninkhoff, B.L., Hartnack, J.N., 2009. Improvements in the coupling interface be-
785 tween FEFLOW and MIKE 11. http://feflow.info/fileadmin/FEFLOW/content_tagung/
786 TagungsCD/papers/29.pdf (accessed 15 April 2018).
787 NASEM - National Academies of Sciences, Engineering, and Medicine, 2016. From
788 Maps to Models: Augmenting the Nation's Geospatial Intelligence Capabilities. The Na-
789 tional Academies Press, Washington, DC. Oreskes, N., Shrader-Frechette, K., Belitz, K.,
790 1994. Verification, validation and confirmation of numerical models in the Earth science.
791 Science 263, 641–646.
792 Pignotti, G., Rathjens, H., Cibin, R., Chaubey, I., Crawford, M., 2017. Comparative
793 Analysis of HRU and Grid-Based SWAT Models. Water 9, 272, 1–20.
794 Pintar, M., Korpar, P., Zupanc, V., 2012. Meritve na lizimetrski postaji v Klečah,
795 Poročilo za leto 2012 (in Slovene). University in Ljubljana, Biotechnical Faculty, De-
796 partment of Agronomy, Center for Agricultural Land Management and Agrohydrology
797 (CUKPA), Ljubljana.
798 Refsgaard, J.C., Storm, B., 1996. Construction, calibration and validation of hydrolog-
799 ical models, in: Abbott, M.B., Refsgaard, J.C. (Eds), Distributed Hydrological Modelling.
800 Water Science and Technology Library, vol 22, Springer, Dordrecht.
801 Reid, M.A., Cheng, X., Banks, E.W., Jankowski, J., Jolly, I., Kumar, P., Lovelly, D.M.,
802 Mitchell, M., Mudd, G.M., Richardson, S., Silburn, M., Werner, A.D., 2009. Catalogue
803 of conceptual models for groundwater-stream interaction in eastern Australia, eWater
804 Cooperative Research Centre Technical Report. eWater Cooperative Research Centre,
805 Canberra.
806 Renger, M., Bohne, K., Facklam, M., Harrach, T., Riek, W., Schäfer, W., Wessolek, G.,
807 Zacharias, S., 2008. Ergebnisse und Vorschläge der DBG-Arbeitsgurppe »Kennwerte des
808 Bodengefüges« zur Schätzung bodenphysikalischer Kennwerte (in German). https://www.
809 boden.tu-berlin.de/fileadmin/fg77/_pdf/publikationen/bodenphysikalischeKennwerte.pdf

(accessed 27 December 2017).

Rieger, W., Winter, F., Disse, M., 2010. Uncertainties of soil parameterisation in process based simulation of distributed flood control measures. Adv. in Geosci. 27, 121–129.

Schulla, J., 2015. Model Description WaSiM (Water balance Simulation Model). Hydrology Software Consulting J. Schulla, Zurich.

Šram, D., Brenčič. M., Lapanje, A., Janža, M., 2012. Perched aquifers spatial model: a case study for Ljubljansko polje (central Slovenia). Geol. 55, 107–116.

Steinman, F., Banovec, P., Gosar, L., Rak, G., Pogačnik, N., Koželj, D., Petkovšek, G., Pipan, G., Artač, M., Šterk, M., Cecowski, M., Cvrle, A., Pranjič, S., 2008. Interaktivna vizualizacija poplavnih obmocij za podporo interventnemu ukrepanju. Ciljni raziskovalni projekt "Znanje za varstvo in mir 2006-2010" (Proj. no. M2-0135) (in Slovene). Republic of Slovenia, Ministry of Defense, Administration of the RS for Civil Protection and Disaster Relief, Ljubljana.

Trefry, M.G., Muffels, C., 2007. FEFLOW: A finite-element groundwater-flow and transport modeling tool. Groundw. 45, 525–528.

UNSW – University of New South Wales, 2007. Soil Moisture Classification. http://www.terragis.bees.unsw.edu.au/terraGIS_soil/sp_water-soil_moisture_classification.html (accessed 03 May 2017).

Urbanc, J., Jamnik, B., 1998. Isotope investigation of groundwater from Ljubljansko polje (Slovenia). Geol. 41, 355–364.

Vrzel, J., Solomon, D.K., Blažeka, Ž., Ogrinc, N., 2018. The study of the interactions between groundwater and Sava River water in Ljubljansko polje aquifer (Slovenia). J. Haydrol. 556, 2018, 384–396.

Vrzel, J., Ogrinc, N., Vižintin, G., 2015. Data preparation for groundwater modelling – Ljubljansko polje aquifer system. RMZ – M& G 62, 167–173.

Wellen, C., Kamran-Disfani, A.R., Arhonditsis, G.B., 2015. Evaluation of the current state of distributed nutrient water quality modeling. Environ. Sci. Technol. 49, 3278–3290.

Wessolek, G., Kaupenjohann, M., Renger, M., 2009. Bodenphysikalische Kennwerte und Berechnungsverfahren für die Praxis (in German). Technische Universität Berlin, Berlin.

Winter, T.C., Harvey, J.W., Franke, O.L., Alley, W.M., 1998. Ground water and surface water a single resource, Circular 1139. U. S. Geological Survey, Dakota.

Woessner, W.W., 2000. Stream and fluvial plain ground water interactions: rescaling hydrogeologic thought. Groundw. 38, 423–429.

Supplementary material

Table S1: Lithological composition of the potential model layers (ML).

ML	Lithology
1	Gravel, sand, gravel with sand and silt
2	Conglomerate, clay, conglomerate with lens and clay
3	Gravel with clay, sand with clay, gravel with narrow lines of conglomerate, gravel with sand and silt
4	Conglomerate is predominate
5	Gravel with sand and silt

Table S2: Linear correlations (R^2) between observed and calculated real evapotranspiration and trend of the hydraulic head after the calibration (period: Jan 2010–Dec 2014).

Correlation		ET_{ref}	Elevation of the hydraulic head							
			P-084	P-013	P-086	P-032	P-035	P-036	P-096	P-102
ET_{real}		0.87	-	-	-	-	-	-	-	-
Hydraulic head	$\sum$	-	**0.83**	0.70	0.67	0.56	0.57	0.6	0.70	0.66
	2010	-	**0.82**	0.61	0.62	0.46	0.47	0.50	0.68	0.54
	2011	-	**0.79**	**0.72**	0.69	0.68	0.69	**0.74**	0.63	**0.76**
	2012	-	**0.71**	0.57	0.14	0.38	0.38	0.38	0.25	0.43
	2013	-	**0.74**	**0.71**	**0.86**	**0.78**	**0.81**	**0.87**	**0.74**	**0.90**
	2014	-	0.66	0.64	**0.80**	0.69	**0.72**	**0.81**	0.70	0.84

Table S3: Correlations (R^2) between observed and calculated real evapotranspiration and trend of the hydraulic head after the validation (period: Jan 2009–Dec 2009).

Validation		ET_{ref}	Elevation of the hydraulic head							
			P-084	P-013	P-086	P-032	P-035	P-036	P-096	P-102
ET_{real}		0.47	-	-	-	-	-	-	-	-
H. head	2009	-	0.53	0.53	**0.84**	**0.69**	**0.72**	**0.83**	**0.78**	**0.87**

Recharge Components ($m^3 s^{-1}$)

The Sava River				Percolation	Underflow		Comments
Medno-Brod	Brod-Roje	Roje-Ježica	Medno-Šentjakob		Trnovo	Dravlje	
0.06-0.13	0.20-2.36	1.35	1.62				Žlebnik (1968)
			1.34-1.74				Žlebnik (1969)
			1.47-1.74				Pleskovič (1969)
			2.5				Brilly (1989)
			0.7-4.3				Brilly et al. (2002)
				3.2	0.2	0.05	Andjelov et al. (2005)
2.3-8.1				3.2	0.25		Total
5.76–11.59							Sum

Discharge Components ($m^3 s^{-1}$)

Sava - downstream of Šentjakob	Pumping	Direct outflow	Underflow	ET	Comments
3.26			(unreliable data)		Brilly (1989)
1.3-2					Brilly (2002)
	0.92	0.3		1.5	Andjelov et al. (2005)
4.02–5.98					Total

Table S4: Estimated components of a groundwater budget in Ljubljansko polje (m3 s-1) (Andjelov et al., 2013).

Recharge Components ($m^3 s^{-1}$)

The Sava River				Percol-ation	Underflow						Comments
Medno-Brod	Brod-Roje	Medno-Šentjakob	Downstream of Šentjakob		Trnovo	Dravlje	Roje	Črnuče	Stanežiče	Outflow	
0.096	0.183	1.102	1.772	0.500	0.316	0.117	1.141	0.035	0.240	2.791	Calibration
3.153					4.640						Sum
0.098	0.001	1.116	1.608	0.609	0.179	0.052	1.302	0.041	0.163	2.868	Validation
2.823					4.605						Sum
0.191	0.275	1.178	1.2433	0.500	0.168	0.131	0.509	0.015		0.552	$^3H/^3He$
2.421					1.375						Sum
4.296-8.037											Total

Discharge Components ($m^3 s^{-1}$)

The Sava River		Pumping	Underflow					Comments
Upstream of Šentjakob	Downstream of Šentjakob		Dravlje	Roje	Črnuče	Stanežiče	Outflow	
0.001	0	1.376	0.043	0.055	0.026		9.315	Calibration
0.001			9.439					Sum
0.002	0	1.293	0.109	0.012	0.026		9.131	Validation
0.002			9.278 (0.147 without the Outflow)					Sum
1.004E-10	3.507E-7	1.376	0.107	0.036	0.003	0.101	5.079	$^3H/^3He$
1.004E-10			5.326					Sum
6.702 (1.501 without the Outflow) -10.573 (1.442 without the Outflow)								Total
-2.406 – +0.076								Imbalance

Table S5: Water balance after calibration and validation of the steady state groundwater flow model for data observed over the period 2010–2011 and 2013–2014, respectively. Water balance after calibration of the steady state model with the additional parameter-mean residence time.

Recharge Components ($m^3 s^{-1}$)

The Sava River				Percolation	Underflow				Comments
Medno-Brod	Brod-Roje	Medno-Šentjakob	Downstream of Šentjakob		Trnovo	Dravlje	Roje	Stanežiče	Outflow	
0.168	0.801	1.858	0.001	0.00025	0.457	0.186	0.561	0.020	1.149	02.11.2010
2.828					2.373					Sum
0.165	1.215	1.760	0.074	4.819	0.271	0.061	0.130		0.683	01.07.2010
3.214					1.145					Sum
5.201-9.178										Total

Discharge Components ($m^3 s^{-1}$)

The Sava River		Pumping	Underflow				Comments
Upstream of Šentjakob	Downstream of Šentjakob		Dravlje	Trnovo	Roje	Stanežiče	Outflow	
0.287	0.117	1.217	0.234		0.219	0.010	3.809	02.11.2010
4.272								Sum
0.956	0.621	1.476	0.818		1.060	0.314	6.015	01.07.2010
8.207								Sum
5.893-11.260								Total
0.692-2.082								Imbalance

Table S6: Water balance for validated transient state model (after the step five) for two days 02.11.2010 (high water level in the Sava River) and 01.07.2010 (low water level in the Sava River).

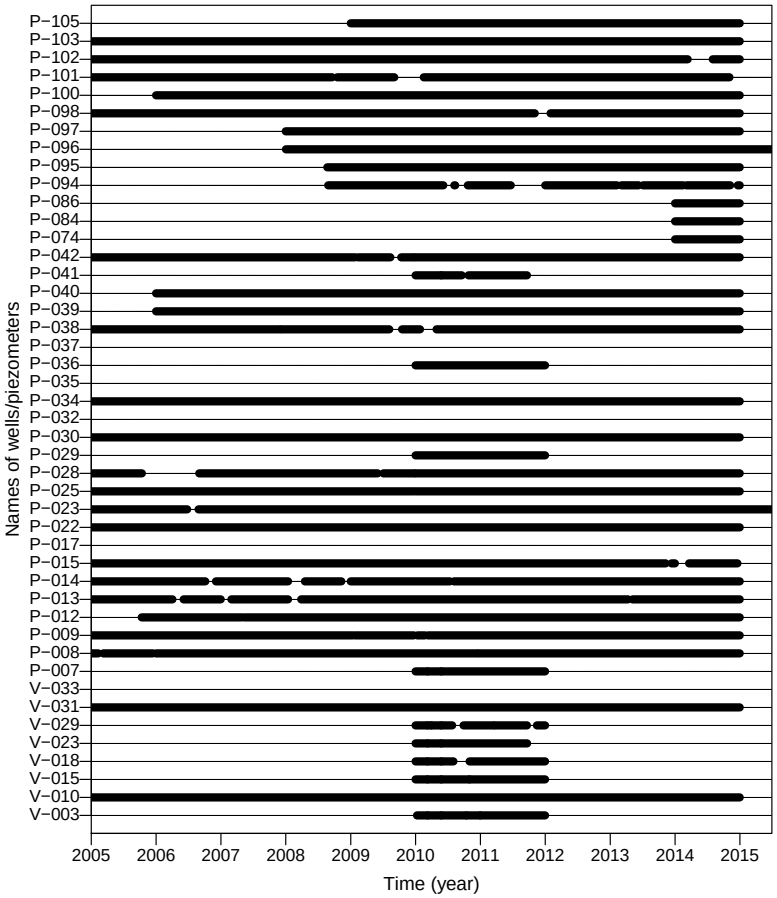


Figure S1: Distribution of observed hydraulic heads over time.

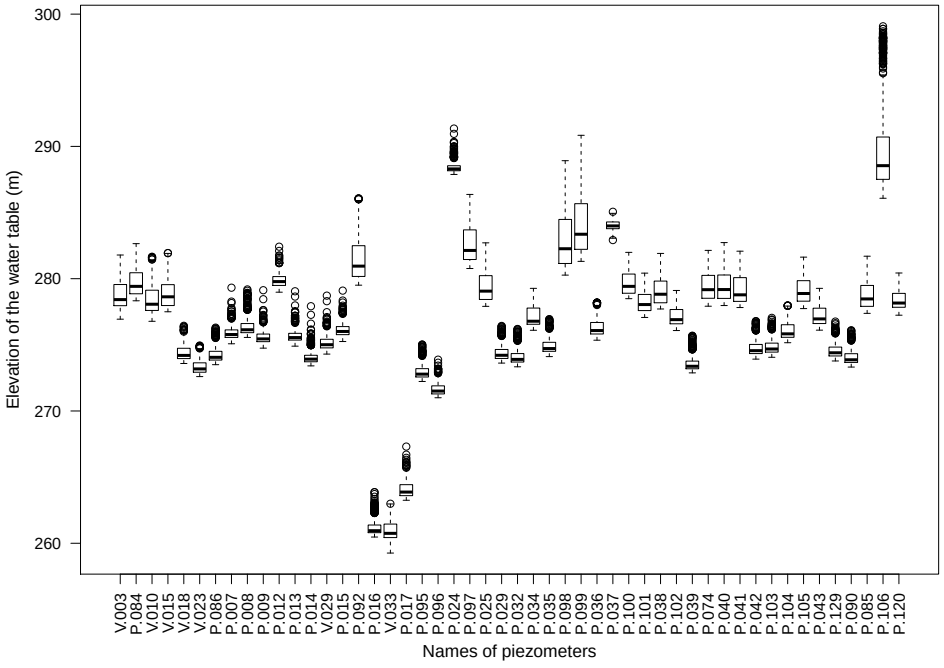


Figure S2: Box plot of hydraulic heads observed in 50 piezometers over the period 2010–2011.

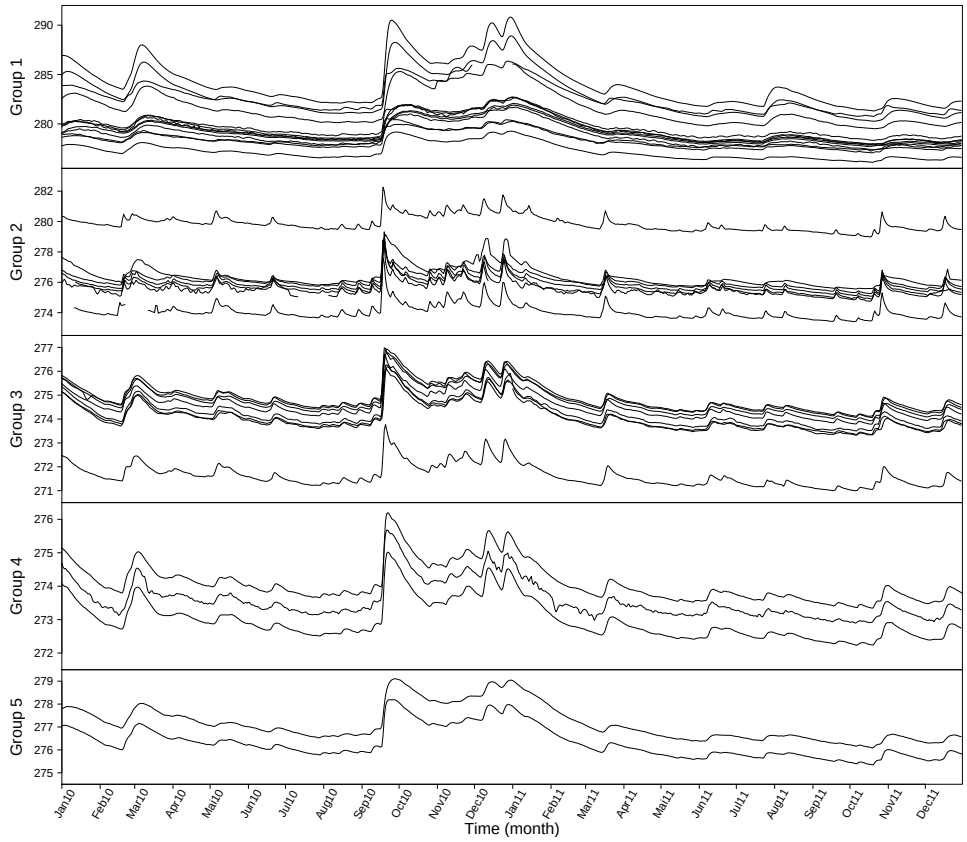


Figure S3: Hydraulic head patterns of the all five groups observed over the period 2010–2011.

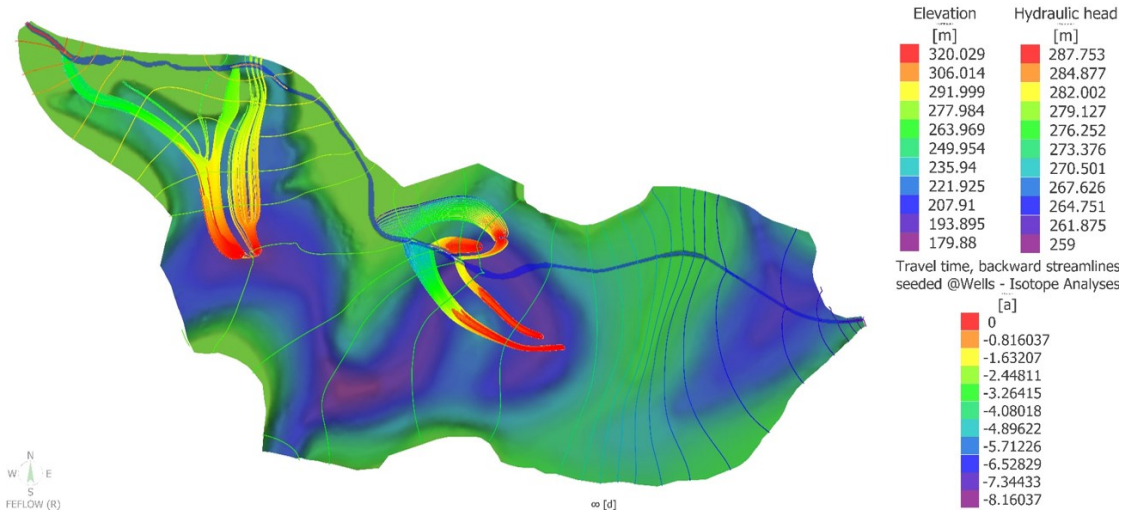


Figure S4: Paths and travel time (in years) of particles from their source to wells, fluid rate budget $m^3\ s^{-1}$, and bedrock elevations.

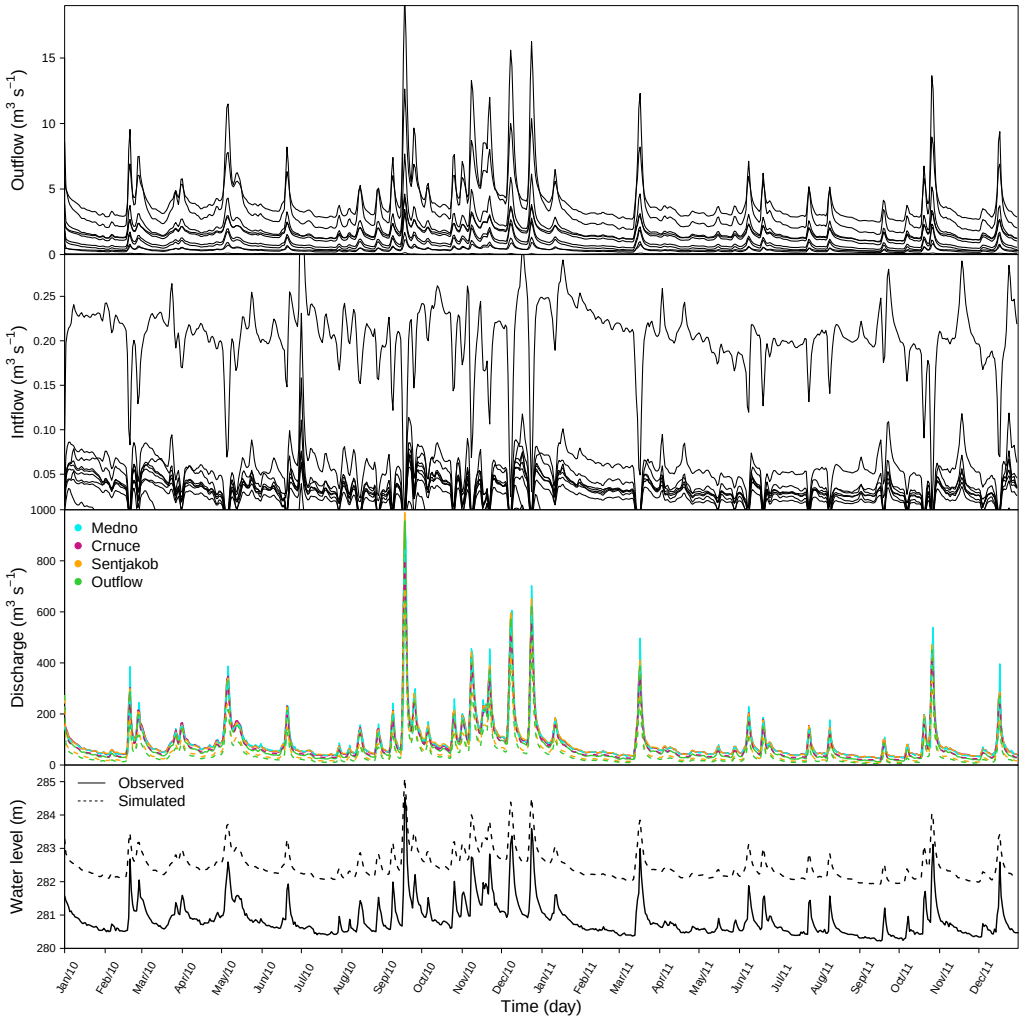


Figure S5: The upper two plots show outflows/inflows (m^3 s^{-1}) for random Sava River cross-sections simulated in MIKE11 with ifmMIKE11 plug-in in FEFLOW. Observed (full lines) and simulated (dash lines) discharges and water levels in the Sava River over the validated period 01.01.2010–31.12.2011.

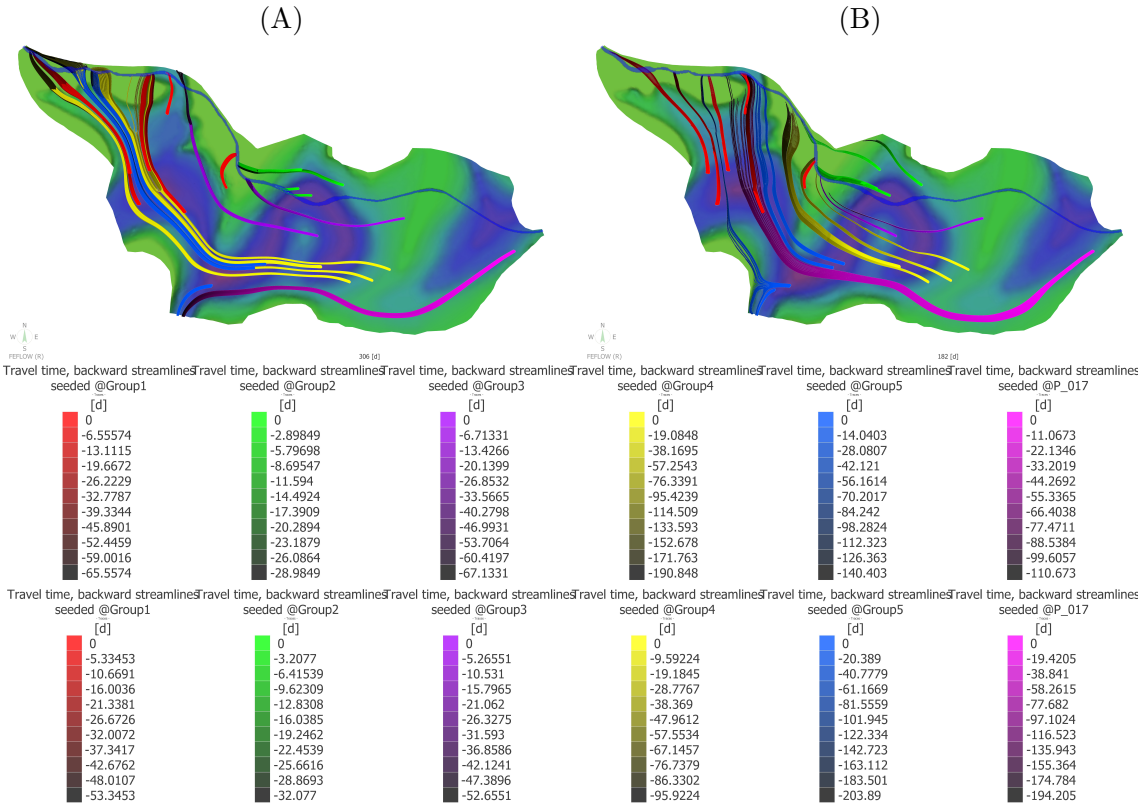


Figure S6: Groundwater flow under different conditions in the Sava River: (A) high discharge—the left figure and the upper legend (06.05.2010); (B) low discharge—the right figure and the lower legend (01.07.2010).

Chapter 4

Forecasting Model

This chapter describes the use of the developed modeling approach described in Section 3.4 for forecasting modeling that is going to be the subject of the new paper entitled "Assessment of the hydrological system behavior under climate change in the Ljubljansko polje, Slovenia" by Janja Vrzel, David Gampe, Ralf Ludwig and Nives Ogrinc. The manuscript will be submitted for the publication in the Science of the Total Environment as a part of the Special Issue "Climate Change and Water".

4.1 Introduction

Gampe, Nikulin, and Ludwig (2016) assessed increased pressure of climate change on the water balance in rivers of Mediterranean basins, including the Sava River Basin (SRB), due to the projected decrease of precipitation and rise of temperature (Figure 4.1). This prediction for the future was the encouragement for determination of the impact that would climate change had on groundwater in the Ljubljansko polje, which, as the main drinking water supply in the region, plays an important role for the local population.

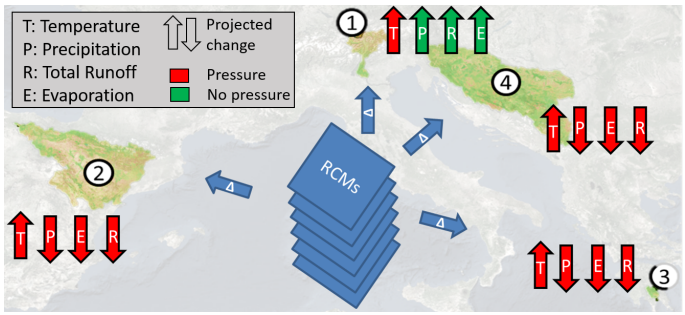


Figure 4.1: Climate change pressure on the water balance of Mediterranean river basins (Gampe, Nikulin, & Ludwig, 2016).

4.2 Methods

The climate pressure assessment is based on 22 simulations of climate projection, derived from combinations of four General Circulation Models (GCMs) forcing different Regional Climate Models (RCMs) and two Representative Concentration Pathways (RCPs) at mbox12 km horizontal resolution provided through the EURO-CORDEX initiative.

The used RCMs are: SMHI-RCA4, DMI-HIRHAM5, KNMI-RACMO22E and CLMcom-CCLM4-8-17. Climate change signals were projected for the period 2035–2065 and compared to the reference period 1981–2010 (Gampe et al., 2016).

The hydrological modeling was done with the modeling framework, which detailed description is provided in 4.2 and it is shown on Figure . The results of the climate models, provided by the partners in the GLOBAQUA project, were applied as input data for the both WaSiM models. The first model has a spatial resolution of 12 km and its domain includes the full Slovenian part of the SRB. The second WaSiM set-up was developed only for the Ljubljansko polje with a spatial resolution of 50 m. Both of them have a daily temporal resolution (see Section 3.4). The WaSiM model, with the Ljubljansko polje as the modeling domain, calculates spatially and temporally distributed percolation which results were used as the input data for the groundwater flow model in FEFLOW. The second WaSiM model, with the modeling domain of the SRB in Slovenia, simulates the Sava River discharge, which results were used as the input data for the MIKE 11 model. This procedure was repeated for the three RCMs (SMHI-RCA4, KNMI-RACMO22E and CLMcom-CCLM4-8-17). Daily WaSiM results for the period 2036–2065 were aggregated to the mean daily values (over one year) for each RCM. The projected data were compared to the results simulated for the reference period 2005–2015 and chronological data. The simulation with a simulated period of 30 years and daily time step was not accomplished so far, because of the time consuming FEFLOW simulation. Such a simulation, for only one RCM, would have to run nearly 30 days.

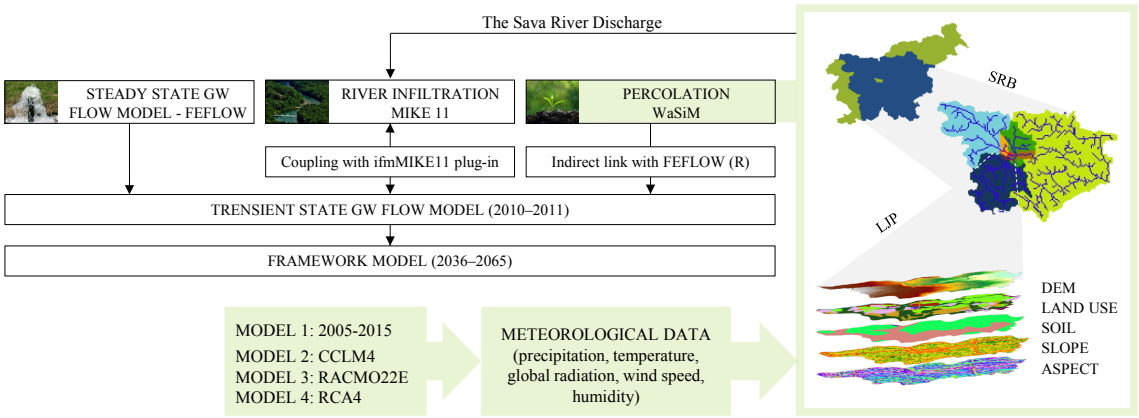


Figure 4.2: Modeling framework.

4.3 Results and Discussion

In the first step, an evaluation of climate conditions in the Ljubljansko polje, projected for the period 2036–2065 with the RCMs, was performed. A comparison of the projected precipitation for the period 2036–2065 and observed precipitation at Bežigrad over the period 1985–2015 shows slightly higher projected precipitation over a calendar year. It should be pointed out that this observation is relevant exclusively for the Ljubljansko polje, while the assessment of the climate pressure on the SRB is based on average values of the climate parameters for the full SRB, where climate conditions vary greatly (Alpine climate, Moderate continental climate and Moderate continental (mid-European) climate) (ISRBC, 2009). This can be the reason for observed deviations from the assessment provided by Gampe et al. (2016).

Figure 4.3 also shows projected percolation for the period 2036–2065. The lowest percolation may be expected at the beginning of the calendar year, late July and early August, while the highest percolation will most likely occur between the middle of September and the middle of November. These two periods have also the largest range between maximal and minimal projected precipitation and percolation.

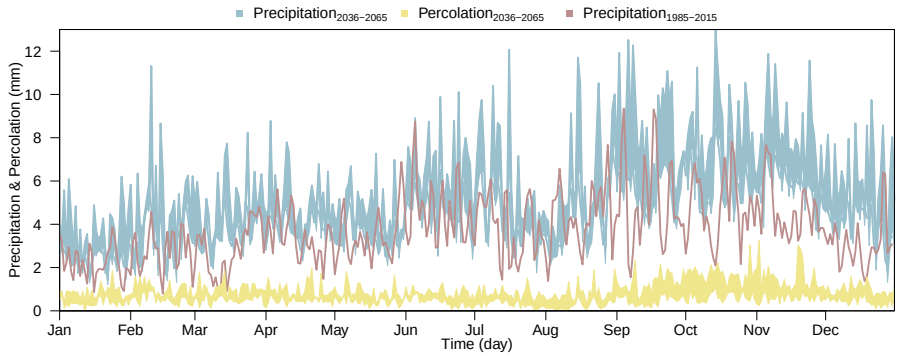


Figure 4.3: Comparison of the simulated precipitation and observed precipitation, and simulated percolation. Precipitation and percolation are given in a range that includes results of all the three RCMs.

Simulated discharge in the Sava River is also slightly higher than discharge observed over the reference time period (2000–2014) (Figure 4.4). Larger ranges between maximum and minimum discharge than between maximum and minimum amount of precipitation was observed. The investigation showed that this interesting observation is an effect of the amount of precipitation upstream from the Ljubljansko polje, which is strongly connected to the Sava River discharge.

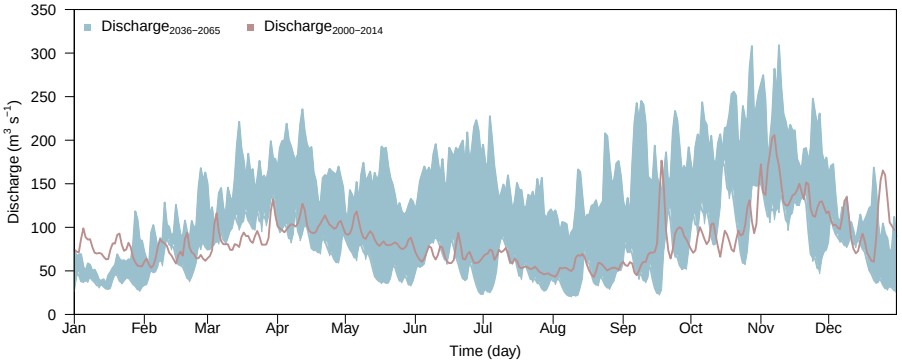


Figure 4.4: The Sava River discharge—observed over the period 2002–2014 and a range of water level simulated under conditions, which were projected with three RCMs.

The results show that drastic changes of the elevation of the hydraulic head in the Ljubljansko polje cannot be expected. Impacts of the RCMs on Kleče (group 1), Jarški prod (group 2) and Hrastje (group 3) are presented in Figure 4.5. The projected hydraulic head in Kleče is slightly higher than it was observed for the reference period (2005–2014). However, this observation does not necessarily mean that rising hydraulic heads are expected in the future, since the reference model also simulated slightly higher hydraulic heads for the group 1. Projected hydraulic heads in groups 2 and 3 are lower than hydraulic heads simulated with the reference model. For this reason, from these observations also

can not be certainly concluded that hydraulic heads will decrease in the future.

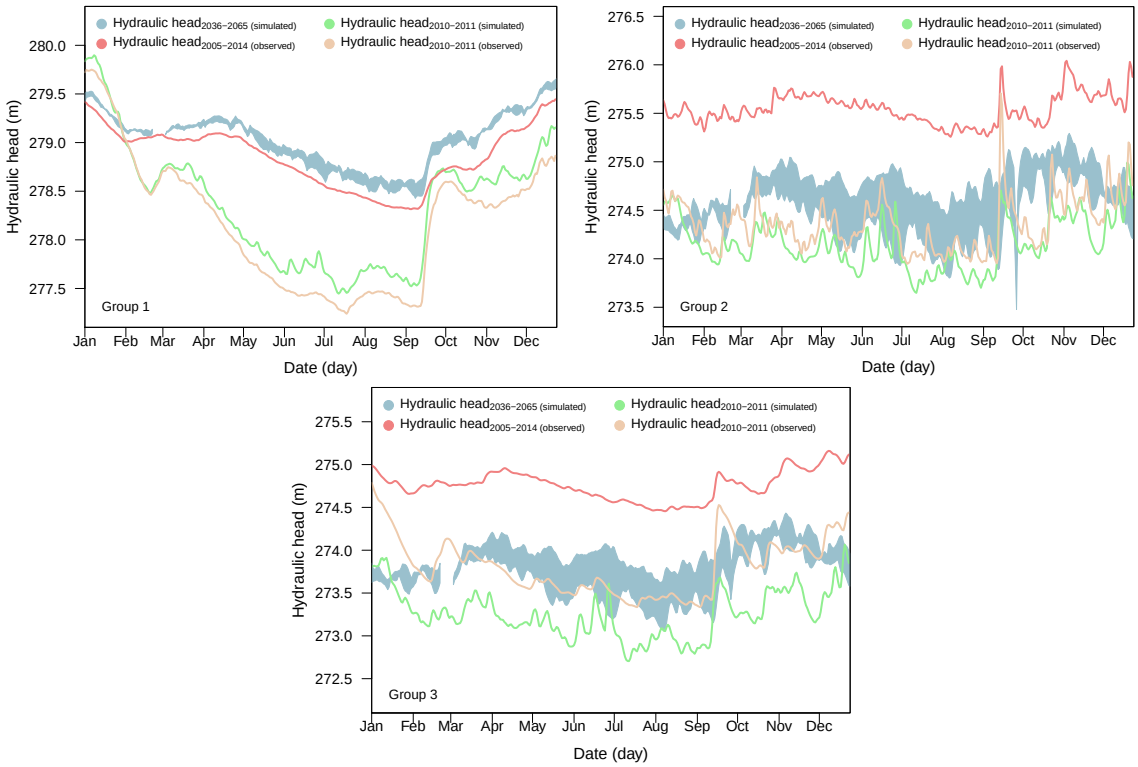


Figure 4.5: Observed, simulated and projected hydraulic heads for groups 1, 2, and 3. Locations of the groups are shown in Section 3.4, Figure 3.

Figure 4.6 and Figure 4.7 show leaching of the Sava River water into the aquifer and *vice versa*, respectively. Figure 4.6 shows that the Sava River–groundwater interface is the most sensitive to climate conditions between Črnuče and Šentjakob, because of the largest discrepancy between the maximum and minimum quantity of gaining groundwater. On the other hand, this flux is quite constant between Tacen and Črnuče (the seepage area for the group 1). Although the leaching of groundwater into the Sava River channel is relatively small, an impact of climate projections on these fluxes might be observed.

A closer look to the projected climate conditions by individual RCMs identifies three scenarios, on which the system reacts differently and therefore they can serve as a tool for even better understanding of the hydrology in the Ljubljansko polje. Sums of daily amounts of local precipitation and percolation, and mean discharge over the period 2036–2065 in the Ljubljansko polje, as well as a sum of precipitation upstream of the Ljubljansko polje, in the Alps, for each of the RCMs are presented in Table 4.1. The CLMcom-CCLM4-8-17 model projected climate conditions with the highest level of local precipitation, which created the largest percolation. Climate conditions, projected with the KNMI-RACMO22E model, force the hydrological models to simulate the greatest Sava River discharge due to the highest level of precipitation in the Alps. The driest hydrological conditions were simulated with climate conditions, which were projected with the SMHI-RCA4 model.

Hydraulic heads under RCMs conditions are quite harmonized in the group 1. On the other hand, they are more diverse in groups 2 and 3, their range is up to 1 m or 0.5 m wide, respectively. This is also connected to the altered sensitivity of the Sava River water–groundwater interface on varied climate conditions (Figure 4.6 and Figure 4.7),

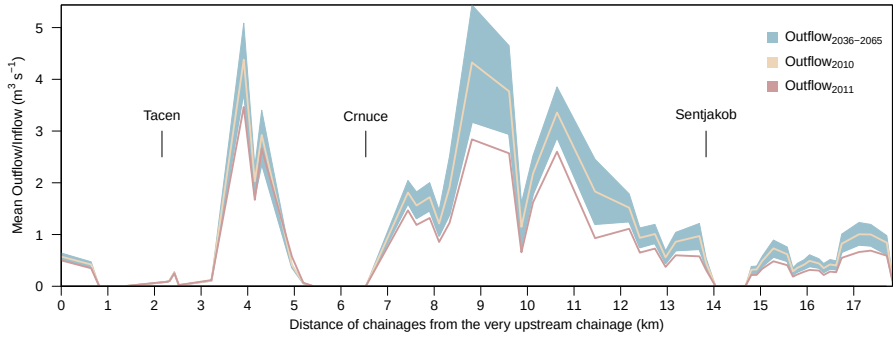


Figure 4.6: Locations where the Sava River water leaches into the aquifer and fluxes quantification for 2010, 2011 and 2036–2065.

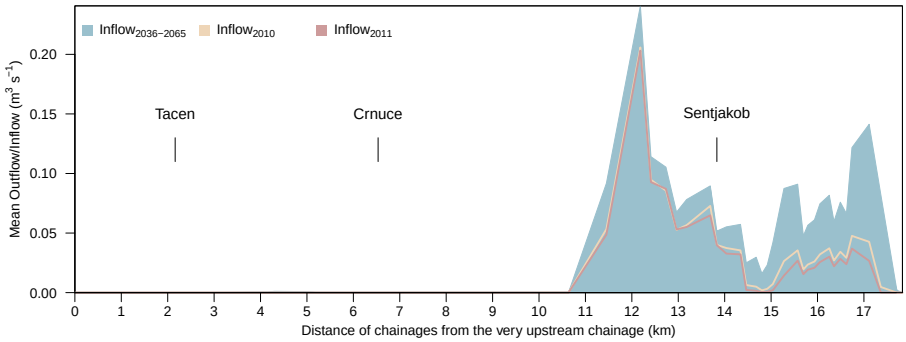


Figure 4.7: Locations where groundwater flows into the Sava River channel and fluxes quantification for 2010, 2011 and 2036–2065.

the main seepage areas for the groups 1, 2 and 3 (see Figure 4 in Section 3.4). These observations are especially interesting in the group 2 where the simulated and observed hydraulic head over the period 2010–2011 in the reference model does not deviate for more than 0.5 m. Two explanations were found for different reactions of hydraulic heads on the RCMs conditions in group 1, 2 and 3. First, a correlation between projected ranges of hydraulic heads and system responsiveness was observed. Faster system responsiveness coincides with the wider range between maximum and minimum hydraulic heads simulated under RCMs conditions. The second observation is that the system is more sensitive in areas where only one groundwater source prevails. In groups 2 and 3 the Sava River water and local precipitation are dominated groundwater sources, respectively, while the contribution of the both groundwater sources in the group 1 is quite equal, which could be the reason for the harmonized projection of hydraulic heads in this area. Fractions of the two main groundwater sources in groups 1, 2 and 3 were estimated and presented in Section 3.3.

4.4 Conclusions

Multi-tools (FEFLOW-WaSiM-MIKE 11) for simulation of hydrodynamics in an aquifer that is sensitive to the surface water, was found to be a very effective approach for the forecasting modeling. It enables precise simulations of surface water, groundwater and

Table 4.1: Sums of local precipitation and percolation, and mean discharge over the period 2036–2065 in the Ljubljansko polje, as well as a sum of precipitation upstream of the Ljubljansko polje, in the Alps.

	CCLM4-8-17	RACMO22E	RCA4
Sum of local precipitation (mm)	1613	1598	1473
Sum of precipitation upstream from the LJP, in the Alps (mm)	1,146,517	1,554,455	842,021
Discharge (m^3 s^{-1})	105	142	77
Sum of percolation (mm)	296	228	284

their interaction. Therefore, it is expected that results will be of a great help for sustainable water management planning in the Ljubljansko polje. According to the presented results of forecasting models, which were forced with the three RCMs for the period 2036–2065, the Ljubljansko polje is not going to suffer due to water scarcity in these 30 years. However, the general projection for the full SRB shows that the water scarcity may happen there in the future. Deeper investigation of water quality and its forecasting are two possible applications of the presented surface-groundwater models.

Chapter 5

Conclusions

This study was set up to explore the water cycle in detail, with an emphasis on the interaction between groundwater and surface water, and identify pressures on water resources. Environmental issues, especially those related to water scarcity and drinking water quality that the world is facing, as well as the demands of the European Union water policy that is regulated by the EU Water framework directive was the inspiration for this work. I believe that we can solve such complex environmental issues only through the collaborative work of environmental scientists specializing in surface water, groundwater and even subsurface water, as well as those expert in measuring either water contaminants or tracers and those who understand the role of water from the societal point of view. Nevertheless, this dissertation represents an incredible achievement resulting from a combination of different scientific fields. Therefore, I wish that this thesis will encourage scientists to perform interdisciplinary work and act as a reminder to stakeholders as to just how complex and sensitive the system is that they manage. Moreover, this research is complementary to the activities performed within the on-going EU project GLOBAQUA (Managing the effects of multiple stressors on aquatic ecosystem under water scarcity).

The next notable contribution to the science is the development of a comprehensive modeling framework capable of running parallel simulations of all the crucial water components. With some additional work, the model is also capable of simulating the transport of water contaminants, climate change and land use change. The diverse mathematical background of these models and the huge database they require are two of the reasons why this work is so demanding and has not been fully implemented into routine work.

The contribution to the science performed within the study has resulted in four publications (three published and one submitted) in SCI international journals. Another paper (in preparation) will be part of a Special issue "Climate Change and Water" in the journal Science of the Total Environment. To date, the work has been presented at twenty-one international conferences (See 5) that include six oral presentations.

The main conclusions of the present research follow the order of scientific articles presented in this dissertation and are summarized as follows:

1. The first paper deals with nutrient patterns (NO_3^- and PO_4^{3-}) in the Sava River at eight locations covering Slovenia, Croatia and Serbia. The results show how these concentrations have changed with time and space, which are the main drivers of their behavior. In general, nutrient concentrations have declined by 58% in the Sava River. However, significantly higher annual mean concentrations of NO_3^- and PO_4^{3-} were observed at locations influenced by intensive agricultural activity in Croatia and Serbia. Nutrient concentrations are also strongly related to riverine flow. The highest NO_3^- concentrations were observed during winter/autumn when leaching from soil was most intensive, while the lowest NO_3^- concentrations were observed

during summer, which are mainly related to the reduction of NO_3^- due to phytoplankton uptake. Alternatively, the highest PO_4^{3-} concentrations are related to low flow conditions during the summer months and the presence of reducing conditions that release inorganic phosphorous from sediments into the water column.

2. The second investigation focused exclusively on determining nutrient and microbiological sources. The research is based on the combined use of the isotope compositions of N and O in NO_3^- and the standard indicators of fecal pollution and microbial source tracking based on the human-associated BacHum and HF183II, the ruminant-associated BacR and the pig associated Pig2Bac genetic Bacteroidetes fecal markers. The first notable result provides evidence of the pressure of NO_3^- on the Sava River water that arises from two different sources: one originating from pristine soils and the second from waste water and manure. The results also show the possibility that atmospheric deposition and commercial fertilizers do not contribute significantly to river NO_3^-. Low levels of isotopic nitrogen and oxygen enrichment, however, suggests possible soil nitrification and an admixture of NO_3^- from waste water and manure. Nevertheless, this hypothesis still requires a deeper investigation in the future. Of concern is the observed human fecal pollution in the Sava River basin that arrives to the Sava River water from the continuous discharge of untreated waste water. Thus, the most important take home massage of this research is that the Sava River needs effective waste water treatment plants as part an overall water management programme.
3. Since rivers are strongly connected to groundwater, it was important to determine how the pressure of anthropogenic activities affecting the SRB are reflected in groundwater. Multiple tools were applied to improve our understanding of the water cycle in the Ljubljansko polje in space and in time under different conditions. The $\delta^{18}O$ and $\delta^{2}H$ fingerprints explain the diversity in the dominant groundwater sources from location to location, while ^{3}H and $^{3}H/^{3}He$ tools are used to determine the groundwater mean residence time. The results reveal a shorter mean residence time in Jarški prod where the Sava River water is the dominant groundwater source, while the longest residence time is in Hrastje, where local precipitation is the dominant source of groundwater. The area having the greatest impact from local precipitation also has the highest NO_3^- concentrations, while the presence of old water in Kleče, which is undetectable using the $^{3}H/^{3}He$ method, was previously unknown.
4. A strong connection exists between groundwater and surface water, which occurs below the surface. However, to understand where, under which conditions and how this interaction takes place, it was necessary to revert to methods that have a mathematical and physical background. This meant making a comprehensive simulation of the complete water cycle in the Ljubljansko polje. The first step involved data pre-processing, including making an evaluation to whether or not the data are appropriate for transforming a conceptual model, which is based, in this instance, on geochemical analyses, into numerical model. Different statistical methods were applied, but the most convincing results were obtained using cross correlation analysis. In general, the system's responsiveness is quicker when the influence of the Sava River water dominates and mean residence time is shorter, whereas the overall responsiveness of the system is slower in the case when groundwater has a longer mean residence time and local precipitation dominates. Next, the two main groundwater sources—the Sava River and local precipitation, which play a key role as boundary conditions in modeling groundwater flow, were simulated individually using MIKE 11 and WaSiM software. Later, the groundwater flow model, simulated using FEFLOW, was coupled with the MIKE 11 software via an ifmMIKE11 plug-in. Addi-

tionally, a link between FEFLOW and WaSiM was established. The results are truly enviable since they provide answers to all our questions, i.e., where, to what extent and under which conditions do groundwater-surface water interactions happen.

5. Further, the link between FEFLOW and WaSiM means the modeling framework is capable of simulating the water cycle under other climatic conditions and land use. The final part of this thesis makes predictions concerning the water cycle for the period 2036–2065. The forecast is positive since it appears that the Ljubljansko polje will not suffer due to water scarcity in the period 2036–2065, as was projected for the SRB as a whole. This comprehensive groundwater flow model has been run under climate conditions simulated using the three Regional Climate Models: SMHI-RCA4, KNMI-RACMO22E and CLMcom-CCLM4-8-17. All three simulations provide different conditions, which was important for improving our understanding of the water cycle. Higher precipitation upstream in the Alps and lower local levels of precipitation create ideal conditions for groundwater-river water interactions. In addition, the river section between Tomačevo and Šentjakob is the most sensitive to climatic changes.

While the findings of this study demonstrate the potential of creating a comprehensive modeling framework by coupling the three software programs together i.e., FEFLOW-MIKE 11-WaSiM, the set up of which is based on geochemical and historical data, opportunities for extending the scope of this thesis remain. For instance, Kleče—the main drinking water pumping station provides an ideal opportunity to perform groundwater studies using a method that is appropriate for estimating old water like the ^{14}C method. Such work would contribute significantly to our understanding of the water cycle in the Ljubljansko polje.

In addition, using newer more modern tools and additional fieldwork will allow a more precise estimate of many of the modeling input data and parameters, albeit this would require drilling. A denser network of piezometers with depths down to the bedrock (especially in areas where there are either a limited number or no piezometers) would allow a better construction of the model's physical domain (geometry of bedrock, multiple model layers). The bedrock is an important driver when it comes to simulating groundwater flow direction and calculating the volume of the aquifer. Multiple model layers can simulate the pressure in an aquifer more realistically, which would be especially useful when modeling the area south from Kleče where layers with low hydraulic conductivity appear. Underground recharge from the Ljubljansko barje also appears to be important for the Ljubljansko polje. Therefore, field observations would make a great contribution to simulating groundwater flow in this region. According to the modeling results, pumping wells from the Pivovarna Laško Union d.o.o. brewery are particularly affected with this water, and therefore the brewery might be interested in such a study.

New possibilities for generating realistic distributions of stream bed properties have the potential for improving our understanding and predictive capabilities for river-groundwater systems, especially when combined with the integrated simulation of river and groundwater flow. The Manning's n, the leaching coefficient and hydraulic conductivity of the clogging layer are the most important parameters. Despite having made field measurements, this work might have been achieved using photogrammetry or remote sensing data.

The WaSiM model could also be improved, especially from a parameterization point of view. Such a parameter is the leaf area index (LAI), for example. Unfortunately, in the period of this doctoral study there was insufficient time to implement the spatially and temporally distributed LAI index, provided by remote sensing. The European Union's Earth Observation Programme Copernicus, however, could provide such data.

The existing groundwater flow model has a great potential for many applications in-

cluding the following: (1) Testing the impact of changing land use on the water cycle. Particularly interesting would be to observe the impact on groundwater-surface water interactions. Huber-García, Meyer, Kok, Verweij, and Ludwig (2018) already projected land use in the Sava River basin up to 2050. (2) Running the forecasting model with daily time steps over the full 30-year period and testing the impacts of climate data at different spatial resolutions, e.g., 12 km and 1 km is possible (Gampe et al., 2016). (3) The model could also be extended into a tracing model for simulating water tracers (e.g., isotopes) and pollutants (e.g., nutrients, pharmaceuticals, heavy metals).

The implementation of such a detailed study in the lower part of the SRB, which has a significantly different climate, would also be interesting. The model framework requires establishing a WaSiM model for the SRB, upstream from the modeling domain. Nevertheless, for such a model it is recommended that unique measurement methods and procedures are implemented in all the countries that belong to the SRB. An importance of a quality water monitoring programs is described in Behmel et al. (2016).

To summarize, the findings of this thesis are important for sustainable groundwater management in the Ljubljansko polje. For example, they are important for Slovenske Elektrarne d.o.o., who manages the Sava River for energy production, the Pivovarna Laško Union d.o.o brewery whose profit depends on groundwater extraction from the Ljubljansko polje, and for the Sava River Commission whose duty it is to manage the Sava River catchment.

Above all, this work is a solid foundation for studies that are currently hydrologically hot topics i.e., the impact of pollution and the effects of climate and land use changes on surface water and groundwater and their interaction. The credit for this must go to following: (1) the strategic location of the Ljubljansko polje—south from the Alps and close to the Adriatic see, because of which the isotopic composition of the Sava River and local precipitation can be easily distinguished, which is not the case in many studies; (2) studying the diverse hydrological processes in the Ljubljansko polje—a relatively small area, where boundary conditions can be easily controlled, makes modeling (on a spatial and temporal scale) easier from a computational point of view, and (3) the ability to simulate, in parallel, key components of the water cycle in the Ljubljansko polje using the modeling framework.

Appendix A

R-script: The WaSiM-FEFLOW Link

1. CONVERTING WaSiM OUTPUTS TO TEXT FILES

```
library(raster)
files_to_read=list.files(pattern="Pattern_Name")
for(i in 1:length(files_to_read)){
  x=raster(files_to_read[i])    #convert WaSiM output files with ending .s into raster files
  y=rasterToPoints(x, fun=NULL)   #convert rasters to points
  NameStr=unlist(strsplit(files_to_read[i], "[.]"))   #define name of new point files
  write.table(y, file=paste(outpath, NameStr[1], "_", NameStr[2], ".dat", sep=""), col.names=TRUE, row.names=FALSE)
  }
```

2. MERGING FILES

```
  # 2.1. Working Directory
setwd("C:/.../")
List=list.files(pattern="dat$")
  # 2.2. Find the third column in the each file
Columns \leftarrow lapply(X=List, FUN=function(x) {
read.table(x, colClasses=c("numeric", "numeric", "numeric"), header=TRUE, sep="")[,3]
  })
  # 2.3. Merge columns into one file (Check if the sequence of columns agree with time steps.)
File1 \leftarrow do.call("cbind", Columns)
  # 2.3. Units
File1 \leftarrow File1[,]/1000
  # 2.4. Check if the new file is right
str(File1)
  # 2.5. Write table
write.table(File1, paste("C:/..."), sep="\t", append=FALSE, quote=TRUE, na="NA", dec=",", row.names=TRUE, col.names=TRUE)
```

3. ADDING COORDINATES

```
  # 3.1. Read table created in the step 2.5
df \leftarrow read.table("D:/...", header=TRUE, sep="\t", dec=",")
  # 3.2 Read a random .dat file (created from ASCII files in the previous steps), which has also X and Y coordinates
xy \leftarrow read.table("D:/...", header=TRUE, sep=" ", dec=",")
  # 3.3 Create new data frame
df_xy=xy[,1:2]
xy_perc \leftarrow merge(df_xy, df, by="row.names")
```

```
8 write.table(xy_perc[,-1], paste("D:/...."), sep="\t", append=FALSE, quote=FALSE, na
    ="NA", dec=".", row.names=FALSE, col.names=TRUE)
```

References

Adu-Gyamfi, J. J. (2013). *Food security in nutrient-stressed environments: Exploiting plants' genetic capabilities*. Developments in Plant and Soil Sciences. San Diego, CA: Academic Press.

Alley, W. M., Reilly, T. E., & Franke, O. L. (1999). *Sustainability of groundwater resources* (U.S. Geological Survey Circular No. 1186). U.S. Geological Survey.

Anderson, M. P., Woessner, W. W., & Hunt, R. J. (2015). *Applied groundwater modeling, Simulation of flow and advective transport*. Second edition. London, UK: Elsevier Inc.

Appelo, C. A. J. & Postma, D. (2004). *Geochemistry, groundwater and pollution*. Second edition. New Yourk: CRC Press.

Behmel, S., Damour, M., Ludwig, R., & Rodriguez, M. J. (2016). Water quality monitoring strategies — a review and future perspectives. *Science of The Total Environment*, *571*(15), 1312–1329. doi:https://doi.org/10.1016/j.scitotenv.2016.06.235

Bernhard, A. (2010). The nitrogen cycle: Processes, players, and human impact. *Nature Education Knowledge*, *3*(10), 25.

Billen, G., Garnier, J., Némery, J., Sebilo, M., Sferratore, A., Barles, A., ... Benoît, M. (2007). A long-term view of nutrient transfers through the seine river continuum. *Science of the Total Environment*, *375*(1-3), 80–97. doi:https://doi.org/10.1016/j.scitotenv.2006.12.005

Boano, F., Camporeale, C., & Revelli, R. (2010). A linear model for the coupled surface-subsurface flow in a meandering stream. *Water Resources Research*, *46*(7), 1–14. doi:10.1029/2009WR008317

Bouwer, H. & Maddock, T. I. (1997). Making sense of the interactions between groundwater and streamflow: Lessons for water masters and adjudicators. *Rivers*, *6*(1), 19–31.

Brunner, P., Therrien, R., Renard, P., Simmons, C. T., & Franss, H.-J. H. (2017). Advances in understanding river-groundwater interactions. *Reviews of Geophysics*, *55*(3), 818–854. doi:10.1002/2017RG000556

Burbery, L. & Ritson, J. (2010). *Integrated study of surface water and shallow groundwater resources of the Orari catchment* (Technical report No. Report No. R10/36). Environmental Canterbury Regional Council.

Calver, A. (2001). Riverbed permeabilities: Information from pooled data. *Groundwater*, *39*(4), 546–553. doi:10.1111/j.1745-6584.2001.tb02343.x

Camporeale, C., Perucca, E., Ridolfi, L., & Gurnell, A. M. (2013). Modeling the interactions between river morphodynamics and riparian vegetation. *Reviews of Geophysics*, *51*(3), 379–414. doi:10.1002/rog.20014

Carr, E. J. & Simpson, M. J. (2018). Accurate and efficient calculation of response times for groundwater flow. *Journal of Hydrology*, *558*, 470–481. doi:https://doi.org/10.1016/j.jhydrol.2017.12.023

Celia, M. A., Bouloutas, E. T., & Zarba, R. L. (1990). A general mass-conservative numerical solution for the unsaturated flow equation. *Water Resources Research*, *26*(7), 1483–1496. doi:10.1029/WR026i007p01483

Chang, C. C. Y., Kendall, C., Silva, S. R., Battaglin, W. A., & Campbell, D. H. (2002). Nitrate stable isotopes: Tools for determining nitrate sources among different land uses in the Mississippi River Basin. *Journal of Fisheries and Aquatic Sciences*, *59*(12), 1874–1885. doi:https://doi.org/10.1139/f02-153

Cheng, R. T. (1978). Modeling of hydraulic systems by finite-elemnt methods. In P. Burnard (Ed.), *Advances in hydroscience* (Vol. 11, pp. 207–284). New York: Academic Press.

Chiang, W.-H. & Kinzelbach, W. (2003). *3d-groundwater modeling with PMWIN*. A Simulation System for Modeling Groundwater Flow and Pollution. Berlin: Springer. doi:10.1007/978-3-662-05549-6

EU-Commission. (2015). Final report summary - INTRAMIF (INitial TRAining network on Mass Independent Fractionation). Retrieved April 8, 2018, from https://www.cordis.europa.eu/result/rcn/164426_en.html

EU-Commission. (2016). The EU Water Framework Directive - integrated river basin management for Europe. Retrieved January 18, 2018, from http://ec.europa.eu/environment/water/water-framework/index_en.html

Coplen, T. B., Herczeg, A. L., & Barnes, C. (2000). Isotope engineering—using stable isotopes of the water molecule to solve practical problems. In P. G. Cook & A. L. Herczeg (Eds.), *Environmental tracers in subsurface hydrology*. Boston: Springer. doi:https://doi.org/10.1007/978-1-4615-4557-6_3

Craig, H. (1957). Isotopic standards for carbon and oxygen and correction factors for mass-spectrometric analysis of carbon dioxide. *Geochimica et Cosmochimica Acta*, *12*(1-2), 133–149. doi:https://doi.org/10.1016/0016-7037(57)90024-8

Craig, H. (1961). Standard for reporting concentrations of deuterium and oxygen-18 in natural waters. *Science*, *133*(3467), 1833–1834. doi:10.1126/science.133.3467.1833

Dansgaard, W. (1964). Stable isotopes in precipitation. *Tellus*, *16*(4), 436–468. doi:10.1111/j.2153-3490.1964.tb00181.x

Delleur, J. W. (Ed.). (2007). *The handbook of groundwater engineering*. Second Edition. New York: CRC Press, Taylor & Francis Group.

Diersch, H.-J. G. (2014). *Feflow, finite element modeling of flow, mass and heat transport in porous and fractured media*. Berlin, Heidelberg: Springer. doi:10.1007/978-3-642-38739-5

Ding, Y., Jia, Y., & Wang, S. S. Y. (2004). Identification of Manning's roughness coefficients in shallow water flows. *Journal of Hydraulic Engineering*, *130*(6), 501–510. doi:10.1061/~ASCE!0733-9429~2004!130:6~501!

Doppler, T., Franssen, H.-J. H., Kaiser, H.-P., Kuhlmanc, U., & Stauffer, F. (2007). Field evidence of a dynamic leakage coefficient for modelling river–aquifer interactions. *Journal of Hydrology*, *347*(1-2), 177–187. doi:https://doi.org/10.1016/j.jhydrol.2007.09.017

EAWAG. (2018). 3H-3He water age. Retrieved March 11, 2018, from http://www.eawag.ch/en/department/wut/main-focus/environmental-isotopes/3h-3he-water-age/

ECRR. (2014). What is the WFD? Retrieved January 18, 2018, from http://www.ecrr.org/

EEA. (2016). Freshwater quality. Retrieved January 20, 2018, from https://www.eea.europa.eu/soer-2015/europe/freshwater

Engel, M. & Macko, S. A. (Eds.). (1993). *Organic geochemistry, principles and applications*. New York: Plenum Press. doi:10.1007/978-1-4615-2890-6

Essink, O. (2000). Groundwater modelling. Retrieved September 2000, from file:///C:/Users/Water/Downloads/gwm1.pdf

EUR-Lex. (2000). Directive 2000/60/EC of the European Parliament and of the Council of 23 October 2000 establishing a framework for Community action in the field of water policy. Retrieved March 11, 2018, from http://data.europa.eu/eli/dir/2000/60/oj

European-Environmental-Agency. (2018). Nutrients in freshwater. Retrieved April 4, 2018, from https://www.eea.europa.eu/data-and-maps/indicators/nutrients-in-freshwater/nutrients-in-freshwater-assessment-published-6

Falkowski, P., Scholes, R. J., Boyle, E., Canadell, J., Canfield, D., Elser, J., ... Steffen1, W. (2000). The global carbon cycle: A test of our knowledge of earth as a system. *Science*, *290*(5490), 291–296. doi:0.1126/science.290.5490.291

Fenech, C., Rock, L., Nolan, K., Tobin, J., & Morrissey, A. (2012). The potential for a suite of isotope and chemical markers to differentiate sources of nitrate contamination: A review. *Water Research*, *46*(7), 2023–2041. doi:https://doi.org/10.1016/j.watres.2012.01.044

Fleckenstein, J. H., Krause, S., Hannah, D. M., & Boano, F. (2010). Groundwater-surface water interactions: New methods and models to improve understanding of processes and dynamics. *Hydrogeology Journal*, *33*(11), 1291–1295. doi:https://doi.org/10.1016/j.advwatres.2010.09.011

Gampe, D., Nikulin, G., & Ludwig, R. (2016). Using an ensemble of regional climate models to assess climate change impacts on water scarcity in European river basins. *Science of The Total Environment*, *573*(15), 1503–1518. doi:https://doi.org/10.1016/j.scitotenv.2016.08.053

Gat, J. R. & Tzur, Y. (1967). *Modification of the isotopic composition of rainwater by processes which occur before groundwater recharge*. International Atomic Energy Agency (IAEA): IAEA.

Gianni, G., Richon, J., Perrochet, P., Vogel, A., & Brunner, P. (2016). Rapid identification of transience in streambed conductance by inversion of floodwave responses. *Water Resources Research*, *52*(4), 2647–2658. doi:10.1002/2015WR017154

Haan, C. T. (2002). *Statistical methods in hydrology*. Second Edition. Iowa: Iowa State University Press.

Hameed, T., Mariño, M. A., DeVries, J. J., & Tracy, J. C. (1997). Method for trend detection in climatological variables. *Journal of Hydrologic Engineering*, *2*(4), 154–160. doi:https://doi.org/10.1061/(ASCE)1084-0699(1997)2:4(154)

Harvey, J. W. & Wagner, B. J. (2000). Quantifying hydrologic interactions between streams and their subsurface hyporheic zones. In J. B. Jones & P. J. Mulholland (Eds.), *Streams and groundwaters* (pp. 3–44). San Diego: Academic Press. doi:10.1016/B978-012389845-6/50002-8

Hebert, C. E. & Wassenaar, L. I. (2001). Stable nitrogen isotopes in waterfowl feathers reflect agricultural land use in western Canada. *Environmental Science & Technology*, *35*(17), 3482–3487. doi:10.1021/es001970p

Hirsch, R. M., Moyer, D. L., & Archfield, S. A. (2010). Weighted regression on time, discharge, and season (WRTDS) with an application to Chesapeake bay river inputs. *Journal of the American Water Resources Association (JAWRA)*, *46*(5), 857–880. doi:https://doi.org/10.1111/j.1752-1688.2010.00482.x

Hirsch, R. M. & Slack, J. R. (1984). Non-parametric trend test for seasonal data with serial dependence. *Water Resources Research*, *20*(6), 727–732. doi:10.1029/WR020i006p00727

Hirsch, R. M., Slack, J. R., & Smith, R. A. (1982). Techniques of trend analysis for monthly water quality data. *Water Resources Research*, *18*(1), 107–121. doi:10.1029/WR018i001p00107

Hoefs, J. (1997). *Stable isotope geochemistry*. Berlin, Heidelberg: Springer. doi:10.1007/978-3-662-03377-7

House, A. R., Thompson, J. R., Sorensen, J. P. R., Roberts, C., & Acreman, M. C. (2016). Modelli ng groundwater/surface water interaction in a managedriparian chalk valley wetland. *Hydrological Processes*, *30*(3), 447–462. doi:10.1002/hyp.10625

Huber-García, V., Meyer, S., Kok, K., Verweij, P., & Ludwig, R. (2018). Deriving spatially explicit water uses from land use change modelling results in four river basins across Europe. *Science of The Total Environment*, *628-629*(1), 1079–1097. doi:https://doi.org/10.1016/j.scitotenv.2018.02.051

Hunt, R. J., Doherty, J., & Tonkin, M. J. (2007). Are models too simple? Arguments for increased parameterization. *Groundwater*, *45*(3), 254–262. doi:10.1111/j.1745-6584.2007.00316.x

Hunt, R. J. & Welter, D. E. (2010). Taking account of unknown unknowns. *Groundwater*, *48*(4), 477. doi:10.1111/j.1745-6584.2010.00681.x

Irvine, D. J., Briggs, M. A., Lautz, L. K., Ryan P. Gordon, J. M. M., & Cartwright, I. (2016). Using diurnal temperature signals to infer vertical groundwater-surface water exchange. *Groundwater*, *55*(1), 10–26. doi:10.1111/gwat.12459

Irvine, D. J., Brunner, P., Franssen, H.-J. H., & Simmons, C. T. (2012). Heterogeneous or homogeneous? Implications of simplifying heterogeneous streambeds in models of losing streams. *Journal of Hydrology*, *424-425*(6), 16–23. doi:https://doi.org/10.1016/j.jhydrol.2011.11.051

ISRBC. (2009). *Sava river basin analysis*. International Sava River Basin Commission.

Janža, M., Meglič, P., & Šram, D. (2011). *Numerical hydrological modelling*. Geological Survey of Slovenia.

Jolly, I., Rassam, D., Pickett, T., Gilfedder, M., & Stenson, M. (2010). Modelling groundwater - surface water interactions in the new generation of river systems models for austria. *CD of Proceedings of Groundwater 2010, Canberra*. 31 October – 4 November 2010.

Kalbus, E., Reinstorf, F., & Schirmer, M. (2006). Measuring methods for groundwater – surface water interactions: A review. *Hydrology and Earth System Science*, *10*(6), 873–887. doi:https://doi.org/10.5194/hess-10-873-2006

Kazemi, G. A., Lehr, J. H., & Perrochet, P. (Eds.). (2006). *Groundwater age*. Hoboken, New Jersey: John Wiley & Sons, Inc. doi:10.1002/0471929514

Kendall, C. & Doctor, D. H. (2011). Stable isotope applications in hydrologic studies. In H. D. Holland & K. K. Turekian (Eds.), *Isotope geochemistry: A derivative of the treatise on geochemistry* (pp. 181–226). Academic Press.

Kendall, C., Elliott, E. M., & Wankel, S. D. (2008). Tracing anthropogenic inputs of nitrogen to ecosystems. In R. Michener & K. Lajtha (Eds.), *Stable isotopes in ecology and environmental science: Second edition* (pp. 375–449). Oxford: Blackwell Publishing Ltd. doi:10.1002/9780470691854.ch12

Kendall, C. & McDonnell, J. J. (1998). *Statistical methods in hydrology*. Amsterdam: Elsevier Science B.V.

Knödel, K., Lange, G., & Voigt, H.-J. (2007). *Environmental geology: Handbook of field methods and case studies* (B. für Geowissenschaften, Ed.). Berlin: Springer Science and Business Media.

Kohn, K. E. (1996). Conceptualization and characterization of ground-water systems using geographic information systems. *Engineering Geology*, *42*(2-3), 111–118. doi:https://doi.org/10.1016/0013-7952(95)00072-0

Konikow, L. F. (1978). Calibration of ground-water models. In *Verification of mathematical and physical models in hydraulic engineering* (pp. 871–93). New York: American Society of Civil Engineering.

Krause, S., Hannah, D. M., & Fleckenstein, J. H. (2009). Hyporheic hydrology: Interactions at the groundwater-surfacewater interface. *Hydrological Processes*, *23*(15), 2103–2107. doi:10.1002/hyp.7366

Kumar, C. P. (2012). Groundwater modelling software – capabilities and limitations. *IOSR Journal of Environmental Science, Toxicology and Food Technology*, *1*, 46–57.

Lapworth, D. J., Baran, N., Stuart, M. E., & Ward, R. S. (2012). Emerging organic contaminants in groundwater: A review of sources, fate and occurrence. *Environmental Pollution*, *163*, 287–303. doi:https://doi.org/10.1016/j.envpol.2011.12.034

Larocque, M. & Broda, S. (2016). Groundwater–surface water interactions in Canada. *Canadian Water Resources Journal / Revue canadienne des ressources hydriques*, *41*(4), 451–454. doi:10.1080/07011784.2016.1176537

Lin, Y.-F., Wang, J., & Valocchi, A. J. (n.d.). Making groundwater recharge and discharge estimate maps in one day, an ArcGIS 9.2 application for water resources research. Retrieved January 14, 2018, from http://www.esri.com/news/arcuser/0408/groundwater.html

Machiwal, D. & Jha, M. K. (2012). Stochastic modelling of time series. In D. Machiwal & M. K. Jha (Eds.), *Hydrologic time series analysis: Theory and practice* (pp. 85–95). Dordrecht, Netherlands: Springer. doi:http://dx.doi.org/10.1007/978-94-007-1861-6_5

Maloszewski, P. & Zuber, A. (1982). Determining the turnover time of groundwater systems with the aid of environmental tracers: 1. Models and their applicability. *Journal of Hydrology*, *57*(3-4), 207–231. doi:https://doi.org/10.1016/0022-1694(82)90147-0

Mayer, B., Boyer, E. W., Goodale, C., Jaworski, N. A., van Breemen, N., Howarth, R. W., ... Paustian, K. (2002). Sources of nitrate in rivers draining sixteen watersheds in the northeastern U.S.: Isotopic constraints. *Biogeochemistry*, *57*(1), 171–197. doi:https://doi.org/10.1023/A:1015744002496

McLachlan, P. J., Chambers, J. E., Uhlemann, S. S., & Binley, A. (2017). Geophysical characterisation of the groundwater–surface water interface. *Advances in Water Resources*, *109*, 302–319. doi:https://doi.org/10.1016/j.advwatres.2017.09.016

Meals, D. W., Dressing, S. A., & Davenport, T. E. (2010). Lag time in water quality response to best management practices: A review. *Journal of Environmental Quality*, *39*(1), 85–96. doi:10.2134/jeq2009.0108

MIKE. (2016). *FePEST in FEFLOW 7.0*. MIKE Powered by DHI.

Monninkhoff, B. (2014). *IfmMIKE11 2.1, DHI-WASY Software*. DHI-WASY GmbH.

Mook, W. G. (2001). *Statistical methods in hydrology* (IHP-V Technical Documents in Hydrology No. 39). International Atomic Energy Agency & United Nations Educational, Scientific and Cultural Organization.

Morgan, K. (2013). Mass spectrometry: Isotope effects. Retrieved February 15, 2018, from https://chem.libretexts.org/Core/Analytical_Chemistry/Instrumental_Analysis/Mass_Spectrometry/Mass_Spectrometry%3A_Isotope_Effects

NRC. (2004). Modeling of hydraulic systems by finite-elemnt methods. In M. P. Anderson & J. L. Wilson (Eds.), *Groundwater fluxes across interfaces* (p. 85). National Research Council. New York: Nacional Academy Press.

Ogrinc, N., Markovics, R., nd Lynn M. Walter, T. K., & Hamilton, S. K. (2008). Sources and transport of carbon and nitrogen in the river sava watershed, a major tributary of the River Danube. *Applied Geochemistry*, *23*(12), 3685–3698. doi:https://doi.org/10.1016/j.apgeochem.2008.09.003

Paniconi, C. & Putti, M. (2015). Physically based modeling in catchment hydrology at 50: Survey and outlook. *Water Resources Research*, *51*(9), 7090–7129. doi:10.1002/2015WR017780

Partington, D., Therrien, R., Simmons, C. T., & Brunner, P. (2017). Blueprint for a coupled model of sedimentology, hydrology, and hydrogeology in streambeds. *Reviews of Geophysics*, *55*(2), 287–309. doi:10.1002/2016RG000530

Patra, H. P., Adhikari, S. K., & Kunar, S. (2016), In *Groundwater prospecting and management* (pp. 7–45). Singapore: Springer. doi:10.1007/978-981-10-1148-1

Pianosi, F. & Wagener, T. (2016). Understanding the time-varying importance of different uncertainty sources in hydrological modelling using global sensitivity analysis. *Hydrological Processes*, *30*, 3991–4003. doi:10.1002/hyp.10968

Poff, N. L. & Zimmerman, J. K. H. (2009). Ecological responses to altered flow regimes: A literature review to inform the science and management of environmental flows. *Freshwater Biology*, *55*(1), 194–205. doi:10.1111/j.1365-2427.2009.02272.x

Reid, M., Cheng, X., Banks, E. W., Jankowski, J., Jolly, I., Kumar, P., ... Werner, A. D. (2009). *Catalogue of conceptual models for groundwater–stream interaction*. eWater Cooperative Research Centre, Canberra.

Ritter, A. & Muñoz-Carpena, R. (2012). Performance evaluation of hydrological models: Statistical significance for reducing subjectivity in goodness-of-fit assessments. *Journal of Hydrology*, *480*, 33–45. doi:http://dx.doi.org/10.1016/j.jhydrol.2012.12.004

Rosenberry, D. O. & LaBaugh, J. W. (2008). *Field techniques for estimating water fluxes between surface water and groundwater*. Techniques and Methods 4–D2. Reston, Virginia: U.S. Geological Survey.

Rosenberry, D. O. & Pitlick, J. (2009). Effects of sediment transport and seepage direction on hydraulic properties at the sediment–water interface of hyporheic settings. *Journal of Hydrology*, *373*(3-4), 377–394. doi:https://doi.org/10.1016/j.jhydrol.2009.04.030

SAHRA. (2005a). Nitrogen. Retrieved March 11, 2018, from http://web.sahra.arizona.edu/programs/isotopes/nitrogen.html

SAHRA. (2005b). Oxygen. Retrieved March 11, 2018, from http://web.sahra.arizona.edu/programs/isotopes/oxygen.html

Salas, J. D. (1993). Analysis and modeling of hydrological time series. In D. R. Maidment (Ed.), *Handbook of hydrology* (pp. 19.1–19.72). New York: McGraw-Hill.

Scanlon, B. R., Healy, R. W., & Cook, P. G. (2015). Choosing appropriate techniques for quantifying groundwater recharge. *Hydrogeology Journal*, *10*(1), 18–39. doi:https://doi.org/10.1007/s10040-001-0176-2

Schmidt, F. (2007). *Laser-based absorption spectrometry* (Doctoral dissertation, Umeå University, Umeå, Sweden).

Schulla, J. (2017). *Model description WaSiM (Water balance Simulation Model)*. Hydrology Software Consulting J. Schulla.

SCI. (2013). The phosphorus cycle. Retrieved February 15, 2018, from https://www.sciencelearn.org.nz/resources/961-the-phosphorus-cycle

Seiler, R. L. (2005). Combined use of ^{15}N and ^{18}O of nitrate and ^{11}B to evaluate nitrate contamination in groundwater. *Applied Geochemistry*, *20*(9), 1626–1636. doi:https://doi.org/10.1016/j.apgeochem.2005.04.007

Shahin, M., Oorschot, H. J. L., & Lange, S. J. (1993). *Statistical analysis in water resources engineering*. Rotterdam: A. A. Balkema.

Shreeja, D. (n.d.). Chemistry and behaviour of phosphorus present in soil. Retrieved April 22, 2018, from http://www.soilmanagementindia.com/nutrient-elements-in-soil/chemistry-and-behaviour-of-phosphorus-present-in-soil/2740

Sidle, W. C. (1998). Environmental isotopes for resolution of hydrology problems. *Environmental Monitoring and Assessment*, *52*(3), 389–410. doi:https://doi.org/10.1023/A:1005922029958

Solomon, D. K. & Cook, P. G. (2000). ^{3}H and ^{3}He. In R. Michener & K. Lajtha (Eds.), *Environmental tracers in subsurface hydrology* (pp. 397–424). Boston, MA: Springer. doi:https://doi.org/10.1007/978-1-4615-4557-6_13

Soong, D. T., Prater, C. D., Halfar, T. M., & Wobig, L. A. (2012). *Manning's roughness coefficients for Illinois streams*. Data Series 668. Reston, Virginia: U.S. Geological Survey.

Sophocleous, M. (2002). Interactions between groundwater and surface water: The state of the science. *Hydrogeology Journal*, *10*(1), 52–67. doi:https://doi.org/10.1007/s10040-001-0170-8

Stein, L. Y. & Klotz, M. G. (2016). The nitrogen cycle. *Current Biology*, *26*(3), R94–R98. doi:10.1002/hyp.10625

Stewardson, M. J., Datry, T., Lamouroux, N., Pella, H., Thommeret, N., Valette, L., & Grant, S. B. (2016). Variation in reach-scale hydraulic conductivity of streambeds. *Geomorphology*, *259*(15), 70–80. doi:https://doi.org/10.1016/j.geomorph.2016.02.001

Stichler, W., Maloszewski, P., & Moser, H. (1986). Modelling of river water infiltration using oxygen-18 data. *Journal of Hydrology*, *83*, 355–365. doi:10.1016/0022-1694(86)90161-7

Takaoka, N. & Mizutani, Y. (1987). Tritiogenic 3he in groundwater in takaoka. *Earth and Planetary Science Letters*, *85*(1-3), 74–78. doi:https://doi.org/10.1016/0012-821X(87)90022-7

Tóth, J. (1999). Groundwater as a geologic agent: An overview of the causes, processes, and manifestations. *Hydrogeology Journal*, *4*(1), 1–14. doi:https://doi.org/10.1007/s100400050

USGS. (2017a). Geophysics for usgs groundwater/surface-water interaction studies. Retrieved January 21, 2018, from https://water.usgs.gov/ogw/bgas/gwsw/

USGS. (2017b). The water cycle. Retrieved January 14, 2018, from https://water.usgs.gov/edu/watercycle.html

Voss1, M., Deutsch1, B., Elmgren, R., Humborg, C., Kuuppo, P., Pastuszak, M., ... Schulte, U. (2006). Source identification of nitrate by means of isotopic tracers in the Baltic Sea catchments. *Biogeosciences*, *3*, 663–676. doi:https://doi.org/10.5194/bg-3-663-2006

Vreča, P., Bronić, I. K., Leis, A., & Demšar, M. (2014). Isotopic composition of precipitation at the station Ljubljana (Reaktor), Slovenia – period 2007–2010. *Geologija*, *57*(2), 217–230. doi:doi:10.5474/geologija.2014.019

Wachniew, P. (2015). Environmental tracers as a tool in groundwater vulnerability assessment. *Italian Journal of Groundwater*, *4*, 19–25. doi:10.7343/AS-108-15-0135

Wang, H. F. & Anderson, M. P. (1982). *Introduction to groundwater modeling, Finite difference and finite element method*. Netherlands: Springer Science & Business Media.

Widory, D., Kloppmann, W., Chery, L., Bonnin, J., Rochdi, H., & Guinamant, J.-L. (2004). Nitrate in groundwater: An isotopic multi-tracer approach. *Journal of Contaminant Hydrology*, *72*(1-4), 165–188. doi:https://doi.org/10.1016/j.jconhyd.2003.10.010

Winter, T. C., Harvey, J. W., Franke, O. L., & Alley, W. M. (1998). *Ground water and surface water, a single resource* (U.S. Geological Survey Circular No. 1139). U.S. Geological Survey.

Xue, D., Botte, J., nad Frederik Accoe, B. D. B., Nestler, A., Taylor, P., Cleemput, O. V., ... Boeckx, P. (2009). Present limitations and future prospects of stable isotope

methods for nitrate source identification in surface- and groundwater. *Water Research*, *43*(5), 1159–1170. doi:https://doi.org/10.1016/j.watres.2008.12.048

Yeh, G.-T. (2000). *Computational subsurface hydrology.* Reactions, Transport, and Fate. New York: Springer. doi:10.1007/978-1-4615-4371-8

Bibliography

Publications Related to the Thesis

Journal Articles

Vrzel, J., Ludwig, R., Vižintin, G., & Ogrinc, N. (2018a). Integrated approach to the study of hydrology in Ljubljansko polje in Slovenia and its simulation. *Environmental Modelling & Software*. Under review.

Vrzel, J. & Ogrinc, N. (2013a). The use of isotopes for characterization of groundwaters and their relation with surface water. *Ekolist: revija o okolju*, *9*, 7–10.

Vrzel, J. & Ogrinc, N. (2015). Nutrient variations in the Sava River Basin. *Journal of soils and sediments: protection, risk assessment and remediation*, *15*(12), 2380–2386. doi:10.1007/s11368-015-1190-7

Vrzel, J., Ogrinc, N., & Vižintin, G. (2015a). Data preparation for groundwater modelling - Ljubljansko polje aquifer system. *RMZ - Materials and geoenvironment*, *62*(3), 167–173.

Vrzel, J., Solomon, D. K., Blažeka, Ž., & Ogrinc, N. (2018). The suty of the interactions between groundwater and Sava River water in the Ljubljansko polje aquifer system (Slovenia). *Journal of Hydrology*, *556*, 384–396. doi:https://doi.org/10.1016/j.jhydrol.2017.11.022

Vrzel, J., Vuković-Gačić, B., Kolarević, S., Gačić, Z., Kračun-Kolarević, M., Kostić, J., ... Ogrinc, N. (2016). Determination of the sources of nitrate and the microbiological sources of pollution in the Sava River Basin. *Science of the total environment*, *573*, 1460–1471. doi:http://dx.doi.org/10.1016/j.scitotenv.2016.07.213

Other publications related to the thesis

Ogrinc, N., Kocman, D., Miljević, N., Vreča, P., Vrzel, J., & Povinec, P. (n.d.). Distribution of h and o stable isotopes in the surface waters of the sava river basin, the major tributary of danube. *Special issue of The Science of the Total Environment*. Under review.

Ogrinc, N., Tamše, S., Zavadlav, S., & Vrzel, J. (n.d.). Evaluation of geochemical processes and nitrate pollution sources at ljubljansko polje aquifer (Slovenia): Stable isotope perspective. *Journal of Hydrology*. Under review.

Vrzel, J., Ludwig, R., Gampe, D., & Ogrinc, N. (n.d.). Assessment of the hydrological system behaviour under climate change in ljubljansko polje, Slovenia. *Special issue of The Science of the Total Environment*. In preparation.

Conference Paper

Vrzel, J. & Ogrinc, N. (2013b). Uporaba izotopov pri raziskavah podzemnih vod. In N. Trdin (Ed.), *Proceedings of 5th Jožef Stefan International Postgraduate School*

Students' Conference. Ljubljana, Slovnia: Jožef Stefan International Postgraduate School.

Vrzel, J. & Ogrinc, N. (2014b). Nitrate origin and distribution in the Sava River Basin. In N. Trdin (Ed.), *Proceedings of 6th Jožef Stefan International Postgraduate School Students' Conference*. Ljubljana, Slovnia: Jožef Stefan International Postgraduate School.

Vrzel, J., Vižintin, G., & Ogrinc, N. (2015b). Conceptual model of Ljubljansko polje aquifer. In A. Rešetič (Ed.), *Proceedings of 7th Jožef Stefan International Postgraduate School Students' Conference*. Ljubljana, Slovnia: Jožef Stefan International Postgraduate School.

Published scientific conference contribution abstract

Anđus, S., Milačić, R., Mitrović, M., Pavlović, P., Ogrinc, N., Vrzel, J., ... Paunović, M. (2015). Upravljanje efektima višestrukih stresora u uslovima nedostatka vode – Globaqua projekat. In A. Đukić (Ed.), *Water 2015*. Belgrade, Serbia: Srpsko društvo za zaštitu voda.

Ogrinc, N., Vrzel, J., Kocman, D., & Vreča, P. (2016). Hydrology and nutrient variations in the sava river basin: Stable isotope approach). In A. N. Ortega, R. Ludvig, & D. B. Cullerés (Eds.), *Managing the effects of multiple stressors on aquatic ecosystems under water scarcity: Book of abstracts of the 1st Globaqua International Conference*. Freising, Germany.

Vrzel, J., Ludwig, R., Meyer, S., Vižintin, G., & Ogrinc, N. (2016a). An integrated modeling approach to assess the surface-groundwater interaction in a sensitive aquifer system (Ljubljansko polje, Slovenia). In *4th International Forum on Integrated Water Management Land, Water, Sources*. Québec city, Canada: International Conference on Source Water Protection.

Vrzel, J., Ludwig, R., Meyer, S., Vižintin, G., & Ogrinc, N. (2017). Hydrodynamic and geochemical analysis of groundwater-surface water interactions (Ljubljansko polje, Slovenia. In K. Posavec & T. Marković (Eds.), *Book of abstracts: 44th Annual Congress of the International Association of Hydrogeologists (IAH)*. Dubrovnik, Croatia: The International Association of Hydrogeologists.

Vrzel, J., Ludwig, R., Vižintin, G., & Ogrinc, N. (2016). Study groundwater-surface water interactions and its modelling to improve understanding of dynamics in the Ljubljansko polje aquifer system (Slovenia). In A. N. Ortega, R. Ludvig, & D. B. Cullerés (Eds.), *Managing the effects of multiple stressors on aquatic ecosystems under water scarcity: Book of abstracts of the 1st Globaqua International Conference*. Freising, Germany.

Vrzel, J., Ludwig, R., Vižintin, G., & Ogrinc, N. (2017). A study of the Ljubljansko polje aquifer system behaviour and its simulations using multi-tools. In *AGU Fall Meeting*. New Orleans, Louisiana, USA: American Geophysical Union.

Vrzel, J., Ludwig, R., Vižintin, G., & Ogrinc, N. (2018b). Multi-tool simulations to assess the hydrological system behavior of the Ljubljansko polje aquifer under climate change conditions. In I. L. Jeuness & S. Pincebourde (Eds.), *Diversity of local responses to the impacts of climate change on water*. Tours, France: International Conference Climate Change and Water 2018.

Vrzel, J. & Ogrinc, N. (2014a). Multiple stressors in the Sava River watershed. In *Programme and abstracts of IASWS 13th International Symposium*. Grahamstown, South Africa: IASWS International Symposium.

Vrzel, J., Ogrinc, N., & Vižintin, G. (2015b). Development of the conceptual model - Ljubljansko polje aquifer (Slovenia). In I. Ristović (Ed.), *Mining and environmen-*

tal protection: Proceedings, 5th International symposium mining and environmental protection. Vrdnik, Serbia: Faculty of Mining and Geology in Belgrade.

Vrzel, J., Solomon, D. K., & Ogrinc, N. (2014). Study of the interactions between surface and groundwater in Ljubljansko polje aquifer. In V. Žunič (Ed.), *Program and abstract book of 8th Young Researchers' Day*. Ljubljana, Slovenia: Jožef Stefan Institute.

Vrzel, J., Tamše, S., Solomon, D. K., & Ogrinc, N. (2013). Groundwater tracers in Ljubljana aquifer. In A. Demény (Ed.), *Book of abstracts of 10th Applied Isotope Geochemistry Conference*. Budapest, Hungary: Akadémiai Kiadó.

Vrzel, J., Vižintin, G., & Ogrinc, N. (2014). Hidrološki model Ljubljanskega polja. In B. Rožič, T. Vrbovšek, & M. Vrabec (Eds.), *Abstracts and field trips of the 4. Slovenian Geological Congress*. Ankaran, Slovenia: Faculty of Natural Sciences and Engineering in Ljubljana.

Vrzel, J., Vižintin, G., & Ogrinc, N. (2015a). Conceptual model of Ljubljansko polje aquifer. In *Abstracts, FEFLOW Conference*. Berlin, Germany: DHI.

Vrzel, J., Vižintin, G., & Ogrinc, N. (2015c). Hydrogeological modelling of Ljubljansko polje aquifer. In N. Kavčič (Ed.), *Program and abstract book of 9th Young Researchers' Day*. Ljubljana, Slovenia: Jožef Stefan Institute.

Vrzel, J., Vižintin, G., & Ogrinc, N. (2015d). Modelling of Ljubljansko polje aquifer. In O. Nives, D. Potočnik, & J. Faganeli (Eds.), *Dynamics of biogeochemical systems: Processes and modeling: Conference program and abstracts*. Piran, Slovenia: National Institute of Biology & Jožef Stefan Institute.

Vrzel, J., Zavadlav, S., Tamše, S., Solomon, D. K., & Ogrinc, N. (2013). Evaluating the vulnerability of groundwater resources using groundwater tracers. In D. Lisjak, P. Dušak, & S. Kralj (Eds.), *Program and abstract book of 7th Young Researchers' Day*. Ljubljana, Slovenia: Jožef Stefan Institute.

Unpublished scientific conference contribution abstract

Vrzel, J., Ludwig, R., Meyer, S., Vižintin, G., & Ogrinc, N. (2016b). *Study of surface-groundwater interactions at the reach scale: Ljubljansko polje (Slovenia)*. 48. Jahrestreffen des Arbeitskreises Hydrologie, Munich, Germany.

Vrzel, J., Ludwig, R., & Ogrinc, N. (2017). *A link between WaSiM and FEFLOW*. WaSiM User Conference 2017, Munich, Germany.

Biography

The author of this thesis Janja Vrzel was born on March 20, 1987 in Murska Sobota, Slovenia. She finished her primary education in Sveti Jurij ob Ščavnici, Slovenia and secondary education at the Gimnazija Franca Miklošiča in Ljutomer, Slovenia. She started her studies at the Faculty of Natural Sciences and Engineering, University of Ljubljana, Slovenia in 2006. In 2012, she was awarded a Diploma degree in Geology for the thesis entitled "Hydrogeological analysis of shallow and deep aquifer relation in Radenci area" from the University of Ljubljana, Ljubljana, Slovenia. In the same year, she was selected as a PhD candidate at the Jožef Stefan International Postgraduate School, Ljubljana Slovenia, under the supervisor of Prof. Dr. Nives Ogrinc from the Department of Environmental Sciences, Jožef Stefan Institute, Ljubljana, Slovenia, co-supervisor Prof. Dr. Ralf Ludwig from the Department of Geography, at the Ludwig-Maximilians-Universität-München in Munich, Germany and the second co-supervisor Assoc. Prof. Dr. Goran Vižintin from the Department of Geotechnology, Mining and Environment, University of Ljubljana, Slovenia. The first part of the research took place at the Jožef Stefan Institute in Ljubljana, although her employer—the Ecological engineering institute d.o.o. was located in Maribor, Slovenia. She continued with the research for the next few years at the Ludwig-Maximilians-Universität-München in Munich. For her work, she uses interdisciplinary approach for better understanding of the complicated surface and underground hydrology as a one system, such as isotopes, long term historical data and simulations of hydrological processes with different modeling tools. During the PhD studies, she attended several workshops and summer schools on the topics of geochemistry (use of stable isotopes in environmental sciences), hydrological modeling, catchment hydrology, natural resource management and energy systems under changing environmental conditions, and presented her work at several local and international conferences around Europe, North America and South Africa.